



UNIVERSITÀ DEGLI STUDI DI
SASSARI



A.D. MDLXII

**Scuola di Dottorato di Ricerca in
Scienze e Biotecnologie dei Sistemi Agrari e Forestali
e delle Produzioni Alimentari**

Indirizzo

Agrometeorologia ed Ecofisiologia dei Sistemi Agrari e Forestali

XXV CICLO

**AGRICULTURAL WATER DEMAND ASSESSMENT
USING THE SIMETA# MODEL**

Dr. Noemi Mancosu

Direttore della Scuola

Prof. Alba Pusino

Coordinatore di indirizzo

Prof. Donatella Spano

Docenti guida

Prof. Donatella Spano

Dr. Richard L. Snyder

Anno Accademico 2011-2012

The journey is the destination

ACKNOWLEDGMENTS

Many people have contributed to the realization of this dissertation in several ways. Some of them with technical and scientific support, others with friendship and continuous encouragement, but everybody has been essential for my Ph.D. experience. To all these people I want to express my sincere gratitude.

Firstly, my supervisors Prof. Donatella Spano and Dr. Richard L. Snyder for their guidance and patience during my study. I sincerely thank them for their expert advice and technical assistance, contributing to my professional growth.

I would also like to thank Prof. Sandro Dettori, Chair of the Department of Science for Nature and Environmental Resources (DipNET)-University of Sassari, all the professors, researchers, administrative and technical staff of the department.

I am grateful to all the people and institutions that have made possible the realization of this thesis providing data and information, in particular Dr. Luca Mercenaro, Dr. Andrea Motroni, Dr. Antonella Garippa, Ing. Giuseppe Bosu, Consorzio di Bonifica della Sardegna, Laore, Agris, ARPA Sardegna, and Regione Autonoma della Sardegna.

I would further like to thank Sara Sarreshteh and Morrie Orang for the collaboration on the development of the SIMETAW# model, and Dr. Andrea Peano for providing the software necessary for the manipulation of the future climate data.

I would like to thank the Euro-Mediterranean Center on Climate Change (CMCC) for providing future climate projections data.

I want to thank my lovely friends and colleagues, Dr. Valentina Bacciu and Dr. Valentina Mereu, for their helpful advices, for showing me the positive aspect of this work, and for teaching me to consider even problems in an optimistic prospective. Love you!!

I am also grateful to my friends Gwen Tindula and Dr. Tom Shapland for revising my thesis with their precious suggestions, Prof. Kyaw Tha Paw U, Prof. Aliasghar Montazar, Dr. Mimar Alsina, the Biomet group, and all the staff of the LAWR department of the University of California, Davis, who made my work and my stay a pleasant one.

I would also like to thank all my colleagues of the Ph.D. school XXV cycle; we had such a good time together, especially during dinners!!!

A special round of thanks to all my colleagues of the DipNET, Dr. Serena Marras, Dr. Costantino Sirca, Dr. Michele Salis, Dr. Simone Mereu for continuous exchange of opinions useful for my work.

I also thank Dr. Rita Marras for keeping me updated on reports, deadlines and activities of the Ph.D school.

A very special thanks to all my friends, Italians and Americans, too many to list here, who always cheered me up during tough times and with whom I shared many a laughter.

And last but not least, a special thanks to my family, who shared with me the happiness and difficulties during these years, encouraging and supporting me every day. I will always grateful for all your unconditional love. You are always in my heart!!!

Noe

TABLE OF CONTENTS

ACKNOWLEDGMENTS	III
ABSTRACT	VIII
RIASSUNTO	VIII
CHAPTER 1: INTRODUCTION	1
1. MEDITERRANEAN WATER SCARCITY	14
1.1. Climate change impact on Mediterranean irrigation requirement	15
1.2. The Italian water demand	19
1.3. Agricultural water use in Sardinia	24
2. CROP WATER REQUIREMENT	30
2.1. The soil water balance	30
2.2. Methods to evaluate evapotranspiration	37
2.2.1. The energy balance	39
2.2.2. Meteorological data method to compute ET_o	47
2.3. Crop coefficient	53
3. WATER SCARCITY MANAGEMENT	55
3.1. Adaptation strategies	55
3.1.1. Irrigation systems	57
3.1.2. Scheduling of irrigation management strategies	60
4. OBJECTIVES	63
REFERENCES	64

CHAPTER 2: INVESTIGATION ON THE REFERENCE EVAPOTRANSPIRATION DISTRIBUTION AT REGIONAL SCALE BY ALTERNATIVE METHODS TO COMPUTE THE FAO PENMAN-MONTEITH EQUATION

ABSTRACT	80
1. INTRODUCTION	81
2. MATERIALS AND METHODS	83
2.1. Experimental site description	83
2.2. Data collection and ET_o computation	86
2.3. Alternative ET_o estimation methods for partial stations	88
2.4. Spatial interpolation models for ET_o data	93

3. RESULTS AND DISCUSSION	97
3.1. Estimating daily ET_o by the FAO Penman-Monteith and Hargreaves-Samani methods for full stations	97
3.2. Performance of alternative ET_o computation methods	99
3.3. Interpolation model test	103
4. CONCLUSIONS	108
REFERENCES	109

CHAPTER 3: PROCESSES AND FUNCTIONS OF SIMETAW# - A NEW MODEL FOR PLANNING WATER DEMAND IN AGRICULTURE	117
ABSTRACT	117
1. INTRODUCTION	118
2. THE SIMETAW# MODEL DESCRIPTION	122
2.1. Weather input data and ET_o computation	122
2.2. Crop-soil input data	126
2.3. The weather generator	128
2.4. Crop coefficient values and corrections	131
2.5. Crop evapotranspiration	133
2.6. Water balance calculations	134
2.7. Evapotranspiration of applied water	134
2.8. Determination of the stress coefficient and fraction of potential yield	138
2.9. Rain-fed Agriculture	141
3. MATERIALS AND METHODS	141
3.1. Datasets	141
3.2. Weather data simulation	143
3.3. Statistics	143
4. RESULTS AND DISCUSSION	145
4.1. Simulation of the crop evapotranspiration and irrigation scheduling	145
4.2. Assessment of the accuracy of the weather generator	157
5. CONCLUSIONS	160
REFERENCES	161

CHAPTER 4: ASSESSMENT OF CLIMATE CHANGE IMPACT ON CROP WATER REQUIREMENT IN SARDINIA USING THE SIMETA# MODEL	169
ABSTRACT	169
1. INTRODUCTION	169
2. MATERIALS AND METHODS	171
2.1. Preliminary activity	171
2.2. Scheme of methodology	173
2.3. Data collection	174
2.4. Impact of climate change on irrigation water requirement	178
3. RESULTS AND DISCUSSION	180
3.1. The current irrigation water demand	180
3.2. Impact of climate change on future irrigation water demand	184
3.3. Assessment of adaptation strategies	195
4. CONCLUSIONS	196
REFERENCES	197
GENERAL CONCLUSIONS	203

ABSTRACT

Water scarcity is nowadays one of main world issues, and because of the climate change projections, it will be more important in future. The first step is to compute how much water crops need relative to climate conditions, in order to estimate the depth of storage water required to satisfy future agricultural water demand. In this study, starting from the computation of the regional map of reference evapotranspiration (ET_o) zones from climate station data points, the impact of climate changes on crop irrigation requirement in Sardinia was estimated. The SIMETAW# model was used to quantify the actual and future irrigation requirement for some economically important crops for the region, considering an integrated approach that accounts for soil, crop management, and irrigation system data. The model provided detailed information about the crop water demand by the ET_o zones. This approach presented possible adaptation strategies and demonstrated a sustainable way for water savings, improving irrigation management, and water productivity.

RIASSUNTO

La carenza idrica è attualmente uno dei problemi più sentiti a livello mondiale, e a causa delle proiezioni del cambiamento climatico, lo sarà ancor di più in futuro. Calcolare la richiesta idrica colturale in relazione alle condizioni climatiche è il primo passo utile per la stima del volume idrico necessario per soddisfare le future esigenze del comparto agroalimentare. In questo studio, partendo dalla realizzazione della mappa regionale dell'evapotraspirazione di riferimento (ET_o) utilizzando dati punto stazione, è stato stimato l'impatto del cambiamento climatico sulla richiesta irrigua colturale in Sardegna. La domanda irrigua attuale e futura di alcune colture economicamente importanti per la regione è stata quantificata attraverso l'applicazione del modello per la stima del bilancio idrico del suolo SIMETAW#. Attraverso un approccio integrato che tiene conto delle caratteristiche del suolo, della gestione colturale e del sistema di irrigazione utilizzato, il modello ha fornito informazioni dettagliate sulla richiesta idrica colturale nelle diverse aree ET_o . Tale approccio ha consentito l'applicazione di possibili strategie di adattamento che hanno dimostrato essere una soluzione sostenibile per il risparmio idrico, migliorando la gestione irrigua ed incrementando la produttività dell'acqua.

CHAPTER 1: INTRODUCTION

Water is the most important resource for life. Water has been the main issue on the international agenda for the last 30 years, starting with the 1st International Conference on Water (Mar de la Plata, 1977), following with the International Conference on Water and the Environment (Dublin, 1992), to conclude with the 1st World Water Forum (Marrakech, 1997). Since then, this topic has been considered to be increasingly important.

The concept of water resources is multidimensional, and it goes over the physical connotation. In fact, not only the quantity is considered important, measured in flows and stocks, but also the quality. Water is a natural and environmental resource that acquires a socio-economic connotation. Nowadays, the term “water” is linked to the concept of water scarcity, and there are many ongoing studies and projects to assess the world water demand and its availability.

Water is divided in two types of resources:

- the renewable water resources: the long-term average annual flow of rivers (surface water) and groundwater.
- the non-renewable water resources: groundwater bodies (deep aquifers) that have a negligible rate of recharge on the human time scale, and for this reason can be considered non-renewable.

The natural and anthropogenic water cycle is showed in Figure 1, where the total amount of precipitation is split between evapotranspiration, surface runoff, infiltration, and ground water recharge. Big vertical arrows show the total annual precipitation and evapotranspiration over the land and the ocean ($1,000 \text{ km}^3 \text{ yr}^{-1}$), which include annual precipitation and evapotranspiration in the major landscapes ($1,000 \text{ km}^3 \text{ yr}^{-1}$) presented by small vertical arrows. The direct groundwater discharge, which is globally estimated to be about 10% of total river discharge (Church, 1996), is included in river discharge.

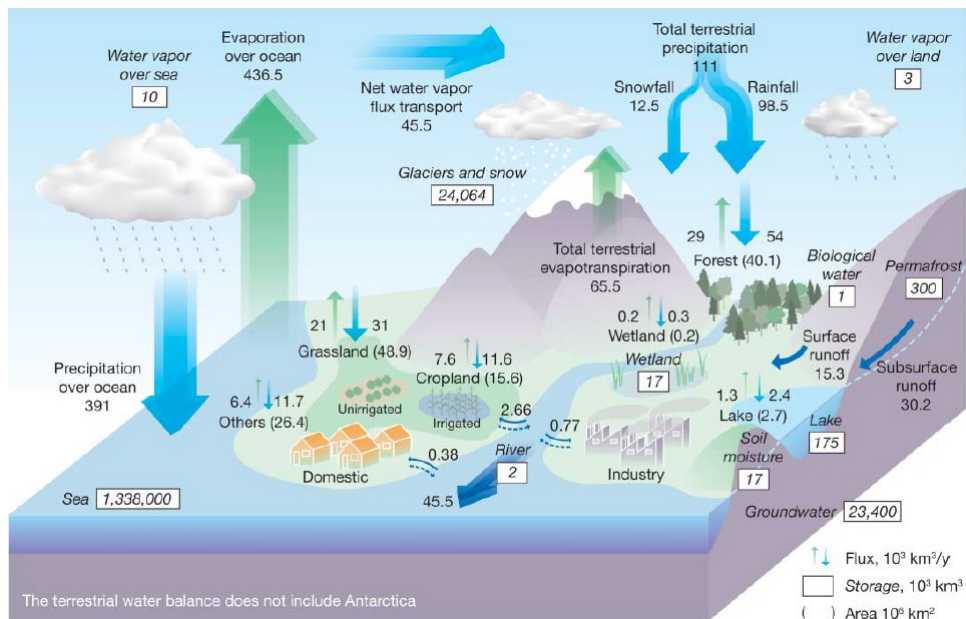


Figure 1. Global hydrological fluxes (1,000 km³ yr⁻¹) and storages (1,000 km³) with natural and anthropogenic cycles. (Oki and Kanae, 2006).

Falkenmark and Rockström (2004) defined blue water as the liquid water above and below the ground (rivers, lakes, groundwater, etc.), and green water as the soil water in the unsaturated zone derived from precipitation. The portion of water that is directly used and evaporated by non-irrigated agriculture, pastures, and forests is defined as green water.

Blue and green water are both considered to be renewable resources in the broad sense, but only blue water is evaluated in the strict sense.

Blue water includes natural and actual renewable water resources. Natural renewable water resources are the total water resource amounts of a country, both surface water and groundwater, which are generated through the hydrological cycle. The amount is computed on a yearly basis.

The method used to assess the renewable water resources by country was first described in FAO/BRGM (1996). The method computes the total renewable water resources (TRWR) of a country and assess the dependency ratio from neighboring countries.

Internal renewable water resources (IRWR) are the volume of the water resources (surface water and groundwater) generated from precipitation within a country or catchment:

$$IRWR = R + I - (Q_{OUT} - Q_{IN}) \quad (1)$$

where:

R = surface runoff. It is the total volume of the long-term annual average flow of surface water generated by direct runoff from endogenous precipitation;

I = groundwater recharge. It is generated from precipitation within the country;

Q_{OUT} = groundwater drainage into rivers (typically, base flow of rivers);

Q_{IN} = seepage from rivers into aquifers.

Surface water and groundwater are usually studied separately, even if the two concepts often overlap. Surface water flows can contribute to groundwater replenishment through seepage in the river bed. Aquifers can discharge into rivers and contribute to their base flow, the sole source of river flow during dry periods.

External renewable water resources (ERWR) are considered resources that enter from upstream countries through rivers (external surface water) or aquifers (external groundwater resources).

ERWR are separated into two categories: natural and actual ERWR.

The natural ERWR are equal to the volume of average annual flow of rivers and groundwater that enter into a country from neighbouring countries.

The actual ERWR take into account the quantity of flow reserved by upstream (incoming flow) and/or downstream (outflow) countries through formal or informal agreements or treaties.

Most of the inflow consists of river runoff, but it can also consider groundwater transfer between countries. Therefore, the actual resource takes into account the resources shared with neighbouring countries (geopolitical country constraints).

Unlike the natural ERWR, the actual ERWR vary with time and consumption patterns; therefore, it must be associated to a specific year.

The total renewable water resources are the sum of IRWR and ERWR.

All these parameters facilitate the analysis of how different countries depend on the water resources of their neighbours. The dependency ratio of a country is an indicator that expresses the part of the water resources originated outside the country as:

$$\frac{IRW}{IRWR+IWR} \times 100\% \quad (2)$$

with:

$$IWR = SW_{IN}^1 + SW_{IN}^2 + SW_{PR} + SW_{PL} + GW_{IN} \quad (3)$$

where:

IWR= total volume of incoming water resources from neighbouring countries.

IRWR= internal renewable water resources;

SW_{IN}^1 = volume of surface water entering the country that is not submitted to treaties;

SW_{IN}^2 = volume of surface water entering the country that is secured through treaties;

SW_{PR} = accounted flow of border rivers;

SW_{PL} = accounted part of shared lakes;

GW_{IN} = groundwater entering the country.

A country with a dependency ratio equal to zero does not receive any water from neighbouring countries. While a country that possesses a dependency ratio equal to 100% receives all its water from outside without producing any.

The total water resources in the world are estimated in the order of $43,750 \text{ km}^3 \text{ yr}^{-1}$ distributed throughout the world. At the continental level, America has the largest share of the world's total freshwater resources with 45%, followed by Asia with 28%, Europe with 15.5 %, and Africa with 9% (FAO, 2003a). In terms of resources per inhabitant in each continent, America has $24,000 \text{ m}^3 \text{ yr}^{-1}$, Europe $9,300 \text{ m}^3 \text{ yr}^{-1}$, Africa $5,000 \text{ m}^3 \text{ yr}^{-1}$, and Asia $3,400 \text{ m}^3 \text{ yr}^{-1}$ (FAO, 2003a).

The world map of IRWR (Figure 2) shows the most critical situations all over Africa and the Middle East, with IRWR values that range from 0 to 150 mm yr^{-1} .

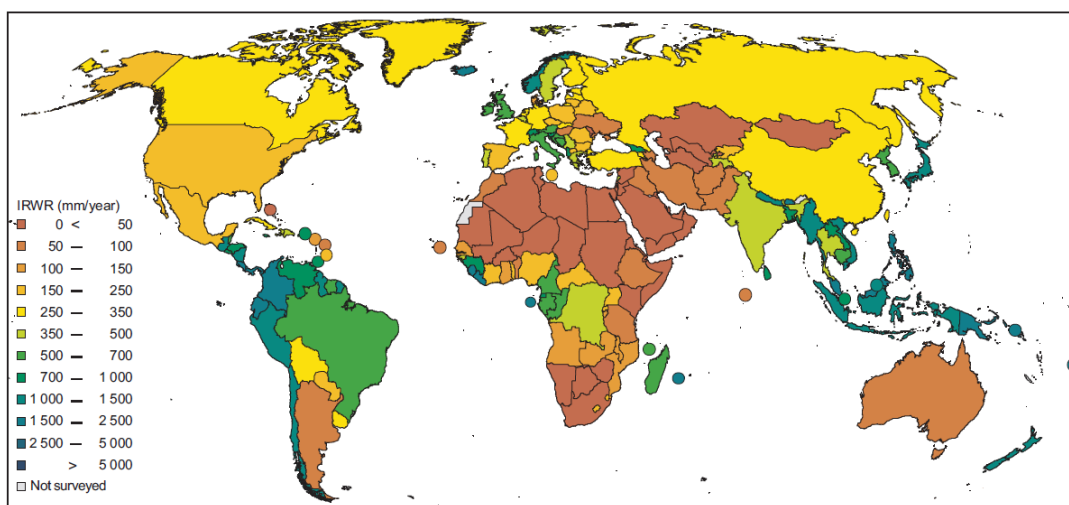


Figure 2. World map of internal renewable water resources (IRWR) per country (FAO, 2003a).

Such sources are taken into consideration separately from natural renewable water resources. They include:

- the reuse of urban or industrial wastewaters (with or without treatment) mostly in agriculture, but increasingly in industrial and domestic sectors;
- the production of freshwater by desalination of brackish or saltwater (mostly for domestic purposes).

Despite the vast amount of water on the planet, the balance between water demand and water availability has reached a critical level in many areas of the world. This is due to a misuse of the water resources, but also to the impact of climate change. The Intergovernmental Panel on Climate Change (IPCC) Fourth Assessment Report declares that climate change is expected to exacerbate the current stress on water resources by population growth and economic and land-use change, including urbanization. In relation with the scenarios described in the IPCC Special Report on Emissions Scenarios (SRES, 2000), changes in precipitation and temperature lead to changes in runoff and water availability that affect crop productivity (IPCC, 2007a).

As pointed out by Bates et al. (2008), climate model simulations for the 21st century are consistent in projecting precipitation increases at high latitudes and parts of the tropics, and decreases in some subtropical and lower mid-latitude regions (Figure 3).

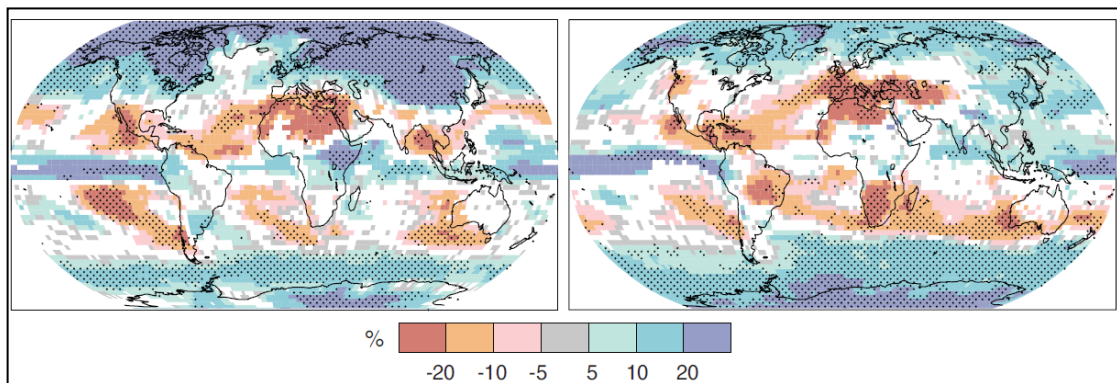


Figure 3. Relative changes in precipitation (in percent) for the period 2090-2099, relative to 1980-1999. Values are multi-model averages based on the SRES A1B scenario for December to February (left) and June to August (right). White areas are where less than 66% of the models agree in the sign of the change and stippled areas are where more than 90% of the models agree in the sign of the change (IPCC, 2007a).

FAO (2011) declared that crop productivity is predominantly weather based, rather than determined by long-term climate, and the following changes are the factors that affect it:

- changes in mean weather (temperature and rainfall);
- changes in variability or distribution of weather;
- combination of changes in the mean and changes in its variability.

The rising atmospheric CO₂ concentration, associated with higher temperature, changes with precipitation patterns. Altered frequencies of extreme events will have significant effects on crop production (Figure 4). As a result, consequences for water resources and pest/disease distributions are expected. In fact, melting of winter snow and reduced storage of precipitation as snow causes a reduction in water availability. Moreover the sea level rise affects low lying coastal areas, and the intrusion of saline water influences the quality of freshwater aquifers.

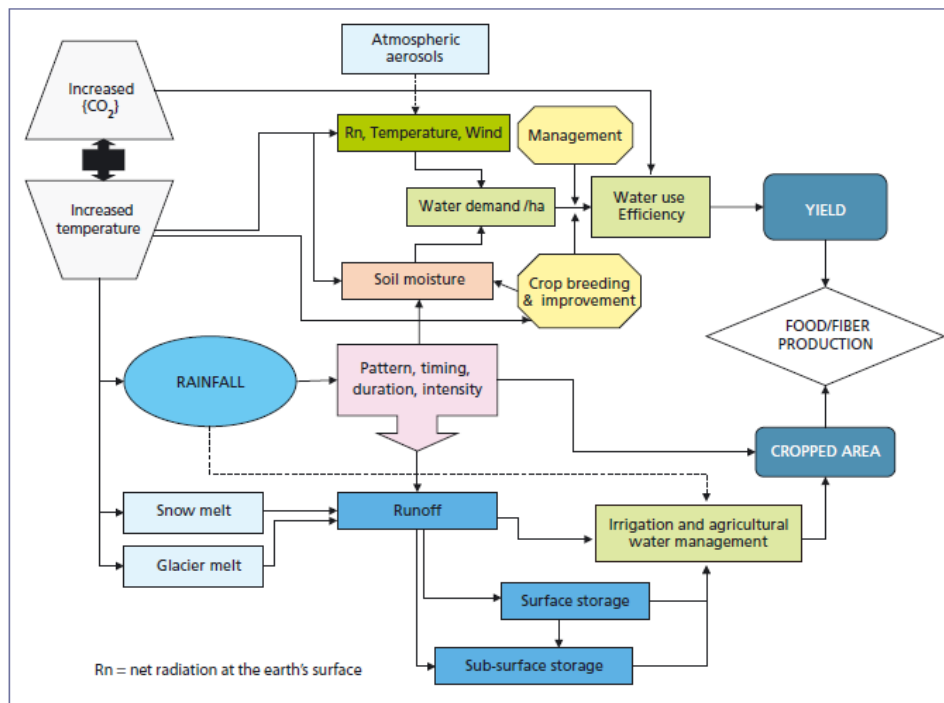


Figure 4. The agricultural production cycle as impacted by climate change (FAO, 2011).

The following changes have been declared in IPCC (2007a):

- depending on the SRES emission scenario and climate models considered, global mean surface temperature is projected to rise in a range from 1.8°C (with a range from 1.1°C to 2.9°C for SRES B1) to 4.0°C (with a range from 2.4°C to 6.4°C for A1) by 2100;

- many semi-arid areas (e.g., the Mediterranean Basin, western United States, southern Africa, and north-eastern Brazil) will have a greater frequency of droughts;
- the decrease in water resources due to climate change in drought-affected areas are projected to increase in extent, with the potential for adverse impacts on multiple sectors, e.g. agriculture, water supply, energy production, and health. In Asia, the large contiguous areas of irrigated land that rely on snowmelt and high mountain glaciers for water will be affected by changes in runoff patterns, while highly populated deltas are at risk from a combination of reduced inflows, increased salinity, and rising sea levels;
- there is a high probability that in the future, heavy rainfall events will increase in many regions, even where the mean annual rainfall is projected to decrease. In addition, the increase of the frequency and severity of floods and droughts poses challenges to society, physical infrastructure, and water quality. It is likely that up to 20% of the world population will live in areas where river flood potential could increase by the 2080s;
- runoff is projected with high confidence to increase by 10 to 40% by mid-century at higher latitudes and in some wet tropical areas (including populous areas in East and South-East Asia), and decrease by 10 to 30% in some dry regions at mid-latitudes and in dry tropics, due to the decrease in rainfall and higher rates of evapotranspiration.

The physical, chemical, and biological properties of freshwater lakes and rivers will also be affected by the increase in temperature. This change is predicted to negatively impact many individual freshwater species, community composition, and water quality.

An increase of evaporative demand from crops, as a result of higher temperature, and the reduction of water availability in regions affected by falling annual or seasonal precipitation, means a reduction in crop yield and agricultural productivity where temperature constrains crop (FAO, 2011). On the other hand, current research confirms that crops would respond positively to elevated levels of CO₂ in the absence of climate change (e.g., Kimball et al., 2002; Jablonski et al., 2002; Ainsworth and Long, 2005). The direct effect of CO₂ enrichment on plant growth and development, also called the

CO₂ fertilization effect, has generally a positive effect on crop yield (Idso and Idso, 1994). In fact, the increase of CO₂ concentration reduces the stomatal conductance and transpiration rates (Olesen and Bindi, 2002). Moreover, the combination of increased water use efficiency and root water uptake capacity modifies the relative crop yield response to elevated CO₂ (Tubiello and Ewert, 2002).

Precipitation and soil moisture are important factors that hinder crop production, even though the increase in atmospheric CO₂ concentration counteracts the negative effect, potentially causing the crops to be less water stress sensitive (Brown and Rosenberg, 1997; Singh et al., 1998). Changes in precipitation patterns, intensity and frequency of extreme events, soil moisture, runoff, and evapotranspiration fluxes have already been observed, and more important changes are expected for the future (Bates et al., 2008). Sillmann and Roeckner (2008) estimated that extreme precipitation is projected to increase significantly in most regions of the world, especially in those regions that are already relatively wet under present climate conditions. Analogously, dry spells are expected to increase, particularly in those regions that are characterized by dry conditions in the present-day climate, such as European regions (Figure 5).

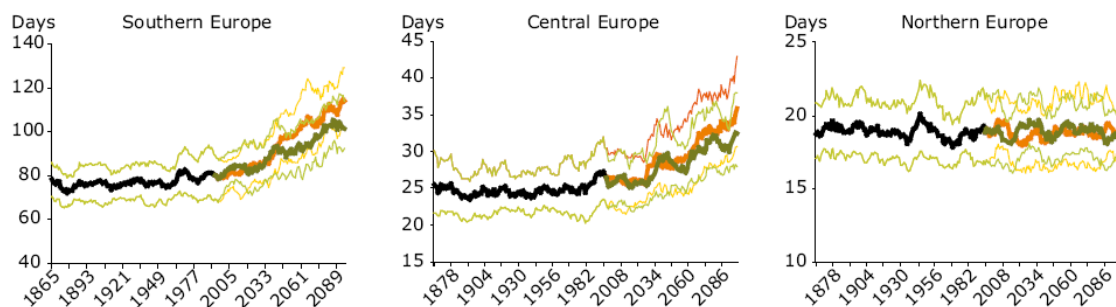


Figure 5. Simulated land average maximum number of consecutive dry days for different European regions (1860–2100) (Sillmann and Roeckner, 2008).

Nowadays, 12% of the land surface is used for cultivation, and another 22% is used for pastures and rangelands (Leff et al., 2004). Shiklomanov (1997) estimated that the agricultural sector uses two-thirds of the world water withdrawals, which accounts for 90% of the total water consumption in the world in the period from 1961 to 2004. On the world average, agriculture is the largest water user sector, accounting for approximately 70% of the total water withdrawals (Johnson et al., 2001).

FAO (2003a) reported that more than 80% of global agricultural land is rain-fed; irrigated land, representing a mere 18% of global agricultural land, produces 1 billion

tonnes of grain annually, or about half the world's total supply. This is because yields of irrigated crops are on average 2–3 times more than their rain-fed counterparts. As pointed out by Shiklomanov (1998), the smallest values for specific water withdrawals are observed in northern Europe, and they are between 300-5,000 m³/ha, while in southern and eastern European countries, they amount to 7,000-11,000 m³/ha. In the USA, the specific water withdrawal for irrigation is estimated to be between 8,000-10,000 m³/ha. In the countries of Asia, Africa, Central and South America, where there is a great variety of climatic conditions, crop composition, and watering techniques, the values for specific water withdrawal range from 5,000 - 6,000 m³/ha to 15,000 - 17,000 m³/ha. The biggest values for specific water withdrawal are observed in regions of Africa (20,000-25,000 m³/ha).

Such water-stressed basins are located in northern Africa, the Mediterranean region, the Middle East, the Near East, southern Asia, northern China, Australia, the USA, Mexico, north-eastern Brazil, and the west coast of South America (Figure 6). An increase in irrigation water demand, particularly in the aforementioned countries, is projected as a result of climate change.

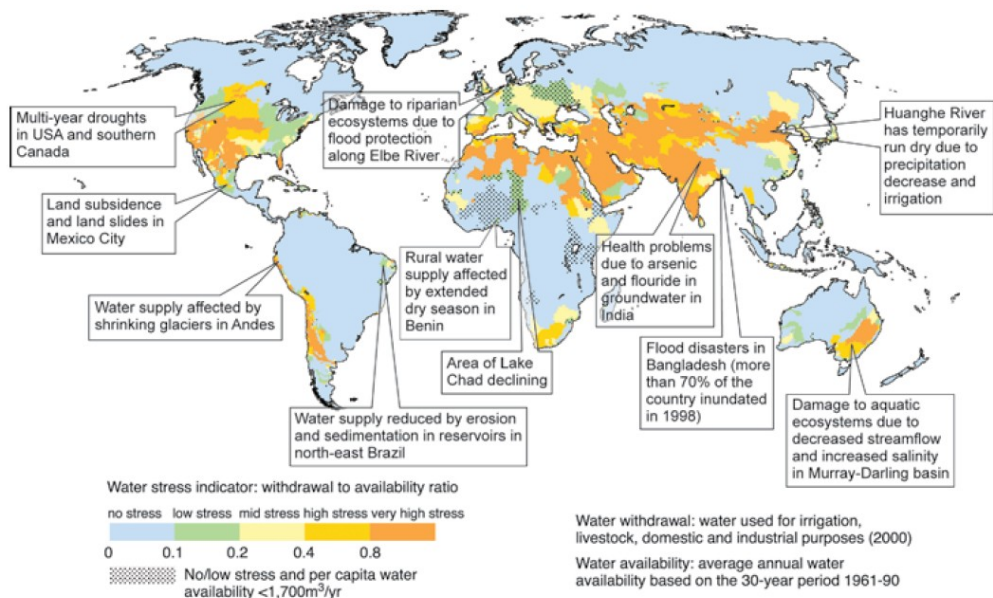


Figure 6. Examples of current vulnerabilities of freshwater resources and their management; in the background, a water stress map based on WaterGAP (Alcamo et al., 2003a).

Fischer et al. (2007) estimated that irrigation water requirements are expected to increase over 50% in developing regions, and by about 16% in developed regions.

Estimations of irrigation water requirements were computed from 2000 to 2080, with the largest relative increases occurring in Africa (+300%) and Latin America (+119%).

Populations estimates for such water-stressed basins range between 1.4 billion and 2.1 billion (Vörösmarty et al., 2000; Alcamo et al., 2003b; Oki et al., 2003; Arnell, 2004). About 7% of the world's population lives in areas affected by water scarcity (Fischer and Heilig, 1997), and the situation will be exacerbated by 2050 (Figure 7 a, b).

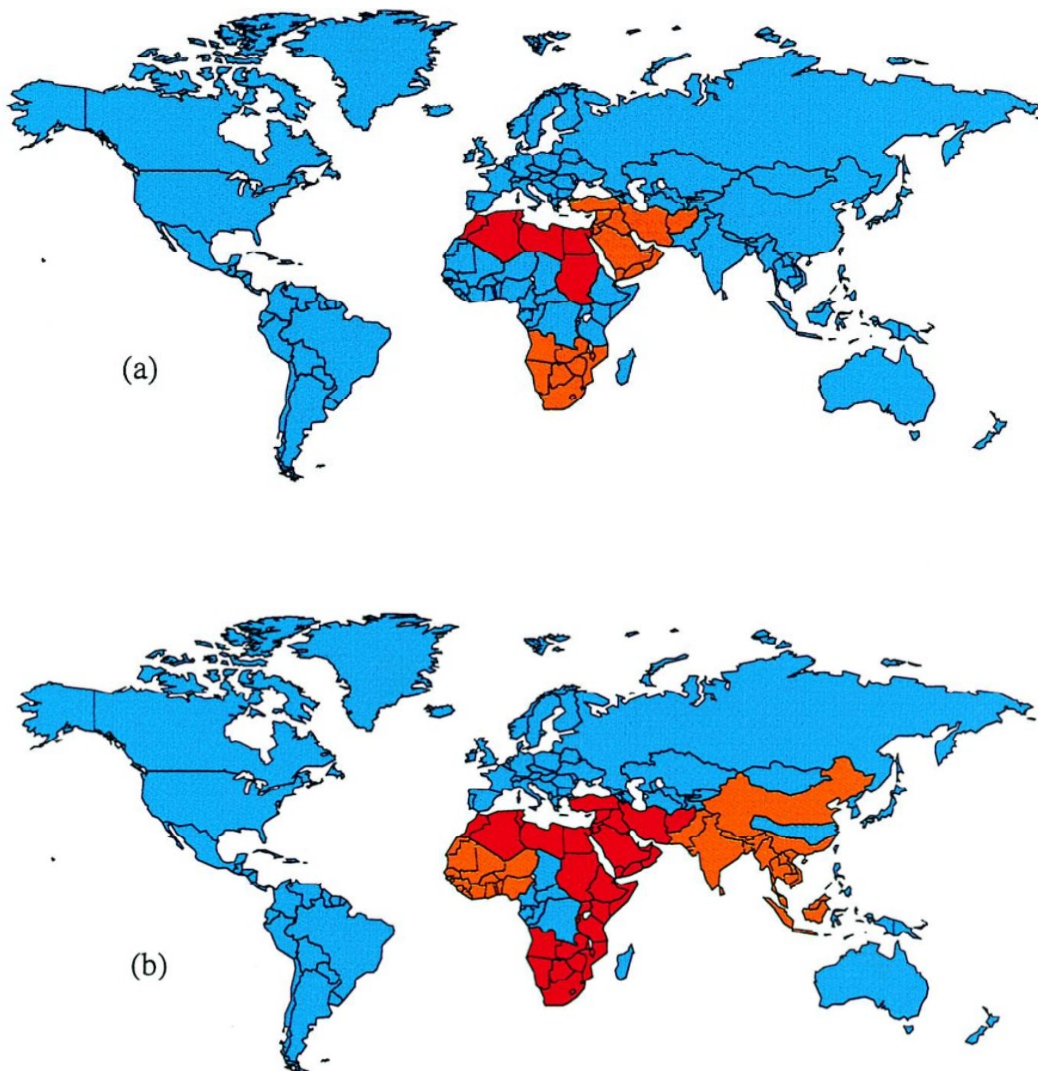


Figure 7. Global water scarcity now (a) and in 2050 (b). Red is used for regions that present less than 1,000 m³ per person per year, orange between 1,000 and 2,000 m³ per person per year and blue for value greater than 2,000 m³ per person per year (data from Fischer and Heilig, 1997; source: Wallace, 2000).

Africa and the Middle East possess the most critical values of annual renewable freshwater resources. In fact, according to Wallace (2000), populations in the North-Africa belt (from Morocco to Egypt, including Sudan) had less than 1,000 m³ of water

per hectare per year in 2000, whereas populations in the Middle East and Southern Africa had between 1,000 to 2,000 m³/ha per year. The estimates made by Wallace for North, East, and South Africa, and the Middle East, determines that the available water per capita will drop below 1,000 m³ per capita per year before 2050. Moreover, as estimated by Roetter and Van Keulen (2008), the median population growth projection for 2025 is 7.8 billion, compared with the present 6.4 billion; the highest projection is 8.3 billion, while the lowest projected population is 7.3 billion. For the year 2050, the average projection is around 9 billion. In Asia, the population will grow by 650 million people between now and 2025, indicating an annual growth rate of approximately 1%. Therefore, it can be assumed from the growth rate that a higher food demand shall be expected in the future, which will have a direct effect on water usage in agriculture.

Rijsberman (2006) reports that the International Water Management Institute (IWMI) estimated that a 29% increase in the amount of irrigated land will be required by the year 2025 under a base scenario that included optimistic assumptions on productivity growth and efficiency. FAO (2002a, 2003b, 2003c) and Shiklomanov (1998) had comparable results. FAO (2000) estimated a 34% increase in irrigated area and a 12% increase in irrigation diversions. Shiklomanov (1998) projected a 27% increase in irrigated diversions.

A significant relationship between renewable water resources of a country and the capacity for food production is evident, especially for poor countries and those affected by water scarcity. For these countries, the regional water scarcity can be alleviated by importing certain commodities, especially food, as agricultural and livestock production, that consume great quantities of water (Allan, 1996). This theory is well known as the “virtual water” concept. Virtual water is defined as the volume of water consumption required to produce commodities traded to an importing or exporting nation (or any region, company, individual, etc.). Virtual water takes into account both blue and green water. Allan (1997) termed such food imports as “virtual water imports” due to the fact that they are equivalent to a transfer of water to an importing country. Hanasaki et al. (2010) showed that the global virtual water export of five crops (barley, maize, rice, soybean, and wheat) and three livestock products (beef, pork, and chicken) is 545 km³ yr⁻¹. Of the total virtual water exports, 61 km³ yr⁻¹ (11%) were blue water (i.e. irrigation water), and 26 km³ yr⁻¹ (5%) were nonrenewable and

nonlocal blue water. North and South America are the major regions from which virtual water export flows originate, while East Asia, Europe, Central America, North Africa, and West Asia are the major destinations for all water sources (Figure 8).

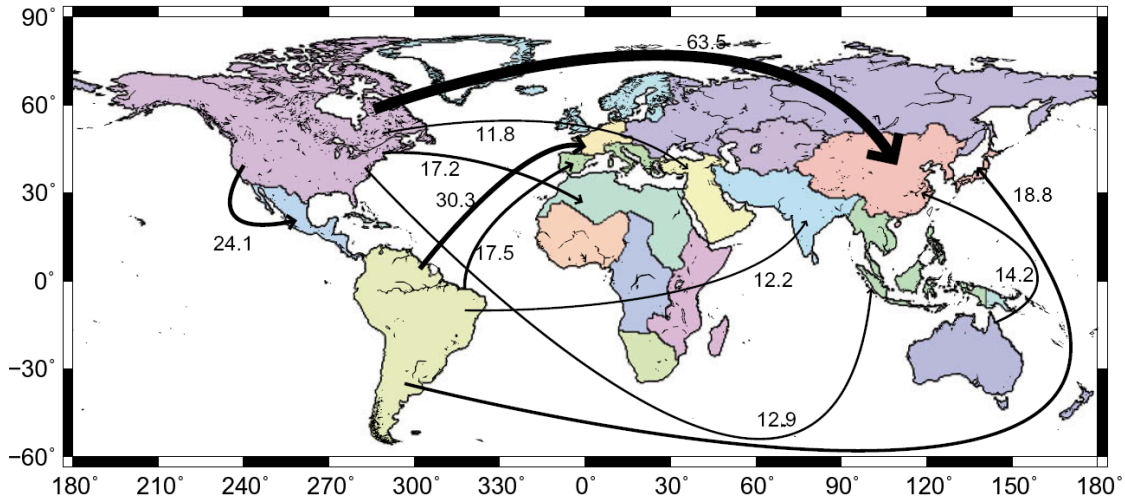


Figure 8. World map of virtual water exports, total virtual water exports (flows exceeding 10 km³ yr⁻¹ are shown), (Hanasaki et al., 2010).

Africa and Asia are considered water-scarce continents because of the high concentration of countries affected by this problem (Cosgrove and Rijsberman, 2000; Smith et al., 2000). Many countries in these two continents are net importers of cereal grains. In the late 1990s, the annual net cereal grains imported into the two continents amounted to over 110 million tons, absorbing all the surplus of the rest of the continents (FAO, 2002b).

Cereal imports have played a crucial role in compensating local water deficits. Yang et al. (2003) estimated the water resources threshold with respect to cereal imports for Africa and Asia. Below the threshold, the demand for cereal import increases exponentially with decreasing water resources. This means that in the next 30 years, many poor and populous countries will drop below the threshold due to their rapid population growth and the depletion of fossil groundwater.

During the past two decades, irrigated areas expanded relatively rapidly in various countries in Africa, including Egypt, Algeria, Libya, and Tunisia (Table 1). With the exception of Egypt, where irrigated croplands cover 100% of the total land, the irrigated areas range between 7 and 45% of the total cropland in the aforementioned countries.

Table 1. Water resources and changes in irrigated areas, 1980–1999.

	Algeria	Egypt	Israel	Libya	Morocco	Tunisia
<i>Water resources, m³/per capita, per year (1998)</i>						
Internal	460	43	289	100	1071	371
External	13	841	20	0	0	64
Total	473	884	309	100	1071	435
<i>Water withdrawal, m³/per capita, per year</i>						
	180 (1990)	921 (1993)	407 (1989)	880 (1994)	433 (1992)	376 (1990)
<i>Irrigated areas, 1000 ha</i>						
1980	253	2445	203	225	1217	243
1985	338	2497	233	300	1245	300
1990	384	2648	206	470	1258	300
1995	555	3283	199	470	1258	361
1999	560	3300	199	470	1305	380
Changes %	121.34	34.97	-1.97	108.89	7.23	56.38
<i>Irrigated area as % of total crop land</i>						
	7	100	45.5	22	13	7.8

Source: Yang and Zehnder (2002). Data for water resources are from WRI (2001). Data for irrigation are from FAO (2001). Data for the proportion of irrigated area in total cropland are from World Bank (2000).

Yang and Zehnder (2002) observe that in 1998–99, cereal imports accounted for 52% of the total supply in the six countries combined. Under the baseline scenario, cereal demand in the six countries as a whole will increase above the 1998-99 level by 22% and 38% in 2010 and 2020, respectively. Under a scenario of increased consumption, cereal demand will rise above the 1998-99 level by 26% in 2010 and 47% in 2020. This means that the international trade in food grains and other agricultural products has played and will continue to play a critical role in water-scarce countries. Therefore, it will not be easy for some countries to meet food demands without importing.

The import of virtual water poses various questions in relation to the concept of “Food Security”. The World Food Summit of 1996 established that “Food security exists when all people, at all times, have physical and economic access to sufficient, safe, and nutritious food to meet their dietary needs and food preferences for an active and healthy life”. Three core concepts are at the base of the food security theory:

- 1) food availability: the amount of food constantly available;
- 2) food access: the ability to have sufficient resources to obtain appropriate foods for a healthy diet;
- 3) food utilization: it means using appropriate products based on basic knowledge of nutrition, water, and adequate sanitary conditions.

Nevertheless, the necessity of other countries to meet the food requirements of their populations creates uncertainties mostly related to the policies of importing

countries. In fact, water scarcity related to the food import demand can have an adverse impact on the stability of the world food economy. On the other hand, “virtual water” food imports are a valid way to create economic growth in water-scarce countries, and to maximize the value of their limited water supplies.

The overall conclusion is that a large share of the world’s population, up to two-thirds, will be affected by water scarcity over the next several decades (Shiklomanov, 1991; Raskin et al., 1997; Seckler et al., 1998; Alcamo et al., 1997, 2000; Vörösmarty et al., 2000; Wallace, 2000; Wallace and Gregory, 2002).

As pointed out by Qadir et al. (2003), the sustainable management of available water resources at the global, regional, and site-specific level is necessary. The first step to achieve this objective is to compute how much water is needed by crops in regards to climate conditions. Once the crop water requirement is assessed, the application of some easy water management strategies may be valuable for the sustainable utilization of water resources. Scheduling irrigation management strategies, modifying agricultural practices, and improving irrigation systems are just a few practices that can lead to a more efficient agricultural water management. Moreover, the implementation of policy measures, followed by the establishment of farmer advisory schemes, could be the key for a future agricultural and economic growth in countries affected by water shortages.

1. MEDITERRANEAN WATER SCARCITY

In the Mediterranean basin, an increase in temperature (1.5 to 3.6°C by the 2050s) and a decreases in precipitation (about 10 to 20%) are expected, based on the climate change projections estimated by the global climate model driven by socio-economic patterns (IPCC, 2001; Iglesias et al. 2000). The combined effects of warmer temperatures and reduced mean summer precipitation would enhance the occurrence of heat waves and droughts. Drought events in the Mediterranean basin have been already observed, and they have occurred more frequently since 1970 (Vogt and Somma, 2000; Wilhite and Vanyarkho, 2000; Hisdal et al., 2001; Iglesias and Moneo, 2005; Iglesias et al., 2007). More water will be required per unit area under drier conditions, and peak irrigation demands are also predicted to rise due to the increased severity of heat waves (Parry, 2000).

Irrigation is important for crop production in many Mediterranean countries because of the high evapotranspiration and restricted rainfall. The demand of water for irrigation is projected to rise in a warmer climate, increasing the competition between the agricultural and urban sectors, as well as industrial users of water (Arnell, 1999).

1.1. Climate change impact on Mediterranean irrigation requirement

In the Mediterranean countries, water is not simply important, but absolutely essential (Figure 9). Water availability is at present the most significant limiting factor for crop yields in the Mediterranean countries, due to pronounced seasonal precipitation gradients, generally poor soils with low water holding capacities, and extensive water use for irrigation in competition with other sectors of the economy (Baric and Gasparovic, 1992; Lindh, 1992). In the estimations reported by FAO (1993), agriculture in the Mediterranean accounts for virtually all olive oil produced worldwide, 60% of wine production, 45% of grape production, 25% of dried nuts (mostly almonds, chestnuts, and walnuts), 20% of citrus production, and about 12% of total cereal.



Figure 9. Map of the Mediterranean basin countries (Correia, 1999).

Climatically, the Mediterranean region is characterized by mild temperatures, with winter-dominated rainfall, and dry summers (Wigley, 1992). Nevertheless, climatic conditions may vary significantly, despite some prevailing common characteristics (Correia, 1990, 1996). In fact, northern and northeastern countries

(Spain, France, Monaco, Italy, Former Yugoslavia, Albania, and Greece) are more temperate and humid than southern and southeastern ones (Turkey, Cyprus, Syria Lebanon, Israel, Egypt, Libya, Malta, Tunisia, Algeria, and Morocco). Southern regions are warmer and drier, with endemic water shortages due to low seasonal rainfall and high evapotranspiration rates (Rosenzweig and Tubiello, 1997). Climate change projections tend to exacerbate these differences. In the northern areas for instance, the benefits of the projected climate change will be limited, while the disadvantages will be predominant. Although the increased water use efficiency caused by higher CO₂ concentration will compensate for some of the negative effects of increasing water limitations and extreme weather events, lower harvestable yields, higher yield variability, and reduction in suitable areas of traditional crops could be expected (Maracchi et al., 2005). Moreover, limited moisture due to increasing temperatures and reduced summer rainfall may regionally generate productivity decline and reduction of suitable areas for traditional crops. The trends over the past 25 years in the Mediterranean basin illustrate that in the northern part, wheat yield has increased from 2.1 to 2.7 Mg ha⁻¹, while a reduction of the total cultivated area of wheat was observed (Olesen and Bindi, 2002).

Under the assumption that a global increase of temperatures is expected in the Mediterranean basin (Mannion, 1995), cereal crops requiring periods of vernalization, such as winter wheat, could be negatively affected and their productivity reduced (Pereira and De Melo-Abreu, 2009). On the other hand, olive and citrus production in warmer and drier climates could benefit from increased temperatures by extending their cultivation range northward (Morettini, 1972). Bindi et al. (1992), showed that the suitable area for olive production in the Mediterranean basin may increase with climate warming; moreover, if the current atmospheric CO₂ concentration is doubled, the suitable area for olive cultivation could be enlarged in France, Italy, Croatia, and Greece due to changes in temperature and precipitation patterns. Grapevines are another tree crop that require relatively high temperatures, and may be influenced positively by the increase of temperature. In any case, a balance between increases in temperature, water shortages, and extreme events is required to assess a positive or negative impact of climate change.

In the Mediterranean countries within Europe, the warming is projected to be greatest in summer (from June to August) (Giorgi et al., 2004; IPCC, 2007b). Drier climates may lead to greater irrigation requirements and more frequent irrigation events for those crops with primary growth during the summer season.

In the Mediterranean basin, irrigated agriculture has grown more than ten-fold in the north part since 1961, but only by 40 % in the south, where crops and soils now largely exist in a regime of marginal water supply (FAO, 1993). Water withdrawal by the agricultural sector range from 12% in Yugoslavia to 92% in Morocco (Table 2).

Table 2. Freshwater resources and withdrawals in the Mediterranean countries (*Source: Correia, 1999*).

Country	Population (millions)	Annual Internal Renewable Resources		Annual River Flows		Annual Total Resources		Annual Withdrawals			Percentage of Sectoral Withdrawal		
		Total (km ³)	Per Capita (10 ³ m ³)	From Other Countries (km ³)	To Other Countries (km ³)	Per Capita (10 ³ m ³)	% of External Resources	Total (km ³)	% of Water Resources	m ³ per Capita	Domes- tic	Indus- try	Agricul- ture
Portugal	10.29	34.00	3.45	31.60	-	6.38	46	10.50	16	1,075	15	37	48
Spain	39.19	110.30	2.82	1.00	17.00	2.84	1	45.85	41	1,188	12	26	62
France	56.14	170.00	2.97	15.00	20.50	3.30	10	43.67	24	778	16	69	15
Italy	57.06	179.40	3.10	7.60	0.00	3.28	5	56.20	30	996	14	27	59
Yugoslavia	23.81	150.00	6.26	115.00	200.00	11.13	44	8.77	3	393	16	72	12
Albania	3.25	10.00	3.02	11.30	-	6.55	54	0.20	1	94	6	18	76
Greece	10.05	45.15	4.43	13.50	3.00	5.84	24	6.95	12	721	8	29	63
Turkey	55.87	186.10	3.19	7.00	69.00	3.46	8	23.75	12	433	24	19	57
Cyprus	0.70	0.90	1.28	0.00	0.00	1.28	0	0.54	60	807	7	2	91
Syria	12.53	7.60	0.57	27.90	30.00	2.83	80	3.34	9	435	7	10	83
Lebanon	2.70	4.80	1.69	0.00	0.86	1.69	0	0.75	16	271	11	4	85
Jordan	4.01	1.02	0.24	0.40	-	0.35	31	0.45	32	173	29	6	65
Israel	4.60	1.70	0.33	0.45	0.00	0.47	30	1.85	86	410	16	5	79
Egypt	52.43	2.60	0.05	55.50	0.00	1.11	96	56.40	97	1,028	7	5	88
Libya	4.55	0.70	0.14	0.00	0.00	0.14	0	2.62	374	692	15	10	75
Malta	0.35	0.03	0.07	0.00	0.00	0.07	0	0.02	92	68	76	8	16
Tunisia	8.18	3.75	0.45	0.60	0.00	0.53	15	2.30	53	317	13	7	80
Algeria	24.96	18.90	0.72	0.20	0.70	0.77	6	3.00	16	160	22	4	74
Morocco	25.06	30.00	1.14	0.00	0.30	1.14	0	10.85	36	412	6	3	92

Egypt is particularly affected by climate changes, and the water withdrawal for the agricultural sector is round 88%. A simulation study by El-Shaer et al. (1997), observed the decrease in potential yield and water use efficiency in wheat and maize in the main agricultural regions of Egypt in relation with possible future climatic variation, even when the beneficial effects of increased CO₂ were taken into account. Eid (1994) suggested that, despite CO₂ enhancement of crop growth, climate change would severely reduce Egyptian maize and wheat yields.

The water deficit is also acute in the Bekaa Valley (Libanon), where potential evapotranspiration exceeds 70% of precipitation (NCRS 1998). Although precipitation was not predicted to decrease, the increase in temperature of 0.6 – 2.1°C would impact the water balance and reduce the available resources. In the Bekaa Valley, a 15%

decrease in available water and 6% increase in irrigation water demand were projected by the year 2020, under a dry and hot scenario (Bou-Zeid and El-Fadel, 2002).

In Spain, a reduction of 17% in nationally available water resources has been predicted (Iglesias et al., 2005). The predicted changes are even greater in southern Spain. Some authors suggest a reduction in precipitation up to 34% for the Guadalquivir basin (Ayala, 2002). Rodríguez Díaz et al. (2007) showed a typical increase between 15 and 20% in seasonal irrigation demand by the 2050s in the Guadalquivir river basin; moreover, the irrigation seasons are also predicted to be longer than at present due to the lower rainfall from April to June. In southern Portugal and southern Spain, the yields are predicted to decrease by up to 3 Mg ha⁻¹ (Maracchi et al., 2005).

Tubiello et al. (2000) showed that 60-90% more irrigation water was required under climate change to keep grain yields of irrigated maize and soybeans in Modena-Italy at current levels.

Moreover, in many countries of the Mediterranean region, the quantity of water that is available (expressed in terms of mean annual volume per capita) is considered an issue, in addition to the uneven distribution of these resources in time and space (Correia, 1999). Taking into account that most irrigation water is applied during the summer season in Mediterranean countries, which also coincides with the main tourism season, a consequential competition between these two sectors is expected. Furthermore, climate change impacts on water pose questions not only about the amount of future water reduction, but also on water quality. In fact, excessive abstraction from coastal aquifers can cause the intrusion of saltwater, diminishing the quality of the groundwater and preventing its subsequent use (EEA, 2009).

1.2. The Italian water demand

Water abstraction in Europe varies by country and sector (Figure 10). In the Nordic countries, the water usages are mostly related to the urban and industrial sectors. The major water usages in Central Europe are for the urban and energy sectors. The most important usage for southern European countries is instead observed in the agricultural sector. In general the European agricultural water consumption is around 24%, mainly distributed in Italy, Spain, Portugal and France (Figure 11).

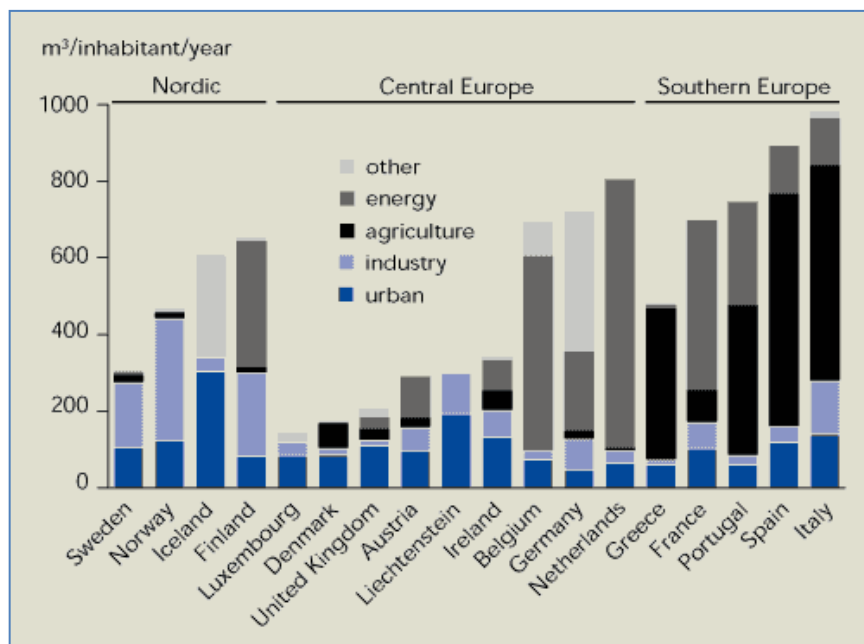


Figure 10. Total water abstraction in European countries by major uses (EEA, 2000).

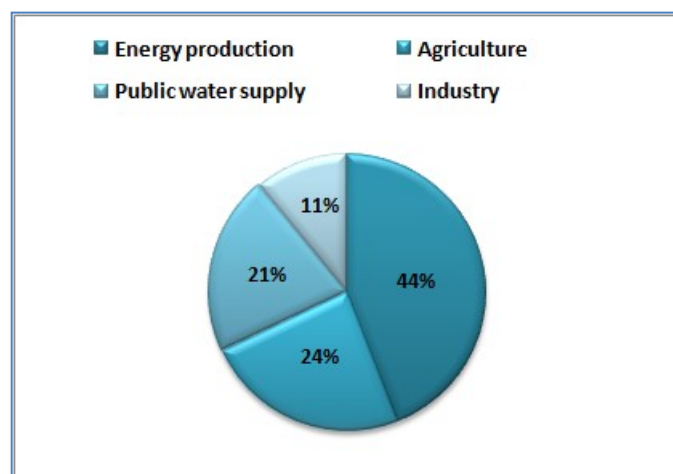


Figure 11. Water use in Europe countries by sector (EEA, 2009).

Water resources are not uniformly distributed over the Italian territory (Figure 12). The northern region contains 59.1% of the potentially usable water resources, whereas the rest of the country accounts for 40.9%.

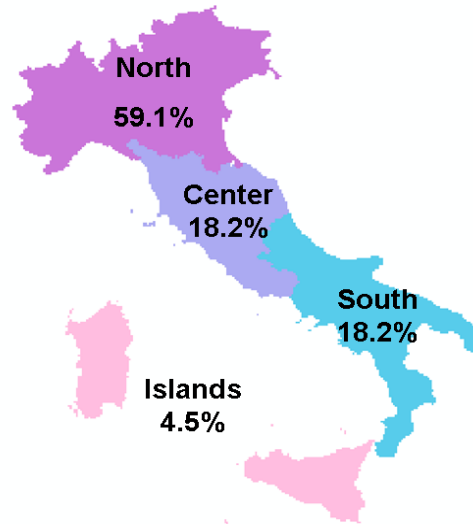


Figure 12. Regional distribution of potentially usable water resources in Italy as a percentage of the total resource (Source: IRSA CNR, 1999).

There are three main rivers in Italy: Po, Arno and Tevere. A study conducted by Legambiente in 2008 shows the water consumption for sector for each river. In the Po river (located in northern Italy), 95% of superficial water is used for irrigation, 3% for domestic purposes, and 2% for industry. Groundwater withdrawal is 47, 33 and 20% for irrigation, domestic usages, and industry respectively. Even though almost all the superficial water resources are used by the agricultural sector, an important percentage of water comes from the ground water resource.

In the Arno river (center of Italy), 63% of superficial water is needed for the public water supply, 19% for aquaculture, 17% for irrigation, and only 1% for the industry sector.

In the Tevere river (center of Italy), considering both water sources together, 37% of water is used for the irrigation supply, 34% for aquaculture, 22% for industry, and 15% for the public water supply.

In Italy, irrigated agriculture contributes more than 50% of the total agricultural production, and more than 60% of the total value of the agricultural products (OECD, 2006). However, the irrigated area encompasses only 21% of total agricultural land in

Italy (EEA, 2009). Northern Italy accounts for the maximum water usages for irrigation (67%), while the needs of the central and southern parts are 5 and 28% respectively (IRSA CNR, 1999). Italy ranks third out of the European countries for water use in the agricultural sector, preceded by Greece and Spain, with 80% and 72% respectively (Legambiente, 2008). Rivers are the main sources of irrigation water (67%), followed by groundwater from wells (27%), and reservoirs (6%) (Todorovic et al., 2007). In southern regions of Italy (Campania, Puglia, Sicily and Sardinia), 80% of irrigation water is drawn from aquifers, causing serious overexploitation problems (Venezian Scarascia et al., 2006).

In an analysis developed by the National Institute of Statistics (Istat) in 2005, the ratio between irrigated area (2.6 million hectares) and irrigable area (2.6 million hectares) in Italy was 65.8% (Table 3).

Table 3. Irrigated and irrigable area by region in Italy (Istat, 2005).

Region	Effectively irrigated cropland (ha)	Potentially irrigable cropland (ha)	Irrigated/Irrigable (%)
Piedmont	379,010	459,495	82.5
Valle D'Aosta	17,219	22,582	76.2
Lombardy	588,752	707,192	83.2
Liguria	4,169	7,722	54
Trentino-Alto Adige	57,044	63,920	89.2
Veneto	275,178	475,284	57.9
Friuli-Venezia Giulia	70,997	94,944	74.8
Emilia Romagna	267,611	556,567	48.1
Tuscany	51,072	130,566	39.1
Umbria	28,699	56,327	50.9
Marches	26,121	48,438	53.9
Lazio	87,337	154,396	56.6
Abruzzo	37,490	56,376	66.5
Molise	12,155	19,468	62.5
Campania	93,743	124,392	75.4
Apulia	236,172	361,240	65.4
Basilicata	47,287	81,450	58.1
Calabria	81,635	119,911	68.1
Sicily	179,869	254,974	70.5
Sardinia	71,849	177,412	40.5
Total	2,613,409	3,972,656	65.8

Sardinia and Tuscany maintain the lowest ratios, where only 40.5 and 39.1% of the total irrigable area was irrigated respectively.

Regions in the northern part of Italy (Piedmont, Lombardy, Veneto, Emilia Romagna, Trentino Alto Adige) have the highest percentages. Those regions are

situated in the Po plain, the largest plain in Italy, and the most profitable area for the agriculture sector with a high irrigation demand (Figure 13).

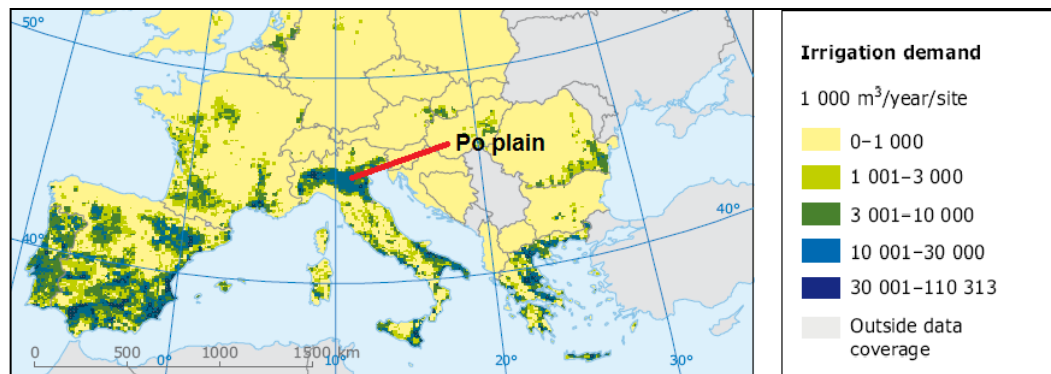


Figure 13. Average irrigation demand per site (10 x 10 km cell) in the south Europe (1,000 m³ per year and site over a simulation period 1995–2002). Source: EEA, 2009.

In the Po plain, tree crops, vines, and fruit trees in particular, account for 20% of the irrigated land (Venezian Scarascia et al., 2006). Fruit tree crops are irrigated almost completely in Trentino Alto Adige (93%), while the percentage is lower in other regions: 72% in Veneto, Friuli Venezia Giulia, and Basilicata; and 61% in Emilia Romagna (Istat, 2002). Data from the agricultural census (2000) shows also that in Trentino Alto Adige, vineyards are one of the main irrigated crops (67%).

Figure 14 gives an idea of the irrigated agriculture in Italy. Citrus crops represent the maximum value (86%). Vegetable crops, in general, and potatoes also maintain high values, 70 and 67% respectively, while cereals have a low value because they are mostly cultivated in rain-fed conditions.

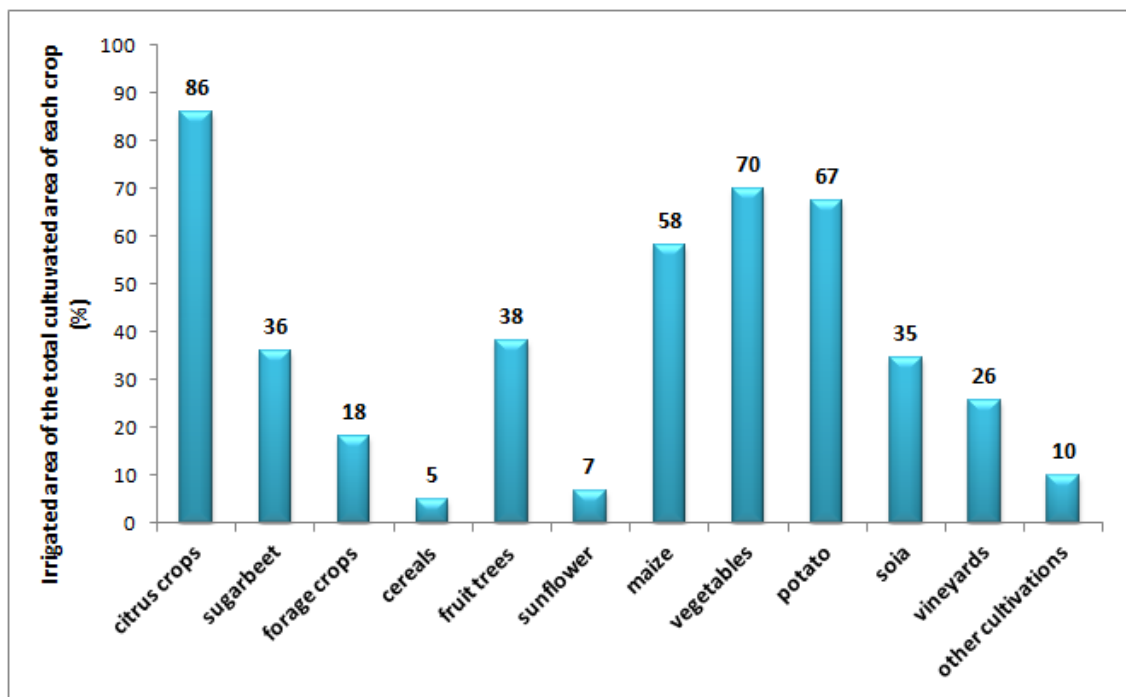


Figure 14. Irrigated crops in Italy (as percentage of total cultivated area of each crop) according to the census in 2000 (Source: Istat, 2002)

The census data of 2000 also presents an idea of the use of irrigation systems. Sprinklers are the predominant system used (42%), followed by furrow irrigation (34%), despite the trend over the last decade where the use of drip irrigation has become more important than furrow systems (Figure 15).

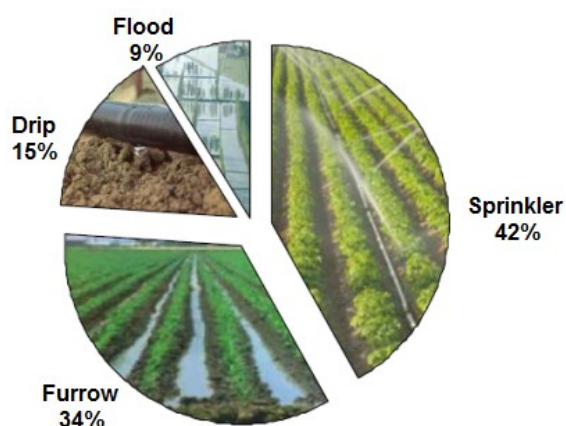


Figure 15. Use of irrigation systems in Italy (Istat, 2002).

Flood irrigation is used in Piedmont and Lombardy for rice production (Figure 16). In these two regions, furrow irrigation is commonly used; while in Veneto and Emilia Romagna, sprinklers are preferred to others system. The utilization of drip systems is particularly developed in southern regions (Apulia and Sicily). Taking into consideration the provisional data from the last Italian agricultural census (2010) and the prior census (2000), the total planted hectares decreased by 2.7% in Italy from 2000 to 2010. In fact, in 2010 the planted area of potatoes, sugar beets, and energy crops diminished by 31, 74 and 40% respectively since 2000. In contrast, forage crop data shows a high increase in planted area since 2000 (214%).

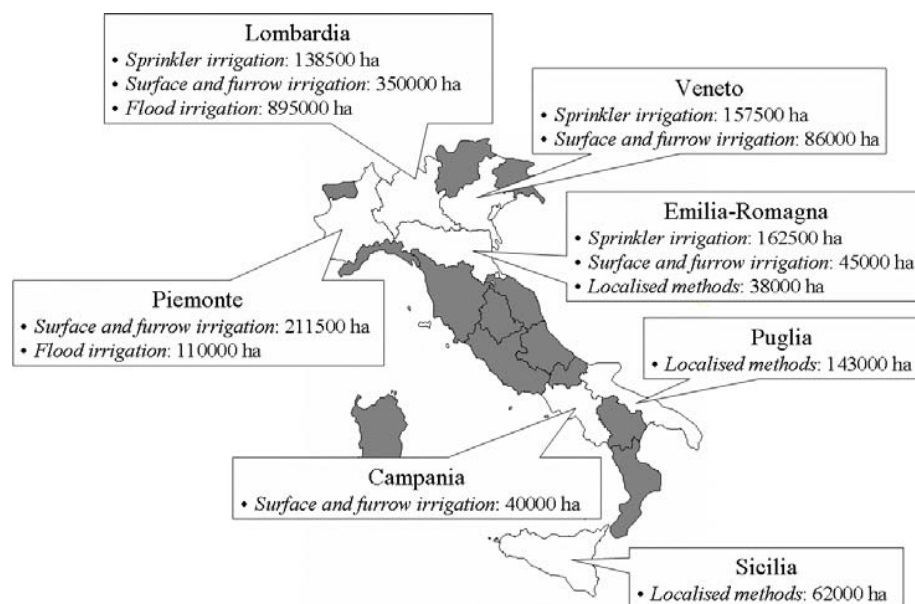


Figure 16. The most utilized irrigation methods in the Italian regions with the highest irrigation surfaces (Todorovic et al., 2007).

1.3. Agricultural water use in Sardinia

The regional policy planning in Sardinia allocates a large portion of the water resources (about 70% of the available freshwater) to satisfy agricultural water requirements (Regione Sardegna, 2006). This is equivalent to have 792 Mm³ of freshwater from an overall potential water use in Sardinia of 1,115 million. More specifically, the potential requirements for existing equipped irrigation area is 643 million of m³ per year, while an additional 149 Mm³ per year are estimated as the requirements of potential irrigation installations in the near future.

Irrigation in Sardinia covers a total potential irrigable area equal to 185,916 ha, even if only about 49% of the potentially irrigable cropland is effectively irrigated, equivalent to 53,108 ha (Regione Sardegna, 2010). The irrigation is managed by nine consortia (Consorzio di Bonifica) distributed where the topography and soil conditions are favorable for irrigated cultivations (Figure 17).

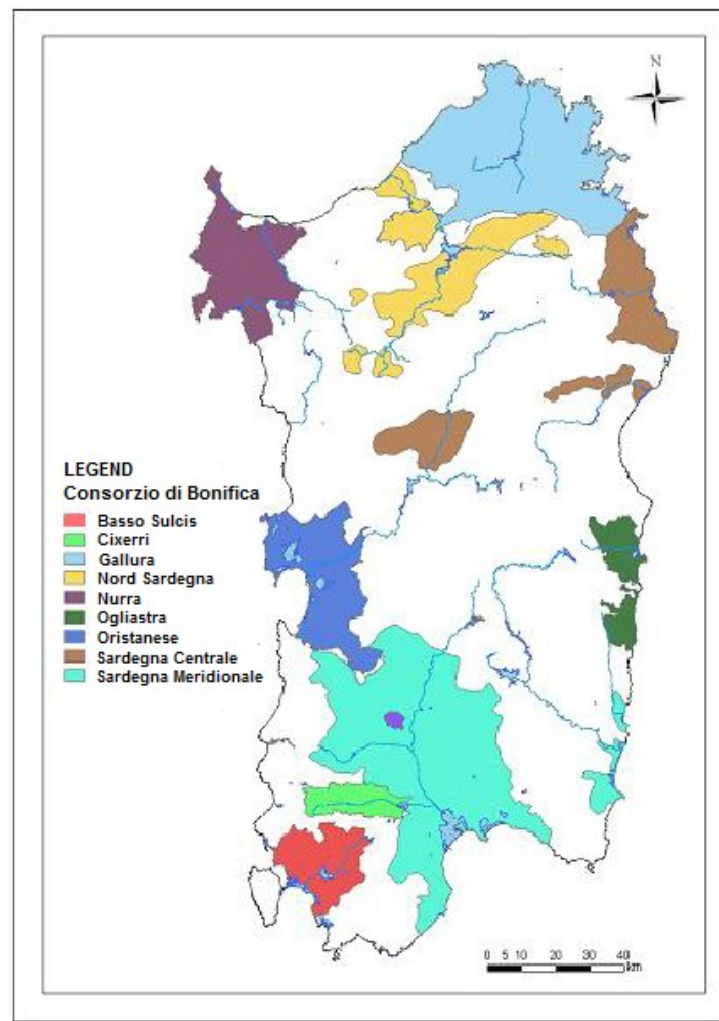


Figure 17. Boundaries of the nine *Consorzio di Bonifica* of Sardinia (Regione Sardegna, 2010).

Crop irrigation requirements on irrigated area are estimated to be equal to 4,766 m³ per ha, while water delivery losses account for an additional 27% of the total (Regione Sardegna, 2006). Therefore, the estimated annual irrigation consumption, considering water losses due to the inefficiency of the delivery and irrigation system, is

around 6,500 m³ per ha. The annual irrigation consumption, related to the areas effectively irrigated, is estimated to be about 350 Mm³.

Currently, the most recent account (2010) of resources available for allocation to different sectors (civil, industrial, agricultural) is based on the water reserves accumulated in the reservoirs of the island, as reported in Table 4.

Table 4. Allocation of available water resources for different sectors (Regione Sardegna, 2010).

Sector	Volume (Mm³)
Agriculture	
Consorzio di Bonifica Basso Sulcis	9.0
Consorzio di Bonifica Cixerri	11.0
Consorzio di Bonifica Nurra	31.0
Consorzio di Bonifica Nord Sardegna	22.0
Consorzio di Bonifica Gallura	24.0
Consorzio di Bonifica Sardegna Centrale	42.5
Consorzio di Bonifica Sardegna Meridionale	100.0
Consorzio di Bonifica Ogliastra	8.5
Consorzio di Bonifica Oristanese	140.0
Others	5.0
Total for agricultural use	393.0
Civil use	228.0
Industrial use	32.0
TOTAL	653.0

The Sardinian water resources are divided into several categories (Figure 18):

- streams, natural and/or artificial;
- lakes, natural and/or artificial;
- transitional water;
- coastal-marine water;
- ground water.

Sardinia contains a total of 39 streams. The main rivers are: the Flumendosa, the Coghinas, the Cedrino, the Liscia, and the Tirso river (Table 5).

Table 5. The main watercourses in Sardinia (Regione Sardegna, 2010).

River	Length (km)	Watershed (Km²)
Tirso	153.60	3,365.78
Coghinas	64.40	2,551.61
Flumendosa	147.82	1,841.77
Flumini Mannu	95.77	1,779.46
Cedrino	77.18	1,075.90

The other streams are characterized by a torrential regime, due basically to rainfall and the close proximity of the mountains to the coast. Rivers have mainly steep slopes in most of their path, and they are subject to major flood events, particularly during late autumn and summer, when the stream can remain dry for consecutive months.

All lakes in the island (32), except for Baratz, are artificial; they are made through barrages of numerous rivers and represent the main water resources of the island.

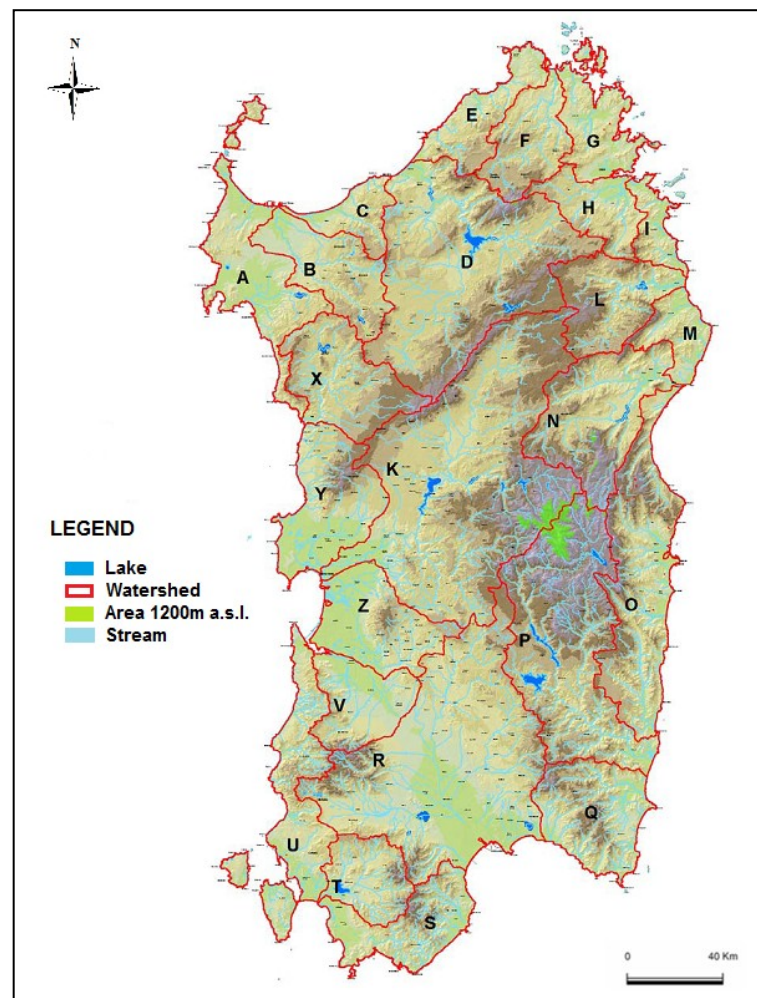


Figure 18. Hydrographical map of Sardinia (Regione Sardegna, 2006).

The regional agricultural sector is characterized by an extensive presence of arable crops and fodder, which cover 51.6% of the actually irrigated area (Figure 19).

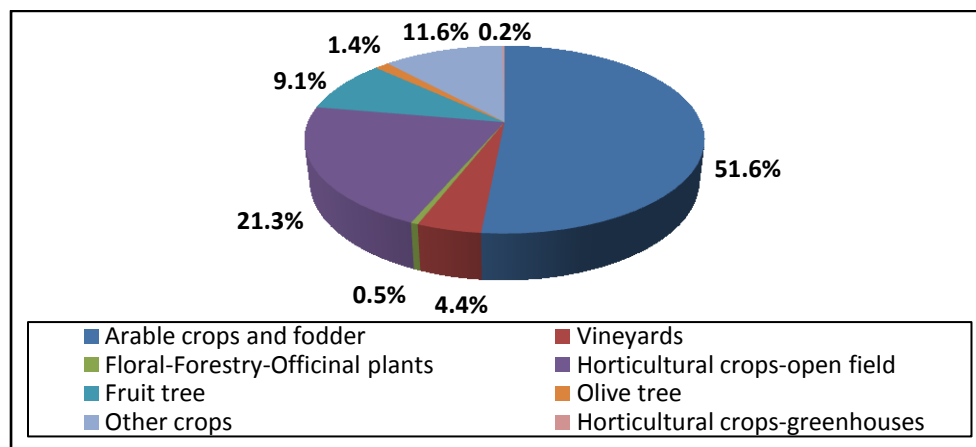


Figure 19. Percentage distribution of irrigated surfaces within the nine regional Consorzi di Bonifica (2005-2007) (source: Regione Sardegna, 2010).

In particular, Sardinia contains a large extension of land with maize cultivation (which is the most widespread crop with 5,507 ha), alfalfa, and grass crops (Istat, 2007).

21.3% of the irrigable land is covered by horticultural crops in open fields. Among the horticultural crops, artichokes are the most representative (44%) of the total area (Istat, 2007).

Fruit tree crops (particularly citrus and peach) represent 9.1% of the irrigated area. The irrigated area planted with vineyards amounts to 4.4%. Less importance is given to olive tree irrigation; the relative percentage of irrigated land is only 1.4% because this type of cultivation is mainly conducted under rain-fed conditions. However, grapevines and olives are considered two of the most economically important cultivations in Sardinia. Even if only 2,314 of the total 18,346 hectares (12.6%) of vineyards are provided by irrigation system (Istat, 2010), viticulture represents a strategic economical sector in Sardinia (Nieddu, 2006).

Olive cultivation is mainly for oil production, and 1,891 of the total 31,212 hectares (6%) are irrigated (Istat, 2010). It is one of the most characteristic crops in Sardinia, considering that around 93% of the municipalities have invested in olive orchards (Idda et al., 2004).

Figure 20 shows the percentages of irrigated area out of the total cultivated area for each crop, or group of crops, in Sardinia for the periods 1982, 1990, 2000 (Istat, 2002).

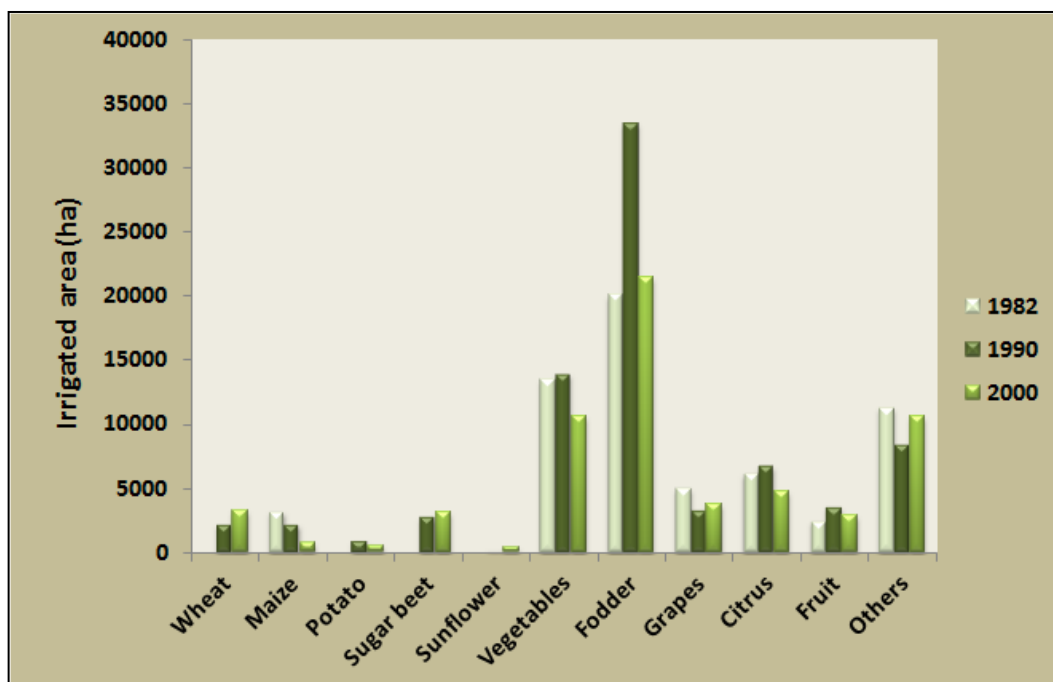


Figure 20. Percentages of irrigated areas out of the total cultivated area for each crop, or group of crops, in Sardinia for the periods 1982, 1990, 2000 (Istat, 2002).

The decrease of irrigated crop percentages was often due to repetitions of several dry years, where the poor precipitation led farmers to reduce the area planted (CRAS, 2006). On the other hand, the regional funding has been the reason for the increasing planted area for crops, such as sugar beets during the 1990s.

The primary irrigation system used in Sardinia is sprinkler irrigation, mainly for forage crops and cereals. Sprinkler systems are used in more than half of the irrigated area and in approximately 30% of the farms (Madau, 2009). The drip irrigation system is used primarily in fruit and horticultural crops (Regione Sardegna, 2010).

In a study conducted by Madau (2009) on the agricultural census data, important changes in the utilization of irrigation equipment during the last ten years have been observed. In fact, in the last years, the spread of sprinkler systems has conspicuously declined. In 2000, the irrigated area equipped with sprinkler systems amounted to more than 62% of the total irrigated area, compared with 52% in 2005 (Figure 21).

Over the past five years, farms that use drip systems have increased from about 28% to over 35%. In 2005, the area irrigated with low volume/drip systems amounted to 31% of the total irrigated area, versus the 19% recorded in 2000.

About 32% of the Sardinian farms adopted furrow irrigation methods, even if the adoption of this method is less than 9% of the regional irrigated area.

Finally, flood irrigation represents the lowest percentage because this method is used only for rice cultivation.

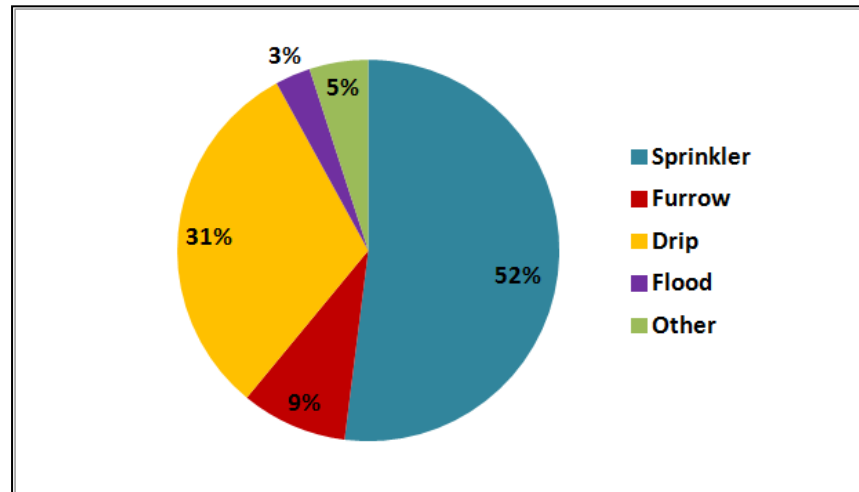


Figure 21. Irrigated area percentage by different irrigation systems in Sardinia in 2005 (data from Madau, 2009).

2. CROP WATER REQUIREMENT

2.1. The soil water balance

The soil water balance is the key concept in the management of water resources, especially for irrigation scheduling. It indicates the variation in the water content of the soil (ΔSW), as a consequence of water input and output (Figure 22), and it is expressed in the following equation (mm):

$$I + P - ET - RO - DP + CR \pm \Delta SF \pm \Delta SW = 0 \quad (4)$$

where I is the amount of water added by irrigation; P is the rainfall on a field; both I and P are considered water inputs, and they might be lost by surface runoff (RO) and deep percolation (DP). Another water input is capillary rise (CR) from a shallow region of the soil towards the root zone. Subsurface inflow (SF_{in}) or outflow (SF_{out}) is a horizontal transfer of water (ΔSF). Some fluxes such as ΔSF , DP , and CR are difficult to assess, and cannot be considered for short time periods (Allen et al., 1998). Evapotranspiration (ET) is the sum of the evaporation and the transpiration processes within the plant and

soil systems. It is considered a water loss from the root zone. The computation of all these fluxes may permit the analysis of the ΔSW over a given time period.

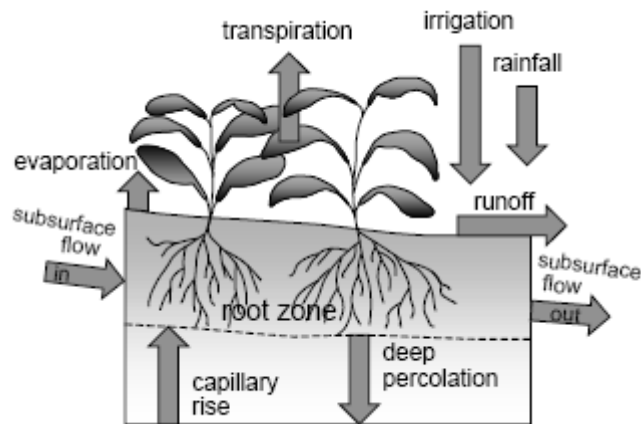


Figure 22. Chart of the soil water balance of the root zone (source: Allen et al., 1998).

Inorganic soil is composed of mixtures of sand, silt, and clay. The soil textural class is determined by the gravimetric percentage of these elements (Figure 23).

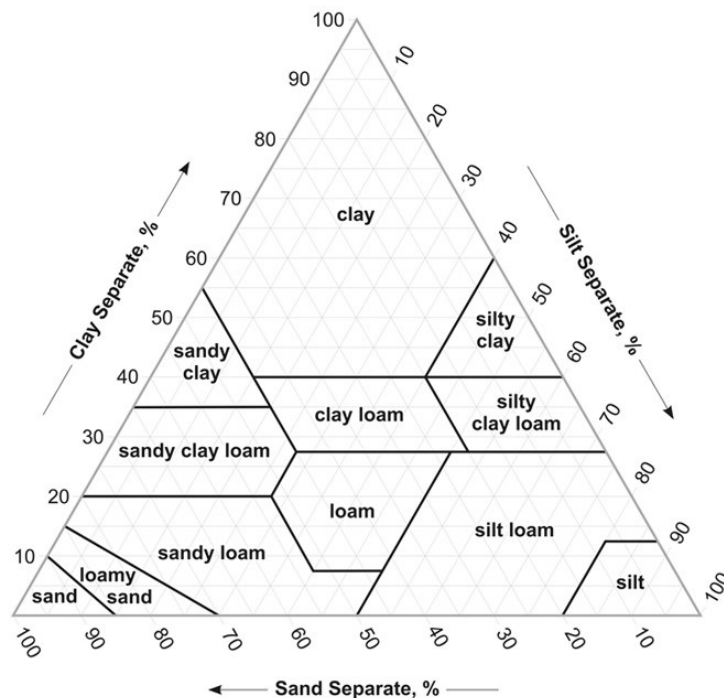


Figure 23. Soil textural classes based on the percentage of sand, silt, and clay (source: <http://soils.usda.gov>).

Some organic materials adhere to the solid particle composition, where air and water fill the pore spaces between the solid particles (Figure 24).

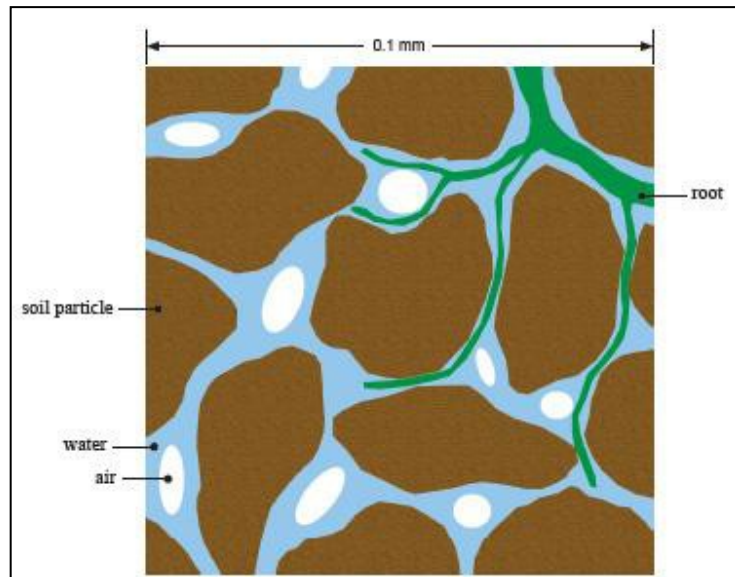


Figure 24. Unsaturated soil is composed of solid particles, organic material and pores. The pore space will contain air and water. (source: Bellingham, 2009).

The soil water system can be expressed as a volume of each single element (Jensen et al., 1990):

$$V = V_s + V_w + V_{av} \quad (5)$$

where V is the total volume of a soil unit, while V_s , V_w , and V_{av} represent solid, water, and air and vapor volume respectively.

The water content in the soil (θ) is expressed as the ratio of the volume of water to the total volume of the soil sample (m^3/m^3):

$$\theta = \frac{V_w}{V} \quad (6)$$

When water fills all the air pores after a heavy rainfall or irrigation, the soil enters saturation (Figure 25).

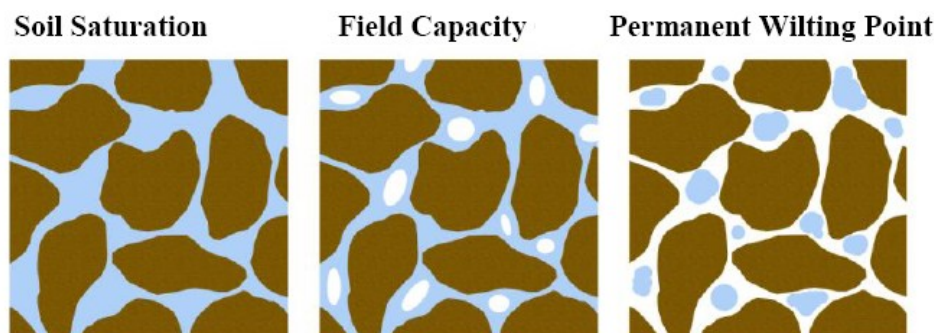


Figure 25. Graphic representation of soil saturation, field capacity and permanent wilting point (source: Bellingham, 2009).

The soil reaches the field capacity (θ_F) typically one or two days after saturation, when the excess water drains from the soil (Ratliff et al., 1983). The amount of water that could be stored in the soil depends on the percentages of the different solid particles. Field capacity is the water holding capacity of the soil (m of water per m of soil depth), where the value of θ_F depends on the considered soil.

As the soil dries, the water retention increases and it becomes more difficult for plant roots to extract water. The soil water retention curve describes the capability of soil to restrain water. Graphically, it represents the soil available water (%) on the y-axis, and the soil matric potential (- bars) on the x-axis (Figure 26).

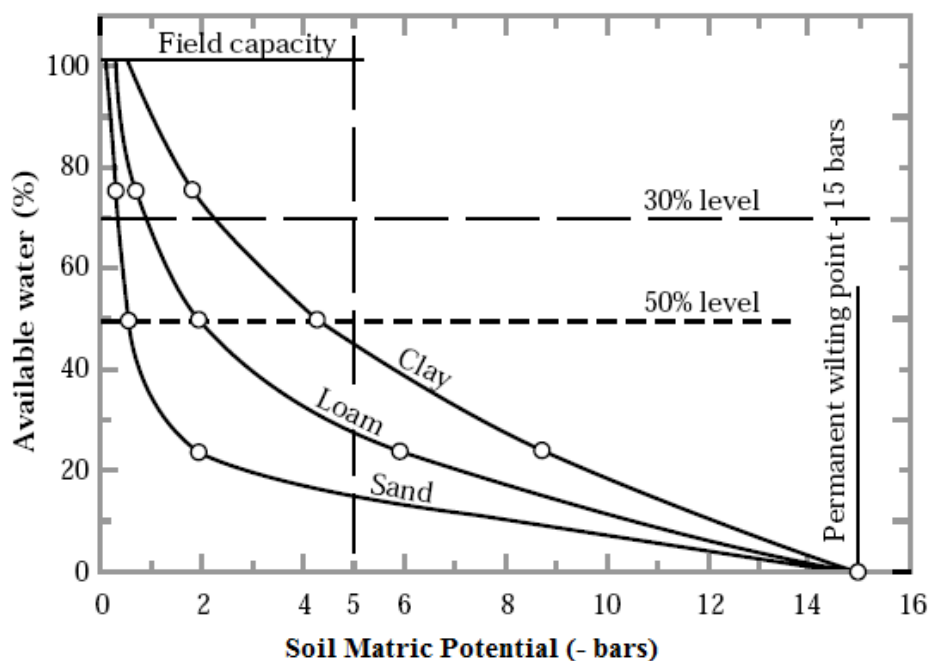


Figure 26. Hypothetical soil water retention curves for typical clay, loam, and sand soil (source: USDA, 1997).

The soil matric potential is a negative number, and a decrease in the value indicates a greater capability of the soil to retain water; this means that there is less water available to the plants roots. The soil water retention curve for three typical soil types is reported in Figure 26. At -15 bars (-1.5 MPa), the soil reaches the permanent wilting point (θ_p), which represents the water holding capacity at which plants will permanently wilt. However, the water content at wilting point depends on the ability of the plant to survive under stressed conditions, root density, the magnitude of the evaporative demand, and the soil retention curve (Jensen at al., 1990).

The water holding capacity of a soil between field capacity and permanent wilting point is defined as the available water holding capacity (θ_A).

The value of the water holding capacity is related to the type and moisture of the soil (Table 6).

Table 6. Water holding capacity (cm/cm depth of soil) at field capacity, permanent wilting point and available water of main texture groups (source: Blencowe et al.,1960).

Texture	Field Capacity	Wilting point	Available water
Coarse sand	0.6	0.2	0.4
Fine sand	1.0	0.4	0.6
Loamy sand	1.4	0.6	0.8
Sandy loam	2.0	0.8	1.2
Light sandy clay loam	2.3	1.0	1.3
Loam	2.7	1.2	1.5
Sandy clay loam	2.8	1.3	1.5
Clay loam	3.2	1.4	1.8
Clay	4.0	2.5	1.5
Self-mulching clay	4.5	2.5	2.0

The water content for each soil layer is a product of θ and the desired soil depth. Thus, the soil water content at field capacity (FC) is the amount of water at a specific depth at θ_F , while the water content at permanent wilting point (PWP) is the water content at a specified soil depth at θ_p .

Figure 27 explains the water content for different soil conditions. Field capacity and permanent wilting point are the maximum and minimum soil water contents (mm) respectively at a specific depth. The available water content (AW) corresponds to the amount of water that the soil stores between field capacity and permanent wilting point at a specified depth ($AW = FC - PWP$). The deficit in water content below FC is defined as the soil water depletion (SWD), while the soil water content (SWC) expresses

the amount of water stored at that depth ($SWC = FC - SWD$). When the soil water content reaches the yield threshold depletion (YTD), plants begin to incur water stress that may negatively influence the yield. Yield threshold (YT) is the water content at yield threshold depletion ($YT = FC - YTD$).

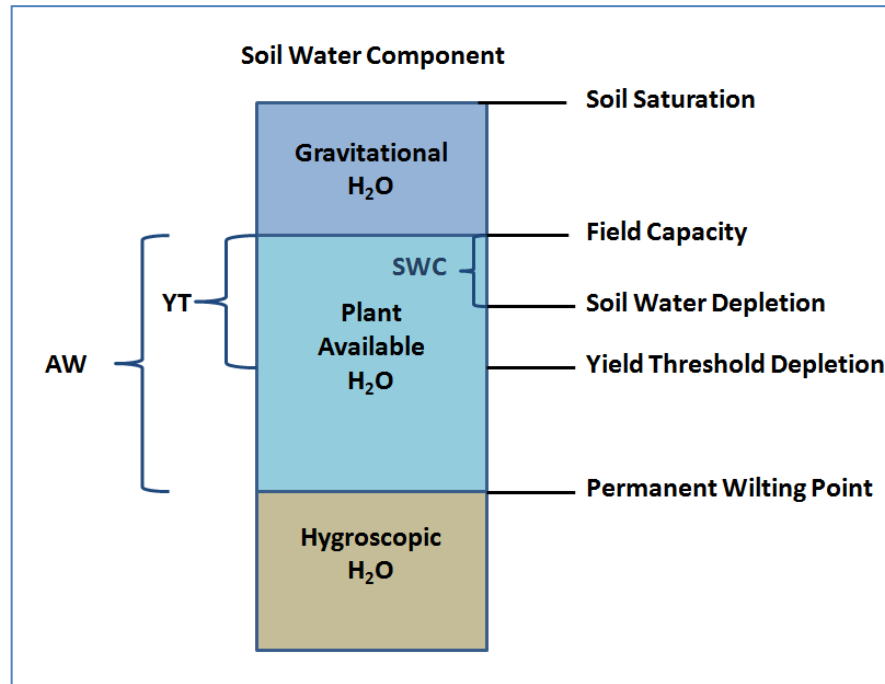


Figure 27. Chart of soil conditions and water content.

Most soils do not have uniform characteristics, and the AW varies with respect to the considered layer. In this case, the plant available water (PAW) represents the water contain at root depth as a sum of AW of each layer:

$$PAW = \sum_{i=1}^n AW \quad (7)$$

where AW is the amount of water stored at the considered layer ($i=1, 2, \dots, n$).

The percentage of PAW that corresponds to the YTD is called the allowable depletion (AD). Generally, AD is about 50% of PAW or $\frac{1}{4}$ of FC within the effective rooting zone for many soils. Therefore, it is possible to compute the YTD as:

$$YTD = PAW \times AD \quad (8)$$

Knowing the *YTD* is the first step to determining the management allowable depletion (*MAD*). The concept of *MAD* (Merriam, 1966), is used to assess irrigation scheduling and avoid plant water stress. The *MAD* is defined as the amount of water that can be depleted between irrigation events without incurring serious water stress.

Ideally, the *MAD* should be less than or at least equal to *YTD*. However, it could be greater than *YTD* depending on the considered crop, its capability to tolerate water stress, roots density and roots depth, and growth period. In fact, with respect to the crop growth, the root system develops deeper with increased *PAW* and *YTD*.

When the *SWD* is expected to exceed the *MAD* (or *YTD*, if *MAD* is equal to *YTD*), the crop requires a certain level of irrigation, the net amount (*NA*), to return the *SWC* to *FC*. The *MAD* is the net amount that needs to be replaced, and it is explained as the product of the gross application (*GA*) and the application efficiency (*AE*), (USDA, 1997):

$$NA = GA \times AE \quad (9)$$

Application efficiency is the ratio of the average depth infiltrated by irrigation water and stored into the plant root zone for use in evapotranspiration. The application efficiency is expressed as a percentage. The gross application is the amount of water that must be applied at each irrigation event to assure that enough water enters the soil and is stored within the plant root zone in order to meet crop needs. *GA* is based on the application rate and the runtime.

Thus, the quantity of water and the frequency of applications depend on the soil *AW* in the plant root zone, the crop grown and stage of growth, the rate of evapotranspiration of the crop, soil *MAD* level, and effective rainfall (R_e). Effective rainfall is a natural water input of the soil water balance, and it is the part of the total rainfall that replenishes the *SWD*. Rainfall lost by runoff or drainage from the soil is not considered R_e . The intensity, duration, and amount of rainfall, as well as the soil water capacity and soil surface conditions, determine the depth of the R_e . According to Snyder et al. (2012), effective rainfall can assume two possible outcomes:

$$R_e = P \quad \text{if } P < SWD \quad (10)$$

if the recorded rainfall is less than the *SWD*, then R_e is considered equal to precipitation;

$$R_e = SWD \quad \text{if } P \geq SWD \quad (11)$$

if the recorded rainfall is more than the SWD , then the effective rainfall equals the SWD .

These relationships mean that if the $R_e = P$, the FC is not achieved; therefore, an irrigation event is necessary to raise the SWD to the FC . Therefore, R_e is a very important parameter for the computation of the soil water balance, and an accurate estimation in comparison to the crop evapotranspiration (ET_c) is critical to determine an optimal irrigation scheduling.

2.2. Methods to evaluate evapotranspiration

As previously mentioned, crop evapotranspiration is one of the outputs of the soil water balance. ET_c , under standard conditions, refers to the evaporative demand from crops that are grown in large fields under optimum soil water conditions, in addition to excellent management and environmental conditions, and achieve full production under the given climatic conditions (Allen et al., 1998). ET_c encompasses the total water used by a specific crop; it includes the direct evaporation from plant leaves and the soil surface, as well as transpiration. ET_c is influenced by several major factors:

- plant temperature;
- ambient air temperature;
- solar radiation (sunshine duration/intensity);
- wind speed/movement;
- relative humidity/vapor pressure;
- soil water availability.

ET_c (mm day^{-1}) is calculated by multiplying the reference crop evapotranspiration, ET_o (mm day^{-1}), by a crop coefficient (K_c) of the considered crop with the equation:

$$ET_c = ET_o \times K_c \quad (12)$$

ET_o is also called potential evapotranspiration, and it is the maximum evapotranspiration that will occur when water is not limited. ET_o is for well-watered, 0.12 m tall grass, usually alfalfa, with a fixed value for canopy and aerodynamic resistance of 70 s m^{-1} and an albedo of 0.23 (Allen et al., 1998).

In addition to soil water balance (section 2.1.), other methods have been developed to estimate ET_o based on:

- lysimeters
- pan evaporation
- energy balance
- meteorological data.

Lysimeters are tanks buried into the experimental field that make it possible to estimate water loss directly by measuring the change of mass or by quantifying the amount of drainage water. The lysimeter has to contain the same soil typology as that of the surrounding area. The lysimeter must also have the same type of grass and growing development. It is only possible to obtain reliable data if uniformity exists between the inside and the outside of the tank.

Pan evaporation measures the rate of evaporation from a shallow, open-faced pan. The water added to the pan should be at the same temperature as the water in the pan. Pan evapotranspiration is classified as case A when the site is a crop field, or case B when referring to a dry surface field or one without a cover crop (Figure 28). Evaporation pans are mounted on an open wooden frame, with the bottom of the pan 15 cm above the ground. The reference ET can be approximated by multiplying the pan evaporation by a parameter called the pan coefficient using the following equation:

$$ET_o = K_p \times E_{pan} \quad (13)$$

where ET_o is the evapotranspiration for a clipped grass reference crop (mm/day), K_p is the pan coefficient, and E_{pan} is the evaporation from the pan. Doorenbos and Pruitt (1977) developed a procedure to predict K_p for Class A evaporation pans. The pan coefficient for Class A pans varies depending on the climate and the type of soil cover surrounding the pan.

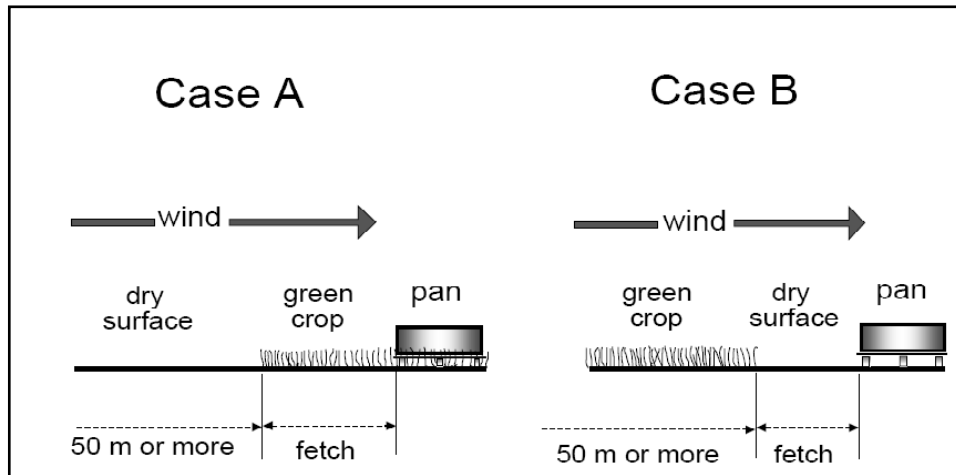


Figure 28. Two cases of evaporation pan siting and their environment (source: Allen et al., 1998).

The energy balance and meteorological data methods to compute evapotranspiration will be discussed in detail in the following sections.

2.2.1. The energy balance

Based on the law of conservation of energy, the energy budget represents the available energy that regulates life processes.

The energy balance is expressed using the following equation:

$$R_n = G + H + LE + M + \Delta S \quad (14)$$

where R_n is net radiation, G is soil heat flux density, H is the sensible heat flux density, and LE is the latent heat flux density. The metabolic term (M), represents the processes of photosynthesis and respiration that occur in the ecosystem. The amount of energy stored in the biomass (ΔS) is generally disregarded.

Thus, the common energy budget equation is considered as follows:

$$R_n = G + H + LE \quad (15)$$

Each flow is measured in W m^{-2} . R_n and G assume a positive value when the flux follows a downward direction, and it is considered negative if it is upward, while H and LE show the inverse situation (Figure 29).

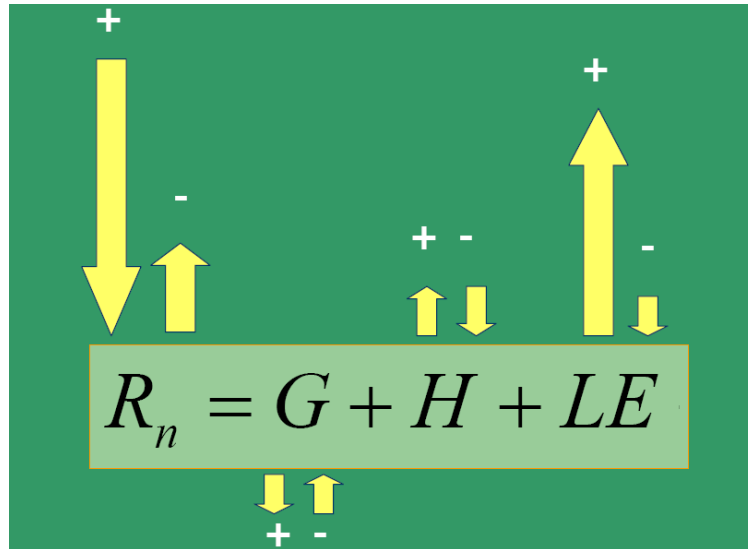


Figure 29. Energy balance equation, direction and sign of terms.

The positive sign of terms symbolizes acquisition of energy by the surface (canopy) from the atmosphere, thus a heating process; the cooling process releases energy, and it is represented by a negative sign.

Net radiation is the main source of energy. It is the electromagnetic energy derived from oscillating magnetic and electrostatic fields that is capable of transmission through empty space at the speed of light.

Net radiation is the sum of longwave (R_l) and shortwave (R_s) radiation, in both the downward (d) and upward (u) direction (Doorenbos and Pruitt, 1975, 1977; Brutsaert, 1982; Wright, 1982; Jensen, 1990; Allen, 1998):

$$R_n = R_{sd} + R_{su} + R_{ld} + R_{lu} \quad (16)$$

Shortwave net radiation (R_s) comprises direct and diffuse radiation, and it is affected by the albedo (α); α is the capability of a surface to reflect radiation back to space.

Direct radiation (Q_s) is the direct beam from the sun to a surface that is horizontal relative to the earth's surface. It is calculated as:

$$Q_s = \tau^m Q_c \cos\alpha \quad (17)$$

where τ^m is the transmission coefficient (relative to sky conditions; can be clear or overcast), Q_c is the extraterrestrial radiation (the solar radiation that follows a direct

beam from the sun but outside the Earth's atmosphere, and it is equal to 1360 W m^{-2}), and α is the angle of incidence from the sun rays to a line perpendicular to the surface of interest.

Diffuse radiation (q) is the amount of radiation that does not arrive on the Earth's surface as direct beam, but it is the radiation scattered by air molecules in the sky and comes from all directions equally. Liu and Jordan (1960) empirically found that about 30% of the depleted radiation reaches the surface as diffuse radiation, and it is calculated as:

$$q = 0.3(1 - \tau^m)Q_c \cos\alpha \quad (18)$$

Upward longwave radiation is expressed as the product of the Stefan Boltzmann constant ($\sigma = 5.675 \times 10^{-8} \text{ J m}^{-2} \text{ K}^{-4} \text{ s}^{-1}$), air temperature (T_a , °K), and emissivity (ε):

$$R_{lu} = \varepsilon\sigma T_a^4 \quad (19)$$

Following the equation presented in Campbell and Norman (1998), downward longwave radiation can be derived as:

$$R_{ld} = (1 - C_1)\varepsilon_a\sigma T_a^4 + C_1(\sigma T_a^4 - 9.0) \quad (20)$$

where C_1 is the fraction of cloud cover in the sky and ε_a is the apparent sky emissivity. ε_a is related to vapour pressure (e , in Pa), and is expressed as:

$$\varepsilon_a = 0.53 + 0.006\sqrt{e} \quad (21)$$

Net radiation is negative during the night and positive during the day. The equation for net radiation can be written in the following manner:

$$R_n = (1 - \alpha)R_s + R_{ld} + R_{lu} \quad (22)$$

as the sum of the longwave radiation and the product of the incoming solar radiation (R_s) and the albedo (α).

Soil heat flux density

Soil heat flux is the energy that is used in heating the soil. G is the conduction of energy per unit area in response to the temperature gradient as expressed by Fourier's Law. Heat is transferred downward into the soil when the soil surface is warmer than below, and it is transferred upward to the soil surface if the soil layers below are warmer. Heat stored in the soil surface contributes to the evaporation of water at the soil surface, heating of the plant canopy by radiation from the surface, and warming of the air and plants by convection of sensible heat to the canopy. Soil temperature is also important because it determines seed germination and plant growth. The soil surface receives energy from net radiation, beginning in the early morning, and conducts heat into the deeper soil layers. Thus, the flux assumes a positive sign and the heat storage process begins. When the net radiation decreases (in the evening), the soil surface becomes cooler and heat that was previously stored in the deep layers is released to the surface. This process continues during the night.

The rate of heat that is released or stored in the soil is expressed as (Jensen et al., 1990):

$$G = -\lambda \frac{\partial T}{\partial z} \quad (23)$$

where λ is the thermal conductivity, ∂T is the temperature gradient within the soil layers, and ∂z is the distance between the considered soil layers.

Thermal conductivity is the ability of a material to conduct heat ($\text{W} \cdot \text{m}^{-1} \cdot \text{K}^{-1}$), and it depends on soil properties and water content. It is also possible to express λ as the product between thermal diffusivity (k) and the volumetric heat capacity (C_v):

$$\lambda = k \times C_v \quad (24)$$

Thermal diffusivity is a property which describes the rate at which heat flows through a material, measured in $\text{m}^2 \text{s}^{-1}$. Volumetric heat capacity is the ability of a given volume of a substance to store internal energy without undergoing a phase change, and it is measured in $\text{J m}^{-3} \text{K}^{-1}$.

Following de Vries equation (1963), C_v is estimated from volume fractions of mineral (V_m), organic matter (V_o), and water as:

$$C_v = (1.93 V_m + 2.51 V_o + 4.19 \theta) 10^6 \quad (25)$$

or considering the soil bulk density (ρ_b) in Mg m^{-3} , the equation can be derived as:

$$C_v = (0.837 \rho_b + 4.19 \theta) 10^6 \quad (26)$$

Thus, the greater the quantity of water that is contained in the soil, the greater the thermal conductivity.

Table 7 reports the thermal conductivity values for some soil materials in dry and wet conditions.

Table 7. Thermal conductivity, (λ), and bulk density (ρ_b) of some soil materials (source: Evett, 2002).

Soil	Dry θ_v	λ $\text{W m}^{-1} \text{K}^{-1}$	Wet θ_v	λ $\text{W m}^{-1} \text{K}^{-1}$	ρ_b Mg m^{-3}	Source
Fairbanks sand	0.003	0.33	0.18	2.08	1.71	1
quartz sand	0.00	0.25	0.40	2.51	1.51	1
sand	0.02	0.9	0.38	2.25	1.60	2
sand	0.00	0.27	0.38	1.77	1.64	3
sand	0.003	0.32	0.38	2.84	1.66	4
gravelly coarse sand (pumice)	0.02	0.13	0.40	0.52	0.76	5
medium and coarse gravel (pumice)	0.01	0.09	0.43	0.39	0.44	5
loamy sand	0.01	0.25	0.40	1.59	1.69	6
loam	0.01	0.20	0.60	1.05	1.18	6
Avondale loam	0.08	0.46	0.23	0.88	1.35-1.45	7
Avondale loam	0.03	0.31	0.30	1.20	1.40	9
silt loam	0.09	0.40	0.50	1.0	1.25	2
Yolo silt loam	0.14	0.49	0.34	1.13	1.25	8
Muir silty clay loam	0.03	0.30	0.30	0.90	1.25	9
silty clay loam	0.01	0.20	0.59	1.09	1.16	6
Pullman silty clay loam	0.07	0.16	0.29	0.89	1.3	10
Healy clay	0.04	0.30	0.30	0.91	1.34	1
Fairbanks peat	0.03	0.06	0.61	0.37	0.34	1
forest litter	0.02	0.10	0.55	0.40	0.21	2

1: de Vries, 1963; 2: Riha et al., 1980; 3: Watts et al., 1990; 4: Howell and Tolk, 1990; 5: Cochran et al., 1967; 6: Sepaskhah and Boerma, 1979; 7: Kimball et al., 1976; 8: Wierenga et al., 1969; 9: Asrar and Kanemasu, 1983; 10: Evett, 1994.

Taking into account that:

$$C_v = C_p \times \rho_s \quad (27)$$

where C_p is the specific heat at constant pressure (J/kg K) and ρ_s is the soil density (Kg of dry soil per m³ of soil), and recalling the different equations used above to describe the concept of thermal conductivity, the soil heat flux equation can be derived as follow:

$$G = -k\rho_s C_p \frac{\partial T}{\partial z} \quad (28)$$

The quantity of heat conducted into the soil can be measured with systems of soil heat flux plates and thermocouples. Estimating the soil heat flux density between two layers (G_1 and G_2), where Δz is the lag distance between them (Figure 30), allows the analysis of the change in stored heat within the soil (ΔS) as:

$$\Delta S = - (G_2 - G_1) \quad (29)$$

The sign of ΔS allows the evaluation of the direction of the flux; a positive sign means that the G_1 layer transfers heat to G_2 , while a negative sign signifies that the heat flux is transferred upward.

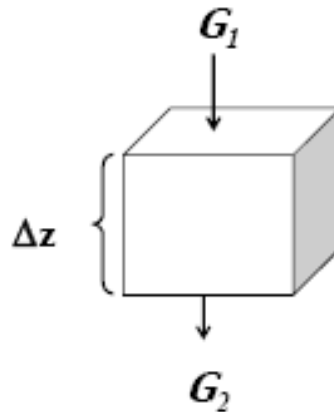


Figure 30. Schematic measuring of soil heat flux.

Therefore, the rate at which heat flows through the soil layers at a depth z below the surface is directly proportional to the temperature gradient.

Sensible Heat Flux

Sensible heat flux is the transfer of energy (heat) away from or to a surface by convection. The sensible heat content of the air depends on the density of the air and the velocity of air molecule transfer through the air. When sensible heat is added to the air, it assumes a positive sign (cooling from the crop surface). The sign is negative when

sensible heat is removed from the air (heating of the crop surface). Sensible heat flux is the heat that is possible to “sense” or “feel”, by measuring with a thermometer.

Sensible heat flux is estimated as:

$$H = -\rho C_p k_a \frac{(T_2 - T_1)}{(z_2 - z_1)} \quad (30)$$

where ρ is the air density, C_p is the specific heat of the air at constant pressure, k_a is the thermal diffusivity, z is the height of the measurement of the heat flux, and T the correspondent temperature at two different heights .

Taking into consideration that k_a is about $(18.9 \cdot 10^{-6}) \times (1 + 0.007 T) \text{ m}^2 \text{ s}^{-1}$ and k is $0.9 \cdot 10^{-6} \text{ m}^2 \text{ s}^{-1}$, it is easy to understand that the heat flux transfer into the air is faster than in the ground.

The concept of resistance to sensible heat flux transfer (r_h) is closely related to H . In fact, the resistance (m s^{-1}) could be explained as:

$$r_h = \frac{(z_2 - z_1)}{k_a} \quad (31)$$

Hence, another way to describe H is :

$$H = -\rho C_p \frac{(T_2 - T_1)}{r_h} \quad (32)$$

where the heat flux density is the result of the ratio of the difference in energy to the resistance.

Latent Heat Flux

The latent heat flux represents the evapotranspiration fraction that can be derived from the energy balance equation if all other components (R_n , G , and H) are known (Allen et al., 1998).

Water molecules are kept together in a liquid state because of the hydrogen bonds. The potential energy of hydrogen bonds in the water is latent in a liquid status. In order to break hydrogen bonds and facilitate evaporation, energy must be added to water.

Sensible heat is the energy used in this process, which allows the change from liquid to vapor status. The consumption of sensible heat indicates a decrease of energy that triggers a reduction of the temperature; thus, a cooling process occurs on the surface. The conversion from sensible heat to latent heat indicates a phase change from the liquid to vapour form of water. In this case, the energy leaves the surface and the flux is considered positive. When condensation occurs, a negative sign is used to describe the flux direction. LE flux is obtained by multiplying the energy gained or released (about 2.45 MJ kg^{-1}) by the mass of water (E , in $\text{Kg m}^{-2} \text{ s}^{-1}$):

$$LE = L \times E \quad (33)$$

The concepts of evapotranspiration and relative humidity are strongly related. In fact, during the evapotranspiration process, the water vapour is added to the atmosphere and the high relative humidity (RH) can hinder the transfer of molecules. Relative humidity is a measure of the water vapour contained in the air, and it is expressed as the ratio of the vapour pressure (e) to the saturation vapour pressure (e_s) at the air temperature (T):

$$RH = \frac{e}{e_s(T)} \times 100 \quad (34)$$

Vapour pressure is the partial pressure due to the water vapor content in the atmosphere, measured in Pascals (Pa) or Kilopascals (kPa). Saturation vapour pressure is the capacity of the air to hold water vapour. When the equilibrium between water molecules escaping and returning to the air is reached, the air is in a condition of saturation vapour pressure. At that moment, the air is said to be saturated since it cannot store any extra water molecules. The number of water molecules that can be stored in the air depends on the air temperature. In fact, e_s is expressed as (Tetens, 1930):

$$e_s(T) = 0.6108 \exp\left(\frac{17.27T}{T + 237.3}\right) \quad (35)$$

where \exp is the exponential function (e^x), and it is valid for the following equations.

The difference between e and e_s is the vapour pressure deficit (VPD):

$$VDP = e_s(T) - e \quad (36)$$

If the air is cooled, without changing e , until the saturation vapor pressure at the cooled temperature (T') is equal to e , the cooled temperature T' is called the dew point temperature (T_d). If the air is diabatically cooled without changing the water vapor content of the air, the sensible heat content and the temperature of the air will decrease until the air becomes saturated and number of water molecules evaporating from a flat surface of pure water is equal the number evaporating from the surface. At that point, the air is at the saturation vapour pressure at the T_d . When the temperature drops slightly below T_d , water will begin to condense on the surface creating dew.

2.2.2. Meteorological data method to compute ET_o

Many equations used to estimate ET_o have been developed so far (Table 8). The choice of the equation is related to the availability of climate data, as well as the location of the study area. In the FAO Irrigation and Drainage Paper No. 24 titled: "Crop Water Requirements" (Doorenbos and Pruitt, 1977), some guidelines were developed and published to provide users solutions that correspond to different availability of data: the Blaney-Criddle, the radiation, the modified Penman, and the pan evaporation methods.

Allen et al. (1998), in the FAO Irrigation and Drainage Paper No. 56 "Crop Evapotranspiration", considered the Penman Monteith equation a standard and the most precise method to estimate ET_o compared with others equations. The FAO Penman Monteith equation combines the energy balance method with the mass transfer method. Penman (1948) is considered the precursor, computing the evaporation from an open water surface from standard climatological records of sunshine, temperature, humidity, and wind speed. The Penman equation takes into account a humid surface, where any kind of resistance is not considered.

Using the Penman equation as a basis for further analysis, Penman and Monteith in 1990 introduced the concept of canopy resistance, applying the equation to a non-wet surface (i.e. plant surface).

Table 8. Some methods to estimate ET_o and relative climate data necessary for each computation.

METHOD	DATA REQUIRED			
	TEMPERATURE	RELATIVE HUMIDITY	SOLAR RADIATION	WIND SPEED
Thorntwaite	×			
Blaney-Criddle	×			
Ivanov	×	×		
Turc	×	×	×	
Cristiansen	×	×	×	×
Hamon	×			
Jensen-Haise	×		×	
Makkink	×		×	
Penman	×	×	×	×
Vanbavel	×	×	×	×
Pristley-Taylor	×	×	×	
Hargreaves	×		×	
Penman-Monteith	×	×	×	×

LE in the Penman equation is the sum of the adiabatic and diabatic processes.

The adiabatic process occurs when there is no exchange of energy. The only source of energy in the adiabatic process is the sensible heat, and a strong relationship between the air temperature and the wet bulb temperature is established (Figure 31).

The wet bulb temperature (T_w) is the temperature that the air (T) assumes if water evaporates into the air until it becomes saturated, without changing the total heat content (enthalpy) in the air and barometric pressure. Wet-bulb temperature is the temperature measured with an aspirated thermometer with the bulb covered by a wet cotton wick. The evaporation of the water from the wick increase e in the air (thus, also the T_d); at the same time air loses energy (sensible heat) to allow water to change from the liquid to vapour phase. Consequently, the air temperature decreases, allowing T and T_d to converge at the same point [$T_w, e_s(T_w)$] in the psychrometric diagram (Figure 31), and the temperature that the air assume is called the wet bulb temperature.

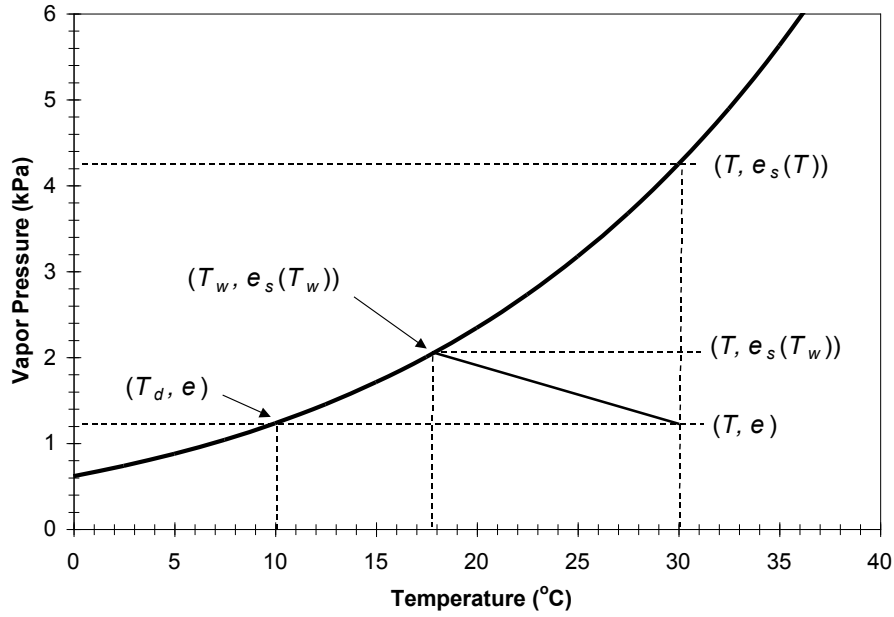


Figure 31. Psychrometric diagram showing the relationship between air temperature (T), wet-bulb temperature (T_w), dew point temperature (T_d), vapor pressure (e), and saturation vapor pressure e_s at T and T_w .

Vapour pressure at T_w is measured as:

$$e_s(T_w) = 0.6108 \exp\left(\frac{17.27T_w}{T_w + 237.3}\right) \quad (37)$$

where e is a function of T_w , T , and barometric pressure (β), and is expressed as:

$$e = e_s(T_w) - 0.000660(1 + 0.00115T_w)(T - T_w)\beta \quad (38)$$

where β is measured in KPa, and it is estimated in relation to the elevation in meters above mean sea level (E_l) (Burman et al., 1987):

$$\beta = 101.3 \left(\frac{293 - 0.0065E_l}{293}\right)^{5.26} \quad (39)$$

Assuming that during the adiabatic process the only source of energy is sensible heat:

$$LE_a = -H_a \quad (40)$$

H_a may be expressed with the following equation, as previously described:

$$H = -\rho C_p \frac{(T-T_w)}{r_h} \quad (41)$$

Moreover, in the adiabatic process, the energy required to raise temperature from T_w to T is equal to that necessary to raise vapour pressure from e to $e_s(T_w)$ (Figure 32).

The slope of the curve between T_w and T is called Δ' , (Figure 32) where:

$$\Delta' = \frac{e_s(T) - e_s(T_w)}{(T - T_w)} \quad (42)$$

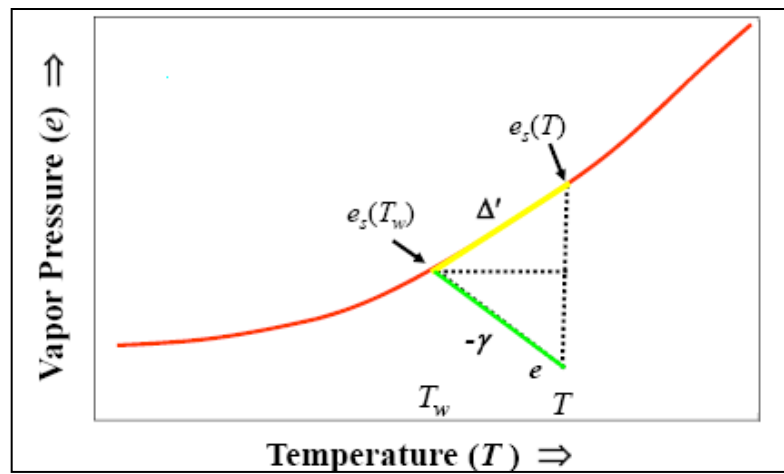


Figure 32. Schematic chart of the adiabatic process.

Δ' is equal to the psychrometric constant ($-\gamma$). All points on γ line have the same enthalpy, but with different proportions between the rates of LE and H , where:

$$-\gamma = \frac{e - e_s(T_w)}{(T - T_w)} \quad (43)$$

The sum of Δ' and γ is equal to the ratio of VPD to the change in temperature:

$$\Delta' + \gamma = \frac{e_s(T) - e}{(T - T_w)} \quad (44)$$

Thus the adiabatic contribution to the LE is:

$$LE = -\frac{\rho C_p}{r_a} \frac{(e_s(T) - e)}{\Delta' + \gamma} \quad (45)$$

where r_a ($s\ m^{-1}$) is the aerodynamic resistance to vapour transfer.

In the diabatic process, an external exchange of energy occurs and $R_n - G \neq 0$.

R_n is the energy input, and it is used for the water vaporization process and/or to increase H . Δ' and $-\gamma$ assume the same meaning during the adiabatic process. The fraction of energy that goes to latent heat is expressed as:

$$LE_d = \frac{\Delta'}{\Delta' + \gamma} R_n \quad (46)$$

while the part of energy that goes to sensible heat is expressed as:

$$H_d = \frac{\gamma}{\Delta' + \gamma} R_n \quad (47)$$

Assuming that:

$$\frac{\Delta'}{\Delta' + \gamma} = \frac{e_s(T) - e_s(T_w)}{e_s(T) - e} \quad (48)$$

then:

$$LE_d = \frac{e_s(T) - e_s(T_w)}{e_s(T) - e} R_n \quad (49)$$

Δ' is considered equal to Δ in $\text{KPa } ^\circ\text{C}^{-1}$ (Tetens, 1930; Murray, 1967) as:

$$\Delta = \frac{4098 e_s(T)}{(T + 237.3)^2} \quad (50)$$

even in conditions of aridity (high VPD), the assumption could be questionable.

Finally, the Penman equation is estimated by the sum of the adiabatic and diabatic processes, and it is expressed as:

$$LE = \frac{\Delta (R_n + G) + \rho C_p (e_s(T) - e) r_a^{-1}}{\Delta + \gamma} \quad (51)$$

Following the suggestion of Allen et al. (2005), G is not considered for daily computations. However, for the monthly estimate it is calculated as:

$$G = 0.07 (T_{mon, i+1} - T_{mon, i-1}) \quad (52)$$

or if $T_{mon, i+1}$ is unknown, it is expressed as:

$$G = 0.14 (T_{mon, i} - T_{mon, i-1}) \quad (53)$$

where T refers to the next (+1), previous (-1), or current (i) monthly mean air temperature respectively.

The aerodynamic resistance ($s\ m^{-1}$) is determined as (Allen et al., 1998):

$$r_a = \frac{\ln\left(\frac{z_m-d}{z_{om}}\right)\ln\left(\frac{z_h-d}{z_{oh}}\right)}{k^2 u_z} \quad (54)$$

where:

- z_m is the height of the wind measurements (m);
- z_h is the height of the humidity measurements (m);
- d is zero plane displacement height (m), and it is considered equal to $0.70 h$, where h is the canopy height;
- z_{om} is the roughness length governing momentum transfer (m);
- z_{oh} is the roughness length governing transfer of heat and vapour (m);
- k is the von Karman's constant, 0.41;
- u_z is the wind speed at height z ($m\ s^{-1}$).

Assuming a constant crop height of 0.12 m and a standardized height of 2 m for wind speed (u_2) and humidity ($z_m = z_h = 2$ m), r_a is computed as:

$$r_a = \frac{208}{u_2} \quad (55)$$

As mentioned previously, the Penman Monteith equation refers to a non-wet surface, taking into consideration the resistance of the canopy (r_c) to vapour transfer, and it can be written as follow:

$$LE = \frac{\Delta (R_n + G) + \rho C_p (e_s(T) - e) r_a^{-1}}{\Delta + \gamma \left(1 + \frac{r_c}{r_a}\right)} \quad (56)$$

where:

$$\gamma \left(1 + \frac{r_c}{r_a}\right) = \gamma^* \quad (57)$$

The canopy resistance is related to the stomatal resistance (r_s) and the leaf area index (LAI) as:

$$r_c = \frac{r_s}{0.5 \times LAI} = \frac{100 \text{ m s}^{-1}}{0.5 \times 2.88} \cong 70 \text{ m s}^{-1} \quad (58)$$

Thus, γ^* is computed as:

$$\gamma^* = \gamma(1 + 0.34u_2) \quad (59)$$

2.3. Crop coefficient

When a crop is grown in large fields under optimum growing conditions, the ratio of the ET_c to the reference crop is known as the crop coefficient (K_c):

$$K_c = \frac{ET_c}{ET_o} \quad (60)$$

The difference between ET_c and ET_o is the result of different factors (Snyder, 2002):

- light absorption by the canopy
- canopy roughness that can affect the turbulence
- crop physiology
- leaf age
- surface wetness

The crop coefficient is dimensionless; it depends on the specific crop at a given growth stage and soil moisture. The distribution of the K_c values during the crop growing season is defined as the crop coefficient curve. As described by Doorenbos and Pruitt (1977), the K_c curve is separated into four stages for field and row crops. In the last part of the growing season, the K_c curve can undergo a decline (Type 1). Crops that do not exhibit a decline of the K_c curve are usually harvested before the onset of senescence (e.g., silage corn and marketable tomatoes). Other crops (Type 2) maintain a fixed K_c value during most of the growing season (e.g., alfalfa, pasture, turfgrass, C-4 species). Figure 33 shows a typical K_c Type 1 curve with a late season K_c decline.

During the initial growth period (A-B), the value of the K_c is generally small because the plant canopy is not completely developed. Most of the crop water use at this time is due to evaporation of the soil surface (bare soil K_c). The crop coefficient of a bare soil depends on the ET_o and the number of days between irrigation events or rainfall. As the canopy develops, the transpiration rate of the crop increases, as well as the K_c . In this period, the increase in the canopy size accounts for the increase in ground cover from 10 to 75%. This period is defined as the rapid growth period (B-C).

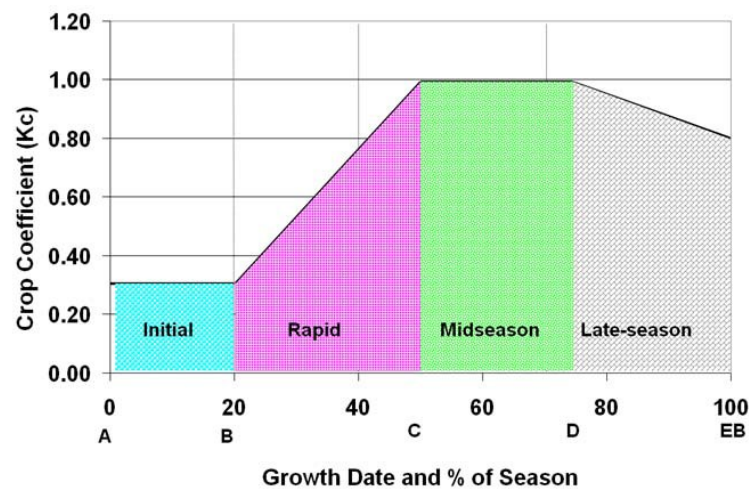


Figure 33. Generalized crop coefficient curve, in relation with the growth date and percentage of season, for field and row crops (Type-1) having a declining K_c during late-season.

Midseason is the stage where 75% of ground cover is present (C-D).

At the onset of the senescence (D-E), the value of the crop coefficient will begin to decrease again, and this stage is defined as late-season.

Deciduous tree and vine crops have K_c similar to field crops, but without the initial period (Figure 34).

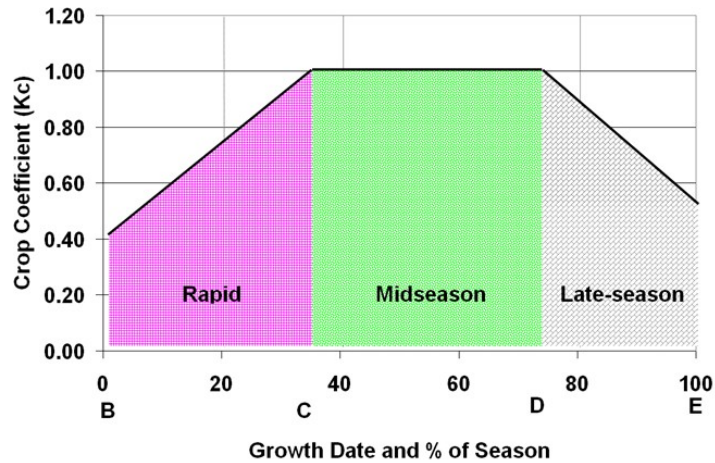


Figure 34. Hypothetical K_c curve for typical deciduous orchard and vine crops.

This kind of curve is characterized by the absence of the initial growth period (Type 3). At leaf out (B), the curve follows a rapid growth, and it distinguishes the beginning of the season. Then, when the crop covers 63% of the ground, the midseason is reached (C-D). At the late season (D-E), the curve begins to decline because of the leaf drop, and the evapotranspiration is near to zero.

Subtropical crops (eg., citrus, olives, avocados) are called Type 4 crops. The K_c for these kinds of crop is assumed to be fixed for the entire season, with corrections in relation to growth, cover crops, and rainfall.

3. WATER SCARCITY MANAGEMENT

3.1. Adaptation strategies

The increase of water scarcity and drought undoubtedly denote the necessity of a more sustainable approach to water resource management. There are many adaptation strategies that can reduce water usages, as well as avoid excessive water consumption.

In the agricultural sector, knowing the actual crop water requirement (CWR) is the starting point to assess and apply adaptation strategies. Crop water requirement is defined as the depth of water needed to meet the water loss through evapotranspiration of a disease-free crop, cultivated in a large field without restrictions on soil conditions (including soil water and fertility), and achieving full potential production under the given growing environment (Doorenbos and Pruitt, 1977). Thus, the CWR includes the total water input necessary to satisfy water losses through the crop evapotranspiration. The amount of water from irrigation needed to satisfy the CWR is defined as the

irrigation requirement (IR). The IR basically represents the difference between the crop water requirement and effective rainfall (Kassam and Smith, 2001). Irrigation provides a way of regulating the seasonal availability of water to match agricultural needs, especially during periods of low rainfall or drought. It is particularly useful for the physiological development of the crop during the growing season, and to increase the yield in both terms of quantity and quality.

Improving the efficiency of the irrigation application rate is the key concept of water saving adaptation strategies. The term "efficiency" is commonly used to indicate "the level of performance" of a system. It means how much water is transported, consumed, and /or used in the production of a commodity. In the agricultural sector, the concept of water use efficiency (WUE) is often used to highlight the relationship between the crop growth development and the amount of water used. WUE could assume different meanings: hydrological and physiological (Stanhill, 1986). In the hydrological sense, it denotes the ratio of the volume of water used productively, i.e., transpired and in some cases also evaporated, from the area under study, to the volume of water potentially available for that purpose, i.e., that reaching the crop growing region via rainfall and irrigation plus that available from the soil. Physiologically, it represents the ratio of the weight of crop water loss to the atmosphere to that of its yield or total dry matter production. Sinclair et al. (1983) linked all meanings of WUE and described this concept as the ratio of biomass accumulation (expressed as carbon dioxide assimilation), total crop biomass, or crop grain yield, to water consumed; therefore, water is expressed as transpiration, evapotranspiration, or total water input into the system.

Improving water use efficiency means increasing water productivity (WP), expressed in economic terms as the agricultural production per unit of water applied (rainfall and/or irrigation). As pointed out by Playán and Mateos (2006), the increase of WP is a way to ameliorate gains in crop yield, reducing the amount of irrigation water. It also could be the solution for food needs accompanying the projected population growth.

Nowadays, many adaptation strategies are implemented to improve WP, starting with the optimal choice of the irrigation system, followed by the choice of the best

cultivar with regards to the soil and climate conditions, concluding with the application of the proper irrigation scheduling in terms of both timing and quantity of water applied.

3.1.1. Irrigation systems

Irrigation systems are designed to supply the water requirements to crops when the natural resources (precipitation) become scarce. The selection of the proper system depends on several factors such as water availability, considered crop, soil characteristics, deep percolation, runoff, evaporation rate, land topography, and the associated installation and maintenance costs.

Irrigation is not only used to supply water to soil affected by water deficit. It is also useful to achieve the following purposes:

- to combat parasites, through products diluted into the water;
- to enrich the soil with nutrients that are dissolved in the water;
- to improve the physical properties of land (e.g., carrying in suspended soil particles that differ from those typical of the soil of the area that would be irrigated);
- to remove excess salinity from the soil;
- to modify the soil pH; (e.g., the submersion of some acidic soils);
- to change the temperature of the soil or plant (e.g., frost protection in orchards).

Irrigation can be performed using different methods of water distribution. Basically, these systems are distinguished into gravity systems, where water moves naturally in the soil by the effect of the gravity force, and pressure systems.

The gravity systems include flood irrigation of the whole field, furrow irrigation using shallow channels to carry water to the crop, and basin irrigation when the water is applied to a levelled surface.

The pressurized systems, also called micro-irrigation, include sprinklers, and drip irrigation systems (surface and subsurface). Sprinkler irrigation is a system that drops water onto the ground, simulating rainfall.

In drip irrigation, water is delivered in small quantities (drops) by nozzles installed in plastic pipes. Surface drip irrigation refers to the use of suspended pipes. This type of irrigation method is usually adopted by orchards or placed into the ground

for vegetables. Drip irrigation reduces water contact with crop leaves, stems, and fruit. These conditions may be less favourable for disease development. When the pipe is buried below the soil surface, subsurface drip irrigation is applied. A well-designed drip irrigation system loses practically no water to runoff, deep percolation, or evaporation. Theoretically, in subsurface drip irrigation, the water losses should be almost null. According to Onder et al. (2005), the surface drip system has more advantages than the subsurface drip method, which is difficult to replace and has higher system costs.

An important parameter used to evaluate the performance of the system is the irrigation efficiency (IE), also known as the application efficiency. IE is defined by the American Society of Civil Engineers (ASCE) On-Farm Irrigation Committee (ASCE, 1978), as the ratio of the volume of water that is taken up by the crop to the volume of irrigation water applied. Many studies have been conducted to determine the IE for different systems. IE for furrow irrigation was estimated between 50 and 73% (Oster et al., 1986; Battikhi and Abu-Hammad, 1994; Chimonides, 1995; Zalidis et al., 1997). For sprinkler irrigation systems, IE values ranged from 54 to 80% (Chimonides, 1995; Zalidis et al., 1997). The best performance occurred in drip irrigation systems, where IE ranged from 80 to 91% (Battikhi and Abu-Hammad, 1994; Chimonides, 1995). Hence, pressurized systems are generally more efficient in transporting water to crops than traditional gravity systems.

In north-eastern Spain, the traditional gravity irrigation systems often maintain efficiencies close to 50% (Playán et al., 2000; Lecina et al., 2005), while properly designed and managed pressurized systems can attain 90% efficiency (Dechmi et al., 2003a, 2003b). Although the traditional gravity approach is still widely used in Europe, particularly in the southern part, it is being replaced (EEA, 2009).

In recent years, several irrigation systems have improved significantly the application efficiency at the farm level, enhancing the irrigation water management. The reason for this recent trend is the interest in achieving the greatest yield for a unit of water applied. The parameter used to assess the water application efficiency is the irrigation water use efficiency, (IWUE). The IWUE is defined as the ratio of the crop yield (Mg ha^{-1}) to the seasonal irrigation water (mm) applied (Kirda, 2004). However, the efficiency of the system depends on the crop, soil conditions, climate, amount and timing of water applied. Previous studies have shown a higher IWUE under subsurface

drip (from 0.0283 to 0.227 Mg ha⁻¹ mm⁻¹), surface drip (from 0.0235 to 0.127 Mg ha⁻¹ mm⁻¹), and sprinkler systems (from 0.0044 to 0.0659 Mg ha⁻¹ mm⁻¹), compared to furrow irrigation (from 0.0086 to 0.056 Mg ha⁻¹ mm⁻¹) (Sammis, 1980; Bogle et al., 1989; Lamm et al., 1995). Ibragimov et al. (2007) compared drip and furrow irrigation. The results using the drip systems have shown an increase in IWUE of 35-103% compared with furrow irrigation, a saving of 18-42% of the applied water. A study on onions by Halvorson et al. (2008) and one conducted on potatoes by Erdem et al. (2006), confirmed that IWUE was higher under the subsurface drip system than the furrow system. Drip irrigation consumes less water than furrow irrigation; consequently, the drip irrigation method yielded higher values of IWUE (Kruse et al., 1990; Erdem et al., 2006). In addition, according to Tognetti et al. (2003), drip irrigation may improve nutrient acquisition in relatively heavy soils (e.g. soils present in the Mediterranean environment), thus accelerating root maturation and the anticipated harvest date.

Hanson and May (2004), in a study on tomatoes conducted along the west side of the San Joaquin Valley in California, found that the yield increased by 12.90–22.62 Mg ha⁻¹ for the drip systems compared to sprinkler systems with similar amounts of applied water. This is possible because a properly managed drip system could reduce percolation below the root zone, giving an IWUE value bigger than in sprinkler irrigation.

A study conducted by Al-Jamal et al. (2001) assessed the differences in irrigation efficiency in onion production for sprinkler, drip, and furrow irrigation systems in Southern New Mexico (USA). The maximum IWUE was obtained using sprinkler systems. The lowest IWUE values were obtained under furrow irrigation systems. These results were due to excessive irrigation under subsurface drip and higher evaporation rates from fields using furrow irrigation.

One option to improve the irrigation water management may be converting from furrow or sprinkler irrigation systems to drip irrigation. In fact, drip irrigation can apply water more precisely and uniformly than furrow and sprinkler irrigation systems. The results would be a potential reduction in subsurface drainage, a higher control of soil salinity, and an increase in yield. On the other hand, the IWUE values depend on the irrigation system, but they are also affected by the canopy interception, the soil type, the

cultural and management practices, and crop variety choice. At the farm level, selecting the appropriate irrigation system means also evaluating the installation and maintenance costs. Thus, a balance among the yield income, water conservation, and the cost to maintain the irrigation system is necessary to increase farmer's profits.

3.1.2. Scheduling of irrigation management strategies

Irrigation water management is a term used in the broad sense to refer to all practices that improve crop yield and reduce excessive water consumption. The main management activity involves irrigation scheduling or determining when and how much water to apply, taking into account the irrigation method and other field characteristics (Holzapfel et al., 2009).

Shifting the planting date is a useful strategy in response to climate change, especially for those crops with a spring-summer growing season. Simulations of irrigation requirements under climate change scenarios, where the planting date was shifted by a month or more into the winter season, showed optimal results (Döll, 2002; Lovelli et al., 2012). In fact, planting earlier in the spring increases the length of the growing season, and it will increase the potential yield if the soil moisture is adequate and the risk of heat stress is low (Maracchi et al., 2005). Otherwise, earlier planting combined with a short-season cultivar would give the best assurance of avoiding heat and water stress (Tubiello et al., 2000). Kucharik (2008) observed that the current yield trend toward earlier maize planting dates appears to have contributed to recent gains in yield between 19 and 53% in several states in the northern and western portions of the Corn Belt (Nebraska, Iowa, South Dakota, Minnesota, Wisconsin, and Michigan). The shorter growing season, due to earlier planting dates, have benefited significantly the yield, an increase between 0.06 and 0.14 Mg ha⁻¹ for each additional day of earlier planting.

In the Mediterranean basin, some orchard crops, such as olives, and grapevines have been traditionally cultivated in rain-fed conditions in the past. Recently, the increase of irrigated land in orchards has been observed because of the yield response to irrigation. In fact, even with low water application, the yield response is greater than that in rain-fed conditions, so that an increasing interest in irrigated agriculture has been observed. For instance, the average olive production under rain-fed conditions was

about 35% lower than that obtained by applying different irrigation treatments, including full irrigation (Gómez-Rico et al., 2007). Intuitively, the application of full irrigation to meet the CWR leads to the maximum yield. Nevertheless, many studies have demonstrated that allowing the plants to experience a certain degree of water stress turned out to be a good way to save water without resulting in a significant reduction in yield. The application of regulated deficit irrigation (RDI) means delivering less water than the crop actually needs. Deficit irrigation has been demonstrated as a useful tool to improve the irrigation management at the field scale for arid and semi-arid conditions (Holzapfel et al., 2009). Analyzing different studies conducted on orchards and field crops, the conclusion in terms of irrigation efficiency would be that providing the full CWR could be ineffective considering yield and gain. The amount of water supply that a crop really needs could be assessed by the installation of sensors into the soil. Once the full crop water requirement is established, the deficit in irrigation related to the ET_c or PAN evapotranspiration can be computed. Fereres and Soriano (2007) showed that the performance of the deficit irrigation has a significantly positive response in tree crops and vines, whereas other studies showed there was no evident benefit in field crops. A study conducted on maize by Yenesew and Tilahun (2009) demonstrated that applying only 50% of the irrigation demand at the initial and late season stages resulted in statistically similar average grain yield and biomass as that of applying the full irrigation requirement throughout the whole season; instead, stressing maize during the mid season stage results in lower yields, indicating that mid season is the most sensitive growing period to water deficit. For Farré and Faci (2009), applying irrigation deficit practices in maize during all of the growing season without incurring significant yield reductions is not possible, unless the stress is limited only during the grain filling phase. On the contrary, promising results have been achieved in tree crop studies. Chaves et al. (2007) analysed the response of regulated deficit irrigation on grapevines. They showed that a decrease of 50% of water applied did not affect the quality and production, even if the response to deficit irrigation depends on the variety and the environmental conditions during the growing season.

Many studies have been conducted on olives under RDI conditions (Patumi et al., 2002; Çetin et al., 2004; Gómez-Rico et al., 2007; Lavee et al., 2007; Tognetti et al., 2006; Melgar et al., 2008; Dabbou et al., 2010). In Italy, the application of a RDI of

33% of the full CWR from the beginning of pit hardening (August–September) to the early fruit veraison in olive trees, limits the yield losses to only 16% (Tognetti et al., 2006). Dabbou et al. (2010) showed that a restitution of 100% of ET_c does not further enhance the yield more than 75%. Furthermore, this choice is also optimal to achieve good oil content. Moreover, the analysis of the oil content showed that this irrigation option does not affect the quality and composition of virgin olive oil. Several previous studies presented contrasting results, observing a reduction in oil content related to the deficit irrigation (Spiegel, 1955; Lavee and Wodner, 1991; Inglese et al., 1996). With respect to water management in olive orchards, the yield is considered significant, in addition to the oil characteristics (e.g.: phenols, fatty acid composition, α -Tocopherol). In Israel, Lavee et al. (1990) showed that a full irrigation during all of the growth season may cause a reduction in the fruit characteristics; complementary irrigation in some occasions during summer drought after pit hardening is effective in doubling the olive production and the oil yield in olive trees compared with rain-fed conditions.

Patumi et al. (2002) mentioned that a restitution of 66% of ET_c is sufficient to achieve good yields, while higher volumes of water (100% of ET_c) produce just a little additional increase in the yield. Moreover, the olive oil composition does not change with irrigation, except for the decrease of the total phenols, but they are not considered detrimental for oil organoleptic characteristics.

Functional relationships between yield and water deficits in citrus have been verified by Shalhevet and Bielorai (1978) and Doorenbos and Kassam (1979). Both studies demonstrated that deficit irrigation affects the yield in relation to the period of the application. In general, flowering, fruit set, and the initial phases of fruit development are considered to be the most critical growth stages. In a study conducted by Castel and Buj (1990) on orange orchards in Spain, the results showed that the deficit irrigation amount during May and June, or from September to March, does not significantly affect the yield production compared with the full irrigation treatment. In addition, no apparent relationship between the fruit quality and water deficit was noticed during flowering, fruit set, or the maturation period. García-Tejero et al. (2010) found that the application of RDI from June to October led to statistically significant differences in quality parameters (total soluble solids and titratable acidity), but the effects are not so clear-cut in terms of tree yield. Nonetheless, the results due to the

reduction of 50% of the irrigation application compared with a full irrigation treatment showed a non-statistically significant reduction in yield production and an increase in IWUE.

OBJECTIVES

Water is a key resource for the development of any human activity, especially for farming. The availability of water for farming is an essential condition for achieving satisfactory and profitable yields, both in terms of unit yields and quality. In order to cope with future estimates of water shortages, some measures aimed at streamlining and optimizing the efficiency of water consumption are needed; this need is particularly acute in the agricultural sector in view of the very considerable volumes of water required for the production cycle of crops. Efficient water management is one of the key elements in the successful operation and management of irrigation schemes. The research activity reported in this work focuses on the assessment of the irrigation water demand for some of the most economically important crops in the region of Sardinia (Italy), and the estimation of climate change impact on future crop water requirements using the SIMETAW# model. This dissertation is divided into three sections.

The first section aims to investigate the distribution of the reference evapotranspiration, applying alternative methods for the FAO Penman-Monteith computation, in order to define ET_o zones to be used for the investigation of the impact of climate change on the irrigation water demand in Sardinia.

The second section shows the skills and functions of the SIMETAW# model, in addition to its potential applications.

The third section aims to compute the irrigation water demand for artichokes, grain and silage maize, olives, grapevines, and citrus using the SIMETAW# model in relation with current and future climate conditions in each ET_o zone of Sardinia. The estimation of the irrigation requirement is the results of the combination of the crop planted areas and management data, soil conditions, and irrigation system information. The final goal of this research activity is the analysis of the application of some possible adaptation strategies in order to reduce the potential climate change impact and to propose a future irrigation management strategy focused on water use efficiency.

REFERENCES

- Ainsworth, E.A., Long, S.P. 2005. What have we learned from 15 years of free-air CO₂ enrichment (FACE)? A meta-analysis of the responses of photosynthesis, canopy properties and plant production to rising CO₂. *New Phytologist*, 165, 351-372.
- Alcamo, J., Döll, P., Kaspar, F., Siebert, S. 1997. Global change and global scenarios of water use and availability: an application of WaterGAP 1.0. University of Kassel, CESR, Kassel, Germany.
- Alcamo, J., Henrichs, T., Rosch, T. 2000. World water in 2025: global modeling and scenario analysis. In: Rijsberman F.R. (Ed.), .World water scenarios analyses. World Water Council, Marseille, France.
- Alcamo, J., Döll, P., Henrichs, T., Kaspar, F., Lehner, B., Rösch, T., Siebert, S. 2003a. Development and testing of the WaterGAP 2 global model of water use and availability. *Hydrological Sciences Journal*, 48, 317–338.
- Alcamo, J., Döll, P., Henrichs, T., Kaspar, F., Lehner, B., Rösch, T., Siebert, S. 2003b. Global estimates of water withdrawals and availability under current and future “business-as-usual” conditions. *Hydrological Sciences Journal*, 48, 339-348.
- Al-Jamal, M.S., Ball, S., Sammis, T.W. 2001. Comparison of sprinkler, trickle and furrow irrigation efficiencies for onion production. *Agricultural Water Management*, 46, 253-266.
- Allan, J.A. 1996. Policy responses to the closure of water resources: regional and global issues. In: Howsam P. (Ed.), *Water Policy: Allocation and Management in Practice*. Taylor and Francis, London, UK, pp. 3–12.
- Allan, J.A. 1997. Virtual water: a long-term solution for water short Middle Eastern economies? Paper presented at the 1997 British Association Festival of Science, University of Leeds, 9 September 1997, UK.
- Allen, R.G., Pereira, L.S., Raes, D., Smith, M. 1998. Crop evapotranspiration: Guidelines for computing crop water requirements. FAO Irrigation and Drainage Paper 56, FAO, Rome.

- Allen, R.G., Walter, I.A., Elliott, R.L., Howell, T.A., Itenfisu, D., Jensen, M.E., Snyder, R.L. 2005. The ASCE Standardized Reference Evapotranspiration Equation. American Society of Civil Engineers, Reston, VA.
- American Society of Civil Engineers (ASCE). 1978. Describing irrigation efficiency and uniformity. *Journal of the Irrigation and Drainage Division*, 104, 35-41.
- Arnell, N.W. 1999. The effect of climate change on hydrological regimes in Europe: a continental perspective. *Global Environmental Change*, 9, 5–23.
- Arnell, N.W. 2004. Climate change and global water resources: SRES scenarios and socio-economic scenarios. *Global Environmental Change*, 14, 31–52.
- Asrar, G., Kanemasu, E.T. 1983. Estimating thermal diffusivity near the soil surface using Laplace Transform: uniform initial conditions. *Soil Science Society of America Journal*, 47, 397-401.
- Ayala, F.J. 2002. Notas sobre los impactos físicos previsible del cambio climático sobre los lagos y humedales españoles. III Congreso Ibérico sobre gestión y planificación de aguas. Sevilla, Spain.
- Baric, A., Gasparovic, F. 1992. Implication of climatic change on the socio-economic activities in the Mediterranean coastal zones. In: Jeftic L., Milliman J.D., Sestini G. (Eds.), *Climatic Change and the Mediterranean*. UNEP, New York, USA, pp.129–174.
- Bates, B.C., Kundzewicz, Z.W., Wu, S., Palutikof, J.P. 2008. *Climate Change and Water*. Eds. IPCC Secretariat, Geneva.
- Battikhi, A.M., Abu-Hammad, A.H. 1994. Comparison between the efficiencies of surface and pressurized irrigation systems in Jordan. *Irrigation and Drainage Systems*, 8, 109-121.
- Bellingham, B.K. 2009. Method for irrigation scheduling based on soil moisture data acquisition. *Proceeding of Irrigation District Conference, United States Committee on Irrigation and Drainage*, 3-6 June 2009, Reno, Nevada, pp. 1-17.
- Bindi, M., Ferrini, F., Miglietta, F. 1992. Climatic change and the shift in the cultivated area of olive trees. *Journal of Agricultura Mediterranea*, 22, 41–44.
- Blencowe, J.P.B., Moore, S.D., Young, G.J., Shearer, R.C., Hagerstrom, R., Conley, W.M., Potter, J.S. 1960. United States Department of Agriculture (USDA), Soil, Department of Agriculture Bulletin 462.

- Bogle, C.R., Hartz, T.K., Nunez, C. 1989. Comparison of subsurface trickle and furrow irrigation on plastic mulched and bare soil for tomato production. *Journal of the American Society for Horticultural Science*, 114 (1), 40-43.
- Bou-Zeid, E., El-Fadel, M. 2002. Climate change and water resources in Lebanon and the Middle East. *Journal of Water Resources Planning and Management*, 128 (5), 343-355.
- Brown, R.A., Rosenberg, N.J. 1997. Sensitivity of crop yield and water use to change in a range of climatic factors and CO₂ concentrations: a simulation study applying EPIC to the central USA. *Agricultural Forest Meteorology*, 83, 171–203.
- Brutsaert, W.H. 1982. *Evapotranspiration into the atmosphere*. Reidel D. Publishing and Co. Dordrecht, Holland, Boston, USA, and London, England.
- Burman, R.D., Jensen, M.E., Allen, R.G. 1987. Thermodynamic factors in evapotranspiration. Proceedings of a conference on irrigation systems for the 21st century. Portland, Oregon (USA), 28-30 Jul 1987, 28-30. In: James L.G. and English M.J. (Eds.). New York, N.Y. (USA) ASCE.
- Campbell, G.S., Norman, J.M. 1998. *An introduction to environmental physics*. Second edition, Springer-Verlag, New York, USA.
- Castel, J.R., Buj, A. 1990. Response of Salustiana oranges to high frequency deficit irrigation. *Irrigation Science*, 11, 121-127.
- Centro regionale agrario sperimentale (CRAS). 2006. Indagine sull'effetto dell'utilizzo delle aree irrigue a integrazione del piano stralcio di bacino regionale-relazione tecnica conclusiva. www.regionesardegna.it
- Çetin, B., Yazgan, S., Tipi, T. 2004. Economics of drip irrigation of olives in Turkey. *Agricultural Water Management*, 66, 145–151.
- Chaves, M.M., Santos, T.P., Souza, C.R., Ortuño, M.F., Rodrigues, M.L., Lopes, C.M., Maroco, J.P., Pereira, J.S. 2007. Deficit irrigation in grapevine improves water-use efficiency while controlling vigour and production quality. *Annals of Applied Biology*, 150, 237–252.
- Chimonides, S.J. 1995. Irrigation management under water shortage conditions. In: Tsiourtis N.X. (Ed.), *Water resources management under drought or water shortage conditions*. Balkema, Rotterdam.
- Church, T.M. 1996. An underground route for the water cycle. *Nature*, 380, 579-580.

- Cochran, P.H., Boersma, L., Youngberg, C.T. 1967. Thermal conductivity of a pumice soil. *Soil Science Society of America Journal*, 31, 454-459.
- Correia, F.N. 1990. Water management in Mediterranean environments. *Proceedings of the European Conference on Water Management*. European Commission and French Ministry of the Environment, La Villete, Paris.
- Correia, F.N. 1996. Water resources under the threat of desertification. *Proceedings of the International Conference on Mediterranean Desertification*. European Commission and Greek Ministry of Agriculture, Crete.
- Correia, F.N. 1999. Water Resources in the Mediterranean region. *Water International*, 24 (1), 22-30.
- Cosgrove, W., Rijsberman, F. 2000. Making water everybody's business, *World Water Vision*. The World Water Council, Earthscan Publications Ltd., London, UK.
- Dabbou, S., Chehab, H., Faten, B., Dabbou, S., Esposto, S., Selvaggini, R., Taticchi, A., Servili, M., Montedoro, G.F., Hammami, M. 2010. Effect of three irrigation regimes on Arbequina olive oil produced under Tunisian growing conditions. *Agricultural Water Management*, 97, 763–768.
- de Vries, D.A. 1963. Thermal properties of soil. In van Vijk W.R. (Ed.), *Physics of plant environment*. North Holland Pub. Co., Amsterdam, pp. 210-235.
- Dechmi, F., Playán, E., Faci, J.M., Tejero, M. 2003a. Analysis of an irrigation district in northeastern Spain: I: Characterisation and water use assessment. *Agricultural Water Management*, 61, 75–92.
- Dechmi, F., Playán, E., Faci, J.M., Tejero, M., Bercero, A. 2003b. Analysis of an irrigation district in northeastern Spain: II. Irrigation evaluation, simulation and scheduling. *Agricultural Water Management*, 61, 93–109.
- Döll, P. 2002. Impact of climate change and variability on irrigation requirements: a global perspective. *Climatic Change*, 54, 269–293.
- Doorenbos, J., Pruitt, W.O. 1975. *Guidelines Crop water requirements*. FAO Irrigation and Drainage Paper 24, Rome.
- Doorenbos, J., Pruitt, W.O. 1977. *Crop water requirements*. FAO Irrigation and Drainage Paper 24, 2nd ed., Rome.
- Doorenbos, J., Kassam, A.H. 1979. *Yield response to water*. FAO Irrigation and drainage Paper 33, Rome.

- Eid, H.M. 1994. Impact of climate change on simulated wheat and maize yields in Egypt. In: Rosenzweig C., Iglesias A. (Eds), Implications of Climate Change for International Agriculture: Crop Modeling Study. US Environmental Protection Agency, Washington, DC.
- El-Shaer, H.M., Rosenzweig, C., Iglesias, A., Eid, M.H., Hillel, D. 1997. Impact of climate change on possible scenarios for Egyptian agriculture in the future. *Mitigation and Adaptation Strategies for Global Change*, 1, 233-250.
- Erdem, T., Erdem, Y., Orta, H., Okursoy, H. 2006. Water-yield relationships of potato under different irrigation methods and regimens. *Scientia Agricola*, 63 (3), 226-231.
- European Environment Agency (EEA). 2000. Report No. 6/2000: Environmental signals - European Environment Agency, Copenhagen, Denmark.
- European Environment Agency (EEA). 2009. Report No 2/2009: Water resources across Europe — confronting water scarcity and drought. European Environment Agency, Copenhagen, Denmark.
- Evet, S.R. 1994. TDR-Temperature arrays for analysis of field soil thermal properties. *Proceedings of the Symposium on Time Domain Reflectometry in Environmental, Infrastructure and Mining Applications*, 7-9 September 1994. Northwestern University, Evanston, Illinois, pp. 320-327.
- Evet, S.R. 2002. Water and energy balances at soil-plant-atmosphere interfaces. Warrick A.A., (Ed.), *The Soil Physics Companion*. Crc Press, Boca Raton, Florida, pp. 127-188.
- Falkenmark, M., Rockström, J. 2004. *Balancing water for humans and nature*. Earthscan, London, UK.
- FAO. 1993. *Production Yearbook, 1961-1993*. United Nations Food and Agriculture Organization, Rome, Italy.
- FAO. 2000. *Agriculture: Towards 2015-30 - Technical interim report*. FAO, Rome, Italy.
- FAO. 2001. FAOSTAT (Statistics Database). On-line information service, FAO, Rome, Italy. www.fao.org.
- FAO. 2002a. *Crops and Drops: Making the best use of water for agriculture*. FAO, Rome, Italy.

- FAO. 2002b. FAOSTAT, On-line Database; www.fao.org.
- FAO. 2003a. Review of world water resources by country. Water Report No. 23. Rome, Italy. <ftp://ftp.fao.org/agl/aglw/docs/wr23e.pdf>
- FAO. 2003b. Agriculture, food and water: a contribution to the world water development report. FAO, Rome, Italy.
- FAO. 2003c. Unlocking the water potential of agriculture. FAO, Rome, Italy.
- FAO. 2011. Climate change, water and food security. FAO water reports No. 36. Rome, Italy. <http://www.fao.org>.
- FAO/BRGM. 1996. Les ressources en eau. Rome.
- Farré, I., Faci, J.M. 2009. Deficit irrigation in maize for reducing agricultural water use in a Mediterranean environment. *Agricultural Water Management*, 96, 383–394.
- Fereres, E., Soriano, M.A. 2007. Deficit irrigation for reducing agricultural water use. *Journal of Experimental Botany*, 58, 147-159.
- Fischer, G., Heilig, G.K. 1997. Population momentum and the demand on land and water resources. *Philosophical Transactions of Royal Society, B: Biological Sciences*, 352, 869–889.
- Fischer, G., Tubiello, F.N., Van Velthuisen, H., Wiberg, D.A. 2007. Climate change impacts on irrigation water requirements: effects of mitigation, 1990–2080. *Technological Forecasting & Social Change*, 74, 1083–1107.
- García-Tejero, I., Jiménez-Bocanegra, J.A., Martínez, G., Romero, R., Durán-Zuazo, V.H., Muriel-Fernández, J.L. 2010. Positive impact of regulated deficit irrigation on yield and fruit quality in a commercial citrus orchard [*Citrus sinensis* (L.) Osbeck, cv. salustiano]. *Agricultural Water Management*, 97, 614–622.
- Giorgi, F., Bi, X.Q., Pal, J. 2004. Mean, inter annual variability and trends in a regional climate change experiment over Europe. II: climate change scenarios (2071–2100). *Climate Dynamic*, 23 (7–8), 839–858.
- Gómez-Rico, A., Salvador, M.D., Moriana, A., Pérez, D., Olmedilla, N., Ribas, F., Fregapane, G. 2007. Influence of different irrigation strategies in a traditional Cornicabra cv. olive orchard on virgin olive oil composition and quality. *Food Chemistry*, 100, 568–578.

- Halvorson, A.D., Bartolo, M.E., Reule C.A., Berrada, A. 2008. Nitrogen effects on onion yield under drip and furrow irrigation. *Agronomy Journal*, 100, 1062–1069.
- Hanasaki, N., Inuzuka, T., Kanae, S., Oki, T. 2010. An estimation of global virtual water flow and sources of water withdrawal for major crops and livestock products using a global hydrological model. *Journal of Hydrology*, 384, (3–4), 232–244.
- Hanson, B., May, D. 2004. Effect of subsurface drip irrigation on processing tomato yield, water table depth, soil salinity, and profitability. *Agricultural Water Management*, 68, 1–17.
- Hisdal, H., Stahl, K., Tallaksen, L.M., Demuth, S. 2001. Have streamflow droughts in Europe become more severe or frequent? *International Journal of Climatology*, 21 (3), 317–333.
- Holzapfel, E.A., Pannunzio, A., Lorite, I., Silva de Oliveira, A.S., Farkas, I. 2009. Design and management of irrigation systems. *Chilean Journal of Agricultural Research*, 69 (1), 17-25.
- Howell, T.A., Tolk, J.A. 1990. Calibration of soil heat flux transducers. *Theoretical and Applied Climatology*, 42, 263-272.
- Ibragimov, N., Evett, S.R., Esanbekov, Y., Kamilov, B.S., Mirzaev, L., Lamers, J.P.A. 2007. Water use efficiency of irrigated cotton in Uzbekistan under drip and furrow irrigation. *Agricultural Water Management*, 90, 112-120.
- Idda, L., Furesi, R., Madau, F.A., Rubino, C. 2004. L'olivicoltura in Sardegna. Aspetti economici e prospettive alla luce di un'analisi aziendale. *Quaderni di Economia e Politica Agraria n. 2, Sezione di Economia e Politica Agraria (Università degli Studi di Sassari). Tipografia Editrice Giovanni Gallizzi, Sassari, Italy.*
- Idso, K.E., Idso, S.B. 1994. Plant responses to atmospheric CO₂ enrichment in the face of environmental constraint: a review of the past 10 years' research. *Agricultural and Forest Meteorology*, 69, 153–203.
- Iglesias, A., Moneo, M. 2005. Drought preparedness and mitigation in the Mediterranean: Analysis of the Organizations and Institutions. *Options Méditerranéennes, CIHEAM, Centre international de Hautes Etudes Agronomiques Méditerranéennes, Paris.*

- Inglese, P., Barone, E., Gullo, G. 1996. The effect of complementary irrigation on fruit growth, ripening pattern and oil characteristics of olive (*Olea europaea* L.) cv. Carolea. *Journal of Horticultural Science*, 71, 257–263.
- Iglesias, A., Rosenzweig, C., Pereira, D. 2000. Prediction spatial impacts of climate in agriculture in Spain. *Global Environmental Change*, 10, 69–80.
- Iglesias, A., Estrela, T., Gallart, F. 2005. Impacts on hydric resources. A preliminary general assessment of the impacts in Spain due to the effects of climate change. Ministerio de Medio Ambiente, Spain.
- Iglesias, A., Garrote, L., Flores, F., Moneo, M. 2007. Challenges to manage the risk of water scarcity and climate change in the Mediterranean. *Water Resources Management*, 21, 775–788.
- Intergovernmental Panel on Climate Change (IPCC). 2001. *Climate change 2001: impacts, adaptation and vulnerability. Contribution of working Group II to the third assessment report of the intergovernmental panel on climate change.* Cambridge University Press, Cambridge, UK.
- Intergovernmental Panel on Climate Change (IPCC). 2007a. *Fourth IPCC Assessment Report (AR4): Climate Change 2007.* Cambridge University Press, Cambridge, UK.
- Intergovernmental Panel on Climate Change (IPCC). 2007b. *Climate Change 2007: The Physical Science Basis. Contribution of Working Group I to the Fourth Assessment Report of the Intergovernmental Panel on Climate Change.* Solomon S., Qin D. Manning M., Chen Z., Marquis M., Averyt K.B., Tignor M., Miller H. L. (Eds.), Cambridge University Press, Cambridge, UK.
- IRSA-CNR. 1999. *Un futuro per l'acqua in Italia.* Eds. M. Benedini, A. Di Pinto, A. Massarutto, R. Pagnotta, R. Passino. Quaderni IRSA-CNR, Roma, Italy.
- Istat. 2002. *V Censimento dell'Agricoltura Italiana.* Roma, Istat. www.istat.it
- Istat. 2005. *Indagine sulla struttura e le produzioni delle aziende agricole (SPA)* http://www3.istat.it/dati/dataset/20070613_00/indexep.html
- Istat. 2007. *Dati annuali sulle coltivazioni (1999-2008).* www.istat.it
- Istat. 2010. *VI Censimento dell'Agricoltura Italiana – I dati provvisori.* Roma, Istat. <http://censimentoagricoltura.istat.it/index.php?id=73>

- Jablonski, L.M., Wang, X., Curtis, P.S. 2002. Plant reproduction under elevated CO₂ conditions: A meta-analysis of reports on 79 crop and wild species. *New Phytologist*, 156 (1), 9-26.
- Jensen, M.E., Burman, R.D., Allen, R.G. 1990. Evapotranspiration and irrigation water requirements. American Society of Civil Engineer, New York, USA.
- Johnson, N., Revenga, C., Echeverria, J. 2001. Managing Water for People and Nature. *Science*, 292 (5519), 1071-1072.
- Kassam, A., Smith, M. 2001. FAO methodologies on crop water use and crop water productivity: expert meeting on crop water productivity. FAO Paper No. CWP-M07, Rome, Italy.
- Kimball, B.A., Jackson, R.D., Reginato, R.J., Nakayama, F.S., Idso, S.B. 1976. Comparison of field measured and calculated soil heat fluxes. *Soil Science Society of America Journal*, 40, 18-24.
- Kimball, B.A., Kobayashi, K., Bindi, M. 2002. Responses of agricultural crops to free-air CO₂ enrichment. *Advances in Agronomy*, 77, 293-368.
- Kirda, C., Cetin, M., Dasgan, Y., Topcu, S., Kaman, H., Ekici, B., Derici, M.R., Ozguven, A.I. 2004. Yield response of greenhouse grown tomato to partial root drying and conventional deficit irrigation. *Agricultural Water Management*, 69, 191-201.
- Kruse, E.G., Bucks, D.A., Von Bernuth, R.D. 1990. Comparison of irrigation systems. *Agronomy*, 30, 475-508.
- Kucharik, C.J. 2008. Contribution of planting date trends to increase maize yields in the central United States. *Agronomy Journal*, 100 (2), 328-336.
- Lamm, F.R., Manges, H.L., Ston, L.R., Khan, A.H., Rogers, D.H. 1995. Water requirement of subsurface drip irrigated corn in northwest Kansas. *Transaction of ASAE*, 38, 441-448.
- Lavee, S., Wodner, M. 1991. Factors effecting the nature of oil accumulation in fruit of olive (*Olea europaea* L.) cultivars. *Journal of Horticultural Science*, 66, 583-591.
- Lavee, S., Nashef, M., Wodner, M., Harshemesh, H. 1990. The effect of complementary irrigation added to old trees (*Olea europaea* L.) cv 'Souri' on fruit

- characteristics, yield and oil production. *Advances in Horticultural Science*, 4, 135–138.
- Lavee, S., Hanoch, E., Wodner, M., Abramowitch, H. 2007. The effect of predetermined deficit irrigation on the performance of cv. Muhasan olives (*Olea europaea* L.) in the eastern coastal plain of Israel. *Scientia Horticulturae*, 112, 156–163.
- Lecina, S., Playán, E., Isidoro, D., Dechmi, F., Causapé, J., Faci, J.M. 2005. Irrigation evaluation and simulation at the irrigation district V of Bardenas (Spain). *Agricultural Water Management*, 73 (3), 223–245.
- Leff, B., Ramankutty, N., Foley, J.A. 2004. Geographic distribution of major crops across the world. *Global Biogeochemical Cycles*, 18, Gb1009.
- Legambiente. 2008. La gestione sostenibile dell'acqua in agricoltura. <http://www.legambiente.it/>
- Lindh, G. 1992. Hydrological and water resources impact of climatic change, in *Climatic Change and the Mediterranean*. In: Jeftic L., Milliman J.D, Sestini G. (Eds.), *Climatic Change and the Mediterranean*. UNEP, New York, USA, pp. 58-93.
- Liu, B.Y.H., Jordan, R.C. 1960. The interrelationship and of direct, diffuse and characteristic distribution total solar radiation. *Solar Energy*, 4 (3), 1–19.
- Lovelli, S., Perniola, M., Scalcione, E., Troccoli, A., Ziska, L.H. 2012. Future climate change in the Mediterranean area: implications for water use and weed management. *Italian Journal of Agronomy*, 7 (e7), 44-49.
- Madau, F.A. 2009. *Aspetti economici dell'agricoltura irrigua in Sardegna*. Rapporto irrigazione INEA, Quintily Grafica, Roma.
- Mannion, A.M. 1995. *Agriculture and environmental change. Temporal and spatial dimensions*. John Wiley & Sons. Chichester, UK.
- Maracchi, G., Sirotenko, O., Bindi, M. 2005. Impacts of present and future climate variability on agriculture and forestry in the temperate regions: Europe. *Climatic Change*, 70, 117–135.
- Melgar, J.C., Mohamed, Y., Navarro, C., Parra, M.A., Benlloch, M., Fernández-Escobar, R. 2008. Long-term growth and yield responses of olive trees to different irrigation regimes. *Agricultural Water Management*, 95, 968–972.

- Merriam, J.L. 1966. A management control concept for determining the economical depth and frequency of irrigation. *Transaction of ASAE*, 9, 492-498.
- Morettini, A. 1972. Ambiente climatico e pedologico. *Olivicoltura*, 12, 219-246.
- Murray, F.W. 1967. On the computation of saturation vapor pressure. *Journal of Applied Meteorology*, 6, 203-204.
- National Center for Remote Sensing (NCRS). 1998. On-going works contributing to desertification studies. Beirut, Lebanon.
- Nieddu, G. 2006. La viticoltura in Sardegna e i vitigni locali. *Saperi e Sapori del Mediterraneo*. Am&d Ed. Cagliari, Italia.
- OECD. 2006. Environmental Indicators for Agriculture. Methods and Results Volume 3. OECD Publishing, Paris.
- Oki, T., Kanae, S. 2006. Global hydrological cycles and world water resources. *Science*, 313, 1068 1072.
- Oki, T., Sato, M., Kawamura, A., Miyake, M., Kanae, S., Musiake, K. 2003. Virtual water trade to Japan and in the world. In: Hoekstra A.Y. (Ed.), *Virtual Water Trade: Proceedings of the International Expert Meeting on Virtual Water Trade*. Value of Water Research Report Series 12, Delft, The Netherlands, pp. 221–235.
- Olesen, J.E., Bindi, M. 2002. Consequences of climate change for European agricultural productivity, land use and policy. *European Journal of Agronomy*, 16, 239–262.
- Onder, S., Caliskan, M.E., Onder, D., Caliskan, S. 2005. Different irrigation methods and water stress effects on potato yield and yield components. *Agricultural Water Management*, 73, 73–86.
- Oster, J.D., Meyer, L., Hermsmeier, L., Kaddah, M. 1986. Field studies of irrigation efficiency in Imperial Valley. University of California, Berkeley. *Hilgardia*, 54 (7), 1-15.
- Parry, M.L. 2000. Assessment of potential effects and adaptations for climate change in Europe. The Europe ACACIA Project. Jackson Environment Institute, University of East Anglia, Norwich, UK.
- Patumi, M., D'Andria, R., Marsilio, V., Fontanazza, G., Morelli, G., Lanza, B. 2002. Olive and olive oil quality after intensive monocone olive growing (*Olea europaea* L., cv. Kalamata) in different irrigation regimes. *Food Chemistry*, 77, 27–34.

- Penman, H.L. 1948. Natural evaporation from open water, bare soil and grass. *Proceedings of the Royal Society A. London*, 193, 120-146.
- Pereira, L.S, De Melo-Abreu, G.P. 2009. Vulnerability of Rainfed and Irrigated Agriculture to Climate Change. In: Eulisse E., Ceccato L. (Eds.), *Climate changes and natural resources: impact on water challenge*. Università Ca'Foscari di Venezia and Civiltà dell'Aqua, Italy, pp. 39-64.
- Playán, E., Mateos, L. 2006. Modernization and optimization of irrigation systems to increase water productivity. *Agricultural Water Management*, 80, 100–116.
- Playán, E., Slatni, A., Castillo, R., Faci, J.M. 2000. A case study for irrigation modernisation: II scenario analysis. *Agricultural Water Management*, 42, 335–354.
- Qadir, M., Boers, Th.M., Schubert, S., Ghafoor, A., Murtaza, G. 2003. Agricultural water management in water-starved countries: challenges and opportunities. *Agricultural Water Management*, 62, 165–185.
- Raskin, P., Gleick, P., Kirshen, P., Pontius, G., Strzepek, K. 1997. *Water futures: assessment of long-range patterns and prospects*. Stockholm Environment Institute, Stockholm, Sweden.
- Ratliff, L.F., Ritchie, J.T., Cassel, D.K. 1983. Field-measured limits of soil water availability as related to laboratory-measured properties. *Soil Science Society of America Journal*, 47, 770-775.
- Regione Sardegna. 2006. Piano stralcio di bacino regionale per l'utilizzazione delle risorse Idriche. www.regionesardegna.it
- Regione Sardegna. 2010. Piano di gestione del distretto idrografico della Sardegna: relazione generale. www.regionesardegna.it
- Riha, S.J., McKinnes, K.J., Childs, S.W., Campbell, G.S. 1980. A finite element calculation for determining thermal conductivity. *Soil Science Society of America Journal*, 44, 1323-1325.
- Rijsberman, F.R. 2006. Water scarcity: Fact or fiction? *Agricultural Water Management*, 80, 5–22.
- Rodríguez Díaz, J.A., Weatherhead, E.K., Knox, J.W., Camacho, E. 2007. Climate change impacts on irrigation water requirements in the Guadalquivir river basin in Spain. *Regional Environmental Change*, 7, 149–159.

- Roetter, R.P., Van Keulen, H. 2008. Food security. In: Roetter R.P, Van Keulen H., Kuiper M., Verhagen J., Van Laar H.H. (Eds.), Science for agriculture and rural development in low-income countries. Springer, Dordrecht, The Netherlands, pp 27–56.
- Rosenzweig, C., Tubiello, F.N. 1997. Impacts of global climate change on Mediterranean agriculture: current methodologies and future directions, an introductory essay. *Mitigation and Adaptation Strategies for Global Change*, 1, 219-232.
- Sammis, T.W. 1980. Comparison of sprinkler, trickle, subsurface and furrow irrigation methods for row crops. *Agronomy Journal*, 72, 701-704.
- Seckler, D., Amarasinghe, U., Molden, D.J., De Silva, R., Barker, R. 1998. World water demand and supply, 1990 to 2025: scenarios and issues. IWMI Research Report 19. IWMI, Colombo, Sri Lanka.
- Sepaskhah, A.R., Boersma, L. 1979. Thermal conductivity of soils as a function of temperature and water content. *Soil Science Society of America Journal*, 43, 439-444.
- Shalhevet, J., Bielorai, H. 1978. Crop water requirements in relation to climate and soil. *Soil Science*, 125 (4), 240-247.
- Shiklomanov, I.A. 1991. The world's water resources. In: Proceedings of the International Symposium to Commemorate 25 Years of the IHP, UNESCO/IHP, Paris, France, pp. 93–126.
- Shiklomanov, I.A. 1997. Assessment of water resources and water availability in the world. World Meteorological Organization/Stockholm Environment Institute, Geneva, Switzerland.
- Shiklomanov, I.A. 1998. World Water Resources: An appraisal for the 21st century. IHP Report. UNESCO, Paris, France.
- Sillmann, J., Roeckner, E. 2008. Indices for extreme events in projections of anthropogenic climate change. *Climatic Change*, 86, 83–104.
- Sinclair, T.R., Tanner, C.B., Bennett, J.M. 1983. Water-use efficiency in crop production. *BioScience*, 34 (1), 36-40.

- Singh, B., El Maayar, M., André, P., Bryant, C., Thouez, J.P. 1998. Impacts of a GHG-induced climate change on crop yields: effects of acceleration in maturation, moisture stress and optimal temperature. *Climatic Change*, 38, 51–86.
- Smith, L., Obeid A., Jensen, H. 2000. The geography and causes of food insecurity in developing countries. *Agricultural Economics*, 22, 199-215.
- Snyder, R.L. 2002. Crop coefficients. In: CNR (Ed.), *Advanced short course on agricultural, forest and micro meteorology*. Firenze, Italy, pp.256-267.
- Snyder, R.L, Geng, S., Orang, M., Sarreshteh, S. 2012. Calculation and simulation of evapotranspiration of applied water. *Journal of Integrative Agriculture*, 11 (3), 489-501.
- Spiegel, P. 1955. The water requirement of the olive tree, critical periods of moisture stress, and the effect of irrigation upon the oil content of the fruit. *Proceedings of 14th International Horticultural Congress, Netherlands*, 1363–1373
- SRES. 2000. *Emission Scenarios. A Special Report of IPCC, WG III. Summary for Policymakers*.
- Stanhill, G. 1986. Water use efficiency. *Advances in Agronomy*, 39, 53–85.
- Tetens, O. 1930. Uber einige meteorologische Begriffe. *Z. Geophys*, 6, 297-309.
- Todorovic, M., Caliandro, A., Albrizio, R. 2007. Irrigated agriculture and water use efficiency in Italy. In: Lamaddalena N., Shatanawi M., Todorovic M., Bogliotti C., Albrizio R. (Eds.), *Water use efficiency and water productivity: WASAMED project*, Bari, CIHEAM-IAMB. *Options Méditerranéennes: Série B. Etudes et Recherches n. 57*. Bari, Italy, pp. 102-138.
- Tognetti, R., Palladino, M., Minnocci, A., Delfino, S., Alvino, A. 2003. The response of sugar beet to drip and low-pressure sprinkler irrigation in southern Italy. *Agricultural Water Management*, 60, 135-155.
- Tognetti, R., d'Andria, R., Lavini, A, Morelli, G. 2006. The effect of deficit irrigation on crop yield and vegetative development of *Olea europaea* L. (cvs. Frantoio and Leccino). *European Journal of Agronomy*, 25, 356–364.
- Tubiello, F.N., Ewert, F. 2002. Modeling the effects of elevated CO₂ on crop growth and yield: a review. *European Journal of Agronomy*, 18(1–2), 57-74.

- Tubiello, F.N., Donatelli, M., Rosenzweig, C., Stockle, C.O. 2000. Effects of climate change and elevated CO₂ on cropping systems: Model predictions at two Italian locations. *European Journal of Agronomy*, 13, 179–189.
- United States Department of Agriculture (USDA). 1997. Irrigation guide, natural resources. www.usda.gov.
- Venezian Scarascia, M.E., Di Battista, F., Salvati, L. 2006. Water resources in Italy: availability and agricultural uses. *Irrigation and Drainage*, 55, 115–127.
- Vogt, J.V., Somma, F. 2000. Drought and drought mitigation in Europe. Kluwer, Dordrecht.
- Vörösmarty, C.J., Green, P.J., Salisbury, J., Lammers, R.B. 2000. Global water resources: vulnerability from climate change and population growth. *Science*, 289, 284–288.
- Wallace, J.S. 2000. Increasing agricultural water use efficiency to meet future food production. *Agriculture, Ecosystems and Environment*, 82, 105–119.
- Wallace, J.S., Gregory, P.J. 2002. Water resources and their use in food production. *Aquatic Sciences-Research Across Boundaries*, 64, 363–375.
- Watts, D.B., Kanemasu, E.T., Tanner, C.B. 1990. Modified heat-meter method for determining soil heat flux. *Agricultural and Forest Meteorology*, 49, 311-330.
- Wierenga, P.J., Nielson, D.R., Hagan, R.J. 1969. Thermal properties of a soil, based upon field and laboratory measurements. *Soil Science Society of America Journal*, 44, 354-360.
- Wigley, T.M.L. 1992. Future climate on the Mediterranean basin with particular emphasis on changes in precipitation. In: Jeftic L., Milliman J.D, Sestini G. (Eds.), *Climatic Change and the Mediterranean*. UNEP, New York, USA.
- Wilhite, D.A., Vanyarkho, O. 2000. Drought: pervasive impacts of a creeping phenomenon. In: Wilhite D.A. (Ed.), *Drought: a global assessment (Vol. I, Ch. 18)*. Routledge, London, UK.
- World Bank. 2000. *The little green data book*. Washington DC: World Bank.
- World Resources Institute (WRI). 2001. Environmental data tables. On-line Database of the World Resources Institute, Washington DC, USA. www.wri.org.
- Wright, J.L. 1982. New evapotranspiration crop coefficients. *Journal of the Irrigation and Drainage Division American Society of Civil Engineer*, 108 (IR2), 57-74.

- Yang, H., Reichert, P., Abbaspour, K., Zehnder, A.J.B. 2003. Water Resources threshold and its implications for food security. *Environmental Science & Technology*, 37, 3048-3054.
- Yang, H., Zehnder, A.J.B. 2002. Water Scarcity and Food Import: A Case Study for Southern Mediterranean Countries. *World Development*, 30 (8), 1413–1430.
- Yenesew, M., Tilahun, K. 2009. Yield and water use efficiency of deficit-irrigated maize in a semi-arid region of Ethiopia. *African Journal of Food, Agriculture, Nutrition and Development*, 9 (8), 1635-1651.
- Zalidis, G., Dimitriads, X., Antonopoulos, A., Geraki, A. 1997. Estimation of a network irrigation efficiency to cope with reduced water supply. *Irrigation and Drainage Systems*. 11, 337-345.

CHAPTER 2: INVESTIGATION ON THE REFERENCE EVAPOTRANSPIRATION DISTRIBUTION AT REGIONAL SCALE BY ALTERNATIVE METHODS TO COMPUTE THE FAO PENMAN-MONTEITH EQUATION

ABSTRACT

Water scarcity is nowadays one of main world issues, and because of the climate change projections it will be more important in future. Reference evapotranspiration (ET_o) is an extremely important agrometeorological variable, useful to assess the irrigation scheduling and management. The FAO Penman-Monteith (PM) equation is considered the most precise method to compute ET_o compared with many others. Sometimes the application of this method is restricted by the lack of the input variables that it takes into consideration. An easy way to compute ET_o is the application of the Hargreaves-Samani (HS) equation because it relies only air temperature data. Depending on the climate characteristics, however, the HS equation does not always provide optimal results. Because of high humidity and sometimes wind speed, Sardinia is one of those regions where the HS application could give poor results, but it does provide alternative methods to estimate ET_o when radiation, humidity, and wind speed data are missing. The accuracy, however, can be improved by calibrating the HS equation for the missing variables in a particular microclimate. In this research, calibration factors for ET_o computed with the HS were developed to obtain more accurate estimates of the PM equation ET_o in regions where climate data were limited. These calibrated HS ET_o values were used to improve the characterization of ET_o over the island. After computing daily ET_o with the PM and calibrated HS equations for all stations in Sardinia over the period of record, the inverse distance weighting (IDW), ordinary kriging (OK), and radial basis function (RBF) interpolation techniques were applied for mapping ET_o data. The substitution method gave optimal and statistically significant results ($RMSE=0.21$) compared with the calibration method ($RMSE=0.39$). Summer reference ET (June, July, and August) ranged from 4.5 to 6.3 mm day⁻¹. Among the three interpolation techniques taken in account, the OK computation better fitted the observed data, followed by the IDW and RBF models. Sardinia was divided into the four ET_o classes: 4.5-5, 5-5.5, 5.5-6, and 6-6.3 mm day⁻¹.

1. INTRODUCTION

Reference evapotranspiration is a parameter that quantifies evaporative demand of the environment, and it is used to estimate water losses from crops using the crop coefficient (K_c) method (Doorenbos and Pruitt, 1977; Jensen et al., 1990; Allen et al., 1998; Mavi and Tupper, 2004). Standardized reference evapotranspiration (ET_o) represents the evapotranspiration from a virtual surface having characteristics that are similar to a broad surface of C-3 species 12-cm tall, cool-season grass assuming no reductions in evaporation due to stress (Allen et al., 1998, 2005).

An accurate ET_o computation is the first step to assess crop water requirement (CWR), which is useful for planning irrigation scheduling. Knowing the actual CWR avoids water wastages due to excessive irrigation application and yield reduction due to under-irrigation.

Many methods to compute ET_o have been developed based on empirical equations that consider air temperature (Thorthwaite, 1948; Blaney-Criddle, 1950; Hargreaves, 1974; Linacre, 1977), theoretical equations which are based on solar radiation (Stanhill, 1961; Jensen and Haise, 1963; Caprio, 1974; Idso et al., 1977; Hargreaves and Samani, 1985), and combination methods (Penman, 1948, 1963; Monteith, 1965; Van Bavel, 1966; Priestley and Taylor, 1972).

The monthly and daily FAO Penman-Monteith equation (PM) from Allen et al. (1998) are identical to the monthly and daily Standardized Reference Evapotranspiration equation reported by the American Society of Civil Engineers (Allen et al., 2005) and the equations are widely considered the most precise method to estimate ET_o when compared to other equations as confirmed by De Souza and Yoder (1994), Chiew et al. (1995), Howell et al. (1997, 2000), Oliveria and Yoder (2000), Walter et al. (2000), Itenfisu (2003), Garcia et al. (2004), Yoder et al. (2005), Gavilán et al. (2006), and Sentelhas et al. (2010).

In some cases, computing ET_o with the PM method is difficult because of the unavailability of required data. In fact, many weather stations lack the sensors needed to record solar radiation, temperature, wind speed, and relative humidity, which are needed for the ET_o calculation. Another common problem is related to missing data due to malfunctioning of the sensors. Procedures to estimate missing parameters were provided by Allen et al. (1998). Following Allen et al. (1998), one can estimate actual vapour

pressure by assuming that the dew point temperature is near the daily minimum temperature. Air temperature differences are sometimes used to estimate missing solar radiation data.

Others have suggested to make use data from a nearby weather station to estimate missing solar radiation and/or wind speed data (Nonhebel, 1994; Hunt et al., 1998; Liu and Pereira, 2001; Trnka et al., 2005; Popova et al., 2006; Jabloun and Sahli, 2008; Sentelhas et al., 2010).

Several studies have used the Hargreaves-Samani (HS) equation, which employs only air temperature data, to estimate ET_o , but HS tends to fail in humid, very dry, and windy regions (Saeed, 1986; Jensen et al., 1990, Amatya et al., 1995; Allen et al., 1998; Temesgen et al., 1999; Samani, 2000; Droogers and Allen, 2002; Xu and Singh, 2002). Therefore, a local calibration for acceptable performance is necessary (Martinez-Cob and Tejero-Juste, 2004; Gavilán et al., 2006; Fooladmand and Haghghat, 2007).

ET_o estimation at the field or basin scale limits the use of the information to locations near the sample point. Estimating data on a regional scale is important to evaluate irrigation planning and crop management decisions (Zhao et al., 2005), and mapping data by a geographic information system (GIS) is a way to extend information in those locations where a direct estimation is not possible. Interpolation techniques range from simple to sophisticated (Stein et al., 1991; Bechini et al., 2000; Schloeder et al., 2001; Dalezios et al., 2002; Markidis et al., 2005; Qian et al., 2005; Zhao et al., 2005; Irmak and Ranade, 2008; Li et al., 2011).

Considering that Mediterranean basin is one of the most affected areas by climate change (IPCC, 2007), an accurate estimate of ET_o spatial distribution is helpful to assess crop water requirement and improve crop irrigation management. Sardinia (Italy) is an island located in the centre of Mediterranean Sea, and it was chosen as case study for this project. The objective of the study was to (1) assess alternative methods to estimate ET_o when missing meteorological variables occur, (2) compare different interpolation methods to predict the distribution of ET_o data at regional scale, and (3) define ET_o zones to be used to investigate the impact of climate change on irrigation water demand.

2. MATERIALS AND METHODS

2.1. Experimental site description

The study was conducted on the island of Sardinia, which is located in the center of the western Mediterranean basin (from 38°N to 41°N, and from 8°E to 10°E) and covers an area of about 24 000 km² (Figure 1).

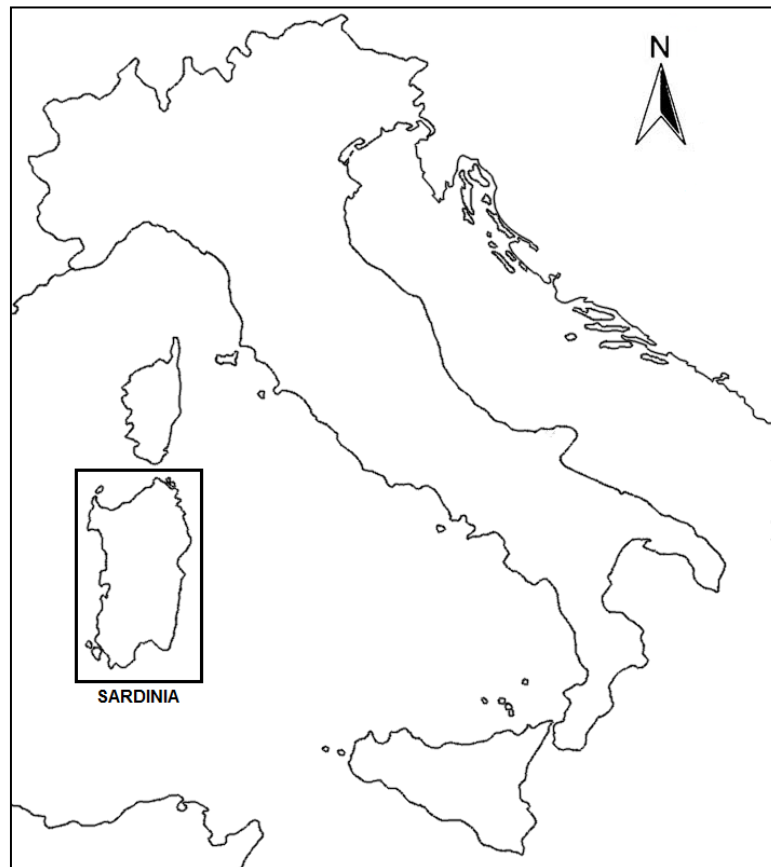


Figure 1. Experimental site.

The schematic geology of Sardinia is shown in Figure 2. It provides a macro-division in the Hercynian basement, post-Hercynian covers and Quaternary deposits. Metamorphic, igneous, and sedimentary rocks are approximately equally represented in the island (Carmignani et al., 2001).

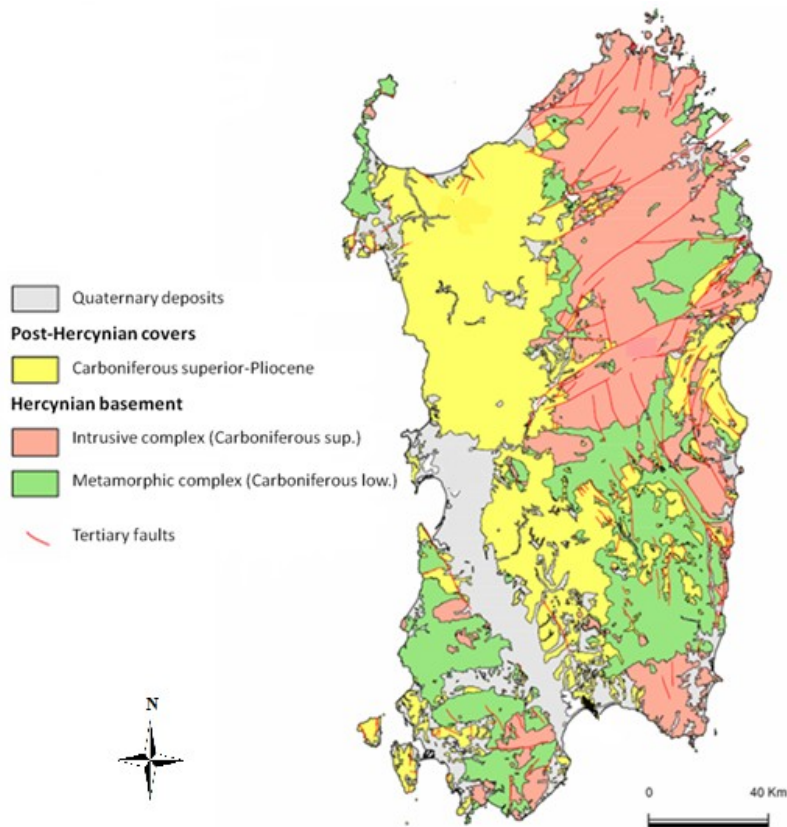


Figure 2. Main geological complex of Sardinia (Carmignani et al., 2001).

The topography in Sardinia varies from plain to hilly and mountainous areas (Figure 3), and the changes in elevation affect the climate conditions (Chessa and Delitala, 1997). In fact climate characteristics are determined by the spatial distribution of the mountain systems.

Sardinia has a Mediterranean climate, characterized by mild and rainy winters and relatively dry and warm summers. During summer (May–September), climate is influenced by the Azores Anticyclone regime that strongly reduces the penetration of Atlantic disturbances into the region, or the formation of local disturbances (Delitala et al., 2000). The presence of a relatively shallow enclosed sea dampens the excess of temperature. The spatial distribution of the average temperature is strongly related to the topography of the island. The mean annual maximum temperature ranges between 16 and 22 °C relative to the elevation classes. Maximum values are recorded for 0-30 m a.s.l., while minimum values are recorded in areas where the elevation is more than 1000 m a.s.l. The minimum annual temperature range between 7 and 14°C; higher values are recorded along the coast, with a proportional reduction of temperature in relation with the increase of the elevation.

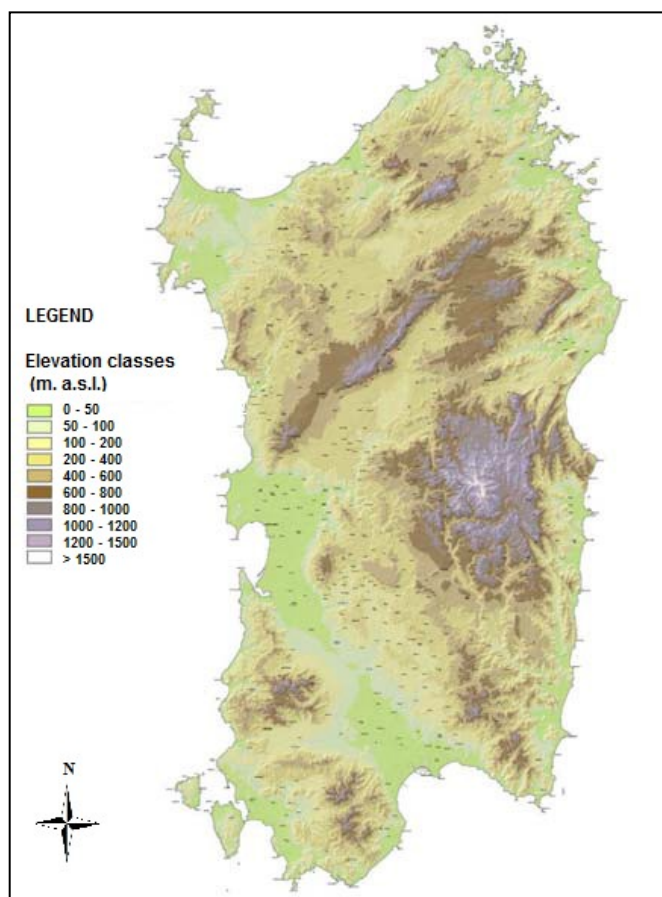


Figure 3. Sardinia topographic map with elevations in m a.s.l. (RAS, 2006).

The periods from March to April and from September to November are the transition phases from winter to summer and from summer to winter, where summer and winter are the two climatic seasons. During winter the mitigating effect of the sea prevails, while in summer the stabilizing effect of the midlatitude anticyclonical dominates, with a clear gradient of temperature in the north-south direction (Chessa and Delitala, 1997).

The mean annual precipitation values range from 400 to 1300 mm with bigger fluctuations on the east coast (ARPAS, 2009). The monthly pattern of rainfall also shows the presence of two seasons: (1) winter, which covers the period from October to April, and (2) summer, which covers the period from May to September. The transition between two seasons is particularly evident during September and October, when rainfall values range from 40-60 mm/month to 80-160 mm/month (Chessa and Delitala, 1997). Between April and May, the differences are less distinct.

The maximum cumulative precipitation occurs in December with 80% of the annual rainfall concentrated from October through April. The minimum values occur during July and August with some rare precipitation on the mountains (Chessa and Delitala, 1997).

Wind from the west and northwest dominate in Sardinia. Annual relative humidity percentages range from 75 to 100% for the maximum and between 45-75% for the minimum.

2.2. Data collection and ET_o computation

This study used meteorological data recorded from the following weather station networks:

- ARPA Sardegna, specialist regional hydro-weather-climate department, (ARPAS);
- Servizio Idrografico Regionale, regional agency for the hydrographical district (ID);

Figure 4 shows the distribution of the 60 meteorological stations in Sardinia that were used in this study.

Following the distinction proposed by Ashraf et al. (1997) weather station networks were divided into partial and full stations. When all variables needed for the PM equation are available, the station is considered a “full” weather station (ARPAS network). If there are insufficient data to calculate the PM ET_o , the station is a “partial” weather station (ID network).

A preliminary analysis of data was performed. For each station, data were organized by both month and year to assess the consistency of the original records. Stations that had more than 10% missing data were not considered for the study. In the end, daily meteorological data from 23 ARPAS network stations from 2000 to 2004, and daily maximum and minimum temperature from 37 stations of the ID network for 2000-2002, were used in this study.

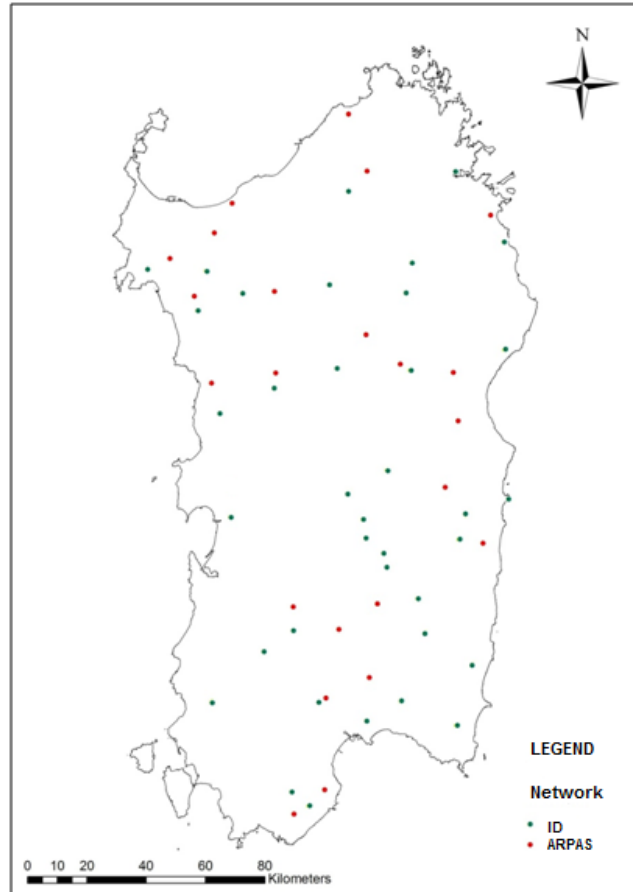


Figure 4. Geographical location of the 60 meteorological stations used in this study, Sardinia.

For each full station the daily reference evapotranspiration for short canopies over the period of record was computed using the standardized PM and HS equations.

FAO-56 Penman-Monteith equation (Allen et al., 1998, 2005) is expressed as:

$$ET_o = \frac{0.408\Delta(R_n - G) + \gamma(900/(T + 273)u_2)(e_s - e_a)}{\Delta + \gamma(1 + 0.34u_2)} \quad (1)$$

where ET_o (mm day^{-1}) is the daily (24-hour) standardized reference evapotranspiration; Δ is the slope of the saturated vapour pressure curve ($\text{kPa } ^\circ\text{C}^{-1}$); R_n is the net solar radiation ($\text{MJ m}^{-2} \text{day}^{-1}$); G is the soil heat flux density estimate ($\text{MJ m}^{-2}\text{day}^{-1}$); T ($^\circ\text{C}$) is the daily mean air temperature at 1.5 to 2 m height, (i.e. the mean of maximum (T_{max}) and minimum (T_{min}) temperatures); u_2 is the average wind speed at 2 m height (m s^{-1}); $(e_s - e_a)$ is the vapour pressure deficit (kPa), where e_s is the saturation vapour pressure at temperature T and e_a is the actual vapour pressure (or the saturation vapour pressure at the dew point temperature); and $\gamma \approx 0.0677 \text{ kPa } ^\circ\text{C}^{-1}$ is the psychrometric constant.

Following the suggestion of Allen et al. (2005) the e_a was calculated from the mean daily dew point (T_d) temperature (°C), which can be estimated from T_{max} and T_{min} and the maximum (RH_{max}) and minimum (RH_{min}) relative humidities. Moreover R_n was estimated from solar radiation, mean daily temperature, the mean daily vapour pressure, and the site latitude and elevation following Allen et al. (2005). For daily calculations, the ground heat flux sums to zero (i.e. $G \approx 0$).

Hargreaves-Samani equation (Hargreaves-Samani, 1985) is expressed as:

$$ET_o = C_o R_a (T + 17.8) \sqrt{T_{max} - T_{min}} \quad (2)$$

where ET_o (mm day⁻¹) is the reference ET ; $C_o = 0.023$ is an empirical constant; R_a is the extraterrestrial solar radiation (MJ m⁻² day⁻¹); T_{max} is the daily maximum air temperature (°C); T_{min} is the daily minimum air temperature (°C); and T is the mean air temperature (°C).

Since they represent the peak ET_o period of the year, the mean daily ET_o rate for the summer months (June, July and August) was computed for all of the full stations. These data were used to determine the ET_o zones for Sardinia.

Finally, a trend analysis between the PM and HS ET_o computation methods and wind speed was performed for the full stations. The PM and HS ET_o and wind speed values were normalized by dividing by the mean value of each variable to allow for a trend comparison between variables.

2.3. Alternative ET_o estimation methods for partial stations

Since for partial stations only the HS ET_o was possible to compute, two alternative methods to estimate the PM ET_o were assessed. The methods were:

a) **Calibration:** Finding a correction factor to estimate PM from HS ET_o using data from the full stations. The correction factor was determined as the slope of a linear regression of PM ET_o versus HS ET_o forced through the origin for each of the full stations (Figure 5). When applied to the partial stations, the factor is multiplied by the HS ET_o value to estimate the PM ET_o at that location. It assumes that the correction factor developed at a full station will also work at a nearby partial station. To test the method, ten pairs of nearby full stations were selected and one was deemed the

“training” and the other the “testing” station (Table 1, Figure 6). The calibration factor was determined using “training” station data. The product of the uncorrected HS ET_o (ET_{hs}) and the calibration factor (K_f) gives: $ET_{HS} = ET_{hs} \times K_f \approx ET_o$, where the lower case subscript (hs) indicates the uncorrected HS ET_o , the upper case subscript (HS) indicates the corrected HS ET_o , and ET_o is the PM ET_o . Using data from the “testing” station, the calibration is evaluated by comparing the ET_{HS} with the PM ET_o (ET_{PM}), which is calculated from the “testing” station dataset.

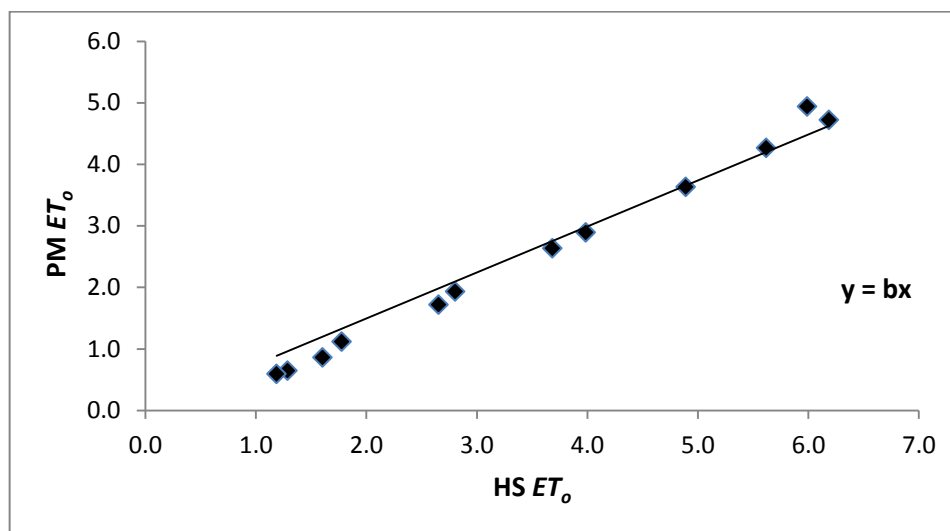


Figure 5. Graphic sample to compute the calibration factor.

Table 1. Ten station pairs chosen as trial set. For each pair the first station was considered the training and the second one was considered the testing.

PAIR	STATION	LONGITUDE E	LATITUDE N	ELEVATION (m a.s.l.)
1	Villa San Pietro	08° 58' 54"	39° 02' 34"	42
1	Decimomannu	08° 59' 09"	39° 19' 21"	20
2	Muravera	09° 35' 55"	39° 25' 09"	4
2	Dolianova	09° 09' 22"	39° 23' 05"	167
3	Macomer	08° 47' 10"	40° 18' 50"	664
3	Modolo	08° 31' 51"	40° 16' 57"	212
4	Dolianova	09° 09' 22"	39° 23' 05"	167
4	Guasila	09° 02' 14"	39° 31' 54"	242
5	Jerzu	09° 36' 23"	39° 47' 35"	46
5	Muravera	09° 35' 55"	39° 25' 09"	4
6	Benetutti	09° 08' 43"	40° 25' 50"	279
6	Nuoro	09° 16' 53"	40° 20' 28"	490
7	Sassari	08° 32' 19"	40° 44' 25"	150
7	Olmedo	08° 21' 44"	40° 39' 43"	32
8	Guasila	09° 02' 14"	39° 31' 54"	242
8	Siurgus Donigala	09° 11' 21"	39° 36' 35"	420
9	Olmedo	08° 21' 44"	40° 39' 43"	32
9	Putifigari	08° 27' 37"	40° 32' 49"	423
10	Aglientu	09° 04' 34"	41° 06' 13"	110
10	Luras	09° 09' 22"	40° 55' 47"	488



Figure 6. Distribution of the full stations chosen as trial set for calibration and substitution method.

b) **Substitution:** Using the temperature data from each partial station and substituting solar radiation, wind speed, and humidity data from a nearby full station provides a method to estimate PM ET_o (ET_{SB}) at partial stations, where ET_{SB} is the PM ET_o calculated using the substitution method. To evaluate the substitution method, the same ten pairs of full stations were used. The solar radiation, wind speed, and humidity data from the “training” station were substituted for the data at the “testing” station to calculate the ET_{SB} estimates of ET_o . Then the ET_{SB} results were compared with the ET_{PM} values that were determined using only data from the “testing” station.

For each station pair, the performance of the two methods was evaluated by regression analysis (Figures 7 and 8).

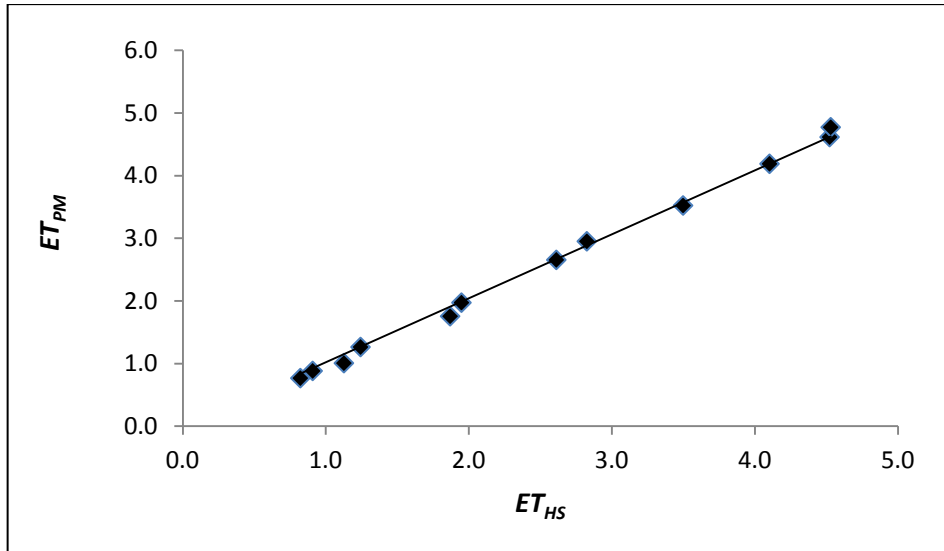


Figure 7. Graphic sample of the linear regression of ET_{PM} versus ET_{HS} for the calibration method.

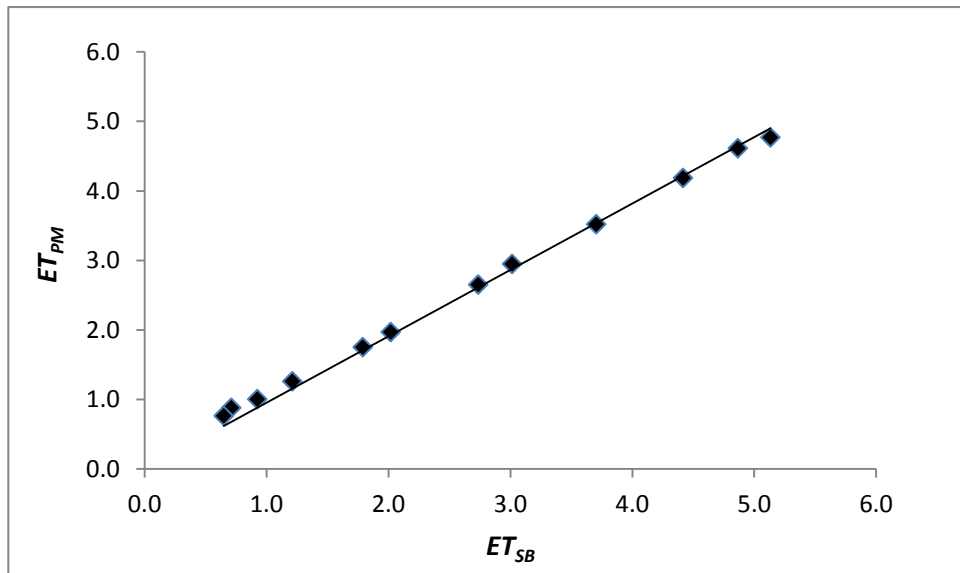


Figure 8. Graphic sample of the linear regression of ET_{PM} versus ET_{SB} for the substitution method.

The monthly mean ET_{PM} (mm day^{-1}) from January through December was regressed against ET_{HS} and ET_{SB} through the origin ($a=0$) using the ten “testing” stations. The slope (b) provides an estimate of the accuracy and R^2 is measure of precision.

The performance of the two alternative PM ET_o estimation methods, and also of the HS ET_o computation was evaluated using the $RMSE$ (mm day⁻¹) calculated with the following equations:

$$RMSE = \sqrt{\frac{1}{n} \sum_{i=1}^n (ET_{HS} - ET_{PM})^2} \quad (3)$$

$$RMSE = \sqrt{\frac{1}{n} \sum_{i=1}^n (ET_{SB} - PM ET_{PM})^2} \quad (4)$$

$$RMSE = \sqrt{\frac{1}{n} \sum_{i=1}^n (HS ET_o - PM ET_{PM})^2} \quad (5)$$

where and ET_{PM} is the PM ET_o , which was calculated with the “testing” station data, ET_{HS} is the calibration estimate, ET_{SB} is the substitution estimate, HS ET_o is the Hargreaves-Samani ET_o computation, and n is the number of samples.

To compare the performance of the different ET_o methods (calibration, substitution and Hargreaves-Samani) for the ten pairs of trial stations, the overall $RMSE$ averages for all methods analyzed were determined and submitted to the double sided t -test. The critical t -value ($P \leq 0.05$) for 18 degrees of freedom ($10 \times 2 - 2$) was 2.1. The hypothesis that the mean $RMSE$ values of different methods were different was accepted when t -value was greater than critical t .

Finally, the daily mean summer PM ET_o value in each partial station was calculated.

2.4. Spatial interpolation models for ET_o data

Three spatial analysis tools of ArcGIS 9.3 software (ESRI, 2008) were chosen to map ET_o . The tools included: inverse distance weighting (IDW), ordinary kriging (OK), and radial basis function (RBF). Moreover, the holdout method and k-fold techniques were used for cross validation.

Inverse Distance Weighting

The inverse distance weighting method estimates the predicted values in an area on the weighted average of neighbour sample values. The weight of each neighbour sample decreases with the increment of the distance.

The general interpolation formula follows (Lloyd, 2005):

$$\hat{z}(u_0) = \frac{\sum_{\alpha=1}^n z(u_\alpha) d_{\alpha 0}^{-r}}{\sum_{\alpha=1}^n d_{\alpha 0}^{-r}} \quad (6)$$

where $\hat{z}(u_0)$ indicates the estimate in a u_0 location, in relation to the number of neighbour sample observations $z(u_\alpha)$; d is the distance between sample point and u_0 . The exponent r determines the power of d on the estimate location; the higher the exponent value, the greater influence at the u_0 location by sample points. In this work a value of two for r was set and four neighbour stations around the estimated point were considered.

Ordinary Kriging

Ordinary kriging is a geostatistical procedure that uses a variogram model. It describes the spatial continuity of the input data to estimate values for an unsampled location (Isaaks and Srivastava, 1989). The relation among sample points and their distance are the fundamental concepts on which the interpolation technique is based. This concept is known as semivariance analysis, and it is evaluated before the kriging application. Semivariance is computed following Goovaerts (1997) as:

$$\gamma(h) = \frac{1}{2N(h)} \sum_{i=1}^{N(h)} [Z(x_i) - Z(x_i + h)]^2 \quad (7)$$

where $\gamma(h)$ is the estimate semivariance at a separation distance, or lag h ; $N(h)$ is the number of pairs for lag h ; $z(x_i)$ and $Z(x_i+h)$ are the observed values at point x_i and x_i+h , separated by h . Therefore, semivariogram is half of the variance, and it expresses the degree of similarity of the variable Z in two points separated by distance lag h .

The spatial correlation among sample points is based on the selection of the semivariogram model and some calibration factors (sill, nugget, range) that better

represent the distribution of the variable. Graphically, semivariogram presents $\gamma(h)$ as the y axis and h as the x axis. The range describes the threshold beyond which points are not correlated. Sill is the asymptote of the curve and represents the maximum value of semivariance. Nugget is the semivariogram model intercept on the y axis. Theoretically for a lag equal to zero, the semivariogram model should pass through the origin of the axes. If it does not occur it could be attributed to measurement errors or spatial sources of variation at distances smaller than the sampling interval. This phenomenon is known as the nugget effect.

Subsequent to semivariance analysis the OK method (Zhang, 2004) was applied:

$$Z = \sum_{i=1}^n \gamma_i Z_i \quad (8)$$

The aim in the OK method is to estimate the value at Z point through the sum of the product of available observations (Z_i) and the weight found in semivariance analysis (γ_i), where the sum is equal to one.

Radial Basis Function

The Radial Basis Function interpolation method minimizes the curvature of the estimated surface that passes exactly through a data point (Zhao et al., 2005). RBF is considered a thin plate interpolation that uses a formula for the surface interpolation from Mitas and Mitasova (1988): given n values of the phenomenon z^j , measured at discrete point x within a certain region of a d -dimensional space to find a function $F(x)$ so that

$$F(x) = z^j \quad (9)$$

where

$$\sum_{j=1}^n |z_j - F(x^j)|^2 w_j + w_0 I(F) = \text{minimum} \quad (10)$$

$$i = 1, 2, \dots, n$$

considering that w_j and w_0 are positive weights and $I(F)$ denotes the smoothness seminorm. According to Talmi and Gilat (1977) and Wahba (1990), the solution for the previous equation is the sum of two components:

$$F(x) = T(x) + \sum_{j=1}^n \lambda_j R(x, x^j) \quad i = 1, 2, \dots, n \quad (11)$$

where λ_j is a coefficient found by the solution of a system of linear equations, $T(x)$ is a ‘trend’ function and $R(x, x^j)$ is a basis function which has a form dependent on the choice of $I(F)$.

For this study a completely regularized spline option was chosen with a power 0.0002 and three neighbour stations around the estimated point were considered.

Cross validation techniques

Validation is a useful way to estimate model precision. For each interpolation method two cross validation techniques were applied: the holdout method and K-fold cross validation. The **holdout method** is the simplest kind of cross validation. The data set was randomly separated into two sets, called the training set, presenting 70% of data, and the testing set with the remaining 30%. To assess how much the model value estimation were different from the observed data (test set), the training set was used.

The model fit a function using the training set only. Then, the function is used to predict the output values for the data in the testing set. The **k-fold cross validation** is more rigorous than the holdout method. The data set was randomly divided into k subsets, and the holdout method is repeated k times; k=10 was used in this study. Each time, one of the k subsets was used as the test set and the other k-1 subsets were collected to form a training set. Then the average error across all ten trials was computed.

The performance of the three interpolation methods for each cross validation technique was assessed through the statistical analysis: mean absolute error (*MAE*), mean bias error (*MBE*), mean relative error (*MRE*) and *RMSE*:

$$MAE = \frac{1}{n} \sum_{i=1}^n \left| \hat{Z}_i - Z_i \right| \quad (12)$$

$$MBE = \frac{1}{n} \sum_{i=1}^n (\hat{Z}_i - Z_i) \quad (13)$$

$$MRE = \frac{1}{n} \sum_{i=1}^n \frac{|Z_i - \hat{Z}_i|}{Z_i} \quad (14)$$

$$RMSE = \sqrt{\frac{1}{n} \sum_{i=1}^n (\hat{Z}_i - Z_i)^2} \quad (15)$$

where n was the number of station points, Z_i and \hat{Z}_i were respectively observed and estimate values at the considered point i ($i=1,2,\dots, n$).

3. RESULTS AND DISCUSSION

3.1. Estimating daily ET_o by the FAO Penman-Monteith and Hargreaves-Samani methods for full stations

A preliminary analysis of data for full stations shows that the PM ET_o values range from 4.5 to 6.3 mm day⁻¹, while HS ET_o values range from 4.7 to 6.7 mm day⁻¹ (Table 2).

Table 2. Statistical summary of Hargreaves-Samani and Penman-Monteith ET_o computation for full stations.

	HS ET_o	PM ET_o
Minimum	4.7	4.5
Maximum	6.7	6.3
Mean	5.6	5.3
Median	5.8	5.3
Standard Deviation	0.5	0.4
Variance	0.2	0.2
Standard Error	0.1	0.1

The trend of ET_o data reported in Table 3 and Figure 9 shows a relation with the wind speed values. In fact, Hargreaves-Samani ET_o tends to overestimate ET_o compared to the PM equation when wind speeds are low (eg., Villa San Pietro, Decimomannu). The opposite situation occurs in those locations characterized by high wind speeds (e.g., Sardara and Domus de Maria). The difference between the two methods is particularly evident in stations that present extreme values for the wind speed. The reverse trend occurs when the wind speed is increasingly less than 2 m s⁻¹, even if some exceptions are noticed (e.g., Modolo and Olmedo).

Table 3. Mean daily ET_o (mm day^{-1}) value using Hargreaves-Samani and Penman-Monteith methods, and daily wind speed ($\text{m s}^{-1}\text{day}$) for full stations during summer months.

STATION	HS (mm day^{-1})	PM(mm day^{-1})	WIND SPEED ($\text{m s}^{-1}\text{ day}$)
Villa San Pietro	5.9	4.5	0.57
Decimomannu	5.9	4.6	0.95
Villagrande Strisaili	5.6	4.5	1.21
Jerzu	5.8	5.0	1.26
Dolianova	6.0	5.1	1.29
Benetutti	6.7	5.3	1.42
Nuoro	5.8	5.0	1.49
Bonnanaro	6.1	5.3	1.59
Guasila	6.0	5.3	1.59
Oliena	6.2	5.5	1.61
Modolo	4.7	5.2	1.76
Muravera	6.1	5.9	1.88
Siurgus Donigala	5.8	5.5	1.94
Putifigari	5.2	5.3	1.95
Olmedo	5.8	5.3	1.98
Sassari	4.9	5.2	1.98
Sorso	5.1	5.1	2.01
San Teodoro	5.2	5.5	2.08
Luras	5.3	5.5	2.36
Macomer	5.5	5.5	2.37
Aglientu	5.0	5.2	2.38
Domus de Maria	5.4	6.3	2.58
Sardara	5.6	6.1	3.26

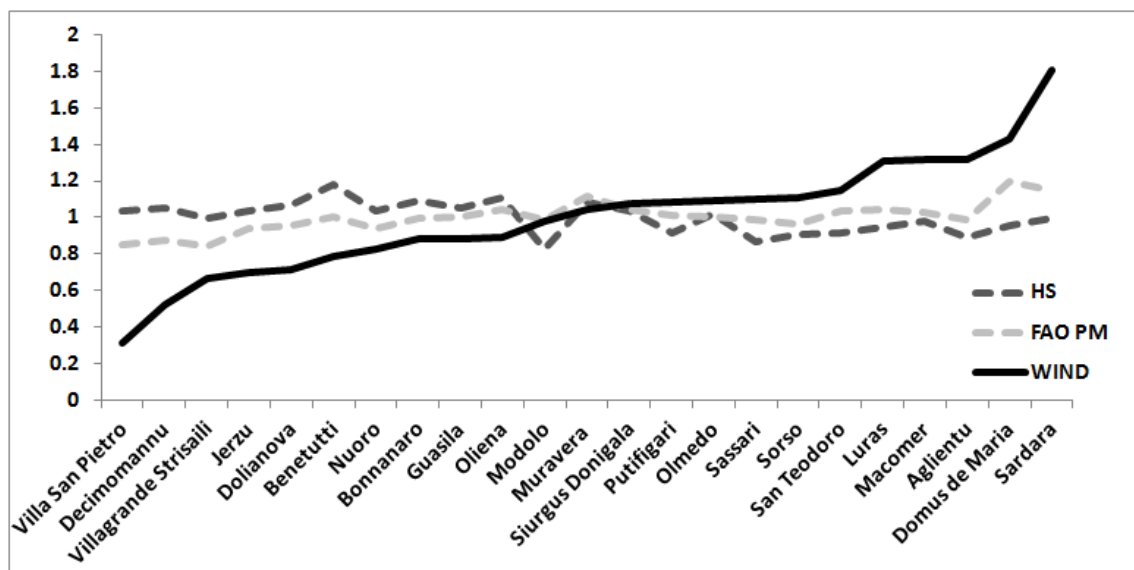


Figure 9. Trend analysis using standardize data of mean daily ET_o values computed by Hargreaves-Samani and Penman-Monteith methods, and daily wind speed for full stations during summer months.

Previous studies have discussed the inaccurate estimate of ET_o using HS computations and have proposed calibration methods to obtain better results. As pointed out by Martínez-Cob and Tejero-Juste (2004) no local calibration is needed for HS computation in windy locations (those where monthly average wind speeds above 2.0 m s^{-1} are frequent), while it is needed for low wind speed locations. Moreover the results showed by Gavilan et al. (2006) confirm that a regional calibration of HS equation in a semi-arid environment must be carried out considering only temperature and wind conditions.

3.2. Performance of alternative ET_o computation methods

The assessment of the calibration and substitution methods for ten station pairs is reported in Table 4. The coefficient of determination (R^2) was always between 0.98 and 1.00. Consequently, there was always a strong correlation between estimated and measured ET_o . The slopes of PM ET_o versus estimated ET_o , however, varied considerably by station pair (Table 4).

Table 4. Slope (b) and coefficient of regression (R^2) for the calibration (ET_{HS}) and substitution methods (ET_{SB}) in relation to ET_o computed using the FAO Penman-Monteith equation.

TRIAL LOCATION	ET_{HS} R^2	ET_{HS} b	ET_{SB} R^2	ET_{SB} b
Villa San Pietro-Decimomannu	1.00	1.02	1.00	0.96
Muravera-Dolianova	0.99	1.22	0.99	1.06
Macomer-Modolo	0.99	0.87	1.00	1.10
Dolianova-Guasila	1.00	0.92	0.99	0.95
Jerzu-Muravera	0.99	0.84	1.00	0.93
Benetutti-Nuoro	1.00	1.00	1.00	1.00
Sassari-Olmedo	1.00	1.20	0.98	1.04
Guasila-Siurgus Donigala	1.00	0.95	1.00	1.00
Olmedo-Putifigari	1.00	0.87	0.99	0.97
Aglientu-Luras	0.99	1.02	1.00	0.93

In some locations, both calibration methods overestimate or underestimate the PM ET_o , whereas, one method will overestimate and the other underestimate at other locations. Except for the Benetutti-Nuoro station pair, where $b=1$ for both methods, b

varied for other sites. For the calibration method, $b > 1$ indicates an underestimation for four of the pairs and $b < 1$ for the other five pairs. The substitution method had $b > 1$ three times and $b < 1$ five times.

The accuracy and precision for both methods was high (Table 5); however, a homogeneous trend was not observed. Differences among HS, substitute, and calibrated estimates of PM ET_o were marked. In some locations (e.g., Benetutti-Nuoro, Villa San Pietro-Decimomannu, Dolianova-Guasila) HS presented much higher *RMSE* values than the other methods. For other station pairs, the difference between HS and the calibrated PM was small (e.g., Jerzu-Muravera, Aglientu-Luras).

Table 5. Annual *RMSE* (mm day^{-1}) values for reference *ET* computed by using HS equation, calibration and substitution methods in ten trial stations (bold fonts depict the lowest values).

TRIAL LOCATION	<i>RMSE</i> HS	<i>RMSE</i> Calibration	<i>RMSE</i> Substitution
Villa San Pietro-Decimomannu	0.90	0.10	0.17
Muravera-Dolianova	0.14	0.65	0.23
Macomer-Modolo	0.17	0.52	0.32
Dolianova-Guasila	0.71	0.31	0.22
Jerzu-Muravera	0.63	0.64	0.26
Benetutti-Nuoro	0.53	0.12	0.07
Sassari-Olmedo	0.33	0.62	0.24
Guasila-Siurgus Donigala	0.42	0.22	0.17
Olmedo-Putifigari	0.43	0.55	0.19
Aglientu-Luras	0.22	0.20	0.28

In five trials of ten, the calibration method had lower *RMSE* than the HS ET_o . In seven trials of ten, the substitution method had lower *RMSE* values than the HS ET_o . For two of three trials where the substitution method had higher *RMSE* than the HS ET_o , the values were lower than those from the calibration method. For the ten trial locations, the mean annual *RMSE* values were 0.45, 0.39, and 0.21 mm day^{-1} respectively for HS, calibration, and substitution methods.

The *t* test ($P \leq 0.05$) showed that the substitution method was significantly different ($P\text{-value} = 0.03$) from the calibration method, while the HS and calibration methods were not statistically different ($P\text{-value} = 0.59$) (Table 6).

Table 6. Average *RMSE* ranking for evapotranspiration estimated with Hargreaves-Samani equation, calibration and substitution methods.

Rank	Method	Average <i>RMSE</i>
1	PM substitution	0.21 ^a
2	PM calibration	0.39 ^b
3	HS	0.45 ^b

The averages followed by the same letter are not statistically different ($P \leq 0.05$).

Therefore, the substitution method was chosen to estimate the PM ET_o for the ID network stations. Figure 10 shows the mean summer ET_o (mm day^{-1}) values for all 60 meteorological stations on a Sardinian digital elevation map (DEM). The summer ET_o ranged from 4.5 to 6.3 mm day^{-1} . Allocation values were homogeneously distributed. The south-west area showed the maximum values, while the central east and extreme south showed the lowest ET_o .

Problems related to missing data make the application of the estimation procedure difficult. As suggested by Ashraf et al. (1997), however, a mixture of full and partial weather stations in a country would be more economical than only full stations in relation to network design and variable interpolation methods. Many different studies were conducted using estimated variables, and difficulties due to missing data were overcome considering various approaches. As suggested by Allen et al. (1998), the use of the wind speed from the nearby station when conditions are uniform has given good results in studies by Popova et al. (2006) for the Trace plain (south Bulgaria), and Sentelhas et al. (2010) in Southern Ontario, Canada. Among methods suggested to estimate solar radiation the results obtained using observed solar radiation data from the nearby station have shown a better performance than the application of estimation procedures when the distance between weather stations is small (Nonhebel, 1994; Hunt et al., 1998; Trnka et al., 2005). In fact, results obtained by Hunt et al. (1998) indicated that it would be preferable to use measured radiation values if the distance between sites is less than 390 km instead of using temperature difference methods such as Hargreaves-Samani. Trnka et al. (2005) confirmed the technique by proving that the accuracy of daily radiation estimates decreased with increasing distance between stations. Indeed, they showed that the R^2 decreased from 0.95 to 0.60 as the distance increased from 17 to 369 km.

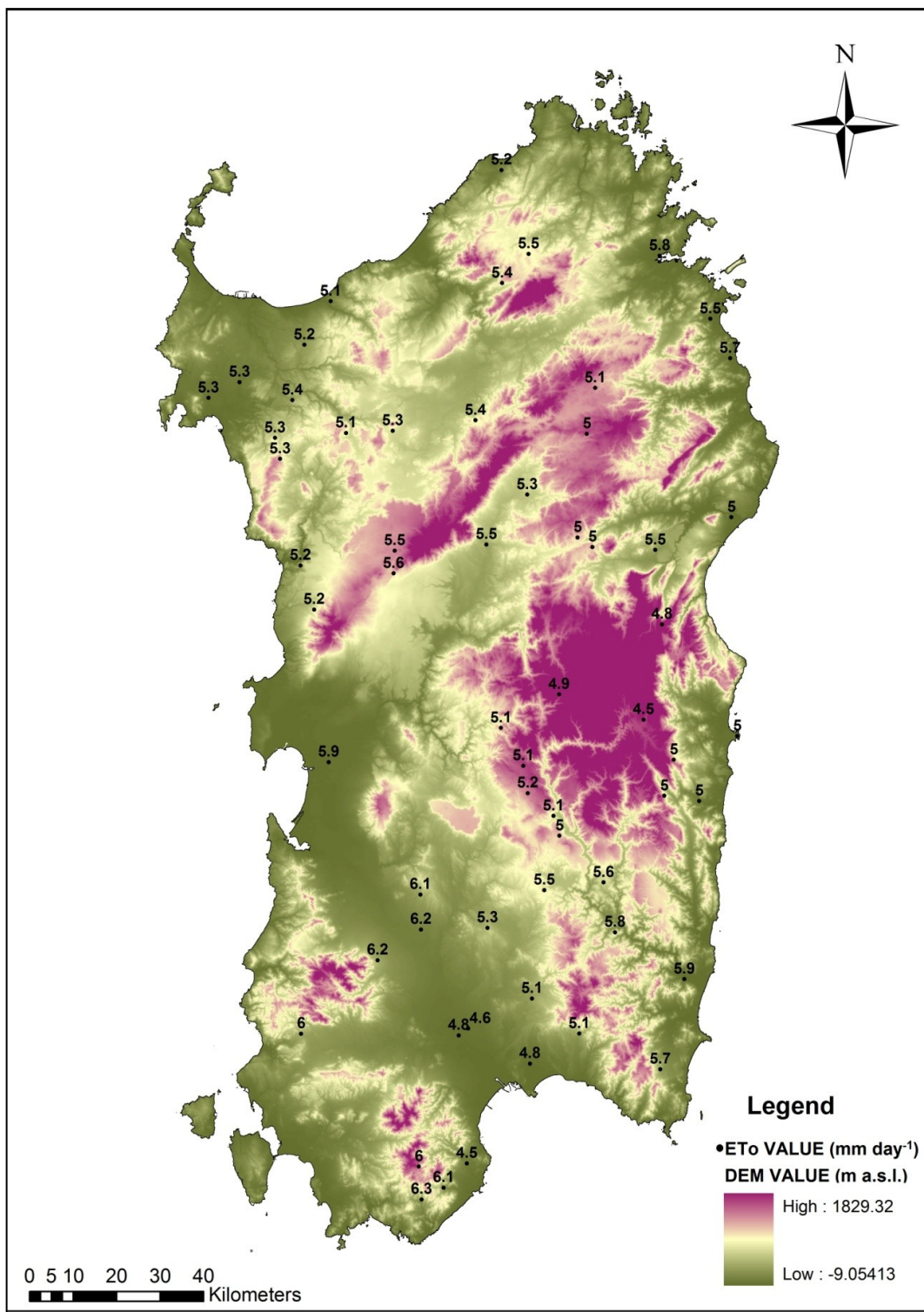


Figure 10. Mean summer ET_0 ($mm\ day^{-1}$) values computed using the FAO Penman-Monteith method for 60 meteorological stations in Sardinia.

3.3. Interpolation model test

The tetra spherical model of the semivariogram successfully fit ET_o values in Sardinia. It takes into account five neighbour stations around a sample point. Sill and nugget were set equal to 0.3 and 0.0, respectively.

The statistical analysis for OK generally showed the best performance (Table 7). RBF often performed poorly. The $RMSE$ values ranged from 0.290 and 0.410 mm day^{-1} for the k-fold validation, and between 0.421 and 0.472 for the holdout method. In terms of k-fold validation, OK showed the lowest $RMSE$ value, while for the holdout method, the RBF interpolation gave the lowest error.

Table 7. Assessment of three interpolation methods as well as two cross validation techniques for ET_o in Sardinia (bold fonts depict the lowest values).

Statistical index	Model	k-fold	holdout
RMSE	IDW	0.290	0.472
	OK	0.250	0.424
	RBF	0.410	0.421
MAE	IDW	0.224	0.279
	OK	0.184	0.258
	RBF	0.333	0.284
MBE	IDW	-0.054	-0.016
	OK	-0.033	0.005
	RBF	-0.044	0.011
MRE	IDW	0.042	0.053
	OK	0.036	0.049
	RBF	0.061	0.054

With respect to mean absolute error, OK had the best performance in both cross validation techniques. RBF gave the highest error (0.333 and 0.284 mm day^{-1}) in both cross validation computations. Taking into consideration the mean bias error, a slight underestimation by k-fold validation for all interpolation models was found. Except for IDW, the holdout computation slightly overestimated ET_o values. The mean relative error confirmed that OK was the optimal interpolation model. Therefore, OK was used to interpolate ET_o data.

The holdout evaluation can have a high variance. The evaluation may depend heavily on which data points end up in the training set and which end up in the test set. Thus, the evaluation may be significantly different depending on how the division is

made. The advantage of the k-fold validation method is that it matters less how the data are divided. Every data point is included in a test set exactly once and in a training set k-1 times. The disadvantage of this method is that the training algorithm has to be rerun k times, which means it takes k times as much computation to make an evaluation. In this work the k-fold validation method gave the best results.

The derived Sardinian ET_o map is shown in Figure 11. The observed summer ET_o ranges were 4.5-5 to 6-6.3 mm day⁻¹, so the map was separated into classes 4.5-5, 5-5.5, 5.5-6, 6-6.3 mm day⁻¹, and each zone represents a range of approximately 0.5 mm day⁻¹. The lowest class is located in the central-east mountains and south coastal zone.

Considering the weather conditions trend for representative stations, Villagrande Strisaili (813 m a.s.l.) had a higher wind speed than Decimomannu (20 m a.s.l.) (Figure 12). On the other hand, Decimomannu had higher air temperature (Figure 13 a, b) and dew point temperature (Figure 14) than Villagrande Strisaili, even though both stations recorded the same solar radiation value (Figure 15).

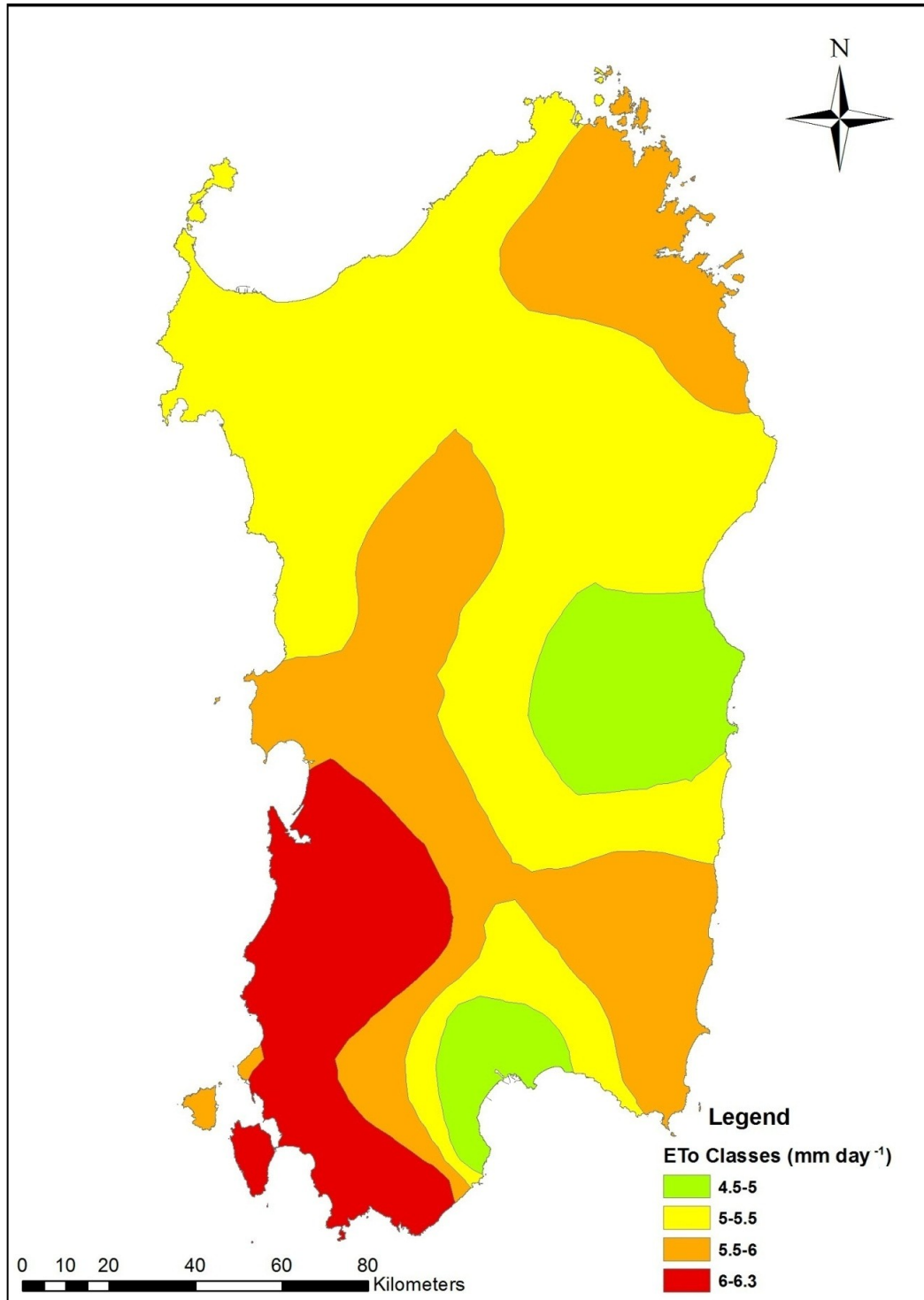


Figure 11. Sardinian summer ET_0 (mm day^{-1}) classes map computed by ordinary kriging.

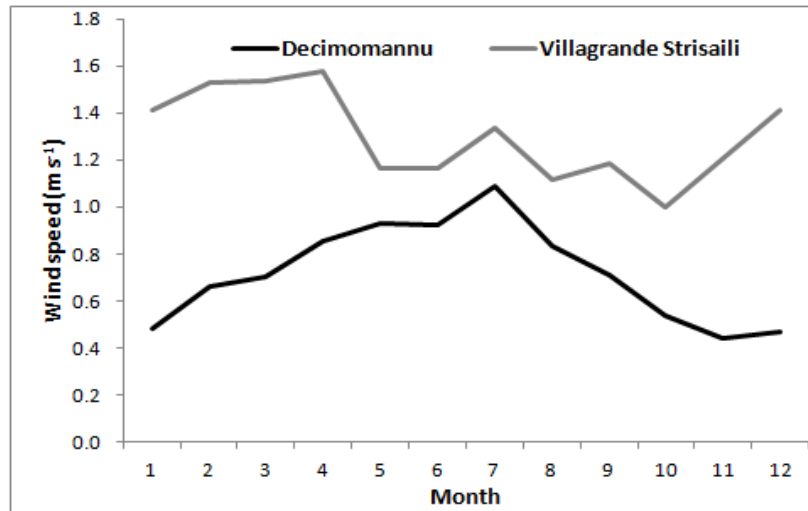


Figure 12. Wind speed annual trend (m s^{-1}) in Decimomannu and Villagrande Strisaili locations.

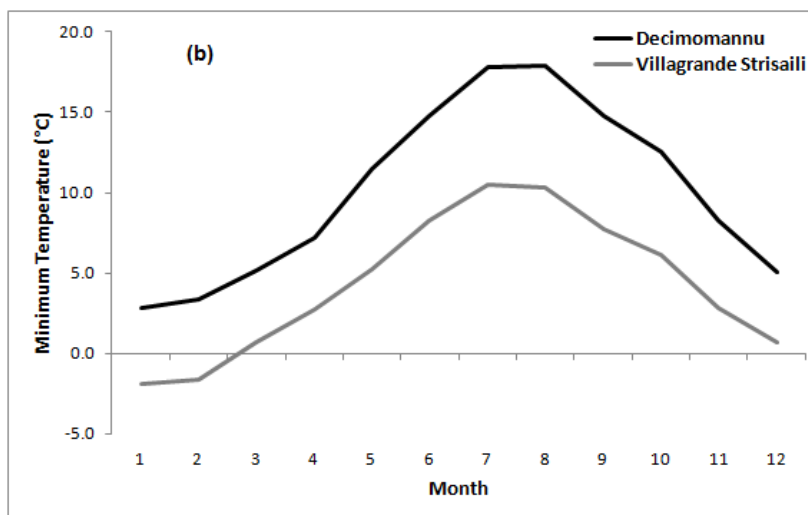
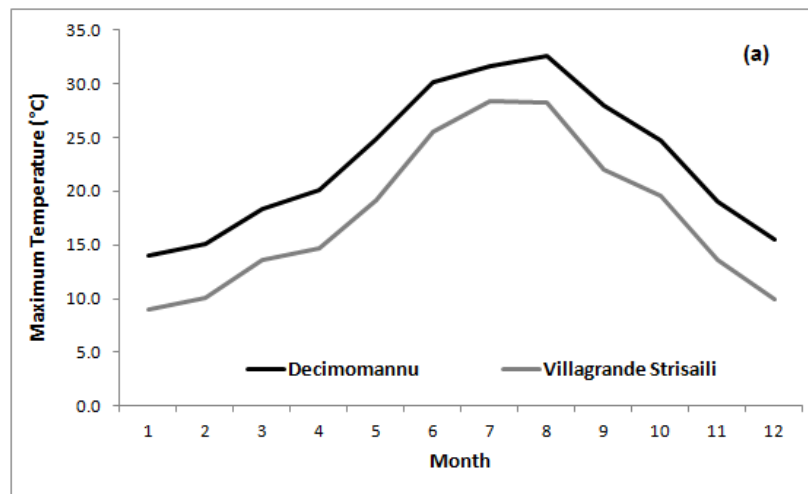


Figure 13. Maximum temperature (a) and minimum temperature (b) annual trends for Decimomannu and Villagrande Strisaili stations.

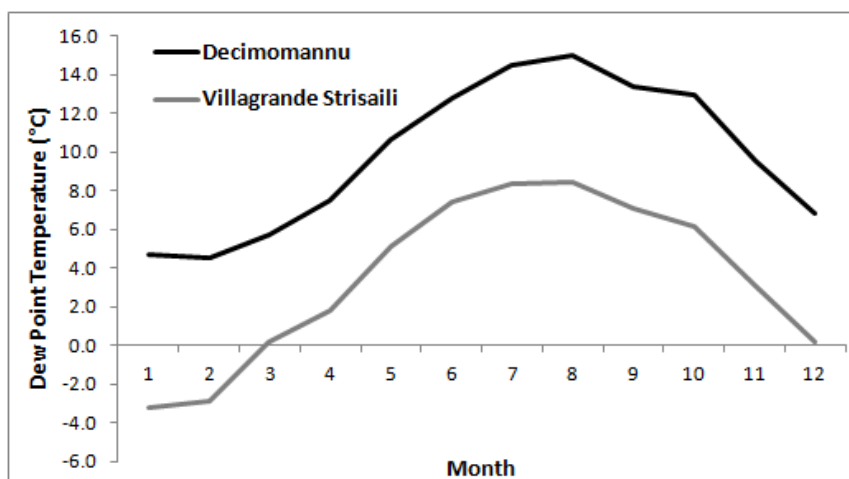


Figure 14. Dew point temperature annual trends (°C) for Decimomannu and Villagrande Strisaili stations.

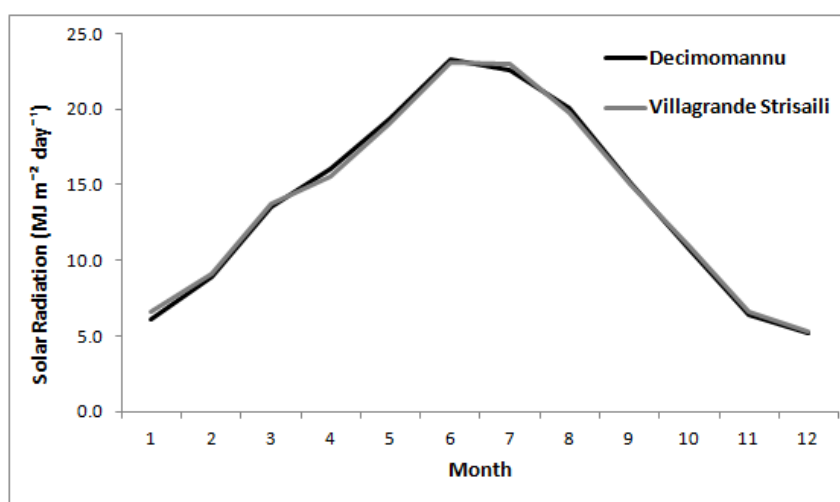


Figure 15. Solar radiation annual trend (MJ m⁻²day⁻¹) for Decimomannu and Villagrande Strisaili locations.

Geographic information system provides many options for interpolation models and procedures. Two common procedures are applied in different studies. One is to calculate first and interpolate later (CI) (De Wit and Van Keulen, 1985; Bouma, 1989; Stein et al., 1988a, b; Li et al., 2011), and the other is to interpolate first and calculate later (IC) (De Wit and Van Keulen, 1985, Li et al., 2011). In this study the CI procedure was considered. Stein et al. (1991) and Bechini et al. (2000) tried both methods, and the CI was considered the best. Otherwise, Li et al. (2011), in assessing both procedures on the yield response factor on winter wheat, discovered that IC was the optimal procedure. On the contrary, Markidis et al. (2005) assessed that the CI and IC procedures were

similar since they had no effect on the performance of the four interpolation methods for the prediction of ET_o .

With respect to different interpolation methods, the ordinary kriging, inverse distance weighting, and radial basis function methodologies are frequently applied. Results similar to those obtained in this study were shown by Zhao et al. (2005) who studied the spatial distribution of air temperature. In fact, RBF produced the worst results, while ordinary kriging showed the smallest prediction errors. The same results were confirmed by Qian et al. (2005) and Schloeder et al (2001), however, not much difference between OK and IDW was observed. Working on temperature, Irmak and Ranade (2008) verified that OK gives better results than the others methods.

Dalezios et al. (2002) investigated spatial variability of ET_o in Greece. They confirmed that the overall results of the kriging technique indicate that geostatistics can be successfully applied to describe the spatial variability of ET_o over large geographical regions.

Several studies consider more sophisticated geostatistical methods. They are based on empirical equation related to the digital elevation map (Hong et al., 2005; Tong et al., 2007) or regression equations that are useful to build a correction model related to local topography and slope gradient (Safanda, 1999; Liu, 2002; Zhao, 2003).

The results obtained from different interpolation methods often show great differences, and it is impossible to declare uniquely which is the optimal method. Comparison among interpolation methods is a way to determine the most advantageous approach for a specific situation.

4. CONCLUSIONS

This study derived a regional ET_o distribution map for Sardinia based on weather station data. To obtain an accurate ET_o computation, the FAO Penman-Monteith and Hargreaves-Samani equations were applied. Results showed that the difference between the FAO Penman-Monteith and Hargreaves-Samani equations were evident in relation to Sardinian climatic characteristics.

Different methodologies were applied to address the missing data problem and interpolation models uncertainty. An easy way to compute the PM equation, even if some weather data are missing, is to make use of observed data from the nearby station

when the climatic and topographic conditions are homogeneous. Using this procedure improved the estimates of PM ET_o with a $RMSE= 0.21$. It performed better than using a correction factor between the FAO Penman-Monteith and the Hargreaves-Samani, which had a $RMSE=0.39$. Among the three interpolation techniques investigated, the ordinary kriging model fitted the observed data better; followed by the inverse distance weighting and the radial bias function.

Using station data points to create a regional map simplifies the zonation of ET_o when large scale computations are needed. Making a distinction based on ET_o classes allows the simulation of crop water requirements for large areas and potentially leads to improved irrigation management and water savings.

REFERENCES

- Allen, R.G., Pereira, L.S., Raes, D., Smith, M. 1998. Crop evapotranspiration. Guidelines for computing crop water requirements. FAO Irrigation and Drainage Paper No. 56.
- Allen, R.G., Walter, I.A., Elliott, R.L., Howell, T.A., Itenfisu, D., Jensen, M.E., Snyder, R.L. 2005. The ASCE Standardized Reference Evapotranspiration Equation. American Society of Civil Engineers, Reston, VA.
- Amatya, D.M., Skaggs, R.W., Gregory, J.D. 1995. Comparison of methods for estimating REF-ET. Journal of Irrigation and Drainage Engineering, 121 (6), 427–435.
- ARPAS. 2009. Analisi agrometeorologica e climatica della stagione piovosa 2008-2009. <http://www.sar.sardegna.it/pubblicazioni/notetecniche/nota2/index.asp>
- Ashraf, M., Loftis, J.C., Hubbard, K.G. 1997. Application of geostatistics to evaluate partial weather station networks. Agricultural Forest Meteorology, 84, 255–271.
- Bechini, L., Ducco, G., Donatelli, M., Stein, A. 2000. Modelling, interpolation and stochastic simulation in space and time of global solar radiation. Agriculture, Ecosystems and Environment, 81, 29–42.

- Blaney, H.P., Criddle, W.D. 1950. Determining water requirements in irrigated areas from climatological and irrigation data. USDA Soil of Conservation Service, Technical Paper 96.
- Bouma, J. 1989. Using soil survey data for quantitative land evaluation. *Advances in Soil Science*, 9, 177-213.
- Caprio, J.M. 1974. The solar thermal unit concept in problems related to plant development and potential evapotranspiration. In: Lieth H. (ed.), *Phenology and Seasonality Modeling. Ecological Studies*. Springer Verlag, New York, pp. 353–364.
- Carmignani, L., Oggiano, G., Barca, S., Conti, P., Salvadori, I., Eltrudis, A., Funedda, A., Pasci, S. 2001. *Geologie della Sardegna – Note illustrative della Carta Geologica della Sardegna a scala 1:200.000 – Memorie Descrittive Carta Geologica d’Italia, Vol. LX*.
- Chessa, P., Delitala, A. 1997. *Il Clima della Sardegna*. Chiarella, Sassari, Italia.
- Chiew, F.H.S., Kamaladasa, N.N., Malano, H.M., McMahon, T.A. 1995. Penman-Monteith, FAO-24 reference crop evapotranspiration and class-A pan data in Australia. *Agricultural Water Management*, 28, 9–21.
- Dalezios, N.R., Loukas, A., Bampzelis, D. 2002. Spatial variability of reference evapotranspiration in Greece. *Physics and Chemistry of the Earth*, 27, 1031–1038.
- De Wit, C.T., Van Keulen, H. 1985. Modelling production of field crops and its requirements. *Geoderma*, 40, 253-267.
- Delitala, A.M.S., Cesari, D., Chessa, P.A., Ward, N.M. 2000. Precipitation over Sardinia (Italy) during the 1946–1993 rainy seasons and associated large-scale climate variations. *International Journal of Climatology*, 20, 519–541.
- De Souza, F., Yoder, R.E. 1994. ET estimation in the northeast of Brazil: Hargreaves or Penman–Monteith Equation? *Proceedings of ASAE International Winter Meeting*, Technical Paper No. 942545, St. Joseph, Michigan.
- Doorenbos, J., Pruitt, W.O. 1977. Guidelines for predicting crop water requirements. *Irrigation and Drainage Paper 24*, 2nd ed. Food and Agriculture Organization of the United Nations, Rome.

- Droogers, P., Allen, R.G. 2002. Estimating reference evapotranspiration under inaccurate data conditions. *Irrigation and Drainage Systems*, 16, 33–45.
- ESRI. 2008. ArcGIS Desktop. Ver. 9.3. Redlands, CA, ESRI Inc.
- Fooladmand, H.R., Haghighat, M. 2007. Spatial and temporal calibration of Hargreaves equation for calculating monthly reference evapotranspiration based on Penman–Monteith method. *Irrigation and Drainage*, 56, 439–449.
- Garcia, M., Raes, D., Allen, R., Herbas, C. 2004. Dynamics of reference evapotranspiration in the Bolivian highlands (Altiplano). *Agricultural Forest Meteorology*, 125, 67–82.
- Gavilán, P., Lorite, I.J., Tornero, S., Berengena, J. 2006. Regional calibration of Hargreaves equation for estimating reference ET in a semiarid environment. *Agricultural Water Management*, 81, 257–281.
- Goovaerts, P. 1997. *Geostatistics for natural resources evaluation*. Oxford University Press, New York.
- Hargreaves, G.H. 1974. Estimation of potential and crop evapotranspiration. *Transactions of the ASAE*, 17 (4), 701–704.
- Hargreaves, G.H., Samani, Z.A. 1985. Reference crop evapotranspiration from temperature. *Applied Engineering Agriculture*, 1, 96-99.
- Hong, Y., Nix, H.A., Hutchinson, M.F., Booth, T.H. 2005. Spatial interpolation of monthly mean climate data for China. *International Journal of Climatology*, 25, 1369–1379.
- Howell, T.A., Steiner, J.L., Schneider, A.D., Evett, S.R., Tolk, J.A. 1997. Seasonal and maximum daily evapotranspiration of irrigated winter wheat, sorghum and corn – Southern High Plains. *Transactions of the ASAE* 40 (3), 623–634.
- Howell, T.A., Evett, S.R., Schneider, A.D., Dusek, D.A., Copeland, K.S. 2000. Irrigated fescue grass ET compared with calculated reference ET. *Proceedings of the 4th ASAE National Irrigation Symposium*, St. Joseph, Michigan, 228–242.
- Hunt, L.A., Kuchar, L., Swanton, C.J. 1998. Estimation of solar radiation for use in crop modeling. *Agricultural and Forest Meteorology*, 91, 293-300.

- Idso, S.B., Reginato, R.J., Jackson, R.D. 1977. An equation for potential evaporation from soil, water and crop surfaces adaptable to use by remote sensing. *Geophysical Research Letters*, 4, 187–188.
- Intergovernmental Panel on Climate Change (IPCC). 2007. Fourth IPCC Assessment Report (AR4): Climate Change 2007. Cambridge University Press.
- Irmak, A., Ranade, P.K. 2008. GIS based estimation of spatial distribution of temperature and evapotranspiration in Nebraska. Proceedings of ASABE Annual International Meeting, June 29 – July 2, 2008, Providence, Rhode Island.
- Isaaks, E.H., Srivastava, R.M. 1989. An introduction to applied geostatistics. Oxford University Press, New York.
- Itenfisu, D., Elliott, R.L., Allen, R.G., Walter, I.A. 2003. Comparison of reference evapotranspiration calculations as part of the ASCE standardization effort. *Journal of Irrigation and Drainage Engineering*, 129 (6), 440–448.
- Jabloun, M., Sahli, A. 2008. Evaluation of FAO-56 methodology for estimating reference evapotranspiration using limited climatic data Application to Tunisia. *Agricultural Water Management*, 95, 707-715.
- Jensen, M.E. Haise, H.R. 1963. Estimating evapotranspiration from solar radiation. *Journal of the Irrigation and Drainage Division. Proceedings of ASCE*, 89, 15–41.
- Jensen, M.E., Burman, R.D., Allen, R.G. 1990. Evapotranspiration and Irrigation Water Requirements. ASCE Manuals and Reports on Engineering Practice No. 70, American Society of Civil Engineers, New York.
- Li, X., Tong, L., Kang, S., Li, F. 2011. Comparison of spatial interpolation methods for yield response factor of winter wheat and its spatial distribution in Haihe basin of north China. *Irrigation Science*, 29, 455–468.
- Linacre, E.T. 1977. A simple formula for estimating evaporation rates in various climates using temperature data alone. *Agricultural Meteorology*, 18 (6), 409–424.
- Liu, Y. 2002. Studies on modeling of mountain climate and forest zone in the middle and the east of the Qilian mountain based on GIS (in Chinese with English abstract). PhD Dissertation, Institute of Geographic Science and Nature Resources Research, CAS, Beijing, China.

- Liu, Y., Pereira, L.S. 2001. Calculation methods for reference evapotranspiration with limited weather data (in Chinese), *Journal of Hydraulics Engineering* 3, 11–17.
- Lloyd, C.D. 2005. Assessing the effect of integrating elevation data into the estimation of monthly precipitation in Great Britain. *Journal of Hydrology*, 308, 128-150.
- Mardikis, M.G., Kalivas, D.P., Kollias, V.J. 2005. Comparison of Interpolation Methods for the Prediction of Reference Evapotranspiration—An Application in Greece. *Water Resources Management*, 19, 251–278.
- Martinez-Cob, A., Tejero-Juste, M. 2004. A wind-based qualitative calibration of the Hargreaves ETo estimation equation in semiarid regions. *Agricultural Water Management*, 64, 251–264.
- Mavi, H.S., Tupper, G.J. 2004. *Agrometeorology-Principles and applications of climate studies in agriculture*. Food Products Press, New York.
- Mitas, L., Mitasova, H. 1988. General variational approach to the interpolation problem. *Computers & Mathematics with Applications*, 16 (12), 983–992.
- Monteith, J.L. 1965. Evaporation and environment. *Proceedings of the 19th Symposium of the Society of Experimental Biology*, Vol. 19, University Press, Cambridge, 205–233.
- Nonhebel, S. 1994. Inaccuracies in weather data and their effects on crop growth simulation results. *Climate Research*, 4, 47-60.
- Oliveira, C.W., Yoder, R.E. 2000. Evaluation of daily reference evapotranspiration estimation methods for a location in the southern USA. ASAE Paper No. 002030. St. Joseph, Michigan.
- Penman, H.L. 1948. Natural evaporation from open water, bare soil and grass. *Proceedings of the Royal Society of London (Ser. A)*, Vol. 193, London, 120–145.
- Penman, H.L. 1963. *Vegetation and hydrology*. Technical Communication 53, Commonwealth Bureau of Soils, Harpenden, England, 125.
- Popova, Z., Kercheva, M., Pereira, L.S. 2006. Validation of the FAO methodology for computing ETo with missing climatic data application to South Bulgaria. *Irrigation Drainage*, 55, 201–215
- Priestley, C.H.B., Taylor, R.J. 1972. On the assessment of surface heat flux and evaporation using large scale parameters. *Monthly Weather Review*, 100, 81–92.

- Qian, Q., Wu, B., Xiong, J. 2005. Interpolation system for generating meteorological surfaces using to compute evapotranspiration in Haihe River Basin. Proceedings of Geoscience and Remote Sensing Symposium, 2005, IGARSS '05. IEEE International, 616-619.
- Regione Autonoma della Sardegna (RAS). 2006. Piano Paesaggistico Regionale, PPR 2006. Relazione Generale. Regione Autonoma della Sardegna. <http://sardegna.territorio.it/j/v/1123?s=6&v=9&c=7424&na=1&n=10>
- Saeed, M. 1986. The estimation of evapotranspiration by some equations under hot and arid conditions. Transactions of the ASAE, 29 (2), 434–438.
- Safanda, J. 1999. Ground surface temperature as a function of slope angle and slope orientation and its effect on the subsurface temperature field. Tectonophysics, 306, 367–375.
- Samani, Z. 2000. Estimating solar radiation and evapotranspiration using minimum climatological data. Journal of Irrigation and Drainage Engineering, 126 (4), 265–267.
- Schloeder, C.A., Zimmerman, N.E., Jacobs, M.J. 2001. Division S-8 nutrient management & soil & plant analysis. Soil Science Society of America Journal, 65,470-479.
- Sentelhas, P.C., Gillespie, T.J., Santos, E.A. 2010. Evaluation of FAO Penman-Monteith and alternative methods for estimating reference evapotranspiration with missing data in Southern Ontario, Canada. Agriculture Water Management, 97, 635-644.
- Stanhill, G.A. 1961. Comparison of methods of calculating potential evapotranspiration from climatic data. Israel Journal of Agricultural Research, 11, 159–171.
- Stein, A., Bouma, J., Van Dooremolen, W., Bregt, A.K. 1988a. Cokriging point data on moisture deficit. Soil Science Society of America Journal, 52, 1418-1423.
- Stein, A., Hoogerwerf, M., Bouma, J. 1988b. Use of soil map delineations to improve (co-)kriging of point data on moisture deficits. Geoderma, 43, 163-177.
- Stein, A., Staritsky, I.G., Bouma, J., Van Eijnsbergen, A.C., Bregt, A.K. 1991. Simulation of moisture deficits and areal interpolation by universal cokriging. Water Resources Research, 27 (8), 1963-1973.

- Talmi, A., Gilat, G. 1977. Method for smooth approximation of data. *Journal of Computational Physics*, 23, 93–123.
- Temesgen, B., Allen, R.G., Jensen, D.T. 1999. Adjusting temperature parameters to reflect well-water conditions. *Journal of Irrigation and Drainage Engineering*, 125 (1), 26–33.
- Thornthwaite, C.W. 1948. An approach towards a rational classification of climates. *Geographical Review*, 38, 55–94.
- Tong, L., Kang, S.Z., Zhang, L. 2007. Temporal and spatial variations of evapotranspiration for spring wheat in the Shiyang river basin in northwest China. *Agricultural Water Management*, 87, 241–250.
- Trnka, M., Žalud, Z., Eitzinger, J., Dubrovsky, M. 2005. Global solar radiation in Central European lowlands estimated by various empirical formulae. *Agricultural and Forest Meteorology*, 131, 54–76.
- Van Bavel, C.H.M. 1966. Potential evaporation: the combination concept and its experimental verification. *Water Resources Research*, 2, 455–467.
- Wahba, G., 1990. Spline models for observational data. In: *CBMS-NSF Regional Conference Series in Applied Mathematics 59*, SIAM. Philadelphia, PA, p. 169.
- Walter, I.A., Allen, R.G., Elliott, R., Mecham, B., Jensen, M.E., Itenfisu, D., Howell, T.A., Snyder, R.L., Brown, P., Echings, S., Spofford, T., Hattendorf, M., Cuenca, R.H., Wright, J.L., Martin, D. 2000. ASCE Standardized Reference Evapotranspiration Equation, p. 209–215. In: Evans R.G., Benham B.L., Trooien T.P. (eds.) *Proc. National Irrigation Symposium*, ASAE, Nov. 14–16, 2000, Phoenix, AZ.
- Xu, C.Y., Singh, V.P. 2002. Cross comparison of empirical equations for calculating potential evapotranspiration with data from Switzerland. *Water Resources Management*, 16, 197–219.
- Yoder, R.E., Odhiambo, L.O., Wright, W.C. 2005. Evaluation of methods for estimating daily reference crop evapotranspiration at a site in the humid Southeast United States. *Applied Engineering in Agriculture*, 21 (2), 197–202.
- Zhang, R.D. 2004. *Applied geostatistics in environmental science*. Science Press and Science press USA, USA.

- Zhao, C. 2003. GIS Assisted Modeling of Potential Ecological Conditions in Zulihe River Watershed of the West-central Loess Plateau, China. PhD Dissertation. Lanzhou University, Lanzhou, China.
- Zhao, C., Nan, Z., Cheng, G. 2005. Methods for modeling of temporal and spatial distribution of air temperature at landscape scale in the southern Qilian mountains, China. *Ecological Modelling*, 189, 209-220.

CHAPTER 3: PROCESSES AND FUNCTIONS OF SIMETAW# - A NEW MODEL FOR PLANNING WATER DEMAND IN AGRICULTURE

ABSTRACT

A successful water management scheme for irrigated crops requires an integrated approach that accounts for water, soil, and crop management. Most existing models are designed only for specific crops and irrigation management, or they are not user friendly, thus their adoption by farmers is limited. The SIMETAW# is a user friendly soil water balance model, developed by the University of California, Davis and the California Department of Water Resource. It is able to assess crop water requirements and generate a hypothetical irrigation scheduling for a wide range of irrigated crops experiencing full, deficit, or no irrigation. The SIMETAW# model computes reference evapotranspiration (ET_o) using the FAO Penman-Monteith (PM) or Hargreaves-Samani (HS) equations. SIMETAW# computes ET_o using observed or simulated daily climate data. The simulated data are generated from monthly means. The model computes the evapotranspiration of the applied water (ET_{aw}), which is the sum of the net amount of irrigation water needed to match losses due to the crop evapotranspiration (ET_c). The net irrigation amounts are determined from a daily water balance using input crop and soil information and the daily ET_c estimates. Using input information on irrigation system distribution uniformity and runoff, when appropriate, the model estimates applied water to each of four quarters of the cropped field (e.g., the 1st quarter is the 4th of the field receiving the least water). The gross application to each quarter is computed as the ET_{aw} divided by the distribution uniformity. Employing the depths of water applied to the four quarters over the season, the actual evapotranspiration (ET_a) is estimated by quarter.

The model is able to estimate the number of irrigation events, the water depth of each application, and, by computing the daily soil water balance, it simulates when the irrigation should be applied. Moreover, setting the crop deficit irrigation and/or rain-fed conditions, the model estimates the reduction of yield relative to full irrigation. Moreover, the SIMETAW# model adjusts ET_o estimates as function of the CO₂ concentration in addition to changes in radiation, temperature, humidity, and wind

speed. Thus, it is a useful tool to assess the impacts of climate change on future irrigation requirement.

A brief evaluation of the SIMETAW# model was carried out, and results of the ET_c , ET_a and ET_{aw} estimate showed a good performance of the model. The weather generator was also tested and results indicate that it is a reliable and useful tool.

The computation of the crop irrigation requirement, using a variety of soil types, crop management, irrigation system, irrigated and rain-fed condition, allows users to identify the most accurate estimates of production and water savings.

1. INTRODUCTION

Irrigation is usually applied to maximize crop yield, but for some regions it is absolutely necessary for production; especially for those countries where the seasonal precipitation gradient is pronounced (e.g., the Mediterranean Basin and other arid-and desert countries) and where agriculture relies heavily on irrigation (Tong et al., 2007). These areas have high productivity when adequate water is available, but because of the high demand for irrigation water, low yields often result if irrigation scheduling is inaccurate or water resources are inadequate (Musick and Dusek, 1980; Singh and Singh, 1995). Agricultural production is vulnerable to the weather conditions and may be strongly influenced by the future climate change projections (IPCC, 2007). In fact, changes in precipitation patterns, intensity and frequency of extreme events, soil moisture, runoff, and evapotranspiration have occurred and substantial changes are expected in the future (Bates et al., 2008). Moreover, world population is expected to grow by around 2.3 billion people, between 2009 and 2050 (Roetter and Van Keulen, 2008, FAO, 2009). Therefore, up to two-thirds of the world population could experience water scarcity over the next several decades (Shiklomanov, 1991; Raskin et al., 1997; Seckler et al., 1998; Alcamo et al., 1997, 2000; Vörösmarty et al., 2000; Wallace, 2000; Wallace and Gregory, 2002). Fischer et al. (2007) estimated that irrigation water demand is expected to increase over 50% in developing regions, and by about 16% in developed regions.

The decrease in water resources, due to climate change in drought-affected areas, is projected to increase in extent and magnitude, with the potential for adverse impacts on multiple sectors, e.g., agricultural and urban water supply, energy

production, and health (IPCC, 2007). Without appropriate water management, the competition between agriculture and other sectors is likely to increase with a progressive worsening of water scarcity (EEA, 2009). Assessing the irrigation requirement is indispensable for water resource planning and to manage the water supply among different economic sectors of a country. Moreover, estimating water needs for the agricultural sector is needed for decision support systems to assess which crop management strategy is more economically convenient, in terms of water usage, crop yield, and satisfactory profits.

Using models to simulate crop water supply and demand is a functional way to estimate the depth of water storage required to satisfy the agricultural sector needs. Models are a decision support tool for regional and on-farm system management and they are helpful to manage sustainable farming systems (Boote et al., 1996). Models are generally defined as simplification or abstraction of a real system (Loomis et al., 1979) that includes a set of mathematical equations to integrate current knowledge from various disciplines (e.g., agrometeorology, soil physics, soil chemistry, crop physiology, and agronomy) to predict crop growth and needs. The use of simulation models is a useful complement to experimental research. Optimal management practices, either strategic or tactic, are often assessed through proven models for making seasonal or within-season decisions (Boote et al., 1996). Models are useful for the analysis and interpretation of results of the behaviour of agronomic systems under diverse environmental conditions and management options. Since 1969, when Brouwer and de Wit produced some of the first models, interest in crop simulation modelling has increased dramatically. A crop model provides a quantitative scheme for predicting the growth, development, and yield of a crop given a set of genetic features and relevant environmental variables (Monteith, 1996). At this time, many crop models have been developed, e.g., CERES group (Crop Environment REsources Synthesis, Ritchie et al., 1985; Jones and Kiniry, 1986), SOYGRO (SOYbean GROwth, Wilkerson et al., 1983; Hoogenboom et al., 1992), EPIC (Erosion Productivity Impact Calculator, Williams et al., 1989; Jones et al., 1991), ALMANAC (Agriculture Land Management Alternatives with Numerical Assessment Criteria, Kiniry et al., 1992), CROPGRO (generic crop growth, Boote et al., 1998), CropSyst (Stockle et al., 2003), the DSSAT cropping system model (Decision Support System for Agrotechnology Transfer, Jones et al.,

2003), the Wageningen models (van Ittersum et al., 2003), the APSIM models (Agricultural Production Systems Simulator, Keating et al., 2003), STICS (Simulator multidisciplinary for Crop Standard; Brisson et al., 2003), and the FAO AquaCrop (Steduto et al., 2009; Raes et al., 2009).

Because of projections for deficits of future water availability, it is necessary to focus the attention on crop water requirement (CWR) in addition to yield. Even though crop models are developed to estimate the CWR beyond the simulation of observed site-specific crop development and yield, the application is still not easy. Despite the punctual and accurate output from crop models, many input variables are required to calibrate, validate, and use the models. The lack of experimental data needed to compute the calibration and validation of the model is an important difficulty that restricts the development and use of crop models. Moreover, applying model output on regional scale could lead to error because of the site specific calibration and validation processes.

Spatialising crop model output requires large amounts of geographical information and crop models are often coupled to geographical information systems (GIS) (Nicoullaud et al., 1999; Heinemann et al., 2002). Another solution is to use spatialisation techniques, e.g., interpolation methods for reference evapotranspiration (ET_o), crop evapotranspiration (ET_c), yield, and yield response (K_y) factor (Cui et al., 1998; Markidis et al., 2005; Tong et al., 2007; Li et al., 2011); however, it is not an easy application.

The estimate of the CWR in relation to climate change scenarios is absolutely necessary to plan water storage requirements and irrigation scheduling. Technical assessment and analysis are needed to determine appropriate management of river basins, to enhance knowledge and provide tools to help farmers, technical staff, the public administration, and policymakers (Perry and Narayanamurthy, 1998; Rosegrant et al., 2001; CGIAR, 2002). The corresponding idea for a decision support system is: “Shall we continue to apply crop models as they exist, or shall we create new models that require an easy approach?” Estimating the CWR at a regional scale requires the application of models that do not explicitly simulate crop growth but do provide estimates of crop water usage for irrigation planning. A number of computerized simulation models based on soil water balance using crop water requirements are

available (Feddes et al., 1974; Kincaid and Heermann, 1974; Rowse et al., 1983; Camp et al., 1988; Smith, 1991; Foroud et al., 1992; George et al., 2000). Among this type of models CROPWAT (Smith, 1991), developed by the Land and Water Development Division of FAO, is perhaps the most well-known. These models have been widely accepted and used by irrigation researchers and other professionals, but their adoption by farmers is limited. Often the models were written for large computers, they were not readily accessible to growers, and they were not user friendly. Furthermore, many models can only be used for irrigation scheduling of a single field, and their application on multiple fields requires several model runs.

Water shortages are common in the State of California, and this has led the University of California, Davis (UCD) and the California Department of Water Resources (CDWR) to develop a program for planning the agricultural water demand in agriculture. The result was the Simulation of Evapotranspiration of Applied Water (SIMETAW) application program (Snyder et al., 2004; Snyder et al., 2012), which is a user friendly soil water balance model that is able to assess the irrigation requirement and generate a hypothetical irrigation scheduling for a wide range of irrigated crops. SIMETAW was originally written in C++, but more recently, the application was re-written in C#, and the new version is called “SIMETAW#”. Unlike other water planning applications, SIMETAW# does account for changes in CO₂ and climate, so it can be applied using climate change projections to provide an estimate of the future reference evapotranspiration and crop water demand. SIMETAW# includes a weather generator that allows the use of either daily or mean monthly climate data to generate up to 30 years of daily weather data. Many improvements were made on SIMETAW# compared with the SIMETAW model. In fact, SIMETAW# computes a daily water balance taking into account a stress coefficient, which is used to account for water deficit effects on crop evapotranspiration. Moreover, SIMETAW# accounts for non-uniformity of irrigation application and the yield reduction for deficit irrigation and rain-fed condition compared with the full irrigation treatment. Another important innovation of the SIMETAW# is the estimate of midseason crop coefficients (K_c) values in relation with local conditions and climate. Input and output data are arranged by zones of equal reference evapotranspiration (ET_o) in order to allow for the computation of seasonal evapotranspiration of applied water (ET_{aw}) for all crops within each zone. Crop

management, weather data, and soil water holding characteristics are the basic inputs to compute ET_{aw} , where ET_{aw} is the depth of water applied that contributes to ET_c . For water resources planning of well watered crops, it is assumed that the net application (NA) depth is equal to the mean depth of water needed to refill the low quarter of an irrigated field to field capacity (FC). If the irrigation is managed in this way, the ET_{aw} is the sum of the NA depths during a cropping season. For each irrigation event, where the mean depth of water applied to the low quarter equals the soil water depletion before irrigation, the gross application minus runoff ($GA-RO$) is determined by dividing NA by the irrigation system distribution uniformity (DU). The $GA-RO$ is the same as the mean depth of infiltrated water over the cropped field. For any given irrigation event, if the NA equals the mean depth of water applied to the low quarter and NA equals the soil water depletion before irrigation, then the DU is approximately equal to the application efficiency (AE).

The combination of different input data (the season start and end date, soil type, crop management, irrigation system, and presence of cover crop) leads to different irrigation requirement estimates (ET_{aw}) that allow farmers and technical staff to identify the most suitable solution in terms of income and water savings. This paper discusses in detail the processes and functions of the SIMETAW# model including the weather simulator, estimate of standardized reference evapotranspiration, adjusting the reference evapotranspiration for climate change, crop coefficients to estimate well-watered crop evapotranspiration, water balance calculations, estimating stress coefficients, adjusting for deficit or no irrigation, and potential applications of the model. Moreover, a brief application of the SIMETAW# model to assess its performance is shown.

2. THE SIMETAW# MODEL DESCRIPTION

2.1. Weather input data and ET_o computation

Weather data are indispensable for the computation of ET_o , which is the first step in estimating well-watered ET_c , deficit and no irrigation corrections for estimating actual crop evapotranspiration (ET_a). SIMETAW# uses either observed or simulated daily climate data to calculate ET_o . The simulated daily climate are generated from monthly values of daily mean data that are (1) input directly or (2) calculated from a set of several years of daily climate data.

SIMETAW# computes ET_o (mm day⁻¹) by the use of the standardized reference equation for short canopies (Allen et al., 2005), which is also known as the FAO Penman-Monteith equation (Allen et al., 1998). It can also compute ET_o using the Hargreaves-Samani (1985) method if only temperature data are available. The data needed to compute ET_o includes: solar radiation (R_s , MJ m⁻²d⁻¹), maximum temperature (T_x , °C), minimum temperature (T_n , °C), wind speed (u_2 , m s⁻¹), dew point temperature (T_d , °C), and rainfall (Pcp , mm). The ET_o equation is:

$$ET_o = \frac{0.408\Delta(R_n - G) + \gamma \left(\frac{900}{T_m + 273} \right) u_2 (e_s - e_d)}{\Delta + \gamma(1 + 0.34u_2)} \quad (1)$$

where Δ (kPa K⁻¹) is the slope of the saturation vapour pressure at the mean daily temperature T_m (°C), e_s and e_d are the saturation vapour pressures at T and T_d , respectively, $\gamma \approx 0.066$ kPa K⁻¹ is the psychrometric constant. The available energy terms are net radiation (R_n , MJ m⁻²d⁻¹) and ground heat flux (G , MJ m⁻²d⁻¹). The R_n is estimated from the input variables and G is assumed equal to zero for daily calculations. For monthly calculations, G is estimated as:

$$G = 0.07(T_{m(i+1)} - T_{m(i-1)}) \quad (2)$$

where $T_{m(i+1)}$ and $T_{m(i-1)}$ are the mean daily air temperatures for the following and previous months, respectively.

Because of the FAO Penman-Monteith equation considers a standardized crop height of 2 m, for wind speeds measured at some height other than 2.0 m, the wind speed at 2 m height (u_2) is estimated as:

$$u_2 = u_z \left(\frac{4.87}{\ln(67.8z_w - 5.42)} \right) \quad (3)$$

where u_z is the wind speed (m s⁻¹) at height z_w (m) above the ground.

Net radiation, expressed as the sum of net short and net long wave radiation, is computed following the procedures in Allen et al. (2005). The first step for the computation of net radiation is the estimate of the extraterrestrial radiation (R_a) calculated for each day using the following equation from Duffie and Beckman (1980):

$$R_a = \left(\frac{24 \cdot 60}{\pi} \right) G_{SC} d_r [\omega_s \sin \delta \sin \phi + \cos \phi \cos \delta \sin \omega_s] \quad (4)$$

where G_{SC} is the solar constant in $\text{MJ m}^{-2} \text{min}^{-1}$ (0.082), σ is the Stefan-Boltzmann constant in $\text{MJ m}^{-2} \text{d}^{-1} \text{K}^{-4}$ (4.90×10^{-9}); ϕ is the latitude in radians converted from latitude (L) in degrees expressed as:

$$\phi = \frac{\pi L}{180} \quad (5)$$

d_r is the correction for eccentricity of Earth's orbit around the sun on day i of the year as:

$$d_r = 1 + 0.033 \cos\left(\frac{2\pi}{365} i\right) \quad (6)$$

δ is the declination of the sun above the celestial equator in radians on day i of the year as:

$$\delta = 0.409 \sin\left(\frac{2\pi}{365} i - 1.39\right) \quad (7)$$

and ω_s is the sunrise hour angle in radians as:

$$\omega_s = \cos^{-1}[-\tan \phi \tan \delta] \quad (8)$$

Net long wave radiation (R_{nl}) in $\text{MJ m}^{-2} \text{d}^{-1}$ is computed as:

$$R_{nl} = -f \varepsilon' \sigma \left[\frac{(T_x + 273.15)^4 + (T_n + 273.15)^4}{2} \right] \quad (9)$$

where ε' is the apparent 'net' clear sky emissivity, f is a cloudiness function, T_x and T_n are respectively maximum and minimum temperature.

The apparent 'net' clear sky emissivity is a function of the actual vapour pressure (e_a , kPa) at the daily mean dew point temperature:

$$\varepsilon' = 0.34 - 0.14 \sqrt{e_a} \quad (10)$$

The ε' is the net emissivity, so:

$$\varepsilon' = \varepsilon_{vs} - \varepsilon_a \quad (11)$$

where ε_{vs} is the emissivity of the grass surface and ε_a is the emissivity of the atmosphere. The cloudiness function uses the measured solar radiation and estimated

clear sky total global solar radiation at the earth's surface (R_{so}) (Jensen et al., 1990; Allen et al., 1998) to adjust for cloudiness:

$$f = 1.35 \frac{R_s}{R_{so}} - 0.35 \quad (12)$$

where R_{so} is function of extraterrestrial radiation and the elevation (E_l) of the weather station:

$$R_{so} = R_a (0.75 + 2.0 \times 10^{-5} E_l) \quad (13)$$

The net solar radiation (R_{ns}) over grass in $\text{MJ m}^{-2} \text{d}^{-1}$ is a function of R_s :

$$R_{ns} = (1 - 0.23) R_s \quad (14)$$

where the saturation vapour pressure (e_s , kPa) is computed as the mean of $e_s(T_x)$ and $e_s(T_n)$.

The actual vapour pressure or saturation vapour pressure (kPa) at the mean dew point temperature from the daily maximum and minimum temperature ($^{\circ}\text{C}$) and maximum (RH_x) and minimum (RH_n) relative humidity (%) is computed as follow:

$$e_a = \frac{e_s(T_x) \frac{RH_n}{100} + e_s(T_n) \frac{RH_x}{100}}{2} \quad (15)$$

The slope of the saturation vapour pressure curve ($\text{kPa } ^{\circ}\text{C}^{-1}$) is function of the mean air temperature (T_m) and the saturation vapour pressure at T_m (e°) (Tetens, 1930; Murray, 1967) as:

$$\Delta = \frac{4099 e^{\circ}}{(T_m + 237.3)^2} \quad (16)$$

The psychrometric constant in $\text{kPa } ^{\circ}\text{C}^{-1}$ is function of barometric pressure (β) in kPa as a function of elevation in meters and latent heat of vaporization ($\lambda \approx 2.45 \text{ MJ kg}^{-1}$) as:

$$\gamma = 0.00163 \frac{\beta}{\lambda} \quad (17)$$

Because increasing CO_2 concentration mainly affects plant physiology (Drake et al., 1997), the SIMETAW# model adjusts the ET_o computation for CO_2 concentration. The current global CO_2 concentration is about 372 ppm and it is projected to reach about

550 ppm by 2050 and more than 700 ppm by 2100 (Prentice et al., 2001). Studies have shown that the stomatal conductance (g_s) of many C_3 plants decreased about 20% when the CO_2 concentration was increased from 372 to about 550 ppm (Drake et al., 1997; Long et al., 2004; Ainsworth and Long, 2005). Following this result, the stomatal conductance of 0.12 m tall C_3 species grass with a current stomatal resistance (r_s) of 100 s m^{-1} should decrease from about 10 mm s^{-1} to 8 mm s^{-1} . Assuming the relationship remains linear beyond the 550 ppm concentration, a correlation regression analysis between the stomatal conductance (mm s^{-1}) and CO_2 concentration (ppm) gives the following equation:

$$g_s = 14.18 - 0.0112 CO_2 \quad (18)$$

For 12 cm tall grass, the canopy resistance (r_c) is related to the r_s and the leaf area index (LAI) as:

$$r_c = \frac{r_s}{0.5 \times LAI} \quad (19)$$

and

$$r_s = \frac{1}{g_s} \quad (20)$$

combining these three equations, the canopy resistance (m s^{-1}) is expressed as a function of CO_2 concentration (ppm) as:

$$r_c = \frac{1000}{1.44(14.18 - 0.0112 CO_2)} \quad (21)$$

2.2. Crop-soil input data

Crop and soil information are input for the SIMETA $\#$ model to calculate the soil water balance and determine hypothetical irrigation schedules. The input data include (1) the crop name, (2) planting and physiological maturity (ending) date, (3) hectares planted, (4) maximum soil and rooting depths, (5) soil water holding characteristics or soil texture, (6) irrigation frequency during the initial growth, (7) allowable depletion (AD), (8) percentage shading of the ground in relation to the growth date, (9) presence of cover crops, (10) irrigation system, (11) the percentage of the full irrigation requirement (PIR), (12) irrigation application rate, (13) the system distribution

uniformity, (14) irrigation runoff fraction (*IRF*) for gravity and poorly designed sprinkler irrigation systems.

Note that default values for application rate and distribution uniformity are determined for the irrigation method categories (1) sprinkler, (2) drip, (3) micro-sprinkler, and (4) gravity (surface) irrigation.

The SIMETA[#] model follows the soil water balance principles described in section 2.1 – “**The soil water balance**” of chapter one. Crop rooting depth, maximum soil depth, and soil water holding characteristics are used to calculate the yield threshold depletion (*YTD*), first information need to compute a crop and soil specific irrigation schedule. Three general categories for the volumetric available water holding capacity (θ_A) in mm of H₂O per mm of soil depth are considered by the model. The program uses $\theta_A = 0.075$, $\theta_A = 0.125$, and $\theta_A = 0.175$ mm of water per mm of soil depth for light (L), medium (M), and heavy (H) soils, respectively. Moreover, some of the most common type of soil and relative θ_A set up in the model can be select. The θ_A value is multiplied by the effective rooting depth (mm) to determine the plant available water (*PAW*) in mm within the soil reservoir. It also assumes that *FC* is double the *PAW*, This assumption has no effect on the water balance calculations, but it is useful for plotting results. The SIMETA[#] model allows for input of the *AD* with a default value *AD*=50%, which is reasonable for most field and horticultural crops. The *YTD* is computed as:

$$YTD = \frac{PAW \times AD}{100} \quad (22)$$

In the SIMETA[#] program, a user can select whether or not to irrigate to irrigate a crop. When the crop is cultivated under rain-fed conditions “R” is selected. When the irrigated option is selected, the irrigation system type can be set as “G” for gravity (surface), “D” for drip (low volume), “S” for sprinkler, and “M” for micro-sprinkler irrigation systems. The default values for system application rates and distribution uniformity percentages (*DU*) are presented in the Table 1. The distribution uniformity for each system was obtained from information reported in the Agricultural Water Use in California (The Centre for Irrigation Technology, 2011).

Table 1. Application rate (mm h^{-1}) and distribution uniformity (%) for gravity and pressurized systems.

System	AR (mm h^{-1})	DU (%)
Gravity	11.2	75
Drip	0.70	85
Micro-sprinkler	1.30	80
Sprinkler	3.20	75

2.3. The weather generator

The weather generator is a useful tool that simulates daily data using either daily or monthly mean data as input. If daily data are input, it first calculates the monthly mean values and then generates the daily simulation. This feature was included to allow for testing of the simulation model and to generate 30 years of data from climate data with fewer years of record. For example, if only five years of data are available, those data are used to calculate monthly means and then the 30 year simulation is generated. The SIMETAW# weather generator follows the principles described in Geng et al. (1986) using either daily or monthly data input. The application program can also use observed daily climate data for calculations. Climate data files include daily values for solar radiation, maximum and minimum temperature, dew point temperature, and wind speed. Daily data files also include precipitation, and the monthly files have the monthly total precipitation and the number of days per month having significant precipitation where significant precipitation is defined as two times the daily ET_o rate. When daily data are generated from monthly climate data, the program forces a negative correlation between rainfall amount and ET_o rate within each month assuming that rainfall amount is inversely related to ET_o .

A gamma and Markov chain modelling approach is often applied to describe rainfall patterns for periods within which rainfall patterns are relatively uniform (Gabriel and Neumann, 1962; Stern, 1980; Larsen and Pense, 1982; Richardson and Wright, 1984). This generalization takes into account the fact that the rainfall patterns are usually skewed toward extreme heavy amounts and the rain status of the previous day tends to affect the present day's condition. The two-state approach consists of a first order Markov chain and a gamma distribution function. Normally, this type of two-state model requires long-term daily rainfall data to estimate model parameters (LONG

method). SIMETAW# uses only monthly averages of total rainfall amount and the number of rainy (*Nrd*) days to obtain all parameters for the Gamma and Markov Chain models (GENG method). As pointed out by Geng et al. (1986) the simplified GENG method performs as well as the LONG method, and both methods perform extremely well relative to observed data. The GENG method includes parameters of two transitional probabilities from: (1) a wet day to a wet day [$P(W/W)$], and (2) a dry day to a wet day [$P(W/D)$]. The gamma function parameters are α and β , where $\alpha \times \beta$ is the mean and $\alpha \times \beta^2$ is the variance of the distribution. Occurrence of a wet day is determined by comparing the computer-generated random uniform deviates with the estimated transitional probabilities using the derived gamma function parameters. The amount of rainfall for a wet day is generated from α and β estimates based on a method developed by Berman (1971). The following empirical relationships between the parameters greatly simplified the number of parameters needed to estimate the four parameters Geng et al. (1986) using the monthly means of the number of wet days and rainfall amount:

- $P(W/D) = 0.75 \times (\text{fraction of wet days in a month});$ (23)

- $P(W/W) = 0.25 + P(W/D);$ (24)

- $\beta = -2.16 + 1.83 \times (\text{per wet day rain amount});$ (25)

- $\alpha = (\text{per wet day rain amount})/\beta.$ (26)

The simulation of wind speed is a simple procedure, requiring only the gamma distribution function, which was previously described.

The temperature, solar radiation, and humidity data typically follow a Fourier series distribution. A model for the variables is expressed as:

$$X_{ki} = \mu_{ki} (1 + \delta_{ki} C_{ki}) \quad (27)$$

where X is the estimated variable, $k = 1$ represents maximum temperature, $k = 2$ represents minimum temperature, and $k = 3$ represents solar radiation. The estimated daily mean is μ_{ki} , C_{ki} is the estimated daily coefficient of variation on the i^{th} day for $i = 1, 2, \dots, 365$ and for the k^{th} variable, and δ_{ki} is a noise factor, assumed to follow a weakly stationary generating process.

The estimated daily mean is function of is the annual mean (α_k), the amplitude of the cosine curve for the k^{th} variable (β_k), and the day of the year when the peak of the corresponding k^{th} variable curve occurs (q_k) as follow:

$$\mu_{ki} = \alpha_k + \beta_k \cos\left(\left[\frac{2(i-q_k)}{365}\right]\right) \quad (28)$$

The SIMETAW# application program uses only the monthly mean data, which simplifies the simulation process. From a study of 34 locations in the USA, the observed coefficient of variation (CV) for temperature variables was inversely related to the means. Then, assuming the same CV for daily data, the monthly CV values were used to determine the daily means. A series of functional relationships between the parameters of the mean curves and the parameters of the coefficient of variation curves made it possible to calculate C_{ki} coefficients from μ_{ki} curves without additional input data. For maximum temperature:

$$C_{1i} = (0.536 - 0.00573\alpha_1) - \exp(-4.63 + 0.0952\beta_1) \cos\left(\frac{2(i-q)}{365}\right) \quad (29)$$

For minimum temperature:

$$C_{2i} = \exp(-0.0466\alpha_2) - \exp(-4.64 + 0.146\beta_2) \cos\left(\frac{2(i-q)}{365}\right) \quad (30)$$

For solar radiation, the mean CVs are more or less constant.

Temperature and solar radiation are associated with rainfall, and the correlation is accounted for using:

$$d_i = 10 (1 - 2f) \quad (31)$$

where d_i is the temperature difference between dry and wet days, and f is the fraction of number of wet days in a year ($f = 0.5$ if $f > 0.5$)

For solar radiation the d_i is defined as:

$$d_i = |410 - 3.12L - 0.35\mu_s| \quad (32)$$

where L is the latitude (degrees + for north) and μ_s is the annual mean daily radiation in langleys ($1.0 \text{ Ly} = 1.0 \text{ cal cm}^{-2} = 1.0 \text{ MJ m}^{-2}$).

2.4. Crop coefficient values and corrections

Default crop coefficient values are included in SIMETAW# using information provided by the FAO 24 (Doorenbos and Pruitt, 1977), FAO 56 (Allen et al., 1998), and several more recent papers. SIMETAW#, however, allows users to update or modify K_c values for local conditions, crop type (see section 2.3-“Crop coefficient” of chapter one), and climate.

The initial growth K_c value for annual field crops is mostly dependent on the soil surface wetting by frequent rainfall or sprinkler irrigation, so the table values for initial growth K_c are typical but not always correct. During the off season (quiescence period for deciduous tree crops, from the harvest to the next planting date for annual crops) and the initial growth, evaporation (E) is the main component of ET . Therefore, the K_c for bare soil is useful to estimate the off-season and the initial growth period ET_c . A two-stage method for estimating soil evaporation presented by Stroosnijder (1987), refined by Snyder et al. (2000) and Ventura et al. (2006) is used to estimate the bare soil K_c values.

During stage 1, the soil evaporation rate is limited only by energy availability to vapourize water. In stage 2, the soil has dried sufficiently that soil hydraulic properties limit the transfer of water to the surface for vaporization. The crop coefficient curves for bare soil were developed with equations for estimating cumulative soil evaporation (CE_s) using the maximum possible cumulative soil evaporation (CE_x) and a soil hydraulic factor $\beta=2.6$. The β factor is soil specific and depends on the rate of water transfer through an unsaturated soil surface layer. However, the value $\beta=2.6$ is believed to be a typical value. For each value of ET_o , the cumulative ET_o (CET_o) was calculated for " d_i " days between irrigation or rainfall events as:

$$CET_o = d_i \times ET_o \quad (33)$$

The maximum possible soil evaporation on each day (E_x) was estimated as:

$$E_x = ET_o \times K_x \quad (34)$$

where:

$$K_x = 1.22 - 0.04ET_o \quad (35)$$

Then, the cumulative maximum soil evaporation was calculated as:

$$CE_x = K_x \times CET_o \quad (36)$$

when

$$\sqrt{CE_x} < \beta, \text{ then } CE_s = CE_x \quad (37)$$

and when

$$\sqrt{CE_x} \geq \beta, \text{ then } CE_s = \beta\sqrt{CE_x} \quad (38)$$

The model estimates the crop coefficients for near-bare soil by cumulative soil evaporation (CE_s), the mean ET_o rate ($\overline{ET_o}$) and the mean number of days between irrigation events as:

$$K_c = \frac{CE_s}{d_i \times \overline{ET_o}} \quad (39)$$

where CE_s represent the ET_c during the off season and initial growth as:

$$CE_s = K_c \times \overline{ET_o} \times d_i \quad (40)$$

Figure 1 shows the bare soil K_c as a function of ET_o rate and a range of soil wetting frequency.

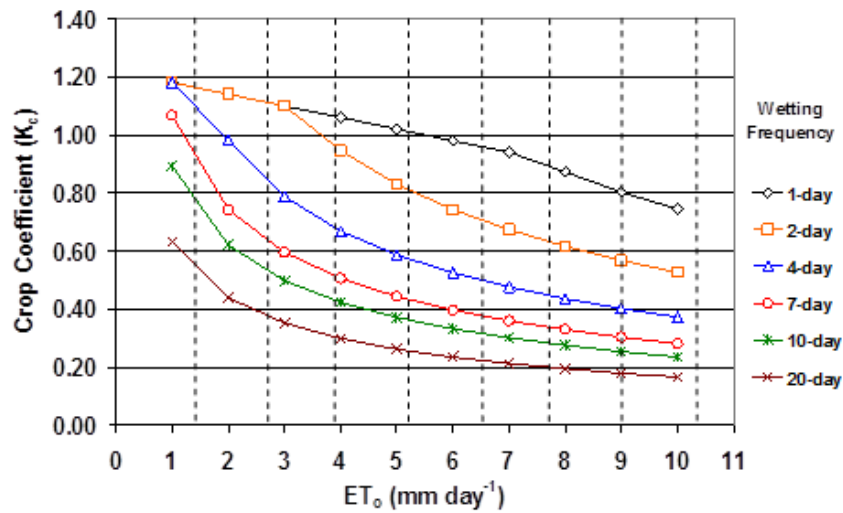


Figure 1. Crop coefficient (K_c) for near-bare soil values (less than 10% shading of the ground) as a function of daily mean ET_o rate and days between significant rainfall or irrigation (>5.0 mm) (based on Ventura et al., 2006).

For deciduous tree and vine crops without ground cover vegetation the K_c values at leaf out (K_{cl}) are set equal to that of the bare soil evaporation on that date. The assumption is that the ET_c for a deciduous orchard or vineyard at leaf out should be about equal to the bare soil evaporation. With ground cover vegetation, the K_c values for deciduous trees and vines are set higher depending on the amount of cover. In general, adding 0.35 to the in-season no-cover K_c for a mature crop, but not to exceed 1.15, is recommended. With immature crops, adding more than 0.35 may be required. For a ground cover vegetation during the off-season, adding 0.35 to the bare soil K_c , but not exceeding 0.90, is recommended. During the off-season, a K_c of 0.90 is used because shading by the trunks and branches are assumed to reduce the ground cover ET slightly below ET_o .

Immature deciduous tree and vine crops use less water than mature crops. The following equation is used to adjust the mature K_c values (K_{cm}) as a function of percentage shading (C_g) by the crop.

$$\text{If } \sin\left(\frac{C_g \pi}{70 \cdot 2}\right) \geq 1.0 \text{ then } K_c = K_{cm} \text{ else } K_c = K_{cm} \left[\sin\left(\frac{C_g \pi}{70 \cdot 2}\right) \right] \quad (41)$$

Initially, SIMETAW# extracts the tabular midseason K_c values from data stored in the program. However, the midseason K_c values are known to vary with climate. The climate correction equation is:

$$K_{cmid} = K_{ctab} + 0.1654(ET_o - 7.3)(K_{ctab} - 1) \quad (42)$$

where K_{cmid} is the corrected midseason crop coefficient and K_{ctab} is the tabular midseason K_c value that is likely to be found during midseason in a climate with $ET_o = 7.3 \text{ mm day}^{-1}$, which is similar to the midsummer ET_o in Davis, California. Clearly, the K_{cmid} values increase as ET_o rises relative to 7.3 mm day^{-1} and it decreases as ET_o falls below 7.3 mm day^{-1} .

2.5. Crop evapotranspiration

During the off-season and the initial growth period the SIMETAW# model estimate the ET_c as the product of ET_o and K_c for near-bare soil. Afterwards, based on crop data input, soil, and irrigation information, K_c curves from the rapid growth to the

late season is determined, and the daily crop evapotranspiration is calculated as the product of ET_o and K_c .

2.6. Water balance calculations

The SIMETAW# model is able to compute the daily water balance for the most common crops (annual and tree crops) in relation to the input data. Because the soil water balance is calculated each day, rainfall runoff onto a cropped field is ignored. Likewise, horizontally transfer of water deep percolation and capillary rise onto a cropped field are also ignored.

The daily soil water balance is computed, and the soil water depletion (SWD) is updated daily by adding the ET_c of the current day to the SWD of the previous day as:

$$SWD_i = SWD_{i-1} + ET_{ci} \quad (43)$$

where i represent the current day and $i-1$ specified the previous day.

The amount of precipitation (Pcp) that is stored and potentially contributes to ET is called effective rainfall (R_e). If rainfall occurs and the Pcp exceeds the SWD , the $R_e = SWD$ and the soil returns to field capacity. If the Pcp event does not exceed the SWD , the $R_e = Pcp$ and the SWD is reduced by an amount equal to the R_e .

If a crop is pre-irrigated, then the SWD is set equal to zero on the day preceding the season. If it is not preirrigated, then the SWD on the day preceding the season is determined by the soil water balance during the off-season before planting or leaf-out.

Some crops are frequently irrigated during the initial growth period. Thus, if an irrigation frequency for the first period is set in the input file, the program will schedule the first irrigation events as established. After the initial growth period, irrigation events occur when the SWD reach a determined maximum threshold depletion. The maximum threshold depletion is known as “management of allowable depletion” (MAD). In fact, because of the crop growth the MAD needs to be estimate in relation to the CET_c and change in water content (ΔSW), while during the initial growth period the $MAD = CE_s$.

2.7. Evapotranspiration of applied water

Evapotranspiration of Applied Water (ET_{aw} , mm) is the sum of the net irrigation applications (ΣNA) during the crop growing season. Computing an estimate of the net

application (NA_e) is the first step for the water balance computation. The NA_e equals the product of application rate (AR) and the hours of runtime (RT):

$$NA_e = AR \times RT \quad (44)$$

Selecting the desired irrigation frequency during midseason, the program estimates of the hours of runtime needed for each irrigation as:

$$RT = \frac{ET_{ms} \times d}{AR} \quad (45)$$

where ET_{ms} is the ET_o during the midseason (mm day^{-1}), and d is the irrigation frequency.

A pressurized irrigation system normally maintains similar distribution uniformity regardless of the water amount applied, so during deficit water conditions, the best irrigation procedure is to maintain the same timing of irrigation and reduce the application amount for each irrigation event. This will generally increase the application efficiency because less water goes to deep percolation and runoff. SIMETAW# keeps the same irrigation timing for fully irrigated and deficit irrigation schedules, but decreases the amount applied at each irrigation event. To do this, the program first calculates a schedule assuming there is adequate water available to avoid yield reduction due to water stress.

In this process, the model calculates the CET_c and estimates the ET_{aw} for an unstressed crop as:

$$ET_{aw} = CET_{c(A-E)} - (YTD_c - YTD_{os}) \quad (46)$$

where $CET_{c(A-E)}$ is the cumulative ET_c during the in-season from stage A to E, YTD_c is the maximum yield threshold depletion (during mid season) and YTD_{os} is the yield threshold depletion during the off-season. At this point in the modelling process, it is impossible to know the real ET_{aw} because the soil water balance is not computed so far, but the equation provides a reasonable estimate for ET_{aw} assuming that there is little effective rainfall and the soil is fairly dry at the end of the season.

The ideal number of full irrigation events (N_{ic}) is function of the ET_{aw} , which is computed as

$$N_{ic} = \frac{ET_{aw}}{MAD_c} \quad (47)$$

where the MAD_c is the management allowable depletion during period midseason. The MAD_c is determined by rounding the NA_e to the next lower integer value.

A typical distribution uniformity percentage is used to estimate the seasonal sum of gross application amounts (ΣGA_c) from the ET_{aw} . After converting the $DU\%$ to a fraction ($DU=DU\%/100$), the seasonal sum of the gross irrigation applications for the fully watered crop (ΣGA_c) is estimated as:

$$\Sigma GA_c = \frac{ET_{aw}}{DU} + \Sigma R_o \quad (48)$$

where ΣR_o (mm) is the estimated sum of the seasonal runoff, or as:

$$\Sigma GA_c = \frac{\Sigma NA_e}{DU} + \Sigma R_o \quad (49)$$

the ΣGA_c (mm) is an estimate of the applied water needed to fully irrigate a crop. Note that the infiltrated water into the cropped field is calculated as $IRF=\Sigma GA_c-\Sigma R_o$. For well designed sprinklers and drip and micro-sprinkler systems, the ΣR_o should be equal to zero. The ΣR_o is computed from the input irrigation runoff percentage (IRP), which is specific to a given irrigation system, and the ΣGA_c . The seasonal irrigation runoff is calculated from the input irrigation runoff percentage (IRP) as:

$$\Sigma R_o = \Sigma GA_c \left(\frac{IRP}{100} \right) \quad (50)$$

After these calculations and knowing the MAD and the N_{ic} , the program is able to compute the soil water balance for a fully irrigated crop.

The water allocation (WA , mm) is the amount of water that is available for the irrigation during a season, and it is computed as:

$$WA = \Sigma GA_c \left(\frac{PIR}{100} \right) \quad (51)$$

where PIR is the percentage of the full irrigation requirement for the crop that is allocated for the cropping season. The $PIR=100$ for full irrigation and $PIR=0$ for rainfed crops.

When water deficit conditions are considered, the $PIR < 100\%$ and the water allocation is lower than for a fully irrigated crop. Thus, the sum of the irrigation depths to the low quarter of a deficit irrigated crop (ΣNA_a) is computed as:

$$\Sigma NA_a = (WA - \sum R_o) \times DU \quad (52)$$

Then, the management allowable depletion for the deficit irrigated crop (MAD_a) is calculated as:

$$MAD_a = \frac{\Sigma NA_a}{N_{ia}} \quad (53)$$

In case of pressurized systems N_{ia} is equal to N_{ic} and the MAD_a is less than the MAD_c .

Because the distribution efficiency of surface (gravity) irrigation depends greatly on the time needed to evenly distribute water across the field, it is difficult to change the application amount for any given irrigation event. Therefore, the SIMETAW# program forces surface irrigation to have a similar management allowable depletion as the fully irrigated crop. During deficit water supply conditions, the number of irrigation events is reduced, but the depth of water applied is similar for each irrigation event. N_{ia} is calculated as the sum of the net applications in deficit condition divided by the management allowable depletion for the fully irrigated crop as:

$$N_{ia} = \frac{\Sigma NA_a}{MAD_c} \quad (54)$$

As the water allocation decreases, the number of irrigation events decreases, while the MAD_a remains slightly less than or equal to MAD_c . Then, the management allowable depletion for the deficit irrigated crop is calculated as:

$$MAD_a = \frac{\Sigma NA_a}{N_{ia}} \quad (55)$$

2.8. Determination of the stress coefficient and fraction of potential yield

Since the SIMETAW# program is able to compute the soil water balance in full irrigation and water deficit conditions, the actual crop evapotranspiration (ET_a) is computed as the product of the well-watered crop evapotranspiration and the stress coefficient (K_s) as:

$$ET_a = ET_c \times K_s \quad (56)$$

The K_s is computed as function of the SWD under deficit water conditions (SWD_a) as:

$$K_s = 1 - \frac{(SWD_a + ET_a - Pcp - NA - YTD)}{(PAW - YTD)} \quad (57)$$

If $K_s=1$, it means that there is no water deficit condition, while a $K_s<1$ implies a water deficit. The cumulative well-watered (CET_c) and actual (CET_a) crop evapotranspiration are computed by summing the daily ET_c rates from the first through the last day of the season as:

$$CET_c = \sum_{i=1}^n ET_{c,i} \quad (58)$$

$$CET_a = \sum_{i=1}^n ET_{a,i} \quad (59)$$

for $i = 1$ to n where n is the number of days in the season.

The ratio of CET_a to CET_c is computed, and the fractional decrease in evapotranspiration (CET_d) due to water stress is calculated as one minus the ratio:

$$CET_d = 1 - \frac{CET_a}{CET_c} \quad (60)$$

The ratio of actual to potential yield (Y_a/Y_c) for a well-watered crop is computed as:

$$\frac{Y_a}{Y_c} = 1 - K_Y \left(1 - \frac{CET_a}{CET_c} \right) \quad (61)$$

where the K_Y are coefficients that relate the relative reduction in cumulative ET to the relative reduction in yield. The K_Y values come from the UN-FAO Publication 33 (Doorenbos and Kassam, 1979). Strictly speaking, this yield ratio estimate is based on the ratio of actual to potential seasonal transpiration. To estimate the transpiration rates would require crop specific, complicated growth and evapotranspiration models that separate evaporation and transpiration from evapotranspiration, and that information is nearly impossible to employ in a model like SIMETAW#, which is designed to roughly estimate the actual to potential yield for a large number of crops with limited input information. Therefore, SIMETAW# uses the assumption that the ratio of CET_a to CET_c is approximately equal to the ratio of CT_a to CT_c , where CT_a and CT_c are the cumulative seasonal transpiration totals for the deficit and fully irrigated crops, respectively.

The FAO 33 publication contains K_Y values for several crops, but K_Y values are not known for all crops. If the K_Y value is unknown for a particular crop, then $K_Y=1.0$ is used. In water stress conditions, the deficit irrigated crop yield is reduced relative to the full irrigation yield. For crops with unknown K_Y values, assuming $K_Y=1.0$ is equivalent to assuming that a 1% reduction in transpiration due to stress will lead to a 1% reduction in biomass production. For crops that produce reproductive parts rather than biomass alone, this is still a fair assumption because, unless there is a severe irrigation deficit, the reduction in transpiration typically occurs later in the season when biomass is accumulating more in the reproductive parts. Thus, this modified version of the FAO 33 approach seems reasonable to obtain estimates of the actual to potential yield ratio for a large number of crops.

Since water application to a cropped field is non-uniform, the SIMETAW# program estimates yield based on the mean depth of water applied to the low, 2nd, 3rd, and high quarter of the field. The low (1st) quarter application is the mean depth of water applied to the one quarter of the field receiving the least amount of water. The high (4th) quarter application is the mean depth of water applied to the one quarter of the field receiving the most water, and the 2nd and 3rd quarters are the mean depths of water applied to the intermediate quarters of the field.

The seasonal mean depth of applied water for a fully irrigated crop is ΣGA_c , and the depth applied to the low (1st) quarter is:

$$\Sigma GA_c \approx ET_{aw}/DU + \Sigma R_o \quad (62)$$

For a deficit irrigated crop, the mean depth of applied water (or water allocation) to the entire crop is:

$$\overline{AW} = \Sigma GA_c \times (PIR/100) \quad (63)$$

and the depth of water applied to the low quarter is:

$$AW_1 = (\overline{AW} - \Sigma R_o) \times DU \quad (64)$$

The high (4th) quarter mean depth applied is computed as:

$$AW_4 = \overline{AW} + (\overline{AW} - AW_1) \quad (65)$$

The 2nd quarter mean depth applied is equal to the sum of AW_1 and 1/3 of the difference between the high and low quarter mean depths applied, so:

$$AW_2 = AW_1 + 1/3(AW_4 - AW_1) \quad (66)$$

The 3rd quarter mean depth applied is equal to the sum of the low quarter depth and 2/3 of the difference between the high and low quarter mean depths applied:

$$AW_3 = AW_1 + 2/3(AW_4 - AW_1) \quad (67)$$

The AW_1 , AW_2 , AW_3 , and AW_4 are the seasonal, actual depths of water applied to the four quarters, so:

$$\overline{AW} = \frac{AW_1 + AW_2 + AW_3 + AW_4}{4} = \Sigma GA_c \times \left(\frac{PIR}{100} \right) \quad (68)$$

SIMETAW# calculates the seasonal CET_a for the deficit irrigated crop by calculating $ET_a = ET_c \times K_s$ on each day of the season. The CET_a is the cumulative ET_a corresponding to a mean depth of applied water to the low quarter for $AW_1 \leq ET_{aw}$. When $CET_a = CET_c$, then $AW_1 = ET_{aw}$. When there is stress, $CET_a < CET_c$ and $AW_1 < ET_{aw}$. The difference between CET_a and AW_1 is the amount of CET_a coming from sources other than irrigation, e.g., effective precipitation, seepage, and stored soil water. The

CET_a corresponds to the depth of water applied to the low quarter (AW_1). Assuming the other three quarters of the cropped field receive the same depth of water from sources other than irrigation, i.e., $CET_a - AW_1$, the estimated CET_a for WA_2 , WA_3 , and WA_4 is $WA_2 + (CET_a - AW_1)$, $WA_3 + (CET_a - AW_1)$, and $WA_4 + (CET_a - AW_1)$, respectively. None of the four CET_a values is allowed to exceed CET_c . The ratio of the seasonal actual to potential evapotranspiration, i.e., CET_a / CET_c , is computed for each quarter and the decrease in the evapotranspiration ratio is computed as: $1 - CET_a / CET_c$ for each quarter. Then the actual to potential yield ratio is computed as: $1 - K_Y (1 - CET_a / CET_c)$ for each quarter. Finally, the mean of the four yield ratios is computed to provide an estimate of the yield effect of the deficit irrigation. This approach accounts for the irrigation system in addition to the irrigation deficit.

2.9. Rain-fed Agriculture

When a crop is grown in rain-fed conditions, there are no irrigations, so the ET_{aw} , DU , and MAD are not computed. The only additions of water are from precipitation. The SIMETAW# program still calculates the daily water balance for a fully irrigated crop because the CET_c information is needed to determine the well-watered yield for the crop. However, the stress function is determined using the SWD , YTD , and PWP as previously discussed. The CET_c and CET_a are determined as in the irrigated crop cases. Finally, the Y_a / Y_c is still determined using the CET_a and CET_c calculations.

3. MATERIALS AND METHODS

3.1. Datasets

To test the performance of the SIMETAW# model, data from three field studies were used. The first experimental study (site 1), was carried out by Bryla et al. (2005) in a peach field [*Prunus Persica* (L.) Batsch], planted at the USDA-ARS San Joaquin Valley Agricultural Research Center in Parlier, California. Peach trees (cv. Crimson Lady) were spaced 1.8 m apart within rows and 4.9 m apart between rows. The soil was fine sandy loam, and the rooting depth was around 1 m. Irrigations were provided by furrow and drip system, and the schedule was based on ET_c measured hourly on two

well-watered peach trees growing in a weighing lysimeter. The lysimeter contained trees of the same variety, age, and planting density as trees in the orchard. Furrow irrigation was applied to the orchard twice per week while drip irrigation was applied every day. Irrigation application occurred from the beginning of April through mid-October. The research project was conducted during 2002 through 2004 and results were used to assess the accuracy of the SIMETAW# model in estimating monthly ET_c and the ΣNA . Weather data necessary to estimate ET_o using the Penman-Monteith equation (Allen et al., 2005) were obtained from the California Irrigation Management Information System (CIMIS) station (Snyder and Pruitt, 1992) nearby the experimental site (Parlier, 36°35'52"N; 119°30'11"W; 103 m a.s.l.). The model estimated ET_c following the procedures described in section 2.5. Then, using crop, soil, and management data reported in the experimental study, the ΣNA for each month for furrow and drip irrigation were estimated.

The second experimental study (site 2), was carried out by Snyder and O'Connell (2007) on navel orange orchard [*Citrus sinensis* (L.) Osbeck] near Lindsay, California in Tulare County. Tree spacing was 5.8 m within rows and 6.1 m between rows. The soil was a fine sandy loam, and the rooting depth was around 1.2 m. Irrigation was applied with micro-sprinklers every 4–6 days during summer. There was no irrigation from October/November through mid-March. A surface renewal (SR) station was set up inside the orchard to measure ET_c , while weather data used to calculate ET_o by the Penman-Monteith equation (Allen et al., 2005) came from the CIMIS station at the University of California Lindcove Field Station (36°21'26"N; 119°03'31"W; 146 m a.s.l.) located 19 km from the study site. Results of daily ET_c , monthly ΣNA , and monthly number of irrigation for the 2003 and 2004 seasons of the experiment were used to assess the performance of the SIMETAW# model. The SIMETAW# model was run every year considering the weather data, soil, and crop management information of the experimental study.

The third experimental study (site 3), was carried out by Snyder et al. (2012) at the Campbell Tract at the University of California, Davis. Wheat (*Triticum aestivum* L. *subsp. aestivum*) variety “Lassik” was cultivated in rain-fed conditions from November 26, 2011 until June 11, 2012. The soil was a Yolo silty clay loam (25% sand, 50% silt, 25% clay) with infiltration rate of about 28.6 mm h⁻¹ and $\theta_A = 0.20$ mm. Rooting depth

was about 1.7 m. The development dates were A (26 Nov.), B (10 Jan.), C (20 Mar), D (15 May), and E (10 Jun), and the percentages for each growth stage from data A were 23% (A-B), 58% (A-C), 87% (A-D), and 100% (A-E). ET_a was computed by using the weighing and floating lysimeters, the surface renewal, and eddy covariance (EC) methods. During early growth, because of the low ET_a values, data were only collected by the two lysimeters. From mid-February on, the EC and SR methods were also used to estimate ET_a . In early May, ET_a from the weighing lysimeter dropped dramatically, and in late May the floating lysimeter measurements resulted also dramatically low. The decrease in early and late May was likely due to the lysimeters running out of water. Thus, considering that the EC and SR observations clearly indicated that the season was longer than indicated by the lysimeter data, an accurate computation of the ET_a was possible by using the EC and SR data at the end of the season. Weather data and ET_o estimates came from the CIMIS station (Davis, 38°32'09"N; 121°46'32"W; 18 m a.s.l.), located about 200 m south of the lysimeters. Following information reported above, ET_a was computed by the use of the SIMETAW# model.

3.2. Weather data simulation

Thirty years of daily weather data were simulated using 29 years of observed mean daily weather data by month (1983-2011) from the California CIMIS weather station of Shafter, California (35°31'59"N; 119°16'52"W; 110 m a.s.l.). The weather data consist of R_s , T_x , T_n , u_2 , T_d , and Pcp . Then, observed and simulated mean daily climate data were compared.

3.3. Statistics

The performance of the model in estimating the ET_c , ET_a , and ΣNA was determined by statistical analyses. Several indexes, including the calculation of correlation and differences between estimated and measured series, were used.

The simulated data were analyzed calculating the Pearson's correlation coefficient (r), root mean squared error ($RMSE$), general standard deviation or relative root mean squared error (GSD), mean absolute error (MAE), mean bias error (MBE), and mean relative error (MRE).

The Pearson's correlation coefficient provides a measure of how strong is the correlation between simulated and observed series, and its range is between -1 and 1. A value of $r = 0$ indicates that there is no linear relationship between simulated and observed values, whereas $r = 1$ indicates a perfect linear relationship.

The *RMSE*, which is defined as the variation between predicted and measured values, expressed in the same unit as the data, (Loague and Green, 1991; Xevi et al., 1996), was used to test the accuracy of the model:

$$RMSE = \sqrt{\frac{1}{n} \sum_{i=1}^n (\hat{Z}_i - Z_i)^2} \quad (69)$$

where n was the number of samples, Z_i and \hat{Z}_i were respectively observed and estimated values for observations $i=1,2,\dots, n$. The *RMSE* was also normalized by dividing it by the observed annual mean (\bar{M}) to obtain the *GSD*:

$$GSD = 100 \times \frac{RMSE}{\bar{M}} \quad (70)$$

To measure the tendency of the model to overestimate or underestimate the measured values the *MBE* was used:

$$MBE = \frac{1}{n} \sum_{i=1}^n (\hat{Z}_i - Z_i) \quad (71)$$

A positive *MBE* indicates the tendency of the model to over predict a variable while a negative bias error implies a tendency to under predict values.

Moreover, *MAE* and *MRE* were used to measure the absolute and relative error between simulated and observed data:

$$MAE = \frac{1}{n} \sum_{i=1}^n \left| \hat{Z}_i - Z_i \right| \quad (72)$$

$$MRE = \frac{1}{n} \sum_{i=1}^n \frac{\left| \hat{Z}_i - Z_i \right|}{Z_i} \quad (73)$$

MAE values near or equal to zero indicate a better match along the 1:1 line comparison of estimated and observed values in the same units as the observations (Rasse et al., 2000). The *MRE* statistic also indicates the match of estimated to observed values, but the value is relative to the observed data.

4. RESULTS AND DISCUSSION

4.1. Simulation of the crop evapotranspiration and irrigation scheduling

The SIMETAW# model estimated the in-season CET_c for peach at site 1 equal to 1026, 1020, and 1048 mm, while the observed values were equal to 1100, 1081, and 1041 mm, in 2002, 2003, and 2004, respectively. As shown in Figures 2-4, the estimated and observed monthly ET_c values followed the same trend. The match between predicted and observed ET_c values during the irrigation season was good. Moreover, for some months, a perfect ET_c estimate was observed, e.g., May and June 2002 (Figure 2) and during the summer of 2004 (Figure 4).

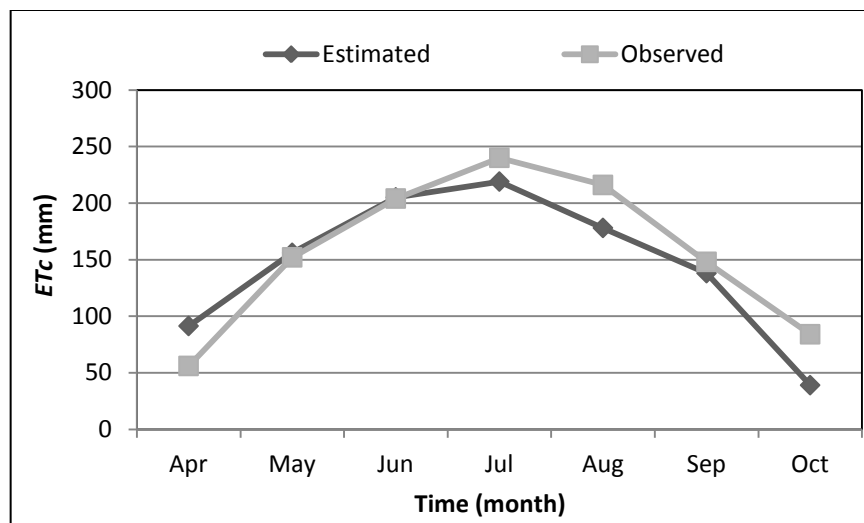


Figure 2. Monthly estimated and observed ET_c (mm) data of peach in site 1 (2002).

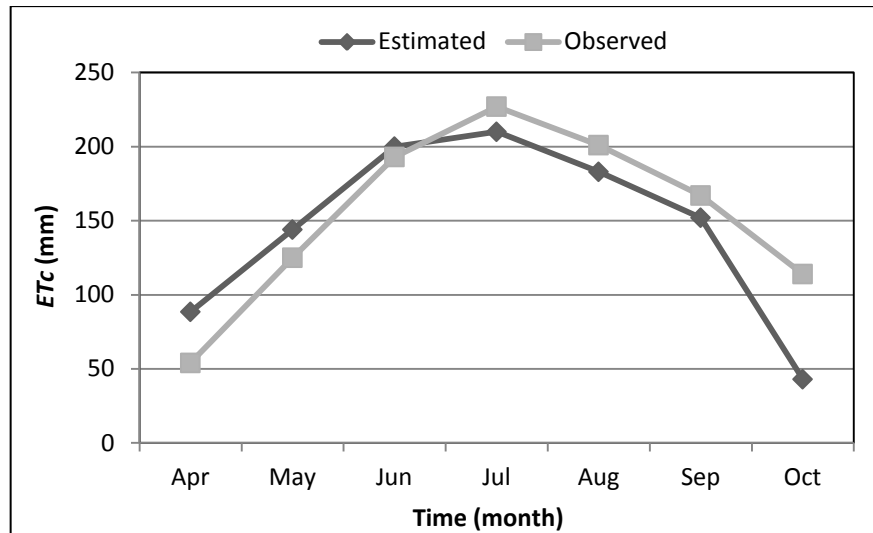


Figure 3. Monthly estimated and observed ET_c (mm) data of peach in site 1 (2003).

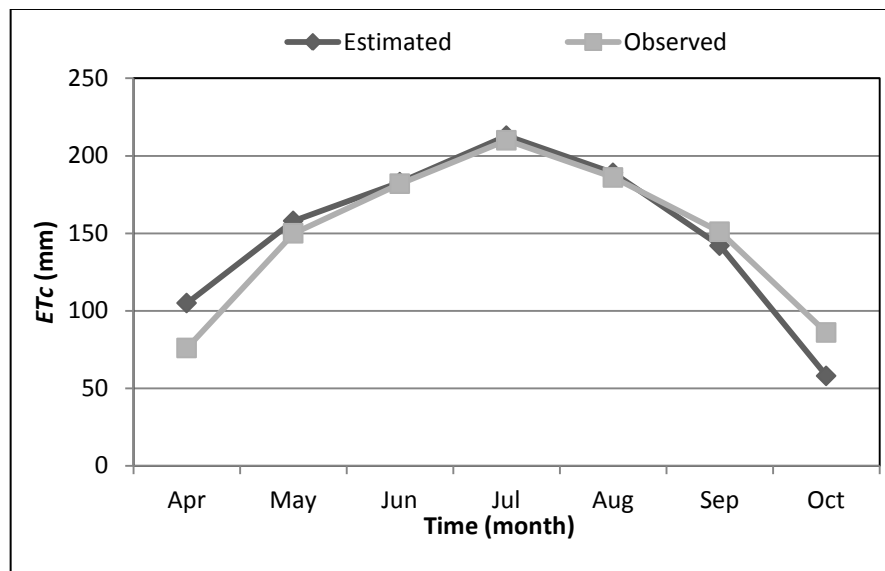


Figure 4. Monthly estimated and observed ET_c (mm) data of peach in site 1 (2004).

Results of the statistical analysis of ET_c estimates at site 1 are shown in Table 3. The Pearson's coefficient values were significant for $p \leq 0.001$ in 2002 and 2004, while r was significant for $p \leq 0.01$ in 2003. Taking into account the indices based on differences between expected and measured data it was noticed a relatively low value of $RMSE$, where the highest value was observed in 2003 ($32.69 \text{ mm month}^{-1}$), while the lowest value was $15.99 \text{ mm month}^{-1}$ in 2004. This, together with a low value of GSD (from 11 to 21%) confirms a good predictive efficiency of the model. The model showed a tendency to underestimate ET_c in 2002 and 2003, although the MBE values (-10.52 and $-8.64 \text{ mm month}^{-1}$) were fairly low. On the contrary, a slightly overestimation of ET_c in 2004 was noticed.

Table 3. Summary of predicted and observed monthly peach ET_c data by year at site 1.

STATISTICAL INDEX	ET_c (2002)		ET_c (2003)		ET_c (2004)	
	Simulated (mm)	Observed (mm)	Simulated (mm)	Observed (mm)	Simulated (mm)	Observed (mm)
CET_c	1026	1100	1020	1081	1048	1041
Min	39	56	43	54	58	76
Max	219	240	210	227	213	210
Samples	7		7		7	
r	0.92***		0.84**		0.95***	
RMSE	27.5		32.69		15.99	
GSD (%)	20		21		11	
MAE	22.05		25.93		11.57	
MBE	- 10.52		- 8.64		1	
MRE	0.22		0.24		0.12	

* $p \leq 0.02$; ** $p \leq 0.01$; *** $p \leq 0.001$; ns=not significant.

The ET_{aw} in 2002 was 990 and 1000 mm for drip and furrow irrigation, respectively, compared with 1029 mm of the observed data.

Results of the estimate of ΣNA for peach in 2002, showed an underestimate in July for both drip and furrow irrigation, while for the rest of the irrigation season the observed and estimated irrigation application followed the same trend (Figures 5 and 6).

A slightly underestimate of ΣNA in July was also observed in 2003 for drip system (Figure 7), while a perfect match between predicted and observed data for the same month, was noticed in 2003 for furrow irrigation (Figure 8), and in 2004 for the drip system (Figure 9). Conversely, considering the furrow irrigation a little overestimation was shown in 2004 (Figure 10). For all three seasons, the model tended to overestimate values during the first part of the irrigation season (from April to June), and to the under predict the ΣNA during the second part (from July to October), considering both irrigation techniques. This could be due to a later leaf out, thus less irrigation needs, than the value set as input of the model (March 1st).

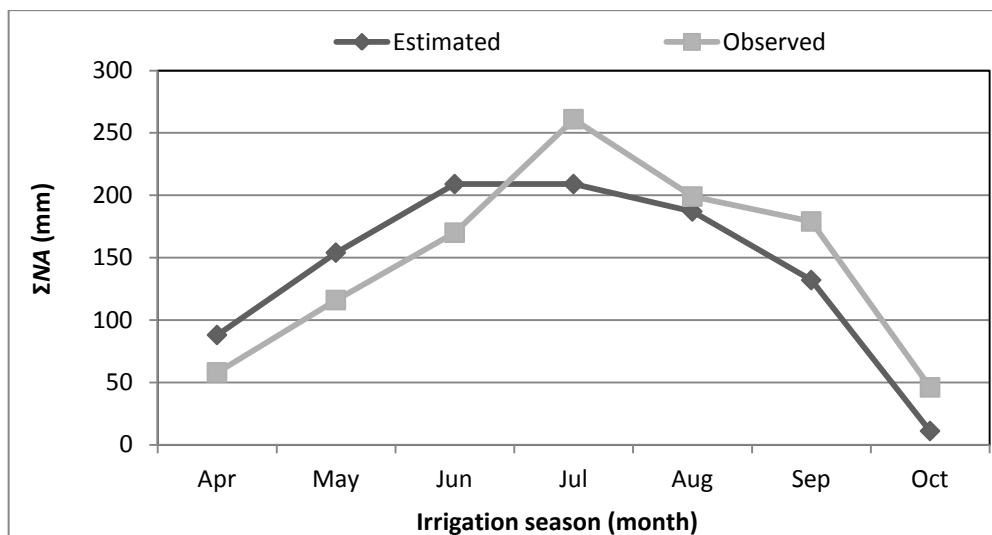


Figure 5. Observed and predicted ΣNA (mm) of peach during the irrigation season by drip system in 2002.

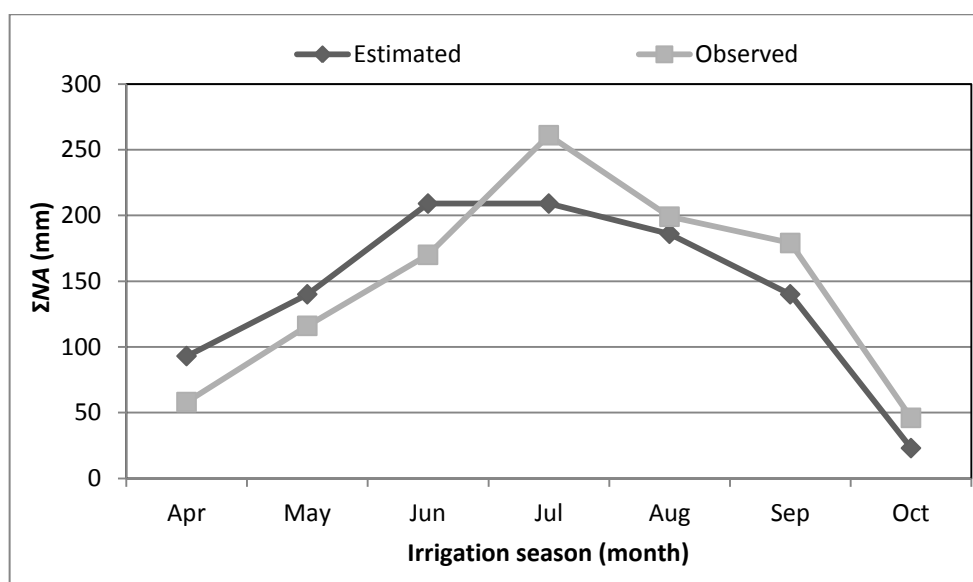


Figure 6. Observed and predicted ΣNA (mm) of peach during the irrigation season by furrow irrigation in 2002.

The ET_{aw} in 2003 was 959 and 954 mm for drip and furrow irrigation, respectively, compared with 935 mm of the observed data. The overestimate trend noticed in 2002 for the first irrigation part was also observed in 2003, while in the second part the underestimated trend is less marked (Figures 7 and 8).

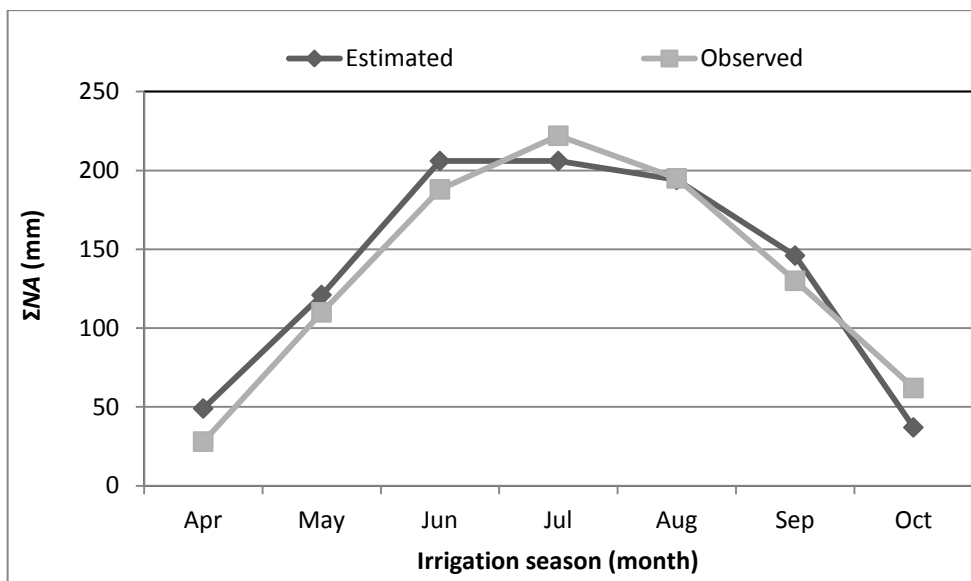


Figure 7. Observed and predicted ΣNA (mm) of peach during the irrigation season by drip system in 2003.

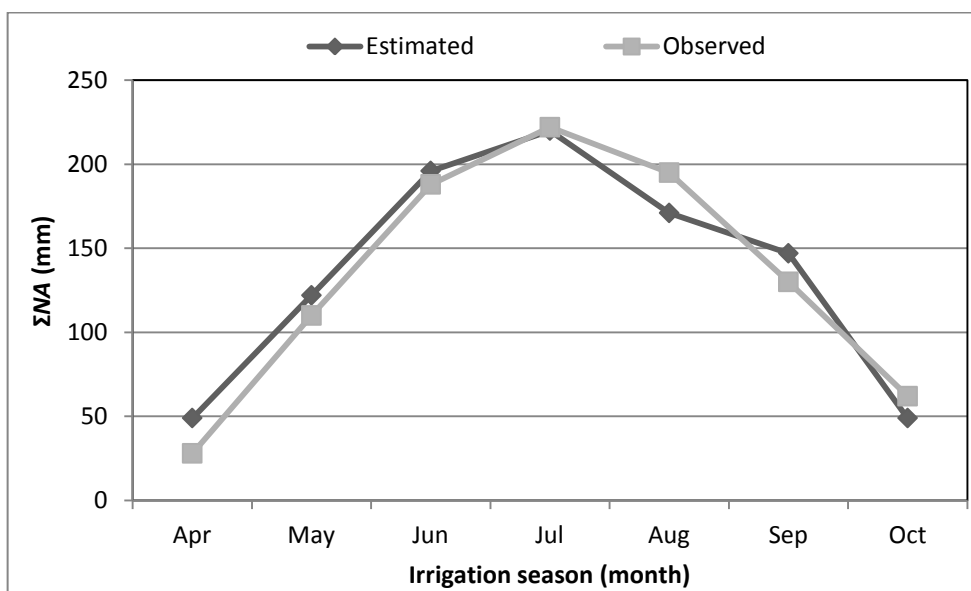


Figure 8. Observed and predicted ΣNA (mm) of peach during the irrigation season by furrow irrigation in 2003.

The ET_{aw} in 2004 was 1007, and 1013 mm for drip and furrow irrigation, respectively, compared with 992 mm of the observed data. The observed and predicted monthly ΣNA values followed the trend almost perfectly (Figures 9 and 10).

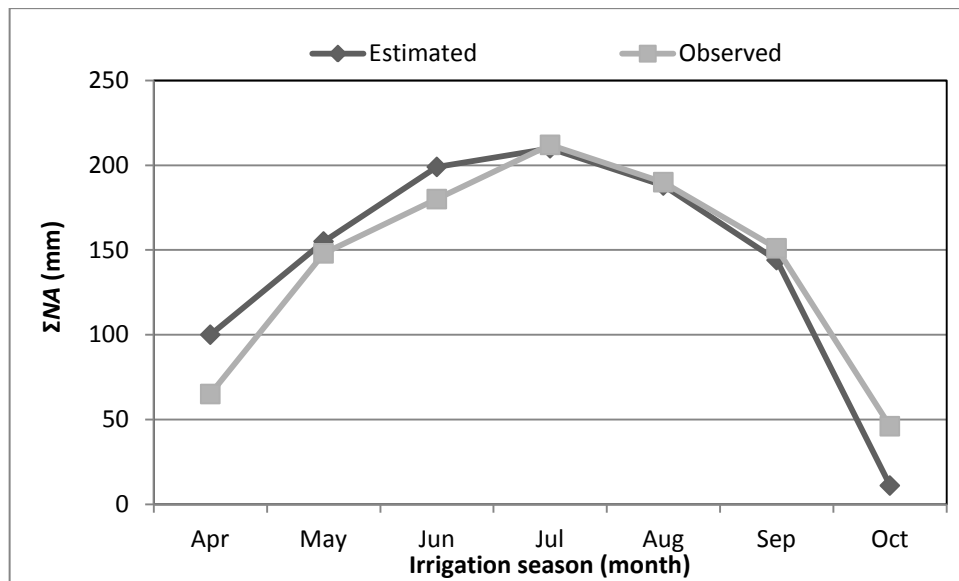


Figure 9. Observed and predicted ΣNA (mm) of peach during the irrigation season by drip system in 2004.

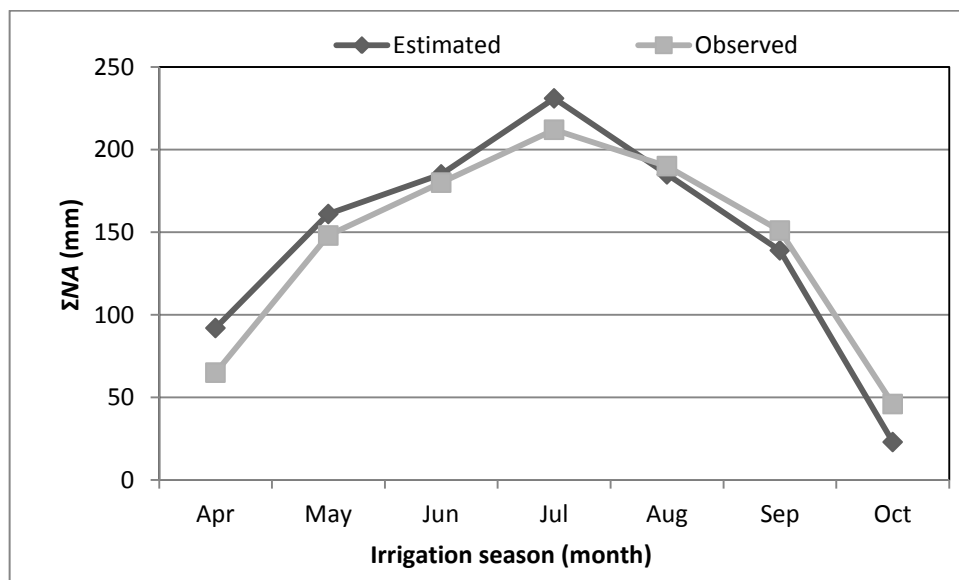


Figure 10. Observed and predicted ΣNA (mm) of peach during the irrigation season by furrow irrigation in 2004.

The summary of the statistical analysis on ΣNA estimate for drip and furrow irrigation is listed in Tables 4 and 5. The Pearson's coefficient values were significant for $p \leq 0.01$ for both drip and furrow irrigation in 2002, while during the other seasons they were significant for $p \leq 0.001$. The *MBE* confirmed the tendency of the model to underestimate ΣNA in 2002, with a greater value for drip system ($-5.57 \text{ mm month}^{-1}$) compared to furrow ($-4.14 \text{ mm month}^{-1}$). Conversely, during 2003 and 2004, the model slightly overestimated ΣNA , and the values ranged between 2.14 and $3.43 \text{ mm month}^{-1}$.

In 2002 higher *RMSE* values were also noticed (38.07 and 34.31 mm month⁻¹), compared with the other seasons (from 15.52 to 20.41 mm month⁻¹).

Table 4. Summary of predicted and observed ΣNA data by month of peach using drip irrigation in site 1.

DRIP	ΣNA (2002)		ΣNA (2003)		ΣNA (2004)	
	Simulated (mm)	Observed (mm)	Simulated (mm)	Observed (mm)	Simulated (mm)	Observed (mm)
STATISTICAL INDEX						
ΣNA	990	1029	959	935	1007	992
Min	11	46	37	28	11	46
Max	209	261	206	222	210	212
Samples	7		7		7	
<i>r</i>	0.86**		0.96***		0.95***	
<i>RMSE</i>	38.07		17		20.41	
<i>GSD (%)</i>	26		13		14	
<i>MAE</i>	36.14		15.43		15.29	
<i>MBE</i>	-5.57		3.43		2.14	
<i>MRE</i>	0.34		0.22		0.22	

* $p \leq 0.02$; ** $p \leq 0.01$; *** $p \leq 0.001$; ns=not significant.

Table 5. Summary of predicted and observed ΣNA data by month of peach using furrow irrigation in site 1.

FURROW	ΣNA (2002)		ΣNA (2003)		ΣNA (2004)	
	Simulated (mm)	Observed (mm)	Simulated (mm)	Observed (mm)	Simulated (mm)	Observed (mm)
STATISTICAL INDEX						
ΣNA	1000	1029	954	935	1013	992
Min	23	46	49	28	23	46
Max	209	261	220	222	231	212
Samples	7		7		7	
<i>r</i>	0.88**		0.97***		0.97***	
<i>RMSE</i>	34.31		15.52		16.82	
<i>GSD (%)</i>	23		11		12	
<i>MAE</i>	32.14		13.86		14.86	
<i>MBE</i>	-4.14		2.71		3.43	
<i>MRE</i>	0.29		0.19		0.18	

* $p \leq 0.02$; ** $p \leq 0.01$; *** $p \leq 0.001$; ns=not significant.

In site 2, the model estimated the CET_c for citrus equal to 936, and 972 mm, while the observed values were 975, and 945 mm, in 2003 and 2004, respectively. As shown in Figure 11, the model under predicted values especially during October and November in 2003, and during March in 2004 (Figure 12). A slightly overestimate was noticed during May for both seasons, and during July and September in 2004. In

general, observed and predicted values followed the same trend, with a particularly good fit during the extreme picks.

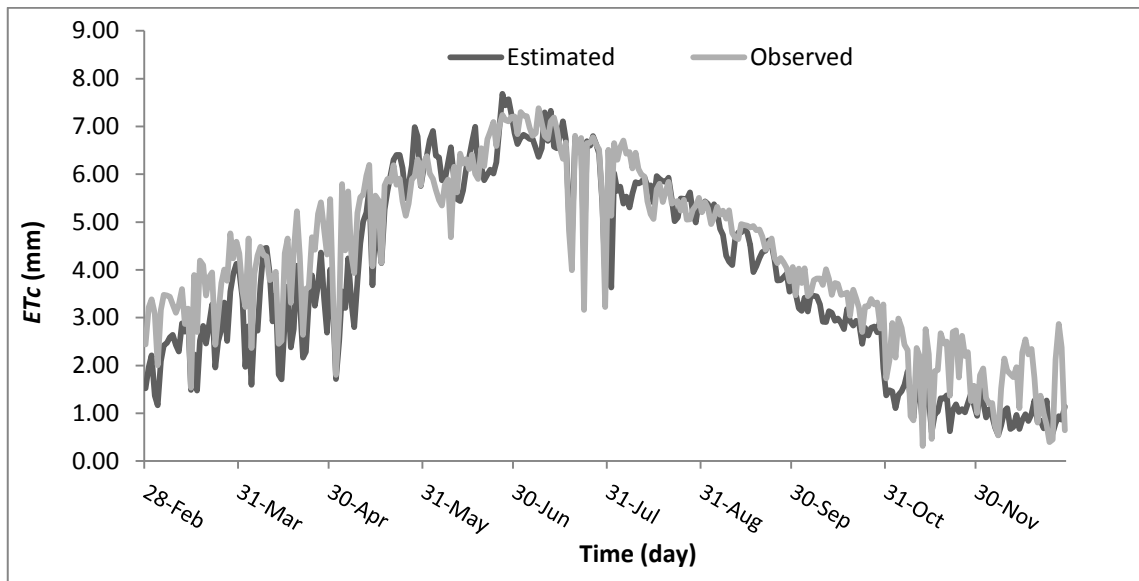


Figure 11. Daily estimated and observed ET_c (mm) data of citrus in site 2 (2003).

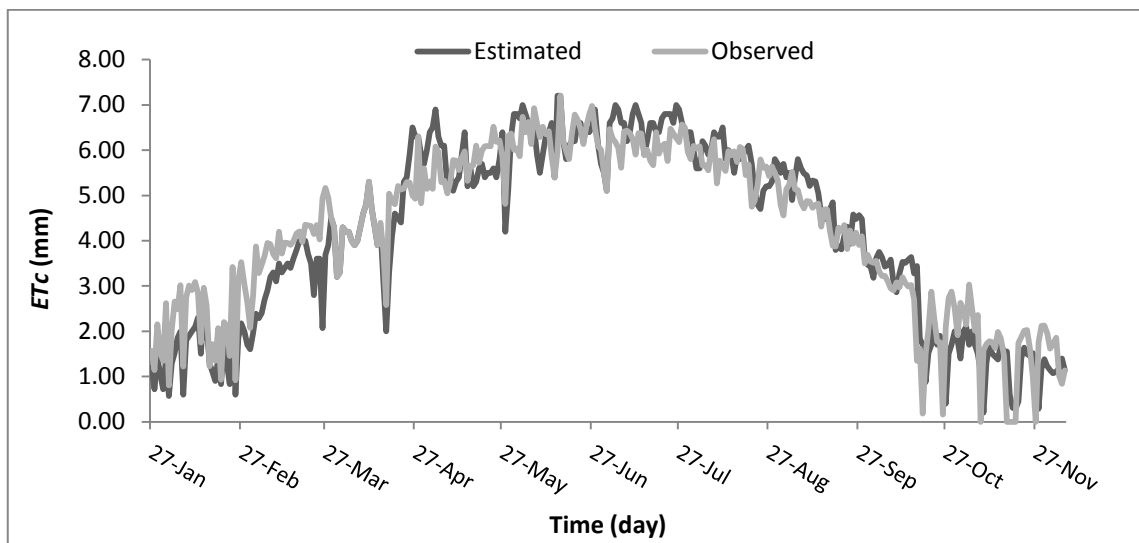


Figure 12. Daily estimated and observed ET_c (mm) data of citrus in site 2 (2004).

The *MBE* confirmed a bigger underestimate in 2003 with $-0.21 \text{ mm day}^{-1}$, while in 2004 an overestimation equal to 0.15 mm day^{-1} was noticed (Table 6). The relative low *RMSE* (0.60 and 0.59 mm day^{-1}) and *MAE* (0.46 and 0.47 mm day^{-1}) confirmed the good predictive capability of the model.

Table 6. Summary of predicted and observed daily ET_c data of citrus in site 2, during the irrigation season.

STATISTICAL INDEX	ET_c (2003)		ET_c (2004)	
	Simulated (mm)	Observed (mm)	Simulated (mm)	Observed (mm)
CET_c	936	975	972	945
Min	1.4	1.7	0.4	0.2
Max	7.7	7.4	7.2	7.2
Samples	184		184	
r	0.92***		0.92***	
$RMSE$	0.60		0.59	
GSD (%)	11		12	
MAE	0.46		0.47	
MBE	-0.21		0.15	
MRE	0.09		0.20	

$p \leq 0.02$; ** $p \leq 0.01$; *** $p \leq 0.001$; ns=not significant.

With respect to ET_{aw} on citrus orchard, the model estimated it was 1117 and 1155 mm compared with 1153 and 903 mm of the observed data, in 2003 and 2004, respectively. Figures 13 and 14 show that the difference between predicted and observed series is particularly marked in March, probably because the model estimate considers the ΣNA all over the month, while the irrigation management of the experimental study considered the irrigation season starting from March 27th in 2003, and march 19th in 2004. Other irregular values were recorded in June and July in 2003, and during April and June in 2004. This could be due because decisions on irrigation timing and duration were made by the ranch management, and an over irrigation in June was maybe counterbalanced with a less irrigation depth in July.

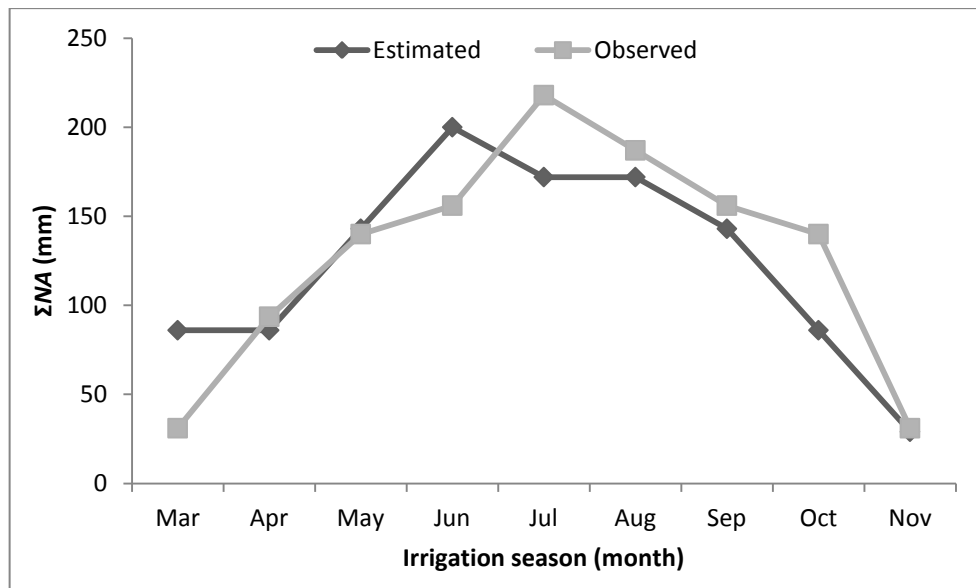


Figure 13. Observed and predicted ΣNA (mm) of citrus during the irrigation season in site 2 (2003).

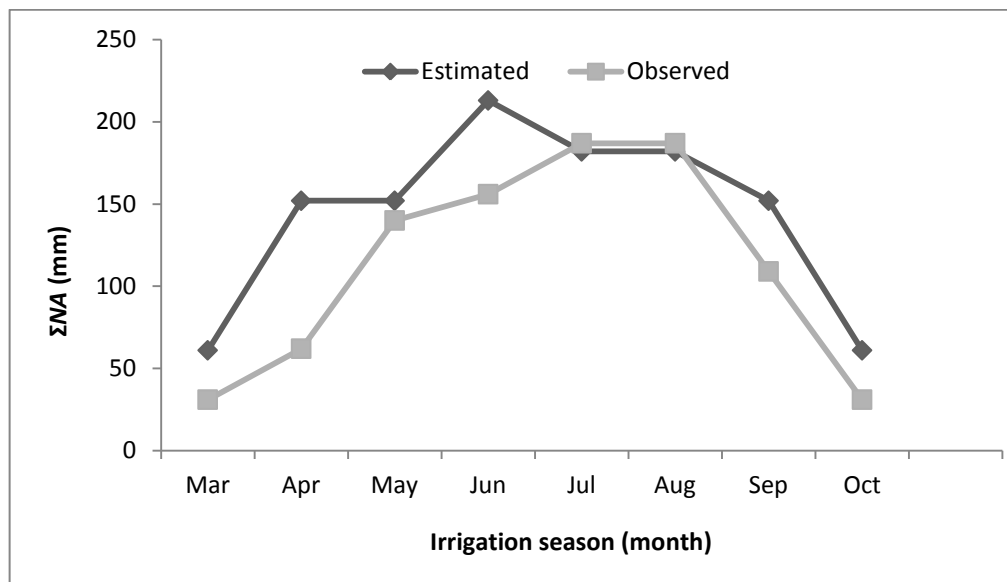


Figure 14. Observed and predicted ΣNA (mm) of citrus during the irrigation season in site 2 (2004).

In the experimental study, the irrigation season was limited only to the period of significant ET_c , although the model simulation determined the necessity of one irrigation event in January and February 2003 (Table 7). Moreover, the irrigation season in citrus orchard ended in mid-October in 2004, compared with mid-November of the previous season; for 2004, the model predicted two irrigation events in November. In general, the number of irrigation predicted by the model and actually applied during the irrigation season were relatively comparable (Table 7). During the irrigation season of

2003, the model estimated 39 irrigation events, an equal amount to that actually applied. In 2004, the model estimated 38 irrigation events, compared to 36 actual applications.

Table 7. Annual estimated and observed number of irrigations (*NI*) in citrus orchard, site 2. (bold fonts depict the irrigation season reported in the experimental study).

	2003		2004	
	estimated <i>NI</i>	observed <i>NI</i>	estimated <i>NI</i>	observed <i>NI</i>
January	1	0	0	0
February	1	0	0	0
March	3	2	2	2
April	3	3	5	4
May	5	5	5	6
June	7	5	7	5
July	6	7	6	6
August	6	6	6	6
September	5	5	5	5
October	3	5	2	2
November	1	1	2	0
December	0	0	0	0

The summary of the statistical analysis reported in Table 8, shows the *r* values significant for $p \leq 0.01$ for both years. The *MBE* denoted the tendency of the model to underestimate the ΣNA in 2003, and to overestimate it in 2004. The index of agreement between simulated and measured data, showed rather satisfactory values.

Table 8. Summary of predicted and observed ΣNA data by month of citrus using in site 2.

STATISTICAL INDEX	ΣNA (2003)		ΣNA (2004)	
	Simulated (mm)	Observed (mm)	Simulated (mm)	Observed (mm)
ΣNA	1117	1153	1155	903
Min	29	31	61	31
Max	200	218	213	187
Samples	9		8	
<i>r</i>	0.83**		0.87**	
<i>RMSE</i>	34.09		43.58	
<i>GSD (%)</i>	27		38	
<i>MAE</i>	26.62		34	
<i>MBE</i>	-3.96		31.5	
<i>MRE</i>	0.33		0.53	

$p \leq 0.02$; ** $p \leq 0.01$; *** $p \leq 0.001$; ns=not significant.

In site 3, the model estimated the CET_a for wheat equal to 475 mm, while the observed value was 465 mm. As shows in Figure 15, the mismatch between observed

and simulated values is marked during the end of the growing season. In fact, a difference of about 20 mm of ET_a in May was computed. Taking into consideration the simulated daily soil water balance data, wheat was affected by weak water stress since May 9th, and it increased to a value of 0.42 at the end of the season. Around May 14th, the stress factor reached a significant value (0.76) that triggered the drop of ET_a values. A slightly overestimation was also noticed during the beginning of the growing season, probably due to the fog interaction, typical of that period of the year (Snyder, personal communication). Overall, the model simulation followed faithfully the observed trend. The statistical analysis showed that the r coefficient, with a value of 0.93, was significant for $p \leq 0.001$.

The $RMSE$ index gave a relatively low value (0.70), which demonstrated the good predictive differences between expected and measured data.

The tendency of the model to overestimate the measured values was indicated by the positive sign of the MBE (0.05 mm day^{-1}). In fact, the monthly ET_a values simulated during the beginning of the growing season were greater than the deficit recorded at the end of the season (Figure 16) As further demonstrated by the MRE (0.51) value, the model confirmed a good performance in the ET_a estimate.

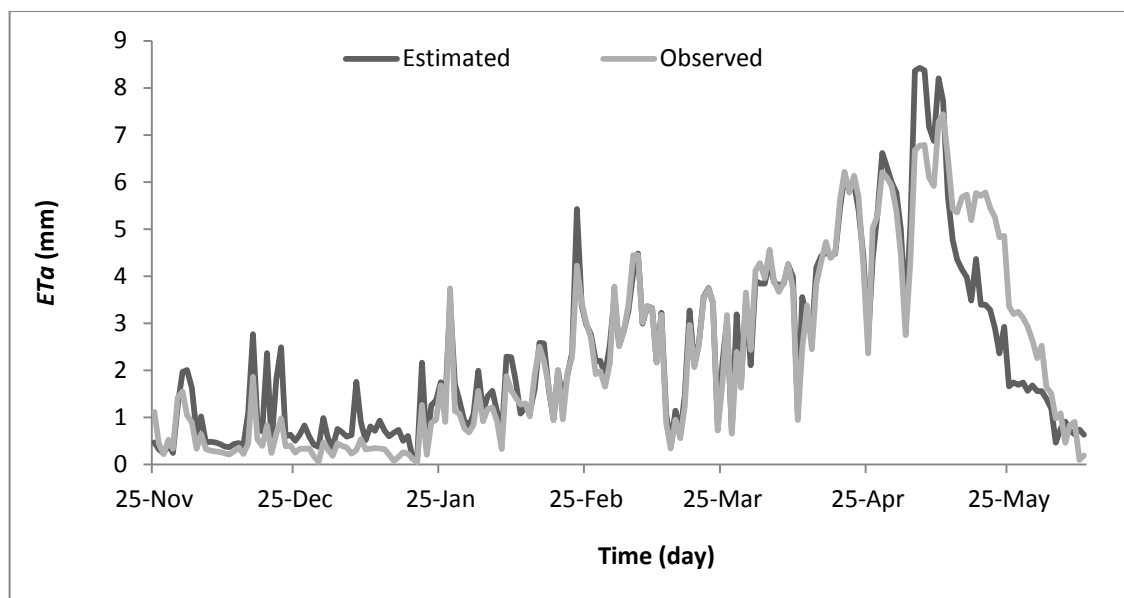


Figure 15 Daily estimated and observed ET_a (mm) data of wheat in site 3.

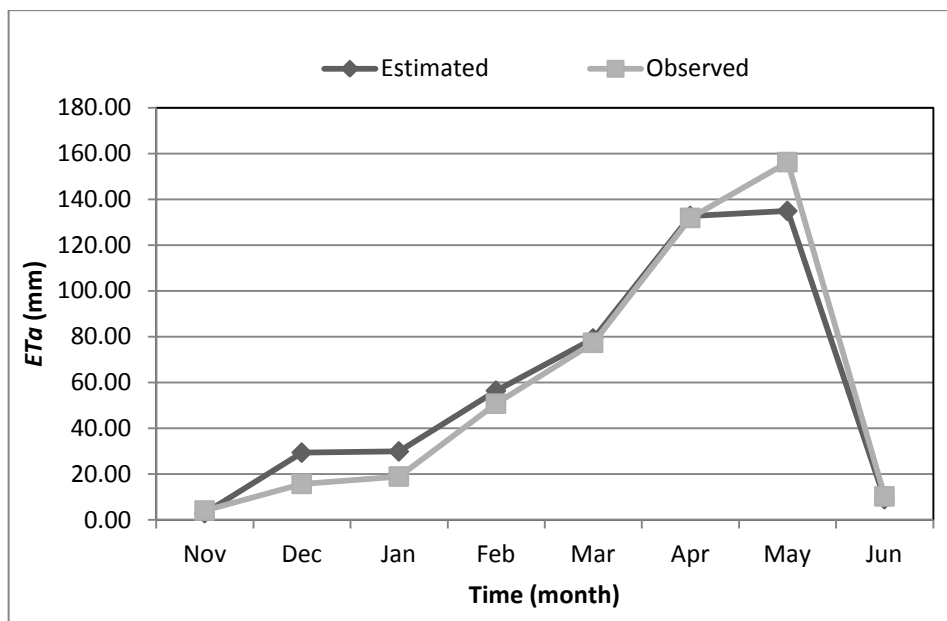


Figure 16. Monthly estimated and observed ET_a (mm) data of wheat in site 3.

The model estimated the ratio of actual to potential yield equal to 0.90. Whereas the irrigated wheat yield in Sacramento Valley from the past ten years was around 4.86 Mg ha^{-1} (UC cooperative extension, 2009), 0.90% of yield reduction means a loss of about 490 kg ha^{-1} . On the other hand, the wheat simulation in irrigated conditions showed the ET_{aw} value equal to $\sim 3800 \text{ m}^3 \text{ ha}^{-1}$. Therefore, the computation of the ratio of actual to potential yield is a useful tool for a roughly computation of the irrigation water use efficiency (IWUE), that helps farmers to estimate the balance between yield loss and installation and maintenance costs of the irrigation system.

4.2. Assessment of the accuracy of the weather generator

The mean daily data simulated over the period of record for Shafter weather station are shown in Figures 17-22. Simulated and measured data showed a uniform trend. The variables that have a seasonal trend, such as solar radiation and maximum/minimum temperature, showed an almost perfect match between observed and simulated series (Figure 17-19). Wind speed (Figure 21) and precipitation (Figure 22) simulations indeed, showed the same trend of the observed series, but with a more marked variability. In general, the weather generator showed a good performance that follows the range of the input data, and without extreme pick values out of the ordinary.

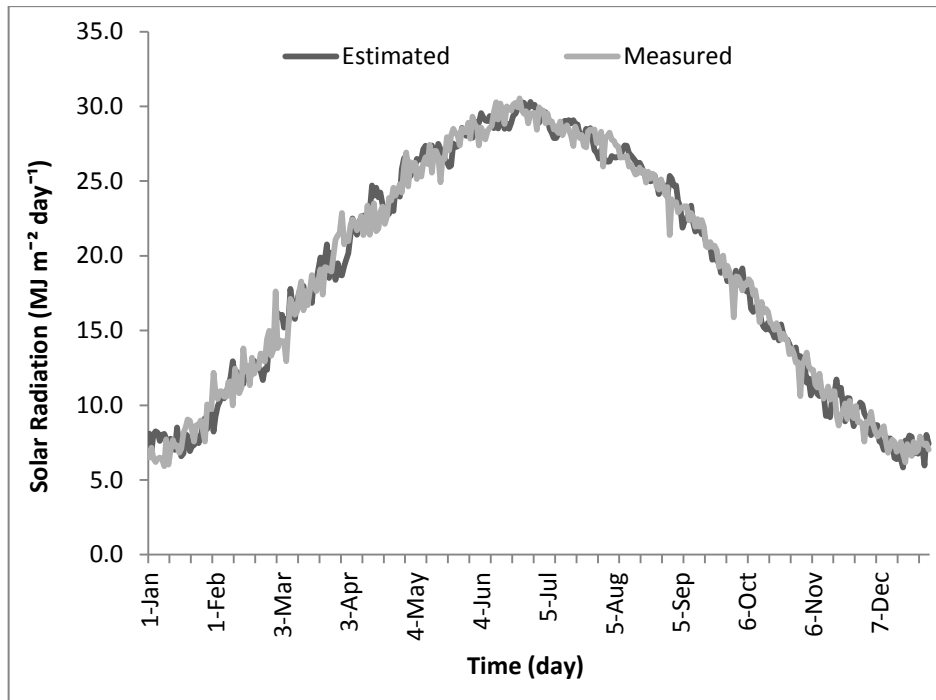


Figure 17. Comparison of measured and simulated mean daily solar radiation at Shafter.

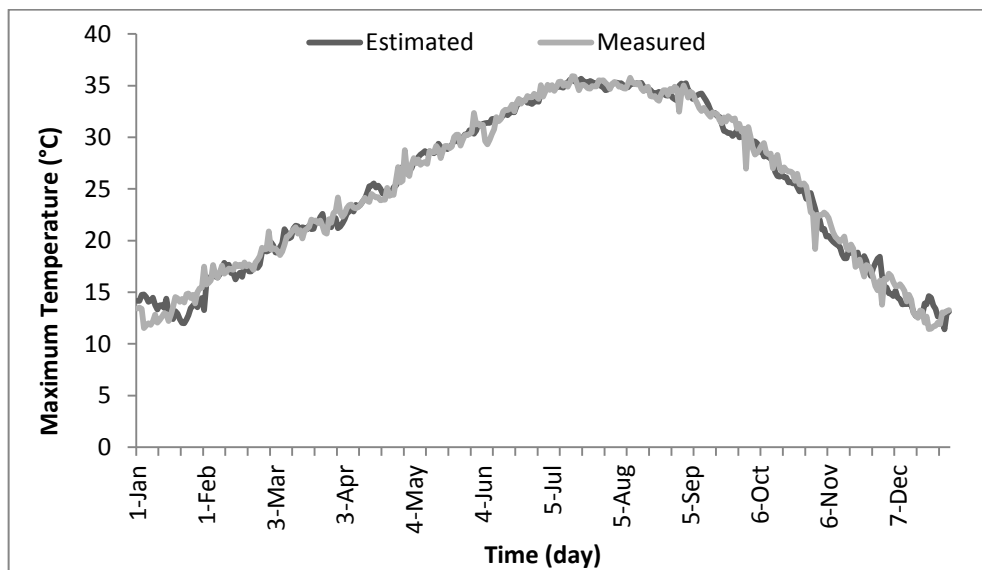


Figure 18. Comparison of measured and simulated mean daily maximum temperature at Shafter.

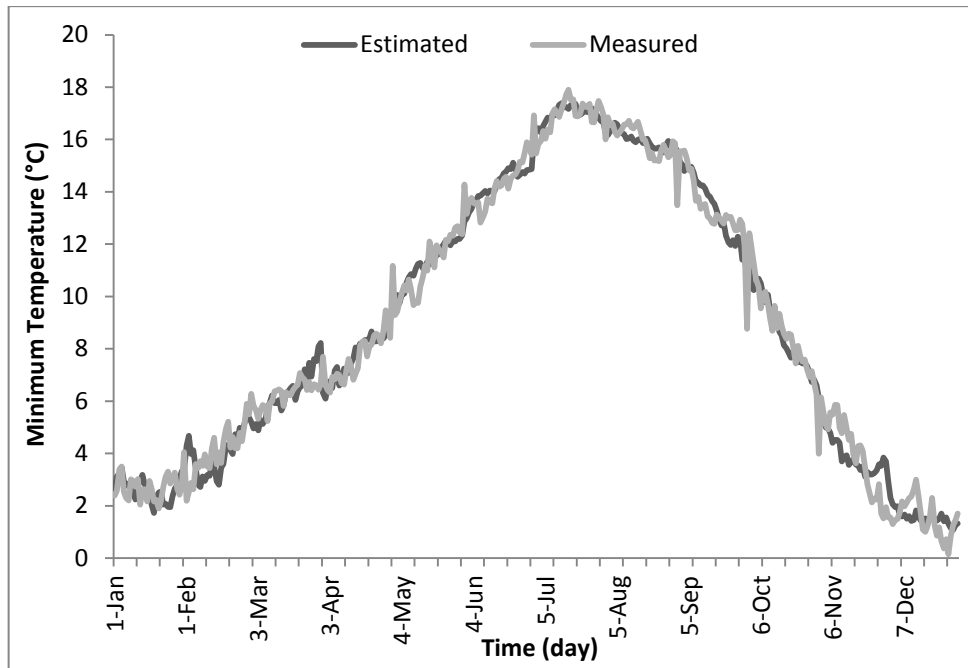


Figure 19. Comparison of measured and simulated mean daily minimum temperature at Shafter.

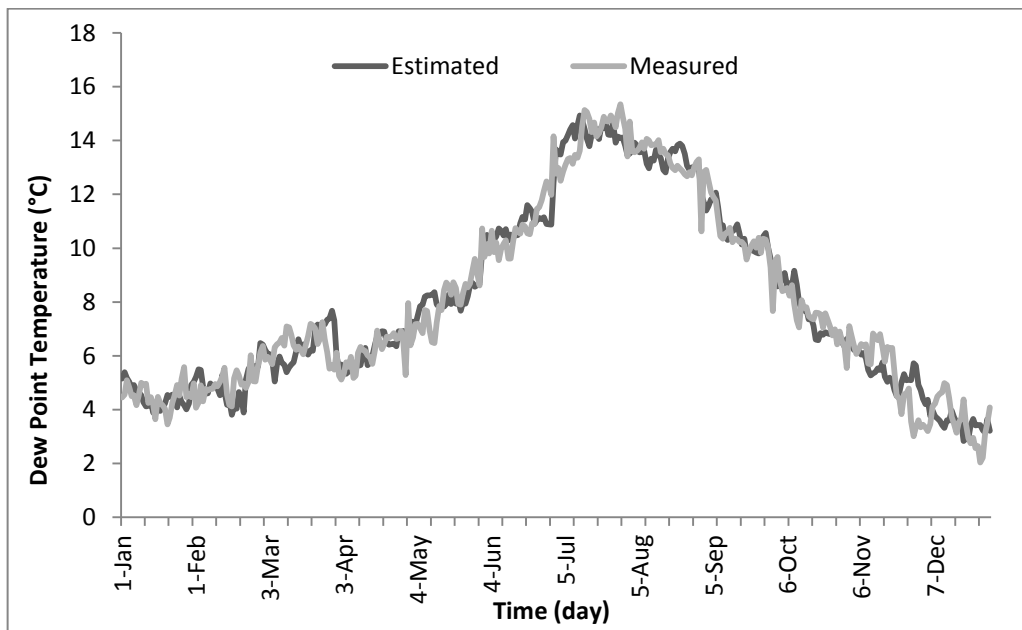


Figure 20. Comparison of measured and simulated mean daily dew point temperature at Shafter.

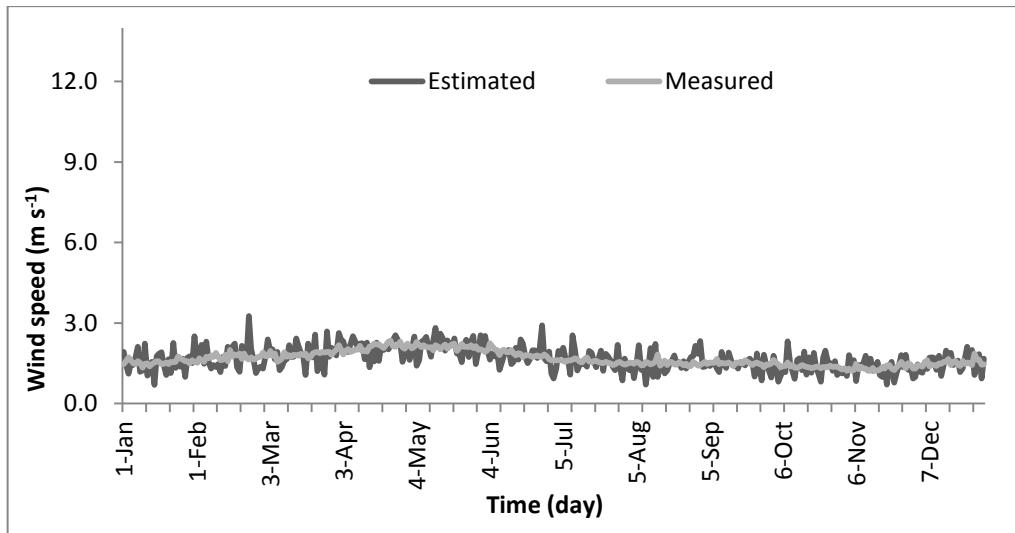


Figure 21. Comparison of measured and simulated mean daily wind speed at Shafter.

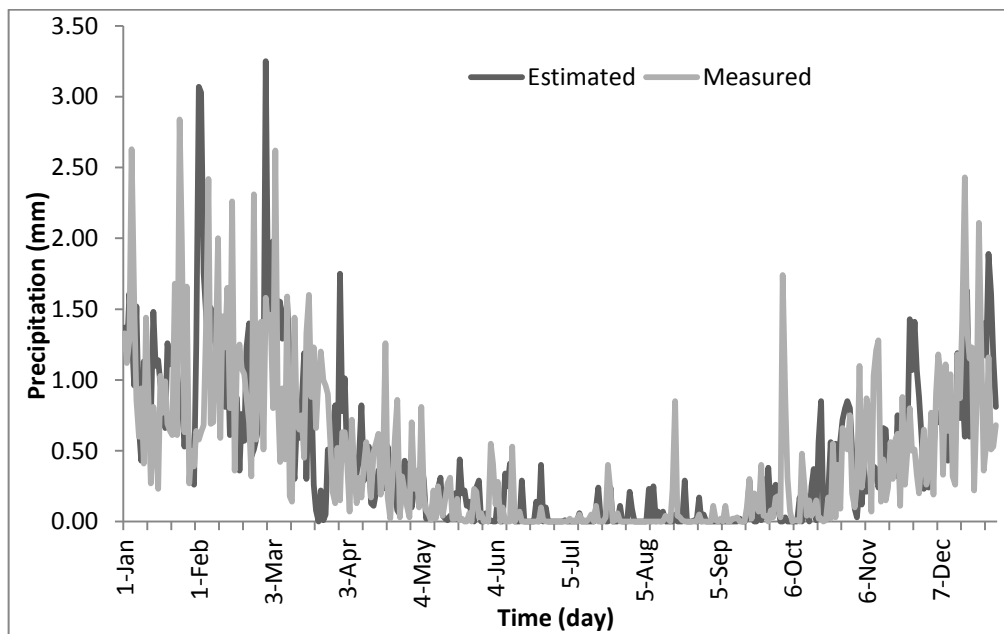


Figure 22. Comparison of measured and simulated mean daily precipitation at Shafter.

5. CONCLUSIONS

SIMETAW# is a soil water balance model that is able to simulate the evapotranspiration of applied water. The daily water balance is an essential part of the program because it helps to determinate the timing of the first and last irrigation events, so that the soil water content starts and ends at levels that are reasonable. The model determines when the crop should be irrigated and how much water should be applied in terms of net and gross application in relation with the considered irrigation system. Then, the sum of the net applications during a season provides information on how

much water is needed to match the seasonal evapotranspiration to produce the crop. Moreover, the possibility to choose the percentage of the full irrigation requirement for the crop, allows one to simulate different adaptation strategies aimed to the increase of the irrigation water use efficiency. The good performance of the weather generator confirmed it is a useful tool for filling the weather data gaps. Moreover, it is an option to assess the irrigation demand by simulating weather data in relation with the future CO₂ concentration. Good results from the ET_c and ET_a estimates suggest a good K_c computation for both the in and off-season. Results of the ET_{aw} simulation indicate that the SIMETAW# model could be used efficiently to evaluate different irrigation strategies, which support irrigation planning and maximize the water productivity.

REFERENCES

- Ainsworth, E.A., Long, S.P. 2005. What have we learned from 15 years of free-air CO₂ enrichment (FACE)? A meta-analysis of the responses of photosynthesis, canopy properties and plant production to rising CO₂. *New Phytologist*, 165, 351-372.
- Alcamo, J., Döll, P., Kaspar, F., Siebert, S. 1997. Global change and global scenarios of water use and availability: an application of WaterGAP 1.0. University of Kassel, CESR, Kassel, Germany.
- Alcamo, J., Henrichs, T., Rosch, T. 2000. World water in 2025: global modeling and scenario analysis. In: Rijsberman F.R. (Ed.), *World water scenarios analyses*. World Water Council, Marseille, France.
- Allen, R.G., Pereira, L.S., Raes, D., Smith, M. 1998. *Crop evapotranspiration. Guidelines for computing crop water requirements*. FAO Irrigation and Drainage Paper No. 56, Rome, Italy
- Allen, R.G., Walter, I.A., Elliott, R.L., Howell, T.A., Itenfisu, D., Jensen, M.E., Snyder, R.L. 2005. *The ASCE Standardized Reference Evapotranspiration Equation*. American Society of Civil Engineers, Reston, VA.
- Bates, B.C., Kundzewicz, Z.W., Wu, S., Palutikof, J.P. 2008. *Climate Change and Water*. IPCC Secretariat Eds., Geneva.

- Berman, M.B. 1971. Generating gamma distributed variates for computer simulation
Rand Corporation, Santa Monica, CA, USA.
- Boote, K.J., Jones, J.W., Pickering, N.B. 1996. Potential uses and limitations of crop models. *Agronomy Journal*, 88, 704-716.
- Boote, K.J., Jones, J.W., Hoogenboom, G. 1998. Simulation of crop growth: CROPGRO model. In Peart R.M., Curry R.B. (Eds.), *Agricultural systems modeling and simulation*. Marcel Dekker, New York, USA, pp. 651-692.
- Brisson, N., Gary, C., Justes, E., Roche, R., Mary, B., Ripoche, D., Zimmer, D., Sierra, J., Bertuzzi, P., Burger, P., Bussiere, F., Cabidoche, Y.M., Cellier, P., Debaeke, P., Gaudillere, J.P., Henault, C., Maraux, F., Seguin, B., Sinoquet, H. 2003. An overview of the crop model STICS. *European Journal of Agronomy*, 18, 309-332.
- Brouwer, R., de Wit, C.T. 1969. A simulation model of plant growth with special attention to root growth and its consequences. In: Whittington W.J. (Ed.), *Root growth*. Proceedings of the 15th Easter School in Agricultural Science. Butterworths, London, UK, p. 224-244.
- Bryla, D.R., Dickson, E., Shenk, R. 2005. Influence of irrigation method and scheduling on patterns of soil and tree water status and its relation to yield and fruit quality in peach. *Hortscience*, 40 (7), 2118-2124.
- Camp, C.R., Christenbury, G.D., Doty, C.W. 1988. Scheduling irrigation for corn and soybeans in the southern coastal plains. *Transaction of ASAE*, 31, 513-518.
- CGIAR. 2002. CGIAR Challenge Program on Water and Food-Revised Full Proposal. CGIAR and IWMI, Colombo, Sri Lanka.
- Cui, Y.L., Li, Y.H., Mao, Z. 1998. The crop-water production function with the influence of reference evapotranspiration taken into account. *Journal of Hydraulic Engineering*, 3, 48-51.
- Doorenbos, J., Pruitt, W.O. 1977. *Crop water requirements*. FAO Irrigation and Drainage Paper 24, 2nd ed., Rome, Italy.
- Doorenbos, J., Kassam, A.H. 1979. *Yield response to water*. FAO Irrigation and drainage Paper 33, Rome, Italy.

- Drake, B.G., González-Meler, M.A., Long, S.P. 1997. More efficient plants: a consequence of rising atmospheric CO₂? *Annual Review of Plant Physiology and Plant Molecular Biology*, 48, 609–639.
- Duffie, J.A., Beckman, W.A. 1980. *Solar engineering of thermal processes*. John Wiley and Sons, New York, USA.
- European Environment Agency (EEA). 2009. Report No 2/2009: Water resources across Europe - confronting water scarcity and drought. European Environment Agency, Copenhagen, Denmark.
- FAO. 2009. *Feeding the world in 2050*. World Summit on Food Security. Rome, Italy.
- Feddes, R.A., Bresler, E., Neuman, S.P. 1974. Field test of a modified numerical model for water uptake by root systems. *Water Resources Research*, 10, 1199-1206.
- Fischer, G., Tubiello, F.N., Van Velthuizen, H., Wiberg, D.A. 2007. Climate change impacts on irrigation water requirements: effects of mitigation, 1990–2080. *Technological Forecasting & Social Change*, 74, 1083–1107.
- Foroud, N., Hobbs, E.H., Riewe, R., Entz, T. 1992. Field verification of a micro computer irrigation model. *Agricultural Water Management*, 21, 215-234.
- Gabriel, K.R., Neumann, J. 1962. A Markov Chain model for daily rainfall occurrence at Tel Aviv. *Quarterly Journal of the Royal Meteorological Society*, 88, 90-95.
- Geng, S, Penning de Vries, F.W.T., Supit, I. 1986. A simple method for generating daily rainfall data. *Agricultural and Forest Meteorology*, 36, 363-376.
- George, B.A., Shende, S.A., Raghuwanshi, N.S. 2000. Development and testing of an irrigation scheduling model. *Agricultural Water Management*, 46, 121-136.
- Hargreaves, G.H., Samani, Z.A. 1985. Reference crop evapotranspiration from temperature. *Applied Engineering Agriculture*, 1, 96-99.
- Heinemann, A.B., Hoogenboom, G., deFaria, R.T. 2002. Determination of spatial water requirements at county and regional levels using crop models and GIS. An example for the State of Parana, Brazil. *Agricultural Water Management*, 52, 177-196.
- Hoogenboom, G., Jones, J.W., Boote, K.J. 1992. Modeling growth, development and yield of grain legumes using SOYGRO, PNUTGRO, and BEANGRO: A review. *Transaction of ASAE*, 35, 2043-2056.

- Intergovernmental Panel on Climate Change (IPCC). 2007. Fourth IPCC Assessment Report (AR4): Climate Change 2007. Cambridge University Press, Cambridge, UK.
- Jensen, M.E., Burman, R.D., Allen, R.G. 1990. Evapotranspiration and irrigation water requirements. American Society of Civil Engineer, New York, USA.
- Jones, C.A., Kiniry, J.R. 1986. CERES-Maize: A simulation model of maize growth and development. Texas A&M University Press, College Station, TX, USA.
- Jones, C.A., Dyke, P.T., Williams, J.R., Kiniry, J.R., Benson, C.A., Griggs, R.H. 1991. EPIC: An operational model for evaluation of agricultural sustainability. *Agricultural Systems*, 37, 341-350.
- Jones, J.W., Hoogenboom, G., Porter, C.H., Boote, K.J., Batchelor, W.D., Hunt, L.A., Wilkens, P.W., Singh, U., Gijsman, A.J., Ritchie, J.T. 2003. The DSSAT cropping system model. *European Journal of Agronomy*, 18, 235-265.
- Keating, B.A., Carberry, P.S., Hammer, G.L., Probert, M.E., Robertson, M.J., Holzworth, D., Huth, N.I., Hargreaves, J.N.G., Meinke, H., Hochman, Z., McLean, G., Verburg, K., Snow, V., Dimes, J.P., Silburn, M., Wang, E., Brown, S., Bristow, K.L., Asseng, S., Chapman, S., McCown, R.L., Freebairn, D.M., Smith, C.J. 2003. An overview of APSIM; a model designed for farming systems simulation. *European Journal of Agronomy*, 18, 267-288.
- Kincaid, D.C., Heermann, D.F. 1974. Scheduling irrigations using a programmable calculator. ARS-NC-12, USDA Agricultural Research Service, Lincoln, Nebraska, USA.
- Kiniry, J.R., Blanchet, R., Williams, J.R., Texier, V., Jones, C.A., Cabelguenne, M. 1992. Sunflower simulation using the EPIC and ALMANAC models. *Field Crops Research*, 30, 403-423.
- Larsen, G.A., Pense, R.B. 1982. Stochastic simulation of daily climate data for agronomic models. *Agronomy Journal*, 74, 510-514.
- Li, X., Tong, L., Kang, S., Li, F. 2011. Comparison of spatial interpolation methods for yield response factor of winter wheat and its spatial distribution in Haihe basin of north China. *Irrigation Science*, 29, 455–468.

- Loague, K., Green, R.E. 1991. Statistical and graphical methods for evaluating solute transport models: overview and application. *Journal of Contaminant Hydrology*, 7, 51-73.
- Long, S.P., Ainsworth, E.A., Rogers, A., Ort, D.R. 2004. Rising atmospheric carbon dioxide: plants face the future. *Annual Review of Plant Biology*, 55, 591-628.
- Loomis, R.S., Rabbinge, R., Ng, E. 1979. Explanatory models in crop physiology. *Annual Review of Plant Physiology*, 30, 339-367.
- Mardikis, M.G., Kalivas, D.P., Kollias, V.J. 2005. Comparison of interpolation methods for the prediction of reference evapotranspiration - an application in Greece. *Water Resource Management*, 19, 251-278.
- Monteith, J.L. 1996. The quest for balance in crop modelling. *Agronomy Journal*, 88, 695-697.
- Murray, F.W. 1967. On the computation of saturation vapor pressure. *Journal of Applied Meteorology*, 6, 203-204.
- Musick, J.T., Dusek, D.A. 1980. Irrigated corn yield response to water. *Transaction of ASAE*, 23, 92-98.
- Nicoullaud, B., Couturier, A., Beaudouin, N., Mary, B., Coutadeur, C., King, D. 1999. Modélisation spatiale à l'échelle parcellaire des effets de la variabilité des sols et des pratiques culturales sur la pollution nitrique agricole. In: Monestiez P. (Ed), *Comptes rendus de l'AIP ECOSPACE*.
- Perry, C.J., Narayanamurthy, S.G. 1998. Farmer response to rationed and uncertain irrigation supplies. IWMI Research Report 24. Colombo, Sri Lanka.
- Prentice, I.C., Farquhar, G.D., Fasham, M.J.R., Goulden, M.L., Heimann, M., Kheshi, H.S., Quere Le, C., Scholes, R.J., Wallace, D.W.R., Archer, D., Ashmore, M.R., Aumont, O., Baker, D., Battle, M., Bender, M., Bopp, L.P., Bousquet, P., Caldeira, K., Ciais, P., Cramer, W., Dentener, F., Enting, I.G., Field, C.B., Holland, E.A., Houghton, R.A., House, J.I., Ishida, A., Jain, A.K., Janssens, I., Joos, F., Kaminski, T., Keeling, C.D., Kicklighter, D.W., Kohfeld, K.E., Knorr, W., Law, R., Lenton, T., Lindsay, K., Maier-Reimer, E., Manning, A., Mearns, R.J., McGuire, A.D., Melillo, J.M., Meyer, R., Mund, M., Orr, J.C., Piper, S., Plattner, K., Rayner, P.J., Sitch, S., Slater, R., Taguchi, S., Tans, P.P., Tian,

- H.Q., Weirig, M.F., Whorf, T., Yool, A. 2001. The carbon cycle and atmospheric carbon dioxide. In: Houghton J.T. (Ed), *Climate change 2001: the scientific basis: contribution of Working Group I to the Third Assessment Report of the Intergovernmental Panel on Climate Change*. Cambridge University Press, Cambridge, (UK), pp. 183-237.
- Raes, D., Steduto, P., Hsiao, T.C., Fereres, E. 2009. AquaCrop-The FAO crop model for predicting yield response to water: II. Main algorithms and software description. *Agronomy Journal*, 101, 438-447.
- Raskin, P., Gleick, P., Kirshen, P., Pontius, G., Strzepek, K. 1997. *Water futures: assessment of long-range patterns and prospects*. Stockholm Environment Institute, Stockholm, Sweden.
- Rasse, D.P., Ritchie, J.T., Wilhelm, W.W., Wei, J., Martin, E.C. 2000. Simulating Inbred-Maize yields with CERES-IM. *Agronomy Journal*, 92, 672-678.
- Richardson, C.W., Wright, D.A. 1984. WGEN: a model for generations daily weather variables. USDA-ARS-8, Springfield, VA, USA.
- Ritchie, J.T., Godwin, D.C., Otter-Nacke, S. 1985. *CERES-Wheat: A simulation model of wheat growth and development*. Texas A&M University Press, College Station, TX, USA.
- Roetter, R.P., Van Keulen, H. 2008. Food security. In: Roetter R.P, Van Keulen H., Kuiper M., Verhagen J., Van Laar H.H. (Eds.), *Science for agriculture and rural development in low-income countries*. Springer, Dordrecht, The Netherlands, pp 27-56.
- Rosegrant, M.W., Cai, X., Cline, S., Nakagawa, N. 2001. The role of rainfed agriculture in the future of global production. In: *Background Paper to the International Conference on Freshwater*, GDI/IFPRI, Bonn, Germany.
- Rowse, H.R., Mason, W.K., Taylor, H.M. 1983. A microcomputer simulation model of soil water extraction by soybeans. *Soil Science*, 136, 218-225.
- Seckler, D., Amarasinghe, U., Molden, D.J., De Silva, R., Barker, R. 1998. *World water demand and supply, 1990 to 2025: scenarios and issues*. IWMI Research Report 19. IWMI, Colombo, Sri Lanka.

- Shiklomanov, I.A. 1991. The world's water resources. In: Proceedings of the International Symposium to Commemorate 25 Years of the IHP, UNESCO/IHP, Paris, France, pp. 93–126.
- Singh, B.R., Singh, D.P. 1995. Agronomic and physiological responses of sorghum, maize and pearl millet to irrigation. *Field Crops Research*, 42, 57-67.
- Smith, M. 1991. CROPWAT: a computer program for irrigation planning and management. FAO Land and Water Development Division, FAO, Rome, Italy.
- Snyder, R.L., Pruitt, W.O. 1992. Evapotranspiration data management in California. Proceedings of the Water Forum '92—Irrigation and Drainage Session, ASCE, New York, 128–133.
- Snyder, R.L., O'Connell, N.V. 2007. Crop coefficients for microsprinkler-irrigated, clean-cultivated, mature citrus in an arid climate. *Journal of Irrigation and Drainage Engineering*, 133 (1), 43-52.
- Snyder, R.L., Bali, K.M., Ventura, F., Gomez-MacPherson, H. 2000. Estimating evaporation from bare or nearly bare soil. *Journal of Irrigation and Drainage Engineering*, 126 (6), 399-403.
- Snyder, R.L., Geng, S., Orang, M.N., Matyac, J.S., Sarreshteh, S. 2004. A simulation model for ET of applied water. *Acta Horticulturae*, 664, 623-629.
- Snyder, R.L., Geng, S., Orang, M.N., Sarreshteh, S. 2012. Calculation and simulation of evapotranspiration of applied water. *Journal of Integrative Agriculture*, 11 (3), 489-501.
- Snyder, R.L., Shapland, T.M., Rejmanek, H. 2012. Evapotranspiration and crop coefficient for winter wheat. University of California, Davis, unpublished report to the California Department of Water Resources on Standard Agreement No. 4600008548, Task # 10.
- Steduto, P., Hsiao, T.C., Raes, D., Fereres, E. 2009. AquaCrop-The FAO crop model for predicting yield response to water: I. Concepts and underlying principles. *Agronomy Journal*, 101, 426-437.
- Stern, R.D. 1980. The calculation of probability distribution for models of daily precipitation. *Theoretical and Applied Climatology*, 28, 137-147.
- Stockle, C.O., Donatelli, M., Nelson, R. 2003. CropSyst, a cropping systems simulation model. *European Journal of Agronomy*, 18, 289-307.

- Stroosnijder, L. 1987. Soil evaporation: test of a practical approach under semi-arid conditions. *Netherlands Journal of Agricultural Science*, 35, 417-426.
- Tetens, O. 1930. Uber einige meteorologische Begriffe. *Z. Geophys*, 6, 297-309.
- The Center for Irrigation Technology. 2011. *Agricultural Water Use in California: A 2011 update*. California State University, Fresno, CA, USA.
- Tong, L., Kang, S.Z., Zhang, L. 2007. Temporal and spatial variations of evapotranspiration for spring wheat in the Shiyang river basin in northwest China. *Agricultural Water Management*, 87, 241-250.
- UC Cooperative Extension. 2009. *Sample costs to produce wheat-Sacramento Valley*. UC Cooperative Extension offices, Davis, California (USA). <http://coststudies.ucdavis.edu>.
- van Ittersum, M.K., Leffelaar, P.A., van Keulen, H., Kropff, M.J., Bastiaans, L., Goudriaan, J. 2003. On approaches and applications of the Wageningen crop models. *European Journal of Agronomy*, 18, 201-234.
- Ventura, F., Snyder, R.L., Bali, K.M. 2006. Estimating evaporation from bare soil using soil moisture data. *Journal of Irrigation and Drainage Engineering*, 132 (2), 153-158.
- Vörösmarty, C.J., Green, P.J., Salisbury, J., Lammers, R.B. 2000. Global water resources: vulnerability from climate change and population growth. *Science*, 289, 284-288.
- Wallace, J.S. 2000. Increasing agricultural water use efficiency to meet future food production. *Agriculture, Ecosystems and Environment*, 82, 105-119.
- Wallace, J.S., Gregory, P.J. 2002. Water resources and their use in food production. *Aquatic Sciences-Research Across Boundaries*, 64, 363-375.
- Wilkerson, G.G., Jones, J.W., Boote, K.J., Ingram, K.T., Mishoe, J.W. 1983. Modeling soybean growth for crop management. *Transaction of ASAE*, 26, 63-73.
- Williams, J.R., Jones, C.A., Dyke, P.T. 1989. *EPIC-Erosion/productivity impact calculator. 1. The EPIC model*. USDA-ARS, Temple, TX, USA.
- Xevi, E., Gilley, J., Feyen, J. 1996. Comparative study of two crop yield simulation models. *Agricultural Water Management*, 30, 155-173.

CHAPTER 4: ASSESSMENT OF CLIMATE CHANGE IMPACT ON CROP WATER REQUIREMENT IN SARDINIA USING THE SIMETAWS# MODEL

ABSTRACT

In the Mediterranean countries, water is essential for agriculture, and water management problems are becoming increasingly serious. Efficient water resource management can help to match available resources and agricultural needs, thereby reducing the risks for crops during periods of drought. Knowing the agricultural water demand is an important factor for developing infrastructure and for managing water delivery to the farm. In order to estimate the volume of storage water required to satisfy the agricultural sector in future, the simulation of the crop water requirement (CWR) is indispensable. The objective of this work was to assess the impact of climate changes on future irrigation requirement (IR) under the A1B emission scenario for the period 2035-2065 (reported year 2050) for some economically important crops in Sardinia. For each homogeneous reference evapotranspiration (ET_o) zone, the SIMETAWS# model was used to estimate the current and future irrigation requirement considering the combinations of planted area, crop management, irrigation system, and soil available water holding capacity data. Climate change was projected to have a negative impact on IR for each crop and area. The increase in ET_o (14%) was more severe with no change in the current CO_2 concentration than the increase in ET_o (9%) for the projected CO_2 level. For summer crops (silage and grain maize), an increase in IR of 5% was projected, while for artichokes and tree crops (citrus, olives, and grapevines) the increase in IR was estimated between 6 and 14% under projected future CO_2 levels. The application of some adaptation strategies, however, can reduce the irrigation water demand and lead to a more sustainable agricultural water use.

1. INTRODUCTION

The increase of the carbon dioxide (CO_2) concentration of the atmosphere contributes to global warming and leads to changes in climate conditions. As well as the increase of temperature and decrease of precipitation in most of the Mediterranean territory (IPCC, 2007), climate change projections also indicate an increasing likelihood of drought (Kerr, 2005) and variability of precipitation in time, space, and intensity that

would directly influence water resource availability (Correia, 1999). Water availability and CO₂ concentration are two of the main factors that affect plant physiology. Increasing evapotranspiration (*ET*) rates are expected with higher temperature, but CO₂ concentration tends to close stomata and decrease *ET* rates (Rosenberg et al., 1990; Kimball, 2004). Increasing CO₂ concentration leads to the partial closure of stomata, reducing conductance, and lowering transpiration rates (Olesen and Bindi, 2002). This response to CO₂ was confirmed by several studies (Curtis, 1996; Lee et al., 2001; Medlyn et al., 2001; Zheng and Peng, 2001; Ainsworth et al., 2002; Long et al., 2004; Ainsworth and Long, 2005; Bernacchi et al., 2007). Increased water-use efficiency results from the decreased stomatal conductance, which reduces water transfer to the atmosphere and consequently *ET* rates (Sellers et al., 1996; Gedney et al., 2006; Kruijt et al., 2008). On the other hand, as pointed out by Kimball et al. (1993) and Bernacchi et al. (2007), lower stomatal conductance rates reduce the transpiration per unit leaf area, but higher CO₂ concentration encourages leaf growth and greater leaf area increases *ET*. Consequently, the reduce conductance and higher leaf area counteract their respective effects on *ET*.

Because the *ET* is controlled primarily by climatic variables (temperature, net radiation, wind speed, and humidity), changes in climatic regimes could effect local hydrological processes (Allen et al., 1991). The increase of global temperature is projected to vaporize more water into the atmosphere from the oceans and other large water bodies. Therefore, the global humidity is likely to increase. The increasing humidity and higher CO₂ concentrations both tend to reduce the transpiration rates and counteract the higher temperature effects on evapotranspiration (Snyder et al., 2010).

Moreover, some authors have recently pointed out that in some areas of the earth the temperature increase is asymmetric, especially in those areas where an increment of cloudiness is observed (Folland et al., 1999; Roderick and Farquhar, 2002). In these areas, the increase of the mean air temperature is simply the result of the temperature increase during night hours when evaporation is less. Therefore, increases in minimum temperature are less likely to increase evapotranspiration, which, in fact, is tending to remain constant or even decrease (Peterson et al., 1995; Viglizzo et al., 1995; Moonen et al., 2002; Todisco and Vergni, 2008). Consequently, many factors need consideration when assessing changes in *ET*.

The combination of long-term changes (e.g., warmer average temperatures) and greater extremes events (e.g., droughts) can have decisive impacts on water demand, with further implications on the ecosystems (Iglesias et al., 2007). Under all climate change scenarios in the Mediterranean region, available water resources are projected to decrease while the irrigation water demand increases (El-Shaer et al., 1997; Döll, 2002; Iglesias, 2002; Fisher et al., 2007).

Water management problems in the Mediterranean basin are becoming increasingly serious (Baric and Gasparovic, 1992; Lindh, 1992; Arnell, 1999; IPCC, 2007). In order to estimate the depth of storage water required to satisfy the agricultural sector in future, estimation of the crop water requirement (CWR), and thus the irrigation requirement (IR) is indispensable. Therefore, the objective of this work is to (1) estimate the climate change impact on IR using the SIMETAW# model, and (2) suggest some possible adaptation strategies to reduce water consumption by agriculture.

2. MATERIALS AND METHODS

2.1. Preliminary activity

The research was conducted on the island of Sardinia, Italy (from 38°N to 41°N, and from 8°E to 10°E). As described in the second chapter, four ET_o classes for the summer period were recognized in Sardinia, where the ranges 4.5-5 and 6-6.3 mm day⁻¹ ET_o classes represent the lowest and highest ranges, respectively (Figure 1). Each zone was identified by a number from one to seven.

Using summer (June-August) data for 2000-2004 from the ARPAS, meteorological network (the specialist regional hydro-weather-climate department), the mean daily ET_o (mm day⁻¹) was calculated. Then, the root mean square error ($RMSE$) was computed between daily ET_o of each station and the daily ET_o averaged over all stations within the zone. The weather station that presented the lowest $RMSE$ value for each zone was chosen to represent the climate of the zone. The weather station chosen for each zone is reported in Table 1.

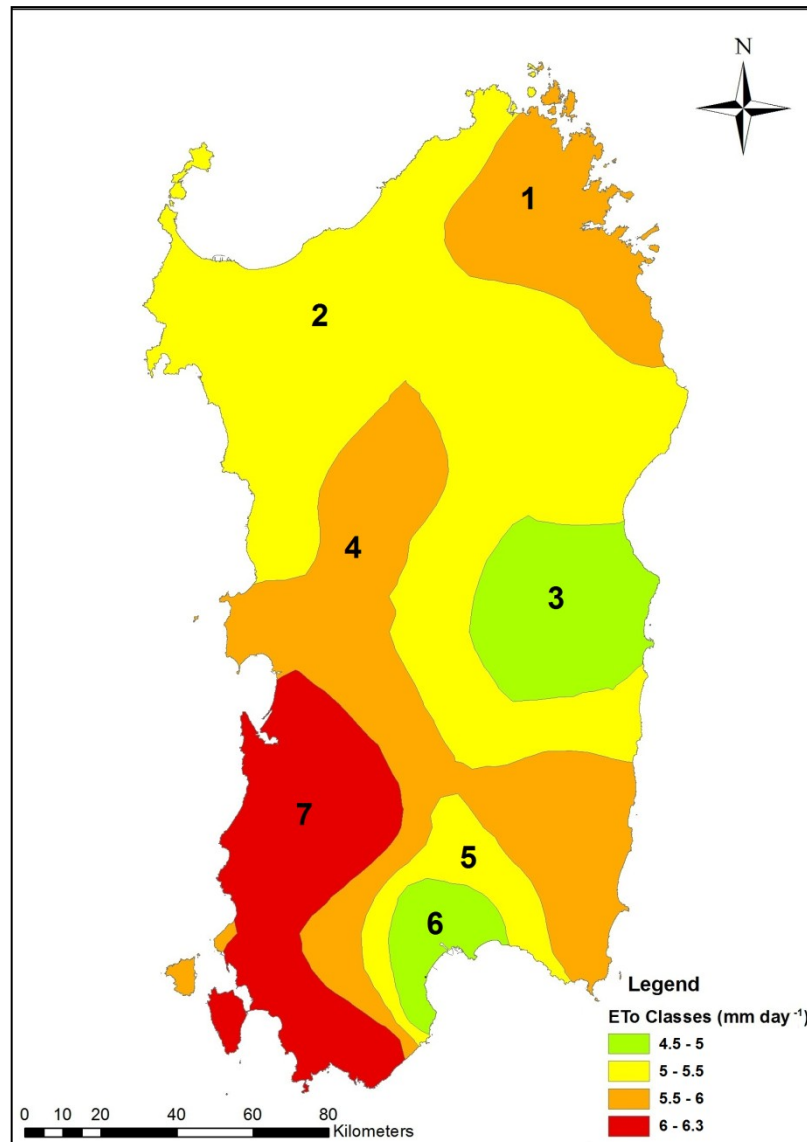


Figure 1. Sardinian ET_0 map (mm day^{-1}). Each number identifies the relative zone.

Table 1. Representative weather station for each ET_0 zone.

ET_0 Zone	STATION	LONGITUDE E	LATITUDE N	ELEVATION (m a.s.l.)
1	San Teodoro	08°38'44"	40°47'36"	13
2	Sassari	08°32'19"	40°44'25"	150
3	Villagrande Strisaili	09°27'28"	39°57'39"	813
4	Siurgus Donigala	09°11'21"	39°36'35"	420
5	Guasila	09°02'14"	39°31'54"	242
6	Decimomannu	08°59'09"	39°19'21"	20
7	Sardara	08°51'26"	39°36'02"	197

2.2. Scheme of methodology

The methodology, in the SIMETAW# model, proposed for estimating the climate change impact on crop irrigation requirement in this study includes the following steps (Figure 2):

- collection of planted area, soil characteristics, and crop management data in Sardinia;
- assessment of the irrigation requirement in relation with the current climate conditions (observed data);
- assessment of the climate change impact on irrigation requirement under climate data delivered by dynamic downscaling of the global climate model (GCM) CMCC-MED through the regional climate model (RCM) COSMO-CLM under the A1B future emission scenario (baseline and future period);
- application of adaptation strategies in the zone that shows the most critical climate projection.

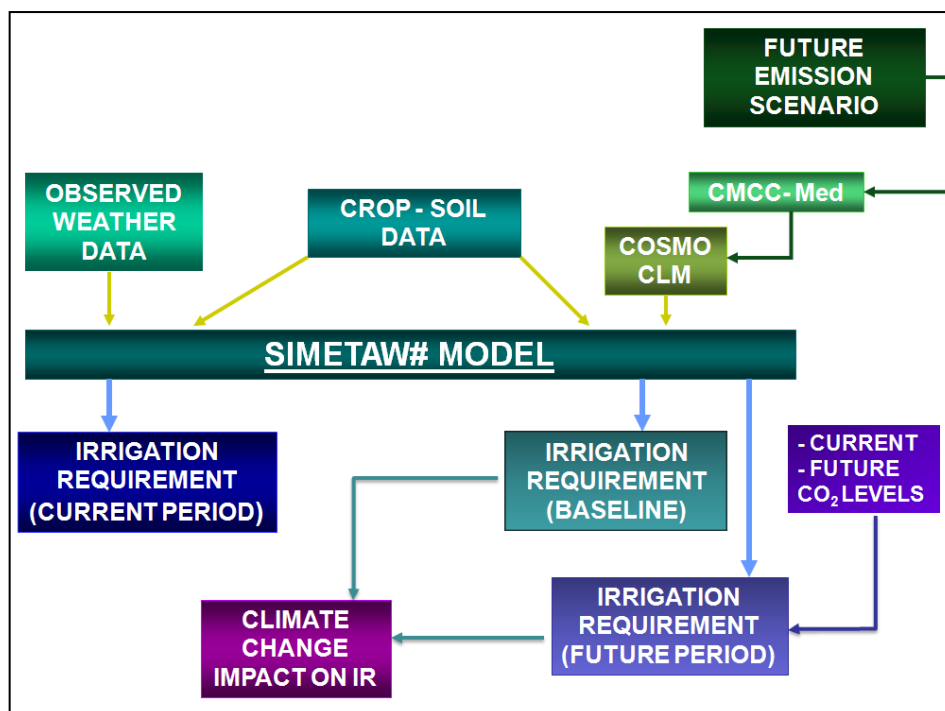


Figure 2. Scheme of methodology.

2.3. Data collection

The input data required to run the SIMETAW# model include the following:

- soil available water holding capacity (θ_A);
- planted area for each crop;
- crop management information.

The soil available water holding capacity data were provided by the specialist regional hydro-weather-climate department of Sardinia. The soil available water holding capacity data (m/m) were divided into three classes (Figure 3) to match categories set into the SIMETAW# model.

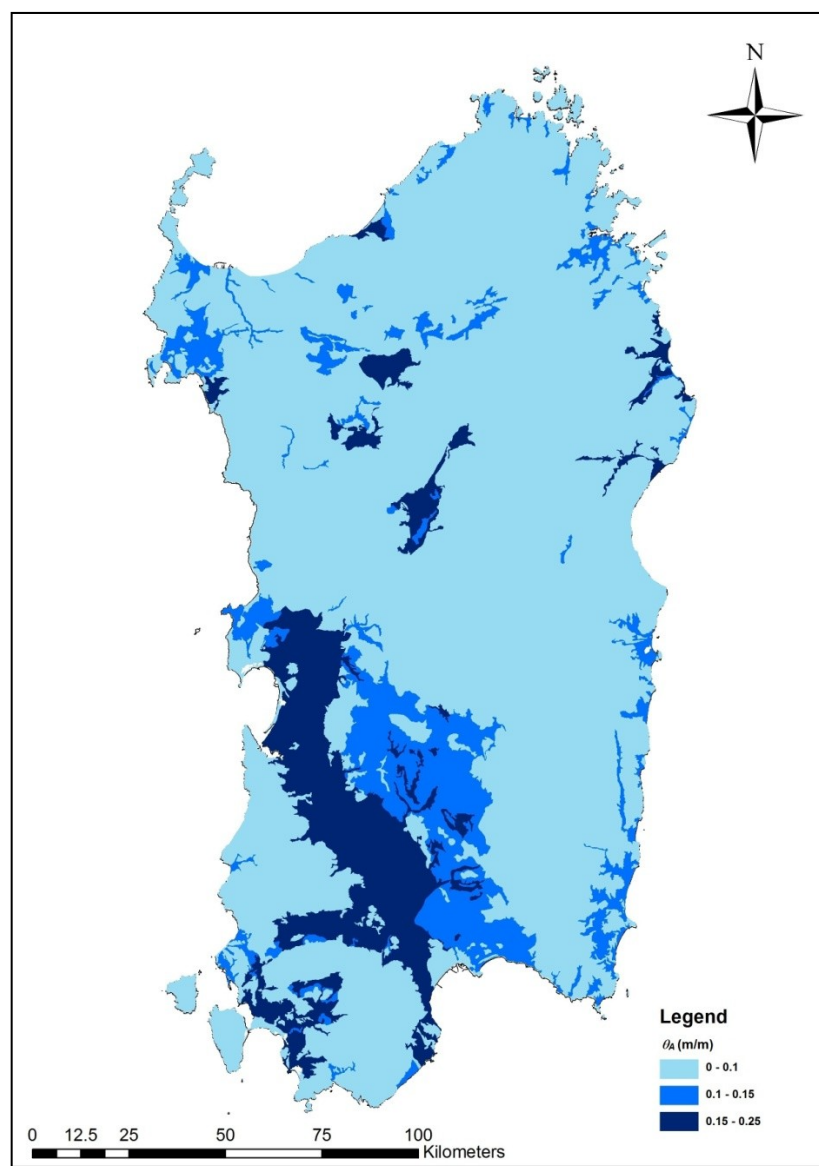


Figure 3. Soil available water holding capacity (θ_A) in Sardinia.

Data related to the cultivated area for each municipality or small homogeneous area during 2010, and irrigation system by crop combinations were provided by the consorzia that manage irrigation in Sardinia (ConSORZI di Bonifica della Sardinia), with the exception for some areas in zone 2. For these municipalities the cultivated area data were provided by the directorate general for agriculture of the Regione Autonoma della Sardegna (Servizio sviluppo, monitoraggio e valutazione - Direzione generale dell'agricoltura e riforma agro-pastorale) from the regional database on products subject to government funding in agriculture,

Crop management data for artichokes, silage and grain maize, olive, grapevines and citrus for each zone were provided by Laore, the agency for technical assistance in agriculture.

In order to match the planted areas, crop management, and soil data in each ET_o zone, the ArcGIS 9.3 software (ESRI, 2008) was used. When a municipality presented more than one class of soil available water holding capacity, the highest class was selected.

In some municipalities within zones 4 and 7, it was difficult to distinguish between grain and silage maize, so these areas were separated into 50% silage and 50% grain.

In some areas of Sardinia, artichokes are cultivated as early season (fresh markets) and, in other regions, they are managed as late season (processed product). In some municipalities, the artichoke cultivation was not distinguished, so zones were divided equally into 50% early and 50% late season.

Zones, 3, 5 and 6 had good records on combinations of crops and irrigation systems. Zones 1, 2, 4, and 7 had limited data irrigation system and crop combinations. In these zones, based on known communication with local inhabitants, the most common irrigation system and crop combinations were (1) sprinkler for maize and artichokes, (2) micro-sprinkler for citrus, and (3) drip systems for olive orchards and grapevines.

The three classes for soil available water holding capacity were: low (L), medium (M) and heavy (H). The used irrigation systems were: sprinkler (SP), drip (DR), and micro-sprinkler (MS). Moreover, to distinguish the two crop management of artichokes, "E" was used to indicate early season and "L" for late season.

Crop management data included the start date (planting for field crops or leaf out for deciduous orchards), end date (when transpiration ceases), maximum rooting depth, beginning and end date for grass or weed ground cover in orchards and vineyards. The typical crop management used in Sardinia is listed in Table 2, although each ET_o zone showed some differences. Type 4 crops have ET all year, so there are no start and end dates for those crops in the table.

Typical distribution uniformity (DU) values for irrigation systems were found in the paper Agricultural Water Use in California (The Center for Irrigation Technology, 2011). The typical DU average values for the major irrigation system types are: 75% for sprinkler, 80% for micro-sprinkler, and 85% for drip irrigation. Tables 3-9 list the summary of crop information for each ET_o zone.

In SIMETAW#, the percentage of the irrigation requirement (PIR) is used to identify the water allocation as a percentage of the full irrigation requirement. In this study, the PIR was set as 100%.

Table 2. Typical crop management in Sardinia.

ANNUAL CROPS				
Crop	Planting (day/month)	End (day/month)	Initial Growth Wetting Frequency	
E-ARTICHOKES	20/06	30/03	every 4 days	
L-ARTICHOKES	15/08	31/05	every 4 days	
MAIZE (grain)	07/05	24/09	every 7 days	
MAIZE (silage)	01/06	15/09	every 3 days	
TREE CROPS				
Crop	Leaf Out (day/month)	End (day/month)	Cover Crop Beginning (day/month)	Cover Crop End (day/month)
CITRUS			01/10	31/05
OLIVES			15/02	31/05
GRAPEVINES	05/03	20/09		

Table 3. Summary of crop information in zone 1.

ZONE 1		
CROP	HECTARES	IRRIGATION SYSTEM
CITRUS	2	100% MS
MAIZE (silage)	29	100% SP
OLIVES	53	100% DR
GRAPEVINES	74	100% DR

Table 4. Summary of crop information in zone 2.

ZONE 2		
CROP	HECTARES	IRRIGATION SYSTEM
CITRUS	23	100% MS
ARTICHOKES	720	22% SP-78% DR
MAIZE (grain)	343	100% SP
MAIZE (silage)	1150	100% SP
OLIVES	1125	11% MS-89% DR
GRAPEVINES	1393	12% SP-88% DR

Table 5. Summary crop information in zone 3.

ZONE 3		
CROP	HECTARES	IRRIGATION SYSTEM
CITRUS	196	50% MS-50% DR
ARTICHOKES	2	100% SP
MAIZE (grain)	56	100% SP
MAIZE (silage)	5	100% SP
OLIVES	219	100% DR
GRAPEVINES	15	100% DR

Table 6. Summary crop information in zone 4.

ZONE 4		
CROP	HECTARES	IRRIGATION SYSTEM
CITRUS	1036	100% MS
ARTICHOKES	1672	8% MS-92% SP
MAIZE (grain)	201	100% SP
MAIZE (silage)	196	100% SP
OLIVES	170	100% DR
GRAPEVINES	138	100% DR

Table 7. Summary of crop information in zone 5.

ZONE 5		
CROP	HECTARES	IRRIGATION SYSTEM
CITRUS	587	15% DR-85% MS
ARTICHOKES	476	1% DR-27% MS-72% SP
MAIZE (grain)	14	100% SP
MAIZE (silage)	90	100% SP
OLIVES	84	14% MS-86% DR
GRAPEVINES	410	1% SP-99% DR

Table 8. Summary of crop information in zone 6.

ZONE 6		
CROP	HECTARES	IRRIGATION SYSTEM
CITRUS	229	5% DR-95% MS
ARTICHOKES	71	4% DR-31% SP-64% MS
MAIZE (silage)	38	100% SP
OLIVES	39	69% DR-31% MS
GRAPEVINES	153	3% MS-97% DR

Table 9. Summary of crop information in zone 7.

ZONE 7		
CROP	HECTARES	IRRIGATION SYSTEM
CITRUS	565	2% DR-98% MS
ARTICHOKES	2063	81% SP-19% MS
MAIZE (silage)	4345	100% SP
OLIVES	225	24% MS-76% DR
GRAPEVINES	199	100% DR

2.4. Impact of climate change on the irrigation water requirement

To compute the IR for the current period, the SIMETAW# model was run in each ET_o zone using the observed data (2000-2004) of the representative weather station for each zone. The evapotranspiration of applied water (ET_{aw}), which is equal to the sum of the net applications (ΣNA), and the sum of the gross applications (ΣGA) was computed for all soil, crop management, and irrigation system combinations as reported in the previous section.

Climate data delivered by dynamic downscaling of the GCM CMCC-MED through the RCM COSMO-CLM (8 Km) under the A1B future emission scenario, provided by the CMCC (Centro Euro-Mediterraneo sui Cambiamenti Climatici) were used to evaluate the climate change impact on IR.

The climate model CMCC-Med is a coupled model atmosphere-ocean-sea-ice based on the climate model CMCC-CM (Scoccimarro et al., 2011) but with a focus on the Mediterranean region. In the CMCC-Med model the global atmospheric component is ECHAM5 (Roeckner et al., 2003) implemented at high-resolution (T159) corresponding to a horizontal grid spacing of about 80 Km ($0.75^\circ \times 0.75^\circ$) with 31 vertical levels.

The ocean component is the global ocean and sea ice model OPA 8.2 (Madec et al., 1998), in its ORCA2 global configuration. The horizontal resolution is $2^\circ \times 2^\circ$ (~200 km) with a meridional refinement near the equator, approaching a minimum 0.5° grid spacing. The model has 31 vertical levels, 10 of which lie within the upper 100 m. ORCA2 also includes the Louvain-La-Neuve (LIM) model for the dynamics and thermodynamics of sea ice (Timmermann et al., 2005). The other component is the Mediterranean sea model NEMO-MFS (Nucleus for European Modelling of the Ocean) (Oddo et al., 2009) with a resolution of ~7 km.

The OASIS3 (Ocean Atmosphere Sea Ice Soil) developed by Valcke (2006) is the coupler among the three models. The coupling is carried out every two hours between atmosphere and ocean, and every eight hours between global ocean and Mediterranean sea models. Heat, mass, and momentum fluxes are computed and provided to the ocean model by the atmospheric model; sea surface temperature and sea surface velocities are provided to the atmospheric model by both ocean models.

The CLM (Rockel et al., 2008) is the climate version of the COSMO model (Steppeler et al., 2003), the operational non-hydrostatic mesoscale weather forecast model developed at the German Weather Service. It can be used with a spatial resolution between 1 and 50 km. The horizontal resolution adopted in the simulation was about 8 km, in order to have a better detail compared with the spatial resolution of 14 km previously developed (Bucchignani et al., 2011).

The A1B scenario belongs to the A1 scenario family of the SRES storylines (IPCC, 2007). The A1 family describes a future world of very rapid economic growth, a global population that peaks in mid-century, declines thereafter, and the introduction of new and efficient technologies. A1 develops into three groups that describe alternative development of energy supply: fossil intensive (A1FI), non-fossil energy sources (A1T), or a balance between all sources (A1B).

Projected daily climate data for the representative seven ARPAS climate stations were extracted from the Sardinia climate for the period 1971 to 2100. The period from 1971 to 2000 was considered the baseline. The period from 2035 to 2065, centered on 2050, which was the reporting year, was considered the future period. The 30 year mean daily data over the baseline and future period were computed. The CO₂ concentration during the future period was estimated at 519 ppm. The FAO (Standardized) Penman Monteith equation (Allen et al., 1998, 2005) was used to compute ET_o .

A SIMETAW# model run using data from 1971 to 2000 gave the baseline scenario for all soil and crop management combinations. Similarly, the ΣNA and ΣGA for the future period were estimated using both ‘current’ and ‘future’ CO₂ concentrations and the impact of climate change on IR was computed.

After identifying the zone that showed the highest increase in annual ET_o and maximum reduction in precipitation under ‘future’ conditions, some adaptation strategies were applied. For maize grain, a shift in planting and harvesting date was

considered. The dates were shifted one month earlier, D-30 days, and one month later, D+30 days, where D represents current typical dates for the zone. For tree crops, the applied water was reduced by 20% by setting $PIR= 80\%$. For citrus, the irrigation system was changed from micro-sprinkler to drip irrigation.

3. RESULTS AND DISCUSSION

3.1. The current irrigation water demand

The summary results for the in-season ET_{aw} and ΣGA (mm) for the current period, using observed data, are listed in Tables 10-14 for each ET_o zone. The ET_{aw} is equivalent to the sum of the net applications during the irrigation season, and the net applications are determined by calculating a daily water balance and irrigating when the soil water depletion exceeds a management allowable depletion (MAD). The ΣGA is the sum of the gross applications, which is estimated as the ET_{aw} divided by the mean irrigation application efficiency for the selected irrigation system. The mean application efficiency is estimated from the system's distribution uniformity and runoff if it occurs.

Zone 7 always had the maximum ET_{aw} values for tree and vine crops (Tables 10-12), and it had an average of precipitation of about 529 mm year⁻¹ with 29 mm during summer months. For the tree and vine crops (Tables 10-12), the lowest ET_{aw} values were observed in zone 3. This zone also had the highest precipitation (880 mm year⁻¹).

Precipitation and especially rainfall distribution (Figure 4) are extremely important for the IR computation. In fact, zones 3 and 6 belong to 4.5-5 mm day⁻¹ ET_o class, but zone 6 has about half as much precipitation, and the result is a higher ET_{aw} for tree and vine crops in zone 6 (Tables 10-12). Zone 2 also showed an higher IR than zone 5, which has the same ET_o class, but with the total precipitation amount in zone 2 slightly higher than in zone 5 (Figure 4). The cumulative ET_o in zone 2 (1,140 mm) was higher than in zone 5 (1,058 mm), but the higher precipitation in zone 2 did not compensate for the higher ET_o , thus zone 2 had a higher IR than zone 5. The same results were obtained in zone 1, where the ET_{aw} values were higher than in zone 4. Zone 1 had slightly less precipitation than zone 4, but the cumulative ET_o was about 120 mm higher in zone 1 than in zone 4.

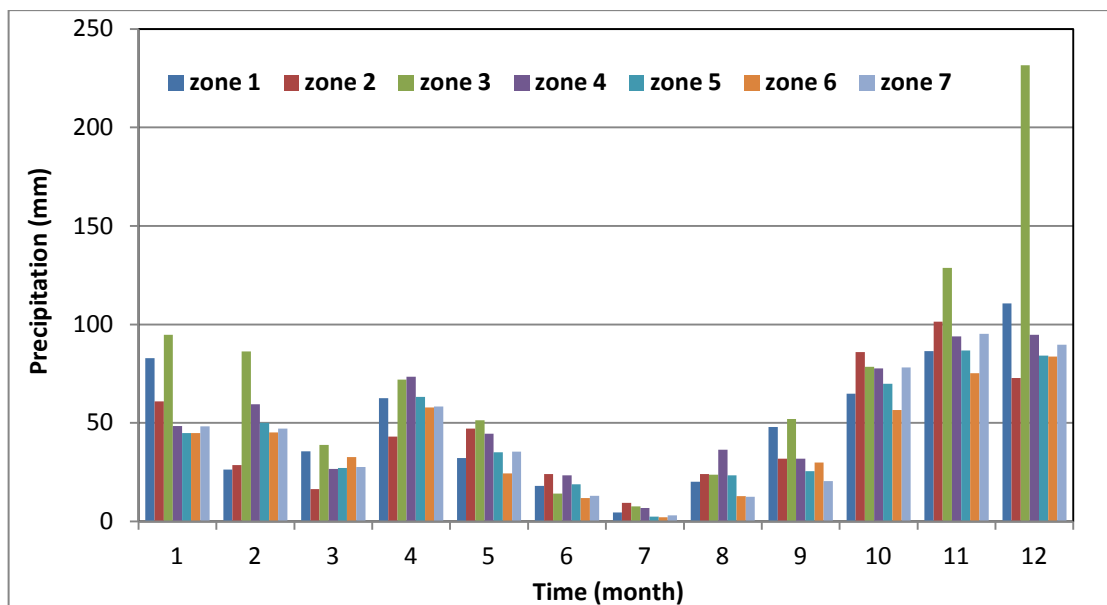


Figure 4. Precipitation distribution in each zone for the current period.

Tree crops are typically not irrigated during the entire growing season in Sardinia. Typically, the irrigation season is from April to October for citrus, from April to September for olives, and from June to August for grapevines (Laore, personal communication). Therefore, the ET_{aw} was computed relative to both the irrigation and the growing season (Tables 10-12).

For citrus, all the irrigation requirement was estimated to be during the irrigation season in zone 3 (Table 10). Similar results were observed for zones 4, 5, 6, and 7 with a percentage of ET_{aw} during the irrigation season close to 100%. In zones 1 and 2 the percentage of ET_{aw} during the irrigation season is lower, and this means that some irrigation events were needed outside of the irrigation season.

For olives (Table 11) the percentage of ET_{aw} during the irrigation season was between 87% (zone 1) and 99% (zone 5). The results again showed the necessity for a few irrigation events before or after the irrigation season, especially in zone 1 (13%). However, considering the percentage of ET_{aw} during the irrigation season for citrus and olives, the irrigation management adopted in Sardinia matched fairly well with the irrigation water demand.

Grapevines are commonly affected by water stress as shown in Table 12. Zone 2 was the area most affected by water stress (65%), followed by zones 1 and 6 (71%). Zone 3, with a 75% value during the irrigation season, was the area less affected by water stress. Actually, in Sardinia both olives and grapevines are commonly grown

under water stress conditions to obtain better production quality (Laore, personal communication). The observations in Tables 11 and 12 were determined assuming no water stress, which partially explains why the results indicate the need for irrigation outside of the irrigation season.

Table 10. Growing and irrigation season (April to October) mean ET_{aw} , growing season ΣGA , and percentage of ET_{aw} during the irrigation season compared with the growing season of citrus.

CITRUS				
Zone	Growing season mean ET_{aw} (mm)	Growing season mean ΣGA (mm)	Irrigation season mean ET_{aw} (mm)	Irrigation season ET_{aw} %
1	596	795	535	90
2	541	676	482	89
3	373	453	372	100
4	515	643	492	96
5	517	633	506	98
6	449	550	437	97
7	633	768	610	96

Table 11. Growing and irrigation season (April to September) mean ET_{aw} , growing season ΣGA , and percentage of ET_{aw} during the irrigation season compared with the growing season of olives.

OLIVES				
Zone	Growing season mean ET_{aw} (mm)	Growing season mean ΣGA (mm)	Irrigation season mean ET_{aw} (mm)	Irrigation season ET_{aw} %
1	579	681	502	87
2	539	644	476	88
3	392	461	360	92
4	496	583	462	93
5	475	571	468	99
6	438	530	430	98
7	568	688	551	97

Table 12. Growing and irrigation season (June to August) mean ET_{aw} , growing season ΣGA , and percentage of ET_{aw} during the irrigation season compared with the growing season of grapevines.

GRAPEVINES				
Zone	Growing season mean ET_{aw} (mm)	Growing season mean ΣGA (mm)	Irrigation season mean ET_{aw} (mm)	Irrigation season ET_{aw} %
1	491	578	349	71
2	536	645	346	65
3	389	458	290	75
4	469	552	350	75
5	475	584	344	72
6	438	531	313	71
7	551	648	395	72

Depending on management, the irrigation water demand for artichokes ranges between 127 and 333 mm (Tables 13), whereas the IR is 399-592 mm for maize (Table 14). The late growing artichokes (L-Artichokes) required less IR than the earlier growing artichokes (E-Artichokes), where the irrigation events occur mostly during the initial growth. The IR of E-Artichokes and grain maize was proportional to the ET_o class, while some differences were noticed for silage probably due to different crop management strategies. In fact, silage planted in April (e.g., zone 1) required less irrigation than that planted at the beginning of June (e.g., zone 4). The same results were observed between zone 2 and 5, where the sowing at the beginning of summertime required more frequent irrigation during initial growth (every 3 days).

Table 13. Summary of the in-season ET_{aw} and ΣGA (mm) of artichokes.

Zone	E-ARTICHOKES		L-ARTICHOKES	
	Growing season mean ET_{aw} (mm)	Growing season mean ΣGA (mm)	Growing season mean ET_{aw} (mm)	Growing season mean ΣGA (mm)
2	301	370	146	183
3	235	313		
4	282	369	189	252
5	274	354	202	257
6	243	314	127	159
7	333	430	226	292

Table 14. Summary of the in-season ET_{aw} and ΣGA (mm) of maize.

Zone	MAIZE (GRAIN)		MAIZE (SILAGE)	
	Growing season mean ET_{aw} (mm)	Growing season mean ΣGA (mm)	Growing season mean ET_{aw} (mm)	Growing season mean ΣGA (mm)
1			449	599
2	498	664	498	664
3	424	565	421	561
4	533	711	475	633
5	508	677	447	596
6			399	531
7	592	789	540	720

3.2. Impact of climate change on future irrigation water demand

The modeling results showed an increase of ET_o values and a decrease of precipitation for the ‘future’ climate conditions in Sardinia (Table 15). With the exception of zone 1, where the decrease of precipitation was only of 1%, most locations had reductions between 10% and 19%. ET_o was projected to increase under the ‘future’ conditions using both ‘current’ and higher CO_2 concentrations. The increase in ET_o rates was approximately double when the ‘current’ CO_2 concentration rather than projected ‘future’ concentration was employed to compute ET_o . The results indicate that zone 4, with an ET_o increase of 6%, under future CO_2 concentration, and a 19% reduction in precipitation, was the most affected location by climate change.

With regards to the rate of regional change in ET_o (Figure 5), the highest increase was in January (9%) and May (7%), while April and September showed the lowest increase. Summertime showed a mean ET_o increase of 5%, and the values were slightly higher during the last months of the year. The rate of change in mean annual regional ET_o was estimated to increase by about 5%, under ‘future’ CO_2 concentration.

Table 15. Changes (%) in cumulative ET_o and precipitation from now to 2050, with current and future CO_2 concentrations in each zone.

Zone	ET_o -current CO_2 (%)	ET_o -future CO_2 (%)	Precipitation (%)
1	7	3	-1
2	7	3	-18
3	11	6	-18
4	11	6	-19
5	10	5	-18
6	9	4	-10
7	9	5	-19

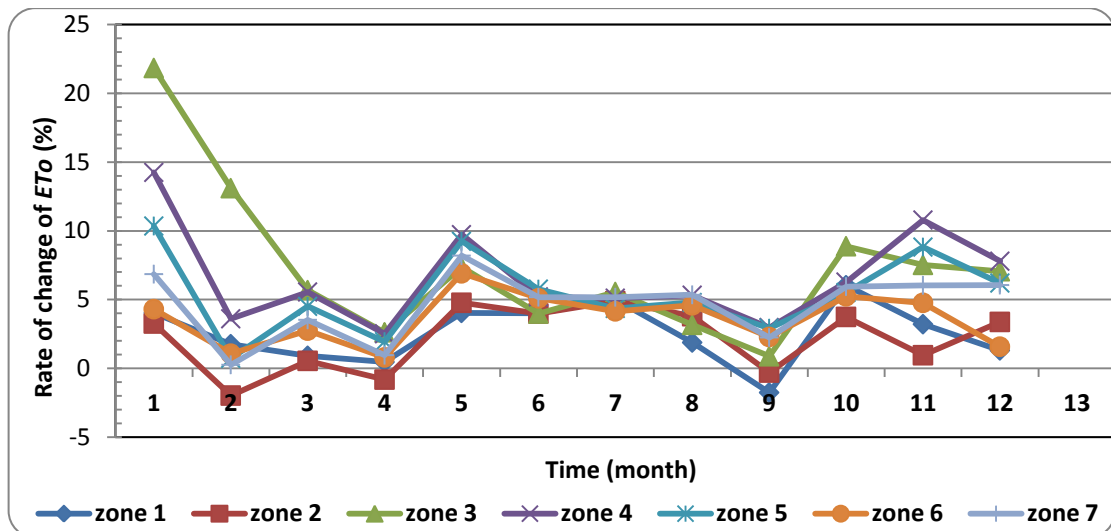


Figure 5 Rate of change (%) in cumulative ET_o at regional level, under future CO_2 concentration, compared with the baseline.

Since the magnitude of the rate of change in ET_o is closely related to different climate change scenarios, GCMs and RCMs, future periods, and equations used to compute ET_o , making a close comparison with other studies is impossible. However considering the limited information value, several studies projected a general increase of ET_o in Mediterranean basin. Rodríguez Díaz et al. (2007) estimated the increase of ET_o , computed by the FAO Penman Monteith method, of about 8% under the A2 and B2 scenarios in 2050 in the Guadalquivir river basin (Southern Spain). In the same region, also Pérez Urrestarazu et al. (2010) showed an increase of ET_o under the A2 and B2 scenarios (2050; 2080). ET_o was computed by the FAO Penman Monteith method, and it was predicted about 14% higher than the baseline by the 2050s and 25% by the 2080s. The increase of ET_o was higher in winter for the A2 scenario, while in B2 the increments were more constant along the year. The summer period presented the maximum difference in ET_o compared with the baseline for both scenarios. Another study conducted by Lhomme et al. (2009) in Tunisia demonstrated that the reference evapotranspiration, computed by the Penman-Monteith method under the A1B scenario, will increase from 14 to 25% and from 8 to 15% in the Northern and Central region (2071-2100), respectively. As pointed out by Kapur et al. (2007), ET_o , estimated by the use of the Hargreaves–Samani equation (Hargreaves and Samani, 1985), is projected to increase up to 15% in Apulia (Southern Italy) under the A2 scenario conditions in the next 100 years.

On the contrary, Lovelli et al. (2010) showed a reduction of ET_o all over the year, with a greater decrease during the spring summer period in 2071 considering the A2 scenario in Southern Italy. Senatore et al. (2011), applying different RCMs and among these the RCM COSMO-CLM with the A1B scenario of the ECHAM5/MPI-OM GCM in Southern Italy, showed that in future (2070–2099) evapotranspiration is expected to increase during wintertime and decrease in summertime.

With respect to the estimate of precipitation trends in future, several studies confirmed a general reduction in Mediterranean basin, considering different GCMs and RCMs. The main changes are expected in the annual distribution, with more rainfall during winter and less in summer. Moriondo et al. (2010) selected the time-slice 2030–2060, simulated by the HADCM3 A2 scenario, to represent the period corresponding to a global average increase of $+2^{\circ}\text{C}$ with respect to the pre-industrial period in Europe. They showed that a clear decrease in rainfall is likely for the regions below 55°N , especially over the Mediterranean basin. Over these areas, the summer period is projected to exhibit a rainfall decrease up to 35% with respect to the baseline. Senatore et al. (2011) showed that the reduction in precipitation of 20% and 21% in Southern Italy was predicted considering the RegCM and CLM regional models, respectively. Both models showed the greatest reduction during the driest period of the year (summer) to varying degrees, with about 60% reduction in July and August. The average reduction during winter (January–March) by CLM was about 20%. Similarly in Southern Italy, precipitation is projected to decrease by almost 90% during summertime in 2071 under the A2 scenario (Lovelli et al., 2010).

According with Ayala (2002) a reduction in precipitation up to 34% for the Guadalquivir basin was also projected. For the same region, Rodríguez Díaz et al. (2007), estimated a reduction of the average annual precipitation of 7 and 1% under the A2 and B2 scenarios in 2050. Decreasing rainfall trends in Turkey have already been observed during the 20th century (Türkeş, 1996); precipitation was projected to decrease more in future in Çukurova plain (Yano et al., 2007). In fact, precipitation was estimated to decrease by about 163, 163, and 105 mm during the period of 1990 to 2100 under the A2 scenario of the CGCM2, ECHAM4 and MRI models, respectively. While for the future period (2070 to 2079) projected mean annual precipitation would decrease

by 133, 56, and 306 mm, equivalent to 25, 12 and 46% decrease according to the CGCM2, ECHAM4 and RCM models, respectively.

In a study conducted by Lhomme et al. (2009), under the A1B scenario, it was demonstrated that in Northern Tunisia in the period 2071-2100 precipitation tends to increase in summer from July to October (up to +12%), but decreases during the rest of the year (down to -44% in April), with an annual mean decrease of 20%. On the other hand, in Central Tunisia, the annual precipitation was projected up by 11% for the same timeframe: precipitation increases from September to February (with a maximum of +94% in October) and then decreases the rest of the year (down to -29% in April).

The estimated future irrigation requirement showed a negative impact for the entire region for each crop taking into consideration the increase in CO₂ concentration. Figures 6-12 list the summary ΣNA and ΣGA (ha m) for each crop computed for the 'current' and the 'future' CO₂ concentration. Moreover, it is shown the rate of change (%) of the future IR from the baseline, computed for both the 'future' and 'current' CO₂ concentrations. In all cases, climate change increased IR more for the 'current' than 'future' CO₂ concentration used with the 'future' climate projection. This means that higher irrigation water demand will be expected in future if the CO₂ concentration does not increase and reduce the effect of higher temperature. Data relatively to ΣNA and ΣGA computed under the 'current' CO₂ concentration are not shown, but the rate of change in IR gives an idea of the magnitude of the increase in irrigation water demand.

Citrus

The most marked difference in the rate of change of IR of citrus was observed in zone 3, with 10 and 21% (Figure 8), considering the two CO₂ concentrations, while in the other locations it was less evident. However, the impact on IR was fairly significant if the 'current' CO₂ concentration was considered (12-21%), especially in zones 3, 4 and 5. Taking into consideration the CO₂ effect, zone 4 (Figure 9) showed the highest impact on irrigation water demand (14%). In addition, this zone has the biggest citrus cropland in Sardinia; the projected 'future' ΣGA is about 1,111 ha m if the CO₂ effect is taken into account, and 1,175 ha m based on the 'current' CO₂ concentration. Zone 5 (Figure 10) shows a significant increase in IR (13%), although the projected 'future' ΣGA (666 ha m) is lower than zone 4, and the land cultivated with citrus is nearly half of zone 4. On the contrary, zone 1 was the least affected area (6%), but also the least

cultivated zone. At regional level, citrus was projected to increase of about 10% considering the future CO₂ condition, and 17% considering the current CO₂ concentration.

Grapevines

With respect to grapevines, zone 2 showed the greatest irrigation consumption (1,393 ha m), although the rate of increase of IR (3%) is relatively low (Figure 7). The highest impact was observed in zone 3 (11%), where irrigating grapevines is uncommon (Figure 8). Conversely, in zones 5 and 7 the rate of change of IR was 8 and 5%, respectively; and these zones showed 'future' ΣGA increases of 368 and 171 ha m, respectively (Figures 10 and 12). The difference in rate of change of IR between the two CO₂ concentrations was less evident in zone 1 and 2. The IR was projected to increase by 5% in zone 7 under the 'future' CO₂ concentration (Figure 12), and 16% under 'current' CO₂ level. Similar trends were observed in the other locations. However, the IR was projected to increase from 3 to 11% under 'future' CO₂ concentration, and from 8 to 16% under 'current' CO₂ values. At the regional level, grapevines are projected to increase the irrigation water demand by 6% considering the 'future' CO₂ concentration and 12% with the 'current' CO₂ condition.

Olives

The impact of climate change on olive orchards was fairly homogeneous all over the region with an increase in IR between 9 and 14% under 'future' CO₂ concentration, and 12 - 22% under 'current' CO₂ concentration. Zone 6 with a lower value was an exception (Figure 11). Zone 2, with an IR increase of 10%, is the main area for irrigated olives in Sardinia (Figure 7); it showed a future irrigation requirement of 1,044 ha m, an amount much greater than in the other areas. In zones 3 and 7 (Figures 8 and 12), growing olives in irrigated condition is typical and the future IR was projected to increase by 164 and 177 ha m, respectively. In these areas, the increase in IR without increasing the CO₂ effect was equal to 22 and 18% for zones 3 and 7, respectively. On the other hand, computing the IR under 'future' CO₂ concentration led to an increase in IR equal to 14 and 12% for zones 3 and 7, respectively. The biggest increase in IR between the two CO₂ concentrations was observed in zone 3 (Figure 8). On a regional level, olive orchards were projected to increase the irrigation water demand by about

11% considering using the ‘future’ CO₂ concentration, and 18% with the ‘current’ CO₂ conditions.

Artichokes

The irrigation water demand for artichokes was projected to increase from 8 to 19% under ‘future’ CO₂ concentrations, and from 13 to 27% under ‘current’ CO₂ values, with the exception for zone 1 that did not grow artichokes, and zone 3 had a small percentage increase in IR. Zones 4 and 7 are the areas where artichokes are commonly planted and it is the area most affected by climate change. The ΣGA was predicted to increase by 788 and 1,049 ha m in zones 4 and 7, respectively (Figures 9 and 12). If the current CO₂ level is used, the ΣGA is predicted to increase by 832 and 1,114 ha m in zone 4 and 7, respectively. Both zones have mainly late seasons artichokes and they showed the highest increases in IR considering both CO₂ concentrations. Zone 5 had the same increase in IR as zone 7, i.e., 19% for ‘future’ and 27% for ‘current’ CO₂ concentrations; however, the area planted to artichokes is lower in zones 5 than 7. The most marked difference in increase of IR for artichokes was observed in zone 3, with an increase in IR of 7 and 19% (Figure 8) for the ‘future’ and ‘current’ CO₂ concentrations, respectively. Zone 3, however, is also the zone with the fewest hectares planted to artichokes. On a regional level, artichokes were projected to increase the irrigation water demand by about 14% considering the ‘future’ CO₂ concentration and 21% using the ‘current’ CO₂ condition.

Maize

The difference in the increase in IR between the two CO₂ concentrations was less evident in maize (a C₄ species) than in the C₃ species. Silage in zone 6 showed the smallest increase in IR among all crops and zones (Figure 11). In fact, an increase of 2% in irrigation water demand was projected when the ‘future’ CO₂ concentration was considered. The increase was about 6% when the ‘current’ CO₂ level was used. Between the two maize types, silage in zones 2 and 3 had higher increase in IR than grain maize (Figures 7 and 8). The opposite situation was observed in zones 4, 5, and 7 (Figures 9, 10, and 12). This inverse situation is probably due to the difference in crop management. In fact, grain maize was sown about the beginning of May in all zones, while silage is typically planted in April in zones 2 and 3, and in June in the others zones. As shown in figure 5, ET_o is projected to increase by 5 and 7% in zones 2 and 3,

respectively; however, the increase in ET_o is even higher in the other zones (about 9%). Thus, silage grown in zones with an earlier planting date was more affected by climate change impact on the ET_o in May than in zones with a later planting date. The irrigation water demand for silage was projected to increase from 2 to 9% under the ‘future’ CO_2 concentration, and from 6 to 13% under ‘current’ CO_2 values.

The irrigation water demand for grain maize was projected to increase from 4 to 6% under ‘future’ CO_2 concentration and from 8 to 10% under ‘current’ CO_2 values. Silage in zone 3 (Figure 8) showed the highest increase in IR (9%). Zone 2 showed an increase in IR of about 7%, and the ΣGA was predicted to increase by 907 ha m using the ‘future’ CO_2 fertilization effect, while it was projected to increase by 936 ha m, with the ‘current’ CO_2 level (Figure 7). Zone 7, with the biggest silage cropped area, is projected to have a 5% increase in IR, but the ΣGA is projected to increase by 3,696 and 3,818 ha m, for the ‘future’ and ‘current’ CO_2 levels, respectively (Figure 12). Zones 3, 4, and 7 showed also the highest increase in IR for grain maize (6%) under the ‘future’ CO_2 levels; the increase in IR was about 9% under the ‘current’ CO_2 level. On a regional level, both silage and grain maize were projected to increase the irrigation water demand by about 5% considering the ‘future’ CO_2 concentration, and 9% using the ‘current’ CO_2 condition.

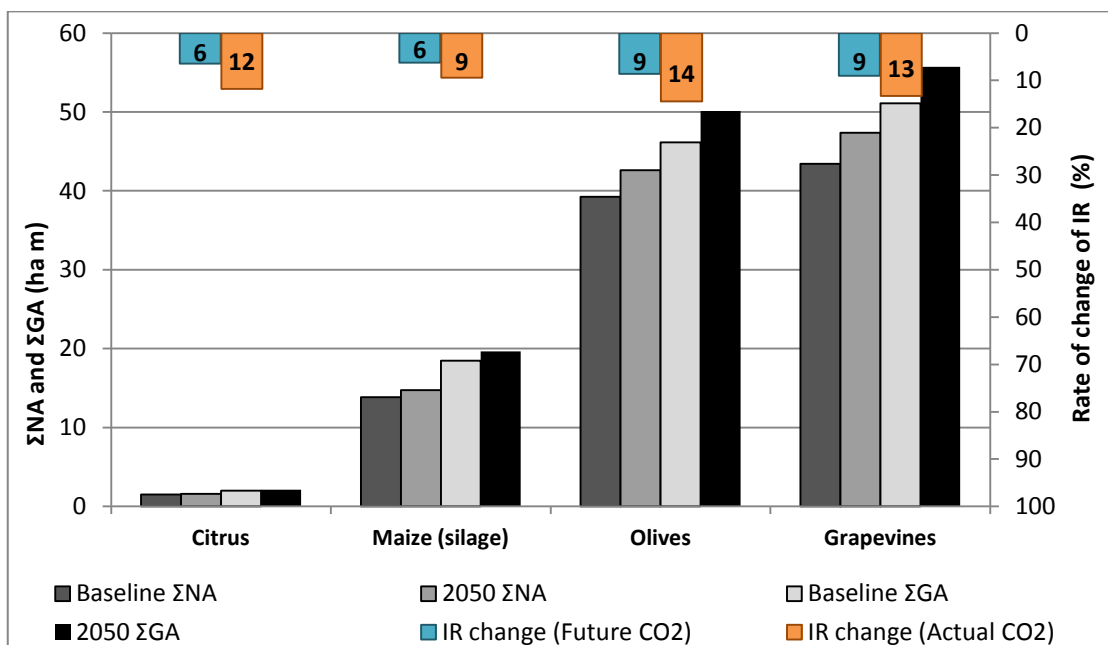


Figure 6. ΣNA and ΣGA (ha m) for the baseline and future period (considering the future CO_2 concentration), and rate of change (%) of the future irrigation requirement compared with the baseline, under the current and future CO_2 concentrations (zone 1).

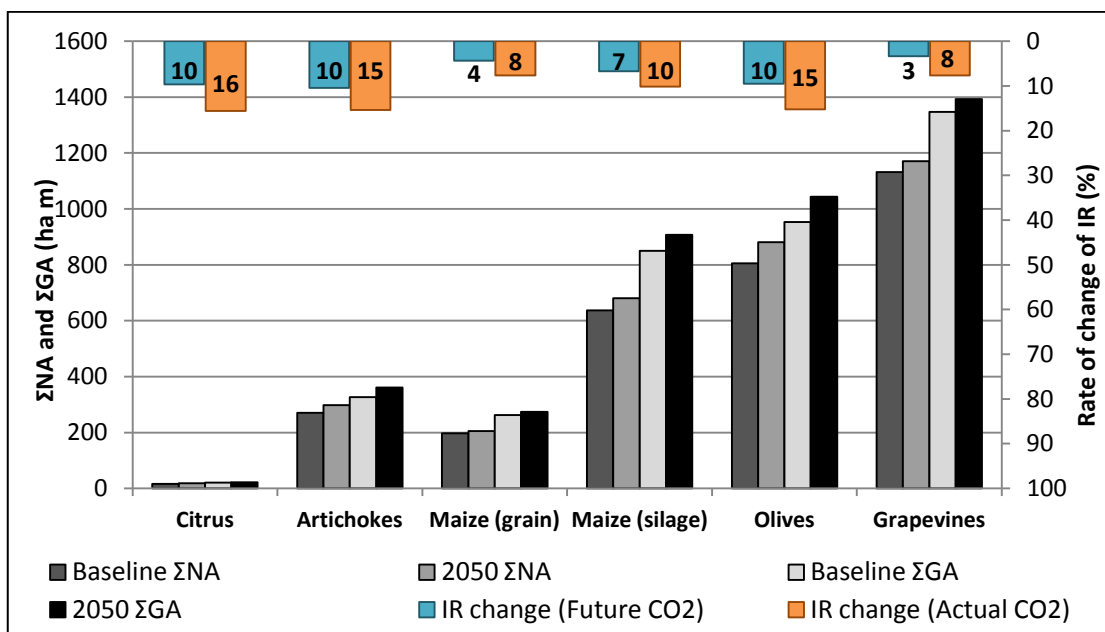


Figure 7. ΣNA and ΣGA (ha m) for the baseline and future period (considering the future CO_2 concentration), and rate of change (%) of the future irrigation requirement compared with the baseline, under the current and future CO_2 concentrations (zone 2).

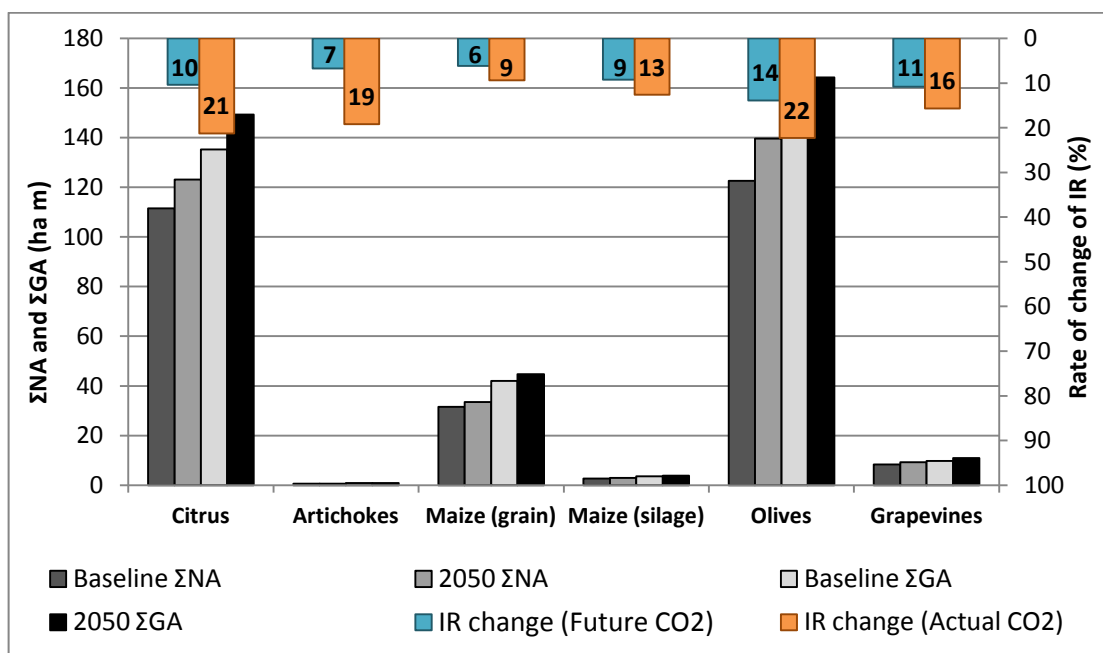


Figure 8. ΣNA and ΣGA (ha m) for the baseline and future period (considering the future CO_2 concentration), and rate of change (%) of the future irrigation requirement compared with the baseline, under the current and future CO_2 concentrations (zone 3).

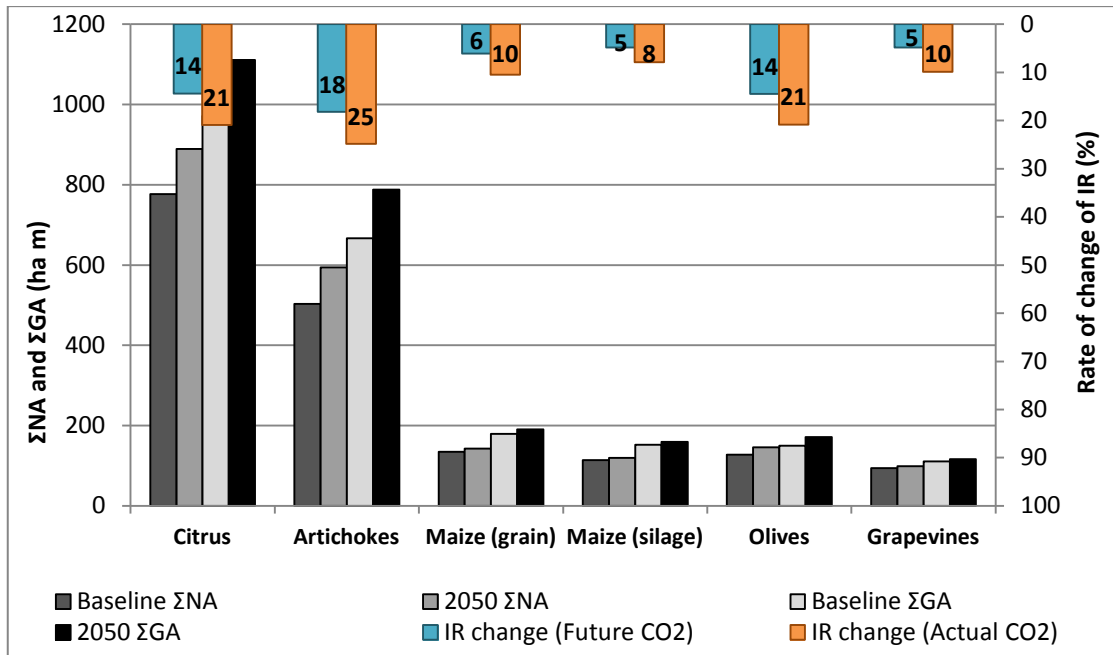


Figure 9. ΣNA and ΣGA (ha m) for the baseline and future period (considering the future CO_2 concentration), and rate of change (%) of the future irrigation requirement compared with the baseline, under the current and future CO_2 concentrations (zone 4).

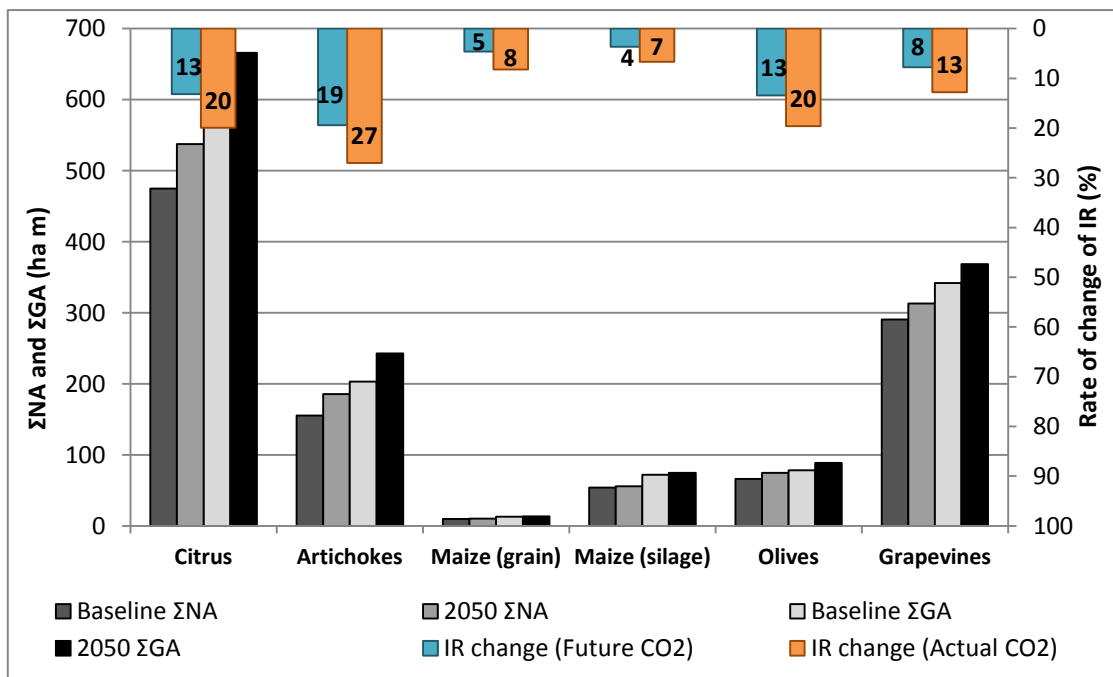


Figure 10. ΣNA and ΣGA (ha m) for the baseline and future period (considering the future CO_2 concentration), and rate of change (%) of the future irrigation requirement compared with the baseline, under the current and future CO_2 concentrations (zone 5).

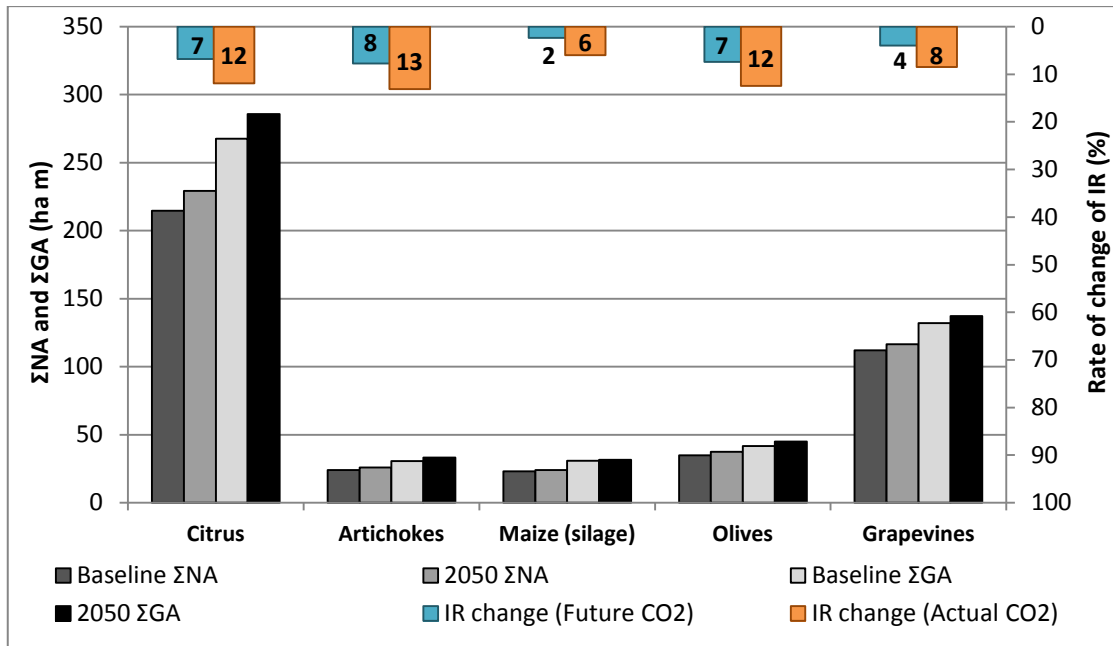


Figure 11. ΣNA and ΣGA (ha m) for the baseline and future period (considering the future CO_2 concentration), and rate of change (%) of the future irrigation requirement compared with the baseline, under the current and future CO_2 concentrations (zone 6).

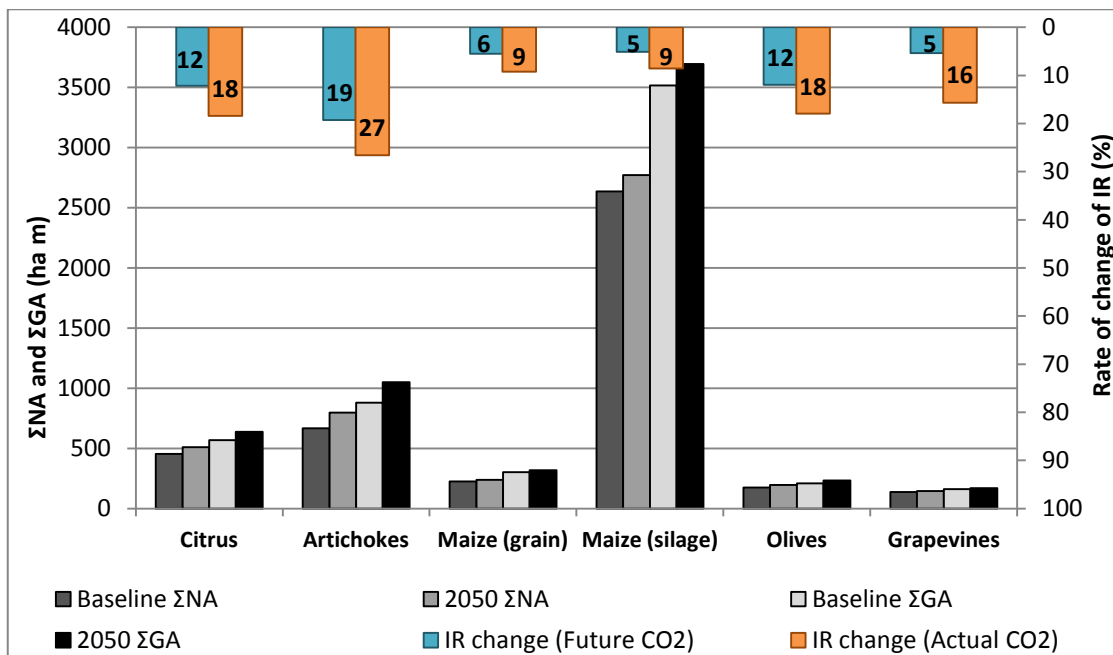


Figure 12. ΣNA and ΣGA (ha m) for the baseline and future period (considering the future CO_2 concentration), and rate of change (%) of the future irrigation requirement compared with the baseline, under the current and future CO_2 concentrations (zone 7).

Irrigation water demand depends on ET_o rates and precipitation patterns, and IR will increase or decrease depending on the cropping season, ET_o , and precipitation. On a regional level, an increase IR demand for the studied crops of about 9 and 15% is

expected under the ‘future’ and ‘current’ CO₂ concentrations, respectively. Zone 4, one of the most important areas for agriculture in Sardinia, was most negatively affected by climate change with an IR increase of 14%. The next two important areas for agricultural production are zone 2 and 7, which showed the lowest increase in IR, with increases of 6 and 8%, respectively. The future IR for Sardinia is projected to increase up to about 119 Mm³ assuming no changes in future crop management. Moreover, without improvement in irrigation application efficiency, the gross application in 2050 was estimated to increase up to ~151 Mm³.

A potential increase in irrigation water demand up to 6% was also projected for the Bekaa Valley (Lebanon) under a dry and hot scenario by the year 2020 (Bou-Zeid and El-Fadel, 2002). Rodríguez Díaz et al. (2007) also showed a typical increase between 15 and 20% in seasonal irrigation water demand by the 2050s in the Guadalquivir river basin. A simulation study conducted by Yano et al. (2007) in the Mediterranean Turkey showed that for the 2070-2079, the irrigation water demand for maize was expected to increase up to 15 and 22% relative to the baseline, based on the CGCM2 and RCM data, respectively. In Southern Italy, Kapur et al. (2007) estimated an increase in irrigation water demand of about 35% for maize, 48% for citrus, 49% for grapevines and 65% and olives, respectively, under the A2 scenario conditions within the next 100 years.

As pointed out by Lovelli et al. (2010), a further increase in irrigation requirement was not expected for autumn-spring crops by the year 2071 in Southern Italy. On the contrary, irrigation needs were projected to increase for spring-summer crops. Based on this study, the impact of climate change on irrigation requirement in Sardinia is also related to summertime, as confirmed by the regional increase in IR for artichokes (14%) and maize (5%). Moreover, both olive orchards and grape vineyards are water stress tolerant crops that grow primarily in the summer, and therefore the IR for olive orchards and grape vineyards is likely to increase. Actually only 6% of olives orchard and 13% of vineyard are irrigated in Sardinia (Istat, 2010); however, in the future, these percentage could rise and deficit irrigation may be needed to stretch water supplies and satisfy irrigation needs. Crops cultivated under rain-fed condition (e.g., wheat) were not considered in this study, but may be in future, because of the likely

reduction in precipitation. Clearly, the application of adaptation strategies to improve water saving is needed.

3.3. Assessment of adaptation strategies

As shown in the previous section, climate change is likely to affect zone 4 the most, and it was therefore chosen to assess how the application of adaptation strategies could lead to a more sustainable agricultural water use. Some changes in crop management were applied to the projected future period to identify the difference in irrigation water demand resulting from a change in on-farm management. Citrus is commonly watered by micro-sprinkler irrigation systems having a mean application frequency of every four days. Reducing the water allocation by 20% results in a percentage of irrigation requirement equal to 80% of a fully irrigated crop. Changing to a drip system with irrigation every second day reduced the ΣGA by 24% in 2050 with a decrease of 11% in yield for the quarter of the field that receives the least amount of water (low quarter) and a mean overall reduction in yield of 3%. Olives and grapevines are already irrigated with drip irrigation systems that have the highest distribution uniformity and potential for the highest application efficiency. Reducing the applied water to 80% of full irrigation for olives and applying water every two days reduced the ΣNA from 874 to 699 mm. Moreover, changing the application frequency from every two to every three days, it was possible to reduce the ΣNA to 693 mm with a yield reduction of only 7% for the low quarter, and a mean yield reduction of 2%.

In grapevines, reducing the applied water to 80% of full irrigation led to a reduction in yield of 5% for the low quarter of a crop. Grain maize, irrigated with sprinklers, showed a reduction in IR by 6%, considering an earlier planting date, while the reduction in IR was greater for a delayed growing season (16%), compared with the crop management currently applied. Other adaptation strategies are also possible including: changing pruning management, reducing or eliminating ground cover between tree and vine rows, modifying agricultural practices, and improving the irrigation systems. Clearly, there are activities that growers can practice to reduce water losses and improve water productivity.

4. CONCLUSIONS

This study aimed to assess the impact of climate change on crop water requirement in 2050 on the Italian island of Sardinia. In general, irrigation requirements increased for the entire region and for all crops. The impact was more severe when ‘current’ rather than ‘future’ CO₂ concentrations were used to account for stomatal closure effects on computed ET_o . On a regional level, an increase in irrigation water demand for the studied crops of about 9 and 15% is projected under ‘future’ and ‘current’ CO₂ concentrations, respectively. Among the crops, maize was the least affected by climate change with an increase in irrigation requirement of 5%. Artichokes were the most affected (14%), followed by olives (11%), citrus (10%), and grapevines (6%), under ‘future’ CO₂ levels. The most important agriculture region in Sardinia (zone 4) was most negatively affected by climate change with an increase in irrigation water demand of about 14% and a reduction in precipitation of 19%. The application of adaptation strategies provided a good way to use water efficiently and to improve the water productivity. For example, applying an irrigation deficit of 20% and using a more efficiency irrigation system for citrus could reduce the ΣGA by 24% in 2050 with a relative small decrease in yield. Moreover, the shift in planting date in grain maize reduced the irrigation requirement by 6% considering an earlier planting date, and 16% considering a delayed planting date, compared with the crop management currently applied.

The methodology applied in this work assumed that crop planting area and other management will not changed in the future, ignoring changes and improvements in technology, genetic, and crop management that will inevitably occur. Some activities that could improve the efficient use of irrigation water are to install and maintain more efficient irrigation systems and to plant more drought tolerant cultivars or new crops.

A comparison with other future emission scenarios can be useful for a better assessment of the magnitude of climate change impacts on irrigation water demand. Moreover, the on-line availability of updated information about crop management and planting distribution would make the research easier, accurate, and detailed. More efforts are needed to improve knowledge about the impacts of climate change in the Mediterranean basin for a future agricultural and economic growth in countries affected by water shortages.

REFERENCES

- Ainsworth, E.A., Long, S.P. 2005. What have we learned from 15 years of free-air CO₂ enrichment (FACE)? A meta-analytic review of the responses of photosynthesis, canopy. *New Phytologist*, 165, 351-371.
- Ainsworth, E.A., Davey, P.A., Bernacchi, C.J., Dermody, O.C., Heaton, E.A., Moore, D.J., Morgan, P.B., Naidu, S.L., Ra, H.S.Y., Zhu, X.G., Curtis, P.S, Long, S.P. 2002. A meta-analysis of elevated [CO₂] effects on soybean (*Glycine max*) physiology, growth and yield. *Global Change Biology*, 8, 695-709.
- Allen, R.G., Gichuki, F.N., Rosenzweig, C. 1991. CO₂-induced climate changes and irrigation-water requirements. *Journal of Water Resources Planning and Management*, 117, 157-177.
- Allen, R.G., Pereira, L.S., Raes, D., Smith, M. 1998. Crop evapotranspiration. Guidelines for computing crop water requirements. FAO Irrigation and Drainage Paper No. 56.
- Allen, R.G., Walter, I.A., Elliott, R.L., Howell, T.A., Itenfisu, D., Jensen, M.E., Snyder, R.L. 2005. The ASCE Standardized Reference Evapotranspiration Equation. American Society of Civil Engineers, Reston, VA.
- Ayala, F.J. 2002. Notas sobre los impactos físicos previsibles del cambio climático sobre los lagos y humedales españoles. III Congreso Ibe'rico sobre gestión y planificación de aguas. Sevilla, Spain.
- Arnell, N.W. 1999. The effect of climate change on hydrological regimes in Europe: a continental perspective. *Global Environmental Change*, 9, 5-23.
- Baric, A., Gasparovic, F. 1992. Implication of climatic change on the socio-economic activities in the Mediterranean coastal zones. In: Jeftic L., Milliman J.D, Sestini G. (Eds.), *Climatic Change and the Mediterranean*. UNEP, New York, USA, pp.129–174.
- Bernacchi, C.J., Kimball, B.A., Quarles, D.R., Long, S.P., Ort, D.R. 2007. Decreases in stomatal conductance of soybean under open-air elevation of [CO₂] are closely coupled with decreases in ecosystem evapotranspiration. *Plant Physiology*, 143, 134-144.

- Bou-Zeid, E., El-Fadel, M. 2002. Climate change and water resources in Lebanon and the Middle East. *Journal of Water Resources Planning and Management*, 128 (5), 343-355.
- Bucchignani, E., Sanna, A., Gualdi, S., Castellari, S., Schiano, P. 2011. Simulation of the climate of the XX century in the Alpine space. *Natural Hazards*, DOI 10.1007/s11069-011-9883-82010.
- Correia, F.N. 1999. Water Resources in the Mediterranean region. *Water International*, 24 (1), 22-30.
- Curtis, P.S. 1996. A meta-analysis of leaf gas exchange and nitrogen in trees grown under elevated carbon dioxide. *Plant, Cell and Environment*, 19, 127-137.
- Döll, P. 2002. Impact of climate change and variability on irrigation requirements: a global perspective. *Climatic Change*, 54, 269-293.
- El-Shaer, H.M., Rosenzweig, C., Iglesias, A., Eid, M.H., Hillel, D. 1997. Impact of climate change on possible scenarios for Egyptian agriculture in the future. *Mitigation and Adaptation Strategies for Global Change*, 1, 233-250.
- ESRI. 2008. ArcGIS Desktop. Ver. 9.3. Redlands, CA, ESRI Inc.
- Fischer, G., Tubiello, F.N., Van Velthuizen, H., Wiberg, D.A. 2007. Climate change impacts on irrigation water requirements: effects of mitigation, 1990–2080. *Technological Forecasting & Social Change*, 74, 1083-1107.
- Folland, C.K., Bader, D., Crowe, M., Jones, P., Plummer, N., Richman, M., Parker, D.E., Rogers, J.S.P. 1999. Workshop on the indices and indicators for climate extremes, Asheville, Breakout Group C Temperature Indices. *Climatic Change* 42, 31-43.
- Gedney, N., Cox, P.M., Betts, R.A., Boucher, O., Huntingford, C., Stott, P.A. 2006. Detection of a direct carbon dioxide effect in continental river runoff records. *Nature*, 439, 835-838.
- Hargreaves, G.H., Samani, Z.A. 1985. Reference crop evapotranspiration from temperature. *Applied Engineering Agriculture*, 1, 96-99.
- Iglesias, A., Ward, M.N., Menendez, M., Rosenzweig, C. 2002. Water availability for agriculture under climate change: understanding adaptation strategies in the Mediterranean. In: Giupponi C., Shechter M. (Eds.), *Climate change and the*

- Mediterranean: socioeconomic perspectives of impacts, vulnerability and adaptation. Edward Elgar, Milan, Italy.
- Iglesias, A., Garrote, L., Flores, F., Moneo, M. 2007. Challenges to manage the risk of water scarcity and climate change in the Mediterranean. *Water Resources Management*, 21, 775–788.
- Intergovernmental Panel on Climate Change (IPCC). 2007. Fourth IPCC Assessment Report (AR4): Climate Change 2007. Cambridge University Press, Cambridge, UK.
- Istat. 2010. VI censimento dell'agricoltura italiana – I dati provvisori. Roma, Istat. <http://censimentoagricoltura.istat.it/index.php?id=73>
- Kapur, B., Steduto, P., Todorovic, M. 2007. Prediction of climatic change for the next 100 years in the Apulia region, Southern Italy. *Italian Journal of Agronomy*, 4, 365-371.
- Kerr, R.A. 2005. Confronting the bogeyman of the climate system. *Science*, 310, 432-433.
- Kimball, B.A. 2004. Global environmental change: implications for agricultural productivity. *Crop, Environment and Bioinformatics*, 1, 251–263.
- Kimball, B.A., Mauney, J.R., Nakayama, F.S., Idso, S.B. 1993. Effects of increasing atmospheric CO₂ on vegetation. *Plant Ecology*, 104 (105), 65-75.
- Kruijt, B., Witte, J.P.M., Jacobs, C.M.J., Kroon, T. 2008. Effects of rising atmospheric CO₂ on evapotranspiration and soil moisture: a practical approach for the Netherlands. *Journal of Hydrology*, 349, 257-267.
- Lee, T.D., Tjoelker, M.G., Ellsworth, D.S., Reich, P.B. 2001. Leaf gas exchange responses of 13 prairie grassland species to elevated CO₂ and increased nitrogen supply. *New Phytologist*, 150, 405–418.
- Lhomme, J.P., Mougou, R., Mansour, M. 2009. Potential impact of climate change on durum wheat cropping in Tunisia. *Climatic Change*, 96, 549–564.
- Lindh, G. 1992. Hydrological and water resources impact of climatic change, In: Jeftic L., Milliman J.D, Sestini G. (Eds.), *Climatic Change and the Mediterranean*. UNEP, New York, USA, pp. 58-93.
- Long, S.P., Ainsworth, E.A., Rogers, A., Ort, D.R. 2004. Rising atmospheric carbon dioxide: Plants FACE the future. *Annual Review of Plant Biology*, 55, 591-628.

- Lovelli, S., Perniola, M., Di Tommaso, T., Ventrella, D., Moriondo, M., Amato, M. 2010. Effects of rising atmospheric CO₂ on crop evapotranspiration in a Mediterranean area. *Agricultural Water Management*, 97, 1287-1292.
- Madec, G., Delecluse, P., Imbard, M., Levy, C. 1998. OPA version 8.1 Ocean general circulation model reference manual. LODYC Technical Report n. 11. Paris, France.
- Medlyn, B.E., Barton, C.V.M., Broadmeadow, M.S.J., Ceulemans, R., De Angelis, P., Forstreuter, M., Freeman, M., Jackson, S.B., Kellomäki, S., Laitat, E., Rey, A., Roberntz, P., Sigurdsson, B.D., Strassmeyer, J., Wang, K., Curtis, P.S., Jarvis, P.G. 2001. Stomatal conductance of forest species after long-term exposure to elevated CO₂ concentration: a synthesis. *New Phytologist*, 149, 247-264.
- Moonen, A.C., Ercoli, L., Mariotti, M., Masoni, A. 2002. Climate change in Italy indicated by agrometeorological indices over 122 years. *Agricultural and Forest Meteorology*, 111, 13–27.
- Moriondo, M., Bindi, M., Kundzewicz, Z.W., Szwed, M., Chorynski, A., Matczak, P., Radziejewski, M. McEvoy, D., Wreford, A. 2010. Impact and adaptation opportunities for European agriculture in response to climatic change and variability. *Mitigation and Adaptation Strategies for Global Change*, 15, 657–679.
- Olesen, J.E., Bindi, M. 2002. Consequences of climate change for European agricultural productivity, land use and policy. *European Journal of Agronomy*, 16, 239-262.
- Oddo, P., Adani, M., Pinardi, N., Fratianni, C., Tonani, M., Pettenuzzo, D. 2009. A nested Atlantic-Mediterranean Sea general circulation model for operational forecasting. *Ocean Science*, 5, 461–473.
- Pérez Urrestarazu, L., Smout, I.K., Rodríguez Díaz, J.A., Carrillo Cobo, M.T. 2010. Irrigation distribution networks' vulnerability to climate change. *Journal of Irrigation and Drainage Engineering*, 136 (7), 486-493.
- Peterson, T.C., Golubev, V.S., Groisman, P.Y. 1995. Evaporation losing its strength. *Nature*, 377, 687-688.
- Rockel, B., Will, A., Hense, A. 2008. The regional Climate Model COSMO-CLM (CCLM). *Meteorologische Zeitschrift*, 17(4), 347–348.

- Roderick, M.L., Farquhar, G.D. 2002. The cause of decreased pan evaporation over the past 50 years. *Science*, 298, 1410-1411.
- Rodríguez Díaz, J.A., Weatherhead, E.K., Knox, J.W., Camacho, E. 2007. Climate change impacts on irrigation water requirements in the Guadalquivir river basin in Spain. *Regional Environmental Change*, 7, 149–159.
- Roeckner, E., Bäuml, G., Bonaventura, L., Brokopf, R., Esch, M., Giorgetta, M., Hagemann, S., Kirchner, I., Kornblueh, L., Manzini, E., Rhodin, A., Schlese, U., Schulzweida, U., Tompkins, A. 2003. The atmospheric general circulation model ECHAM5. Part I: Model description. Report No. 349. Max-Planck-Institut für Meteorologie, Hamburg, Germany.
- Rosenberg, N.J., Kimball, B.A., Martin, P., Cooper, C.F. 1990. From climate and CO₂ enrichment to evapotranspiration. In: Waggoner P.E. (Ed.), *Climate Change and US Water Resources*. John Wiley and Sons, New York, USA, pp. 151-175.
- Scoccimarro, E., Gualdi, S., Bellucci, A., Sanna, A., Fogli, P.G., Manzini, E., Vichi, M., Oddo, P., Navarra, A. 2011. Effects of tropical cyclones on ocean heat transport in a high resolution coupled general circulation model. *Journal of Climate*, 24, 4368-4384.
- Sellers, P.J., Bounoua, L., Collatz, G.J., Randall, D.A., Dazlich, D.A., Los, S.O., Berry, J.A., Fung, I., Tucker, C.J., Field, C.B., Jensen, T.G. 1996. Comparison of radiative and physiological effects of doubled atmospheric CO₂ on climate. *Science*, 271, 1402-1406.
- Senatore, A., Mendicino, G., Smiatek, G., Kunstmann, H. 2011. Regional climate change projections and hydrological impact analysis for a Mediterranean basin in Southern Italy. *Journal of Hydrology*, 399, 70–92.
- Snyder, R.L., Song, Z., Jomaa, I., Moratiel, R., Swelam, A., Shapland, T. 2010. Evapotranspiration response to climate change. *Proceedings of the International Symposium on Climwater 2010, Portugal, 22-27 August 2010, Lisbon*, 91-98.
- Steppeler, J., Doms, G., Schättler, U., Bitzer, H.W., Gassmann, A., Damrath, U., Gregoric, G. 2003. Meso-gamma scale forecasts using the nonhydrostatic model LM. *Meteorology and Atmospheric Physics*, 82, 75–96.
- The Center for Irrigation Technology. 2011. *Agricultural Water Use in California: A 2011 update*. California State University, Fresno.

- Timmermann, R., Goosse, H., Madec, G., Fichefet, T., Etheb, C., Dulière, V. 2005. On the representation of high latitude processes in the ORCA-LIM global coupled sea ice ocean model. *Ocean Modell*, 8, 175-201.
- Todisco, F., Vergni, L. 2008. Climatic changes in Central Italy and their potential effects on corn water consumption. *Agricultural and Forest Meteorology*, 148, 1-11.
- Türkeş, M. 1996. Spatial and temporal analysis of annual rainfall variations in Turkey. *International Journal of Climatology*, 16, 1057-1076.
- Valcke, S. 2006. OASIS3 User Guide (prism_2-5), PRISM Report No 2, 6th Ed., CERFACS, Toulouse, France.
- Viglizzo, E.F., Roberto, Z.E., Filippin, M.C., Pordomingo, A.J. 1995. Climate variability and agroecological change in the Central Pampas of Argentina. *Agriculture, Ecosystems and Environment*, 55, 7-16.
- Yano, T., Aydin, M., Haraguchi, T. 2007. Impact of climate change on irrigation demand and crop growth in a Mediterranean environment of Turkey. *Sensors*, 7, 2297-2315.
- Zheng, F.Y, Peng, S.L. 2001. Meta-analysis of the response of plant ecophysiological variables to doubled atmospheric CO₂ concentrations. *Acta Botanica Sinica*, 43, 1101-1109.

GENERAL CONCLUSIONS

This research provided an overview about the water scarcity issue, focused on the agricultural water demand, future projection of irrigation needs, and ways to improve the water productivity.

The methodology was divided into three steps:

- the investigation on the reference evapotranspiration (ET_o) distribution at the regional scale in Sardinia;
- the assessment of a new soil water balance model, SIMETAW#, for planning agricultural water demand in agriculture;
- the application of the SIMETAW# model to assess the impact of climate change on future irrigation water demand in Sardinia;
- the application of some adaptation strategies in order to use water more efficiently.

The regional ET_o distribution map for Sardinia, based on weather station data, was performed by the use of different methodologies to address the missing data problem and uncertainty in interpolation models. The study of the ET_o distribution at regional scale, with a distinction based on ET_o classes, allowed the application of the SIMETAW# model to estimate the crop water requirements for large areas.

The SIMETAW# model showed a good performance in estimating the potential and actual crop evapotranspiration, suggesting a good crop coefficients (K_c) computation. Moreover, the good performance of the weather generator was confirmed as a useful tool for filling the weather data gaps. These results confirmed that the SIMETAW# model could be used efficiently to evaluate different irrigation strategies, which support irrigation planning and maximize water productivity.

The application of the SIMETAW# model to assess the impact of climate change on future irrigation requirements allowed for an investigation into the magnitude of the future irrigation demand in Sardinia, and the application of some adaptation strategies that lead to improvements in irrigation management and water savings.

This study showed significant results that will be useful for future irrigation planning in agriculture, although more efforts are needed to improve knowledge about the impacts of climate change in the Mediterranean basin for future agricultural and economic growth in countries affected by water shortages.